THÈSE EN COTUTELLE PRÉSENTÉE

POUR OBTENIR LE GRADE DE

DOCTEUR DE L'UNIVERSITÉ DE BORDEAUX ET DE L'UNIVERSITÉ LAVAL

ÉCOLE DOCTORALE DES SCIENCES CHIMIQUES

PROGRAMME DE DOCTORAT EN GÉNIE DES MATÉRIAUX ET DE LA MÉTALLURGIE

SPÉCIALITÉ CHIMIE ET TECHNOLOGIES POUR LE VIVANT

Par **Melissa KOSOVARI**

In vitro systems for bone tissue engineering: Biochemical multi-functionalization with mimetic peptides

Sous la direction de: **Dr. Marie Christine Durrieu** (Université de Bordeaux)
Pr. Gaétan Laroche (Université Laval)

Soutenue le 13/11/2025

Membres du jury:

Mme. F. DJOUAD	Directrice de recherche INSERM, Institute for Regenerative Medecine and Biotherapy	Rapporteur
M. V. HUMBLOT	Directeur de recherche CNRS, Université Besançon	Rapporteur
Mme C. HOESLI	Professeur, McGill University	Examinateur
M. F. HEIM	Professeur, Université de Haute Alsace	Président du jury
Mme. M.-C. DURRIEU	Directrice de recherche INSERM, Université de Bordeaux	Directrice de thèse
M. G. LAROCHE	Professeur, Université Laval	Co-directeur de thèse

Membres invités:

M. L. Vellutini	Professeur, Université de Bordeaux	Invité

Résumé:

Systèmes in vitro pour l'ingénierie tissulaire osseuse: Multi-fonctionnalisation biochimique avec des peptides mimétiques

L'ingénierie des surfaces de biomatériaux fonctionnalisées avec des ligands dérivés de la matrice extracellulaire (MEC) est un domaine multidisciplinaire en expansion, essentiel aux progrès en médecine régénérative. En conditions physiologiques, les cellules perçoivent de multiples signaux de l'échelle nanométrique à micrométrique, qui guident leur comportement et leur destin. La MEC, réseau dynamique et structuré, fournit non seulement un support mécanique mais aussi des signaux biochimiques et biophysiques déterminants via son architecture moléculaire. Les cellules souches mésenchymateuses (CSM), capables d'auto-renouvellement et de différenciations multiples, répondent finement à leur microenvironnement. Leur destinée, notamment ostéogénique, dépend de caractéristiques comme la rigidité, la nanotopographie et la présentation de motifs bioactifs. Les biomatériaux peuvent ainsi être optimisés en incorporant des peptides d'adhésion, mimétiques de facteurs de croissance ou inspirés des protéines de la MEC. Toutefois, les approches limitées à un ou deux peptides ne reflètent pas la complexité multifactorielle de la MEC. Des études récentes démontrent que la co-présentation de plusieurs peptides induit des effets synergiques sur l'expression ostéogénique. La réussite de ces stratégies repose sur une modification de surface précise, où la silanisation joue un rôle clé. Les méthodes classiques, comme l'immersion en solution avec des silanes commerciaux, souffrent de variabilité compromettant la reproductibilité. Pour dépasser ces limitations, une plateforme innovante a été développée sur wafers de silicium: la technique de dépôt à la tournette combinée à l'emploi d'aminosilanes protégés. Cette méthode génère des monocouches auto-assemblées (SAM) homogènes et stables, permettant une présentation contrôlée des ligands, tout en montrant l'importance de la longueur de chaîne alkyle et de la chimie du groupe protecteur dans l'efficacité d'immobilisation. L'activation et la silanisation ont été caractérisées par mesures d'angle de contact, PM-IRRAS et XPS, établissant un protocole reproductible adapté aux évaluations biologiques. Sur cette base, des surfaces de silicium ont été co-fonctionnalisées avec jusqu'à trois peptides différents: RGD (adhésion via intégrines), P15 (mimétique du collagène I) et BMP-2 (activation de récepteurs de facteurs de croissance ostéogéniques). Cette combinaison inédite reconstitue une interface biomimétique complexe et cohérente. Des CSM humaines cultivées sur ces substrats multifonctionnels ont été analysées par RT-qPCR et immunocytochimie. Les résultats révèlent une induction significative des marqueurs ostéogéniques, tant précoces que tardifs, démontrant une différenciation accélérée et robuste, surpassant les substrats fonctionnalisés par un ou deux peptides. En conclusion, ce travail illustre

une avancée majeure en ingénierie de surface des biomatériaux. Il établit qu'une co-fonctionnalisation simultanée de plusieurs peptides, fondée sur une compréhension fine des interactions cellule-MEC, offre un contrôle puissant et reproductible de la différenciation ostéogénique des CSM. Cette stratégie ouvre la voie à de nouvelles interfaces biomimétiques adaptées aux applications de médecine régénérative.

Mots-clés: fonctionnalisation de surface, matrice extracellulaire, silanisation, multi-peptides, cellules souches mésenchymateuses, différenciation ostéogénique

Abstract:

In vitro systems for bone tissue engineering: Biochemical multi-functionalization with mimetic peptides

Engineering biomaterial surfaces functionalized with ligands derived from the extracellular matrix (ECM) is a multidisciplinary and expanding field essential for advances in regenerative medicine. Under physiological conditions, cells perceive multiple signals ranging from the nanometer to micrometer scale that guide their behavior and fate. The ECM, a dynamic and structured network, not only provides mechanical support but also delivers crucial biochemical and biophysical signals through its molecular architecture. Mesenchymal stem cells (MSCs), capable of self-renewal and multiple differentiation pathways, respond finely to their microenvironment. Their fate, particularly osteogenic differentiation, depends on factors such as substrate stiffness, nanotopography, and the presentation of bioactive motifs. Biomaterials can be optimized by incorporating adhesion peptides, growth factor mimetics, or ECM-inspired protein sequences. However, approaches limited to one or two peptides do not fully recapitulate the ECM's multifactorial complexity. Recent studies demonstrate that simultaneous presentation of multiple peptides induces synergistic effects on osteogenic marker expression. The success of these strategies relies on precise surface modification, with silanization playing a key role. Conventional methods such as solution immersion with commercial silanes suffer from variability that compromises reproducibility. To overcome these limitations, an innovative platform was developed on silicon wafers using spin coating combined with protected aminosilanes. This method produces robust and homogeneous self-assembled monolayers (SAMs) that allow controlled ligand presentation while demonstrating the critical influence of alkyl chain length and protective group chemistry on immobilization efficiency. Surface activation and silanization were characterized by contact angle measurements, PM-IRRAS, and XPS, establishing a reproducible protocol suitable for subsequent biological evaluations. On this basis, silicon surfaces were co-functionalized with up to three different peptides: RGD (integrin-mediated adhesion), P15 (collagen I mimetic), and BMP-2 (activation of osteogenic growth factor receptors). This novel combination recreates a complex and coherent biomimetic interface. Human MSCs cultured on these multifunctional substrates were analyzed by RT-qPCR and immunocytochemistry, revealing significant induction of early and late osteogenic markers, demonstrating accelerated and robust differentiation surpassing substrates functionalized with one or two peptides. In conclusion, this work represents a major advance in biomaterial surface engineering. It establishes that simultaneous co-functionalization with multiple peptides, based on the fine understanding of cell-

ECM interactions, provides powerful and reproducible control over MSC osteogenic differentiation. This strategy paves the way for new biomimetic interfaces tailored for regenerative medicine applications.

Key words: Surface functionalization, extracellular matrix, silanization, multi-peptide mesenchymal stem cells, osteogenic differentiation

Unités de recherche

3BIOs group : BIOactive surfaces, BIOmaterials and BIOmimetic tissue-engineered products

Institut de Chimie et Biologie des Membranes et des Nano-objects (CNRS UMR5248 CBMN) Allée Geoffroy Saint-Hilaire – Bât. B14, 33600 Pessac, France

Laboratoire d'Ingénierie de Surface (LIS)

Centre de recherche du CHU de Québec, Axe médecine régénératrice

Hôpital Saint-François d'Assise, 10 rue de l'Espinay, Québec (Québec) Canada G1L 3L5

Contents

Résumé: ii

Abstract: iv

List of tables ix

List of figures x

Abbreviations xii

Acknowledgements xv

Foreword xviii

Introduction 1

Literature Review 3

1 Bone Biology and Mesenchymal Stem Cells in Regenerative Medicine 4

1.1 Bone Tissue Structure and Physiology 4
1.1.2 Mechanisms of Bone Remodeling 7
1.1.3 Advancing Bone Repair: Biomaterials in Bone Tissue Engineering 8

1.2 Stem cells 11
1.2.1 Mesenchymal Stem Cells (MSCs) 12
Bone marrow-derived mesenchymal stem cells (BMSCs) 15
1.2.2 Regenerative effects of MSCs-secreted paracrine factors 16
1.2.3 Clinical Applications and Therapeutic Relevance of MSCs 17

1.3 Signaling Pathways controlling osteogenic Differentiation 21

2 Surface Modification Strategies for Biomaterial Functionalization 26

2.1 Influence of Surface Properties on Cell Behavior 26

2.2 Enhancing Biomaterial Interfaces through Functional Group Modification 31

2.3 Silanization strategies 34

3 Mimicking the Extracellular Matrix: Peptide Functionalization for Osteogenic Platforms 40

3.1 Complexity and Biological Role of the Extracellular Matrix in Bone 40
3.1.1 Cell-cell and cell-matrix interactions in bone microenvironment 42

3.2 Biomimetic Surfaces: Bioactive Cues for Guiding Cell Responses 46
Integrin-binding peptides 47
Collagen-derived peptides 48
Growth factors-derived peptides 49

3.3 Synergistic Effects of Multi-Peptide Functionalization on Cell Differentiation 51

4 Project overview and research objectives 58

4.1 Comparative study on silanization techniques for surface modification 58

4.2 Synergistic effect of multi-peptide functionalized interfaces 59

5 Study 1: Silanization Strategies for Tailoring Peptide Functionalization on Silicon Surfaces: Implications for Enhancing Stem Cell Adhesion 63

5.1 Résumé 64

5.2 Abstract 65

5.3 Introduction 66

5.4 Materials and Methods 69
5.4.1 Materials 69
5.4.2 Sample preparation 70
5.4.3 Surface Characterization 73
5.4.4 Cell culture experiments 74
5.4.5 Statistics 75

5.5 Results 75
5.5.1 Characterization of the biochemical modification of silicon surfaces 75
5.5.2 Water Contact Angle and Atomic Force Microscopy 75
5.5.3 X-Ray Photoelectron Spectroscopy 76
5.5.4 Polarization Modulation Infrared Reflection-Absorption Spectroscopy (PM-IRRAS) 80
5.5.5 Silanization impacts cell adhesion 82

5.6 Discussion 85

5.7 Conclusion 90

6 Study 2: Synergistic Multi-Peptide Interfaces Enhance Early Osteogenic Differentiation of Mesenchymal Stem Cells 92

6.1 Résumé 93

6.2 Abstract 93

6.3 Introduction 94

6.4 Materials and Methods 97
6.4.1 Materials 97
6.4.2 Sample Preparation 98
6.4.3 Polarization Modulation Infrared Reflection-Absorption Spectroscopy 99
6.4.4 Fluorescence Microscopy 99
6.4.5 Cell Culture 99
6.4.6 Immunocytochemistry assays 100
6.4.7 Real-Time Quantitative Polymerase Chain Reaction. 100
6.4.8 Statistical Analysis 102

6.5 Results 102
6.5.1 Polarization Modulation Infrared Reflection-Absorption Spectroscopy 102
6.5.2 Fluorescence Microscopy 104
6.5.3 Gene Expression Analysis of Osteogenic Differentiation by RT-qPCR 108

6.5.4 Immunocytochemistry 111
6.6 Discussion 114
6.7 Conclusions 119
6.8 Supporting Information 121
Conclusion 124
General discussion 124
1. Silanization strategies and impact on biomaterial functionalization 124
2. Multi-peptide functionalization enhances osteogenic differentiation 126
3. Importance of silane molecule in optimizing multi-peptide immobilization 128
4. Unraveling peptide spatial distribution through fluorescence imaging 128
Future Perspectives 131
Appendix A 134
Scientific communications 134
A.1 Publications 134
A.2 Oral Communications 134
A.3 Poster presentation 135
Bibliography 137

List of tables

3.1	Overview of using combinatorial peptide-based surface modifications to enhance biomaterials bioactivity	52
5.1	Root mean square roughness (R rms) calculated by AFM measurements	76
5.2	XPS survey analyses of silicon surfaces after activation, silanization, and RGD grafting	77
6.1	RT-qPCR primer sequences and functions for genes analyzed	101
6.2	Panel of 7 candidate housekeeping genes evaluated	102

List of figures

1.1	Internal structure of human bone	5
1.2	Schematic representation of bone remodeling process	8
1.3	Differentiation potential of MSCs	13
1.4	Overview of the administration routes and targeted diseases for MSC-based clinical trials	19
1.5	Signaling and transcriptional regulation of osteoblast cell lineage, commitment and differentiation	24
2.1	Effects of chemical functional groups on hDPSCs differentiation	27
2.2	The stiffness of living tissues spans a wide range, from a few pascals to gigapascals	30
2.3	Schematic diagram of an ideal single-crystalline SAM on a gold surface	35
2.4	Schematic illustration of the preparation of organosilane-based SAMs	38
3.1	Calcium-dependent cadherin cell-adhesion system. Molecular structure of integrin adhesion complexes	43
3.2	GFOGER hydrogels to restore bone formation	48
3.3	P15-functionalized Ti surfaces for cell attachment and spreading	49
3.4	Schematic illustration of polydopamine coating combined with BMP-2 immobilization on 3D microporous PLGA scaffolds to promote osteogenic differentiation of hADSCs and bone formation	51
3.5	Osteogenic commitment of human bone marrow stromal cells (hBMSCs) after 4 weeks of culture on bare glass surfaces	55
3.6	Ti-BMP-2-GDF-5 coating to enhance cell proliferation and mineral deposition	56
4.1	Chemical structures of the silane molecules utilized in this study	59
4.2	Molecular structures of the ECM-inspired peptides used in this study	61
5.1	XPS high-resolution spectra of Si2p after silanization with APTES, AUTES, and Alk-NH_2 and C1s after RGD grafting	79
5.2	PM-IRRAS spectra after silanization with APTES (a), AUTES (b), and Alk-Phtha (c) onto SiO_2/Au substrates and after RGD peptide grafting	80
5.3	Representative fluorescence images of hBMSCs were seeded for 24 h in a DMEM medium on control (a), APTES+RGD (b), AUTES+RGD (c), and Alk-NH2+RGD (d) substrates in serum-free conditions	82
5.4	Histograms showing the change in cell spreading area of hBMSCs in response to RGD-substrates functionalized with different silanization strategies (A), F-actin expression (B), vinculin-containing focal adhesion area (C) and relative vinculin expression within focal adhesions (D)	84

6.1	PM-IRRAS spectra after silanization with C_{11}-Phtha onto SiO_2/Au substrate, SMPB cross-linker conjugation onto deprotected amino surface and after RGD, BMP2 or P15 peptide grafting	103
6.2	Characterization of single peptide surfaces via fluorescence spectroscopy	104
6.3	Fluorescence spectroscopy characterization of dual and triple peptide surfaces	106
6.4	Gene expression analysis of early osteogenic markers (RUNX2, ALPL), mid-stage marker (COL1A1), and late-stage markers (BGLAP, SATB2) in hMSCs cultured on control and peptide-functionalized surfaces for 3 and 10 days in osteogenic medium	109
6.5	Analysis of SMAD1 and SMAD5 mRNA expression in hMSCs cultured under osteogenic conditions on control or peptide-functionalized substrates for 3 and 10 days	111
6.6	Representative immunofluorescence images of hMSCs showing OPN expression on control (a), BMP2+RGD (b), and BMP2+RGD+P15 (c) conditions at day 5. Histograms showing OPN expression of hMSCs in response to Si-substrates functionalized with different peptide combinations (d) and distribution of OPN fluorescence intensity (e)	113
6.7	Normalized emission spectra of single peptides, dual-peptide and triple-peptide in solution, excited at 405 nm	121
6.8	Unnormalized emission spectra of single peptide surfaces excited at 405 nm	122
6.9	Representative images of hMSCs at the 5-day time point, acquired at 10× magnification	123

Abbreviations

$1,25D_3$ 1,25-dihydroxyvitamin D_3

AFM Atomic Force Microscopy

ALP Alkaline phosphatase

ALS Amyotrophic lateral sclerosis

AMC 7-Amino-4-methylcoumarin

APTES 3-aminopropyl-triethoxysilane

AUTES 11-aminoundecyltriethoxysilane

BMP Bone morphogenetic protein

BMSCs Bone marrow-derived mesenchymal stem cells

BSA Bovine serum albumin

BSP Bone sialoprotein

cDNA Complementary DNA

COL1 Collagen 1

CVD Chemical vapor deposition

DAPI 4',6-diamidino-2-phenylindole

DMEM Dulbecco's modified Eagle medium

DMP1 Dentin matrix protein 1

DMSO Dimethyl sulfoxide

DSPP Dentin sialophosphoprotein

ECM Extracellular matrix

EDC 1-ethyl-3-(3-dimethylaminopropyl) carbodiimide

EDTA Ethylenediaminetetraacetic Acid

EGF-R Epidermal growth factor receptor

EV Extracellular vesicles

FA Focal adhesions

FAK Focal adhesion kinase

FBS Fetal bovine serum

FDA Food and drug administration

FGF Fibroblast growth factor

FITC Fluorescein isothiocyanate

FN Fibronectin

GAG Glycosaminoglycan

GDF5 Growth differentiation factor 5

GF Growth factors

HA hydroxyapatite

hADSCs Human adipose-derived stem cells

HBDs Heparin-binding domains

hDPSCs Human dental pulp stem cells

HLA-DR Human leukocyte antigen – DR isotype

hMSCs Human Mesenchymal stem cells

HSCs Hematopoietic stem cells

HSPGs Heparan sulfate proteoglycans

IGF-R Insulin-like growth factor receptor

iPSCs Induced pluripotent stem cells

MAPK Mitogen-activated protein kinase

MEPE Matrix extracellular phosphoglycoprotein

MGP Matrix Gla protein

MHC Major histocompatibility complex

MS Multiple sclerosis

MSCs Mesenchymal stem cells

OA Osteoarthritis

OCN Osteocalcin

OPN Osteopontin

OPG Osteoprotegerin

Osx Osterix

PBS Phosphate buffered saline

PDGF-R Platelet-derived growth factor receptor

PDMS Polydimethylsiloxane

PEG Poly(ethylene glycol)

PEEK Polyether ether ketone

PD Parkinson's Disease

PLA Polylactic Acid

PLGA poly(lactic-co-glycolic acid)

PM-IRRAS Polarization Modulation-Infrared Reflection-Absorption Spectroscopy

PSC Pluripotent stem cells

PTH Parathyroid hormone

RANKL Receptor Activator of Nuclear Factor-Kb Ligand

RTq-PCR Reverse transcription quantitative polymerase chain reaction

Runx2 Runt-related transcription factor 2

SAMs Self-assembled monolayers

SIBLING small integrin-binding ligand N-linked glycoprotein

SLRPs Small leucine-rich proteoglycans

SMPB Succinimidyl-4-(p-maleimidophenyl) butyrate

SOST Sclerostin

SSPCs Skeletal stem and progenitor cells

TAMRA 5-(and-6)-carboxytetramethylrhodamine

TGF-β Transforming Growth Factor β

TNF Tumor necrosis factor

TSPs Thrombospondins

VEGF Vascular Endothelial Growth Factor

VN Vitronectin

XPS X-ray photoelectron spectroscopy

Acknowledgements

Ever since I was little, my mom has told me that I've been a curious child, always wanting to explore and understand everything around me. Perhaps even then, I already felt a deep need to uncover the "why" behind things.

Four years have passed since this incredible journey began. I've grown in ways I never imagined, and I find myself overwhelmed with gratitude for all the people whose support has made this possible.

Tout d'abord, je souhaite remercier les membres du jury d'avoir accepté d'évaluer mon travail.

Je tiens particulièrement à remercier mes deux directeurs de recherche, Marie-Christine et Gaétan. Le doctorat en cotutelle a été une véritable aventure, elle comporte aussi de défis, et je suis heureuse d'avoir pu la partager avec deux personnes qui s'entendent et se complètent si bien. Merci de m'avoir toujours soutenue, guidée et accompagnée, tout en me laissant la liberté de faire mes propres choix. Je suis aussi très reconnaissante d'avoir eu l'opportunité de participer à de nombreux congrès grâce à vous. Votre appui et vos conseils ont été essentiels tout au long de ce parcours, et partager cette expérience avec vous a été pour moi un véritable privilège.

My journey began in Québec, in January, right in the middle of a snowstorm, and yet, the welcome could not have been warmer.

Je tiens surtout à remercier Andrée-Anne. Merci de m'avoir accueillie dans le laboratoire, pour tous tes enseignements en chimie, si précieux pour le reste de mon doctorat, pour nos réunions improvisées dans le couloir, et pour tes mots d'encouragement qui m'ont toujours aidée à avancer.

I am deeply grateful to everyone at Saint François d'Assise Hospital for welcoming me from the very beginning. A special thanks to Williams for his kindness and for making everything feel lighter, even with his countless "time to panic" post it I kept finding everywhere. Thanks also to Fa, Ghane, Linda, Sergio and Lucia for all the chats and laughter shared together, you made this experience truly memorable, and I feel so fortunate to have met you all.

In Québec, I also met people who are now among my best friends.

Vinicius, Richard, Rosiane, Ariel. Thank you for becoming my second family, for always being there for me, for our adventures, the wonderful moments spent together, and for being the incredible people you are.

Maria, you are my person. Our friendship is the greatest gift this adventure has given me. I could never fully express how grateful I am to have you in my life. You are the most incredible, kind, good-hearted, and amazing person I've ever met. I wish everyone could have a Maria in their life. As I told you when we met: "You are the sun, you light up the room when you enter it". How lucky I am to have such a friend in my life.

Cristina, thank you for asking me to live together four years ago, because since then we've been inseparable. We have shared all the craziness of this adventure, the ups and downs, and beyond that, you've become my "pepito grillo", always understanding me and being the best friend, anyone could ask for. Thank you for always saying, "It will be fine," because in the end, it always is.

Mon aventure continue à Bordeaux, et je tiens à remercier Murielle du fond du cœur. Merci pour tous tes conseils, ton soutien constant, tes mots d'encouragement, et nos moments de discussion qui m'ont toujours fait du bien. Merci aussi de m'avoir accompagnée et de m'avoir fait sentir moins seule dans les moments difficiles. Je suis vraiment heureuse d'avoir croisé le chemin d'une personne aussi exceptionnelle que toi.

Je tiens à remercier Artem et Evgeny pour leur patience face à toutes mes questions « chimiques » et pour leur disponibilité constante.

Je tiens à remercier Luc Vellutini pour sa précieuse contribution à cette thèse, pour l'orientation que ce projet a prise à partir de notre conversation à Québec il y a quatre ans. Merci également pour les échanges scientifiques qui m'ont toujours permis d'apprendre et de progresser.

Je remercie également Thierry Buffeteau, Marc Dussauze et Claire Petuya, qui ont permis d'apporter une véritable valeur ajoutée à ce travail de thèse grâce à leur expérience et à leurs précieux enseignements.

I would like to thank James McGettrick for welcoming me during my stay at Swansea University and for his valuable collaboration, which greatly enriched this work.

I would also like to thank those with whom I have shared part of this journey: Michele, for our philosophical discussions and the countless anecdotes you shared over the years (even if I barely remember any), and Yujie, for her kindness and for always bringing a smile with her.

I would like to thank all the people at CBMN. In particular, thank you to Rosario, Soumaïla, and Lucio for making my last year full of laughter and fun.

Grazie ai miei amici di sempre, con i quali sono cresciuta e senza i quali non sarei la persona che sono oggi. In particolare, grazie a Ilaria, siamo cresciute insieme, da vent'anni a questa parte sei la persona con cui condivido ogni cosa e so che così sarà per sempre. E grazie a Davide, il mio punto fermo e la mia roccia. Grazie per credere in me anche quando io stessa fatico a farlo.

Infine, un grazie immenso alla mia famiglia per avermi sempre sostenuta e incoraggiata.

Grazie a mio fratello e mia sorella, per essere la cosa più preziosa che ho e per essere sempre al mio fianco. Sono incredibilmente fortunata a condividere la vita con voi.

Faleminderit prindërve të mi, që më keni rritur duke më bërë të besoj se në jetë mund të arrija çdo gjë. Që më keni mësuar respektin, forcën dhe vendosmërinë për të ndjekur ëndrrat e mia, dhe që të vlerësoj punën dhe dedikimin në çdo gjë që bëj. Faleminderit për dashurinë, për besimin dhe për të gjitha sakrificat që keni bërë, të cilat më kanë mundësuar të arrij deri këtu.

Faleminderit gjyshërve të mi, që edhe pse larg, gjithmonë i kam ndjerë afër meje. Faleminderit për dashurinë tuaj të pa fund, për besimin që gjithmonë keni pasur tek unë, dhe për mësimet e jetës dhe vlerat e shtrenjta që më keni dhuruar. Ju dua shumë dhe do t'ju mbaj gjithmonë në zemër.

Foreword

This thesis contains two scientific papers that I wrote as first author. These articles are included in this document as chapters 5 and 6.

Article 1

Title: Silanization Strategies for Tailoring Peptide Functionalization on Silicon Surfaces: Implications for Enhancing Stem Cell Adhesion

Authors: Melissa Kosovari, Thierry Buffeteau, Laurent Thomas, Andrée-Anne Guay Bégin, Luc Vellutini, James D. McGettrick, Gaétan Laroche, Marie-Christine Durrieu

Journal: ACS Applied Materials and Interface

State: Submitted March 5th 2024, Published June 4th 2024

Author's contribution: The first author designed and performed the experiments, based on discussions with all the authors. The first author analyzed the data, prepared the figures and drafted the manuscript. T. Buffeteau performed PM-IRRAS measurements. L. Thomas synthetized the Alk-Phtha molecule. J.D. McGettrick performed XPS analysis. All authors reviewed the manuscript.

Article 2

Title: Synergistic Multi-Peptide Interfaces Enhance Early Osteogenic Differentiation of Mesenchymal Stem Cells

Authors: Melissa Kosovari, Marc Dussauze, Claire Petuya, Thierry Buffeteau, Murielle Remy, Luc Vellutini, Artem Zibarov, Gaétan Laroche, Marie-Christine Durrieu

State: Submitted September 2025

Author's contribution: The first author designed and performed the experiments, based on discussions with all the authors. The first author analyzed the data, prepared the figures and drafted the manuscript. M. Dussauze and C. Petuya performed the fluorescence microscopy experiments. T. Buffeteau performed PM-IRRAS measurements. All authors reviewed the manuscript.

Introduction

In vitro platforms have become indispensable tools in biological research, particularly for drug testing, screening, and the initial assessment of cellular responses to new therapies. Before progressing to in vivo studies, it is crucial to acquire comprehensive information about a compound's biological effects, potential toxicity, and mechanisms of action. In the past decades, regenerative medicine has relied increasingly on in vitro models to evaluate the regenerative capacity of stem cells, especially their potential to differentiate into desired tissue types. Human mesenchymal stem cells (hMSCs), for instance, are characterized by their ability to self-renew and differentiate into multiple lineages in vivo, but they reside within a specialized niche, a complex extracellular environment that constantly provides instructive biochemical and physical stimuli. Standard cell culture techniques often fail to replicate this microenvironment, resulting in cellular behaviors that may not accurately reflect physiological responses. To bridge this gap, it is imperative in the field to develop in vitro platforms that closely mimic the native extracellular matrix (ECM). One promising strategy is the incorporation of biomimetic peptides derived from key ECM proteins involved in cell signaling and interactions. Such platforms allow precise control, personalization, and tunability of the cellular microenvironment, enabling researchers to guide cellular differentiation with greater accuracy. By designing in vitro systems that recapitulate the natural ECM, it becomes possible to enhance the reliability of biological testing, improve the predictive value of drug screening, and to ultimately ensure that only the most promising candidates advance to in vivo studies.

This doctoral project is dedicated to advancing the field of regenerative medicine by developing strategies to precisely stimulate and regulate stem cell behavior. The main objective is to establish in vitro platforms capable of supporting rapid and efficient tissue regeneration, with a particular focus on the incorporation of bioactive mimetic peptides that can direct stem cell differentiation towards the osteoblastic lineage. The first part of the thesis establishes the theoretical foundations and background necessary to understand the focus of this study. Chapter 1 introduces the fundamentals of mesenchymal stem cells and bone tissue biology. Chapter 2 reviews surface modification strategies

employed for the functionalization of biomaterials, highlighting their role in enhancing biological interactions. Chapter 3 provides an overview of the extracellular matrix and discusses how mimicking its biochemical and structural cues can be used to guide osteogenic differentiation. Building upon this foundation, Chapter 4 outlines the specific objectives of the PhD project and details the methodological approaches designed to address them. The subsequent chapters present the experimental results in the form of scientific articles. Chapter 5 presents the first scientific article, reporting a comparative study of different silanization strategies, emphasizing their critical influence not only on peptide presentation but also on stem cell behavior. Chapter 6 describes the second scientific article, focusing on the synergistic effects of simultaneously grafting multiple peptides on biomaterial surfaces to better mimic the complexity of the ECM and enhance the efficiency of osteogenic differentiation.

The thesis concludes with a general discussion that integrates the findings across all chapters. This final section summarizes the contributions of the work, reflects on its implications for regenerative medicine, and outlines perspectives for future research directions.

Literature Review

Chapter 1

Bone Biology and Mesenchymal Stem Cells in Regenerative Medicine

1.1 Bone Tissue Structure and Physiology

The skeletal system is indispensable for the human body, fulfilling multiple essential roles. It enables movement, provides internal support, and protects vital organs. Additionally, bone tissue serves as a dynamic reservoir for minerals, primarily calcium and phosphate, thus playing a key role in the regulation of mineral homeostasis. Furthermore, bones are central to hematopoietic function, offering a supportive environment for blood cell production.[1]

Bone tissue is the only connective tissue capable of mineralization under physiological conditions. This process depends on specific bone matrix proteins that promote the nucleation and growth of hydroxyapatite crystals. Structurally, bone is composed of two main components: inorganic and organic.

The inorganic component predominantly consists of hydroxyapatite crystals (primarily calcium phosphate), which impart mechanical strength and resistance to impact and fracture. Importantly, this mineralized matrix is an essential storage site for calcium and phosphate, allowing for rapid mobilization of these ions in states of systemic deficiency.[2]

The organic matrix comprises both cellular and extracellular elements. The cellular component includes osteoprogenitor cells, osteoblasts, osteocytes, and osteoclasts. The extracellular matrix contains type I collagen (the principal fibrillar component), other collagens, glycoproteins, proteoglycans, and various growth factors incorporated within the matrix. The primary role of the organic matrix is to provide structural plasticity, thereby reducing the risk of brittle fractures. Mineral deposition on the type I collagen framework generates a composite structure combining strength and flexibility.[3]

Bone also functions as a reservoir for growth factors, which remain trapped within the matrix and are released during bone remodeling to coordinate tissue growth and repair. The initiation of mineralization occurs on the organic matrix at specific sites determined by bone-derived proteins, ultimately guiding the formation and localization of hydroxyapatite crystals.[4] At the microscale, bone tissue is organized into two main architectural forms: cancellous (trabecular) bone and cortical (compact) bone (Figure 1.1). Cancellous bone features a network of trabeculae interspersed with marrow-filled spaces, resulting in a characteristic spongy appearance and contributing to metabolic activity and shock absorption. Cortical bone, in contrast, is densely packed, providing exceptional hardness and compressive strength necessary for load-bearing function. Bone tissue is richly vascularized. Large arteries branch extensively into arterioles and capillaries, traversing periosteal and endosteal compartments, ultimately delivering oxygen and nutrients to embedded bone cells[5].

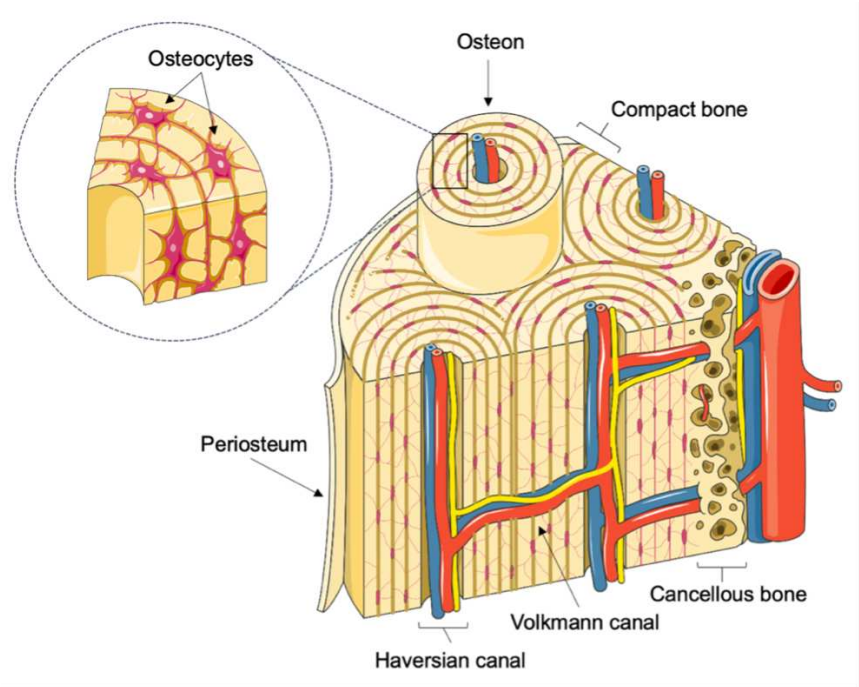


Figure 1.1 Internal structure of human bone. Parts of this diagram were adapted from Servier Medical Art (smart.servier.com).

The cellular component of bone includes several cell types reflecting different stages in the same lineage: osteoprogenitor cells, osteoblasts, osteocytes, all derived from mesenchymal stem cells, as well as osteoclasts, which originate from hematopoietic precursors. The balance between bone formation (osteoblast/osteocyte activity) and bone resorption (osteoclast activity) is fundamental for skeletal

health and tissue remodeling. Dysregulation among these cells underlies the pathogenesis of many bone disorders.

The trabecular zone is particularly significant for bone remodeling, as it houses medullary niches containing osteoprogenitor cells, stem-like precursors committed to the osteogenic lineage. These cells retain multipotency but are primed for differentiation toward mature bone-forming cells. Osteoblasts reside on bone surfaces, where they secrete type I collagen and orchestrate the synthesis of bone matrix, which serves as a substrate for hydroxyapatite deposition. These cells are equipped with membrane receptors for key regulatory factors, including parathyroid hormone, vitamin D (essential for calcium uptake), and estrogen. Histologically, osteoblasts appear as cuboidal cells aligned along trabecular surfaces. The transcription factors Runx2 and Osterix (Osx) are pivotal regulators of osteogenic differentiation. Disruption of Runx2 or Osx activity impairs the commitment of stem cells to the osteoblast lineage, resulting in defective bone formation.[6]

Osteocytes derive from osteoblasts that become entrapped within the mineralized matrix. This process forms mature cells embedded in lacunae, interconnected through an intricate network of canaliculi. Only a part of osteoblasts becomes osteocytes, the rest undergo cell apoptosis. Osteocytes are the primary mechanosensors of bone, translating mechanical stimuli into cellular responses. When mechanical strain or damage occurs, osteocytes secrete signaling molecules that modulate osteoblast activity and direct targeted bone remodeling and repair.[7]

Osteoclasts, by contrast, are large multinucleated cells of hematopoietic origin (macrophage lineage) specialized in bone resorption, a critical process for the continuous renewal and remodeling of skeletal tissue. This function requires osteoclasts to firmly adhere to the bone matrix, solubilize its mineralized component, and subsequently degrade the organic matrix. Physiological microfractures in the bone create accessible surfaces that facilitate osteoclast attachment and initiation of resorption. To maximize resorptive capacity, osteoclasts develop plasma membrane invaginations known as "brush borders", which significantly increase the cell surface area in contact with the bone matrix. Upon adhesion, osteoclasts create a sealed resorption lacuna, the Howship's lacuna, by tight binding mediated through integrins. This enclosed microenvironment is essential to maintain localized acidity and protect surrounding tissues from the destructive actions of the osteoclast. Within the resorption lacuna, osteoclasts acidify the compartment by actively pumping protons (H^+ ions) and chloride ions (Cl^-) into the space via specialized proton pumps and chloride channels, thereby lowering the pH to dissolve hydroxyapatite crystals efficiently. Following mineral dissolution, osteoclasts secrete proteolytic enzymes to degrade the exposed type I collagen matrix, completing the bone resorption

process.[2], [8], [9], [10]. This tightly regulated sequence ensures selective removal of mineralized bone while maintaining skeletal integrity and enabling subsequent bone formation.

1.1.2 Mechanisms of Bone Remodeling

Bone remodeling is a continuous physiological process, with approximately 10% of the skeleton undergoing renewal annually. This process predominantly occurs at sites subjected to frequent mechanical stress, as remodeling is initiated in response to microfractures.[2] The fundamental functional unit in bone remodeling is the Bone Multicellular Unit (BMU), which includes osteoclasts and osteoblasts that coordinate bone resorption and formation.[11] Activated osteoclasts are responsible for bone resorption, they dissolve the mineralized matrix and degrade the organic components of the bone. During resorption, osteoclasts release growth factors and cytokines sequestered within the extracellular matrix. These signaling molecules stimulate the proliferation and differentiation of osteoprogenitor cells into mature osteoblasts, which subsequently synthesize new bone matrix. Pre-osteoblasts play a critical regulatory role by producing factors that influence osteoclast differentiation. Of particular importance is RANKL (receptor activator of nuclear factor-$\varkappa$B ligand), a cytokine secreted by pre-osteoblasts that binds to the RANK receptor on pre-osteoclasts, promoting their maturation into multinucleated, bone-resorbing osteoclasts. Conversely, osteoprotegerin (OPG), a soluble receptor produced in the bone microenvironment, binds to RANKL and inhibits its interaction with RANK, thereby preventing osteoclast differentiation.[12] The relative production of RANKL and OPG is dynamically regulated to meet the skeletal tissue's remodeling demands (Figure 1.2).

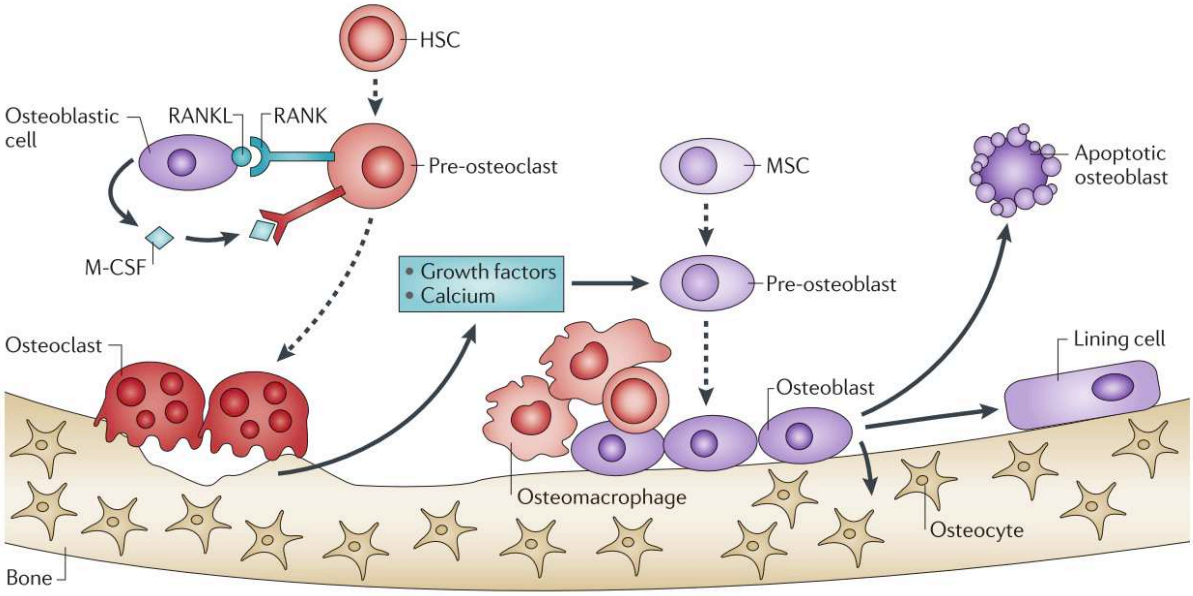


Figure 1.2 Schematic representation of bone remodeling process.[13]

This tightly controlled interplay between osteoclasts and osteoblasts ensures a balance wherein the volume of resorbed bone is matched by an equivalent amount of new bone formation. Disruption of this balance underlies the pathogenesis of various bone diseases. Peak bone mass is typically achieved by the end of the growth period, namely late adolescence. Attaining a high peak bone mass is crucial, as it correlates with greater skeletal strength and a reduced risk of bone fragility later in life when cellular activity naturally declines. Therefore, strategies to maximize peak bone mass during youth are essential for long-term skeletal health.[14], [15]

1.1.3 Advancing Bone Repair: Biomaterials in Bone Tissue Engineering

The increase in human life expectancy has led to a growing demand for effective bone interventions[16]. Autologous bone grafts remain the gold standard for treating bone defects due to their unique biological composition, which includes osteogenic cells, osteoinductive growth factors, and an osteoconductive matrix. These autografts are harvested from the patient's own bone, most commonly the iliac crest of the pelvis, and transplanted to the defect site. Despite their regenerative potential, autografts present several limitations, such as restricted graft volume, donor site morbidity, risk of injury, infection, and post-operative pain. Allogeneic bone tissue, obtained from cadaveric donors, represents an alternative graft source that addresses some limitations related to autograft availability and harvesting complications[5]. However,

allografts (as well as xenografts) tend to exhibit poor integration and vascularization within the host tissue and carry risks of immune rejection and pathogen transmission, which can compromise clinical outcomes[10]. Moreover, some defects are so extensive that most autografts alone cannot heal the lesion, often resulting in uncontrollable necrosis and resorption of the bone graft.[5] Critical bone defects are defined by bone lesions longer than twice the diameter of the long bone diaphysis. Critical-sized bone defects are defined as bone lesions longer than twice the diameter of the diaphysis of the affected long bone. These large defects continue to pose significant challenges in orthopedic surgery. They arise from various causes, including trauma, infection, tumors, and developmental abnormalities, which collectively increase the complexity of clinical management.[17]
The limitations of current techniques for reconstructing bone defects, alongside the ongoing development of new therapies, have contributed to the emergence of regenerative medicine as a dynamic research field in recent years. This interdisciplinary domain merges biological sciences with engineering approaches to create novel biological substitutes aimed at advancing human health. Central to regenerative medicine are three key components: biomaterials or scaffolds, cells, and bioactive molecules. Together, these elements work synergistically to repair damaged bone tissue. The rise of regenerative medicine stems from the urgent need to address previously untreatable bone injuries and diseases, thereby expanding the scope of available clinical treatment options.[16]
Within the broader field, bone tissue engineering has become one of the fastest-growing areas of research. It focuses on promoting bone repair and regeneration by integrating scaffolds, well-incorporated cells, and osteoinductive growth factors.[10] Designed to serve as alternatives to traditional bone grafts, tissue-engineered constructs must overcome the limitations of conventional grafting methods while preserving essential properties such as osteoconductivity, osteoinductivity, and osteogenicity.[5] Osteoinductivity refers to a biomaterial's ability to stimulate the differentiation of stem cells into osteoblastic lineages under the influence of the local microenvironment. Effective biomaterials bind and recruit cells critical to bone regeneration.[16] Notably, bone morphogenetic proteins (BMPs) and vascular endothelial growth factor (VEGF) have been identified as vital factors that promote osteoinduction within scaffolds.[10] Osteoconduction describes the capacity of a scaffold to support bone cell growth by providing a pathway for tissue integration and cell migration. This process heavily depends on interactions between bone tissue and biomaterials, mediated through cellular behaviors such as adhesion, proliferation, and migration. Brånemark first proposed bone integration as the direct connection between implanted scaffold materials and bone tissue[18]. Osteoblasts colonize the implant surface by depositing an extracellular matrix layer, which initiates

new bone formation. Osseointegration is considered the final stage in the healing process around implants and it can be enhanced by modifying prosthetic surfaces using chemical or physical treatments and by influencing bone metabolism surrounding the implant.[14], [19], [20] Biomaterials are a crucial element of bone tissue engineering, working together with cells and bioactive agents to promote bone repair and regeneration. Scaffolds made from biomaterials provide temporary mechanical support and mimic the extracellular matrix, creating a favorable environment for cells to attach, proliferate, and differentiate, which is essential for forming new bone tissue.[16], [17], [21]

Materials used in scaffolds generally fall into metals, ceramics, and polymers. Metals like titanium alloys are widely used for load-bearing implants due to their strength and elastic modulus similar to bone, though they often require surface modifications to enhance biological performance.[22] Magnesium alloys offer the added benefit of biodegradability but require careful control of corrosion.[23] Other metals used medically, such as stainless steel and cobalt-based alloys, pose significant challenges before clinical use due to corrosion-related toxic ion release. This can cause inflammation, allergic reactions, and tissue damage, ultimately reducing their biocompatibility.[1] Metal scaffolds typically require surface modification before implantation to enhance cell adhesion, proliferation, and the adsorption of essential biomolecules. A successful approach involves integrating cell-recognizable ligands and signaling growth factors onto the scaffold surface, thereby promoting cellular communication and organization.[17]

Bioceramics are widely used in bone tissue engineering due to their excellent biocompatibility, biodegradability, osteoconductivity, and osteoinductivity. Common examples include hydroxyapatite, β-tricalcium phosphate, biphasic calcium phosphate, and bioglass. These materials resemble natural bone minerals and support bone cell growth and new bone formation. Their porous, three-dimensional structures provide mechanical support while enabling nutrient flow and tissue integration, making them suitable for repairing large bone defects.[24]

Scaffold materials for bone repair continue to be an area of intense research, with particular emphasis on both processed organic polymers and synthetic polymers. Among the organic options, collagen stands out as it is the primary component of the native bone extracellular matrix. Clinically, collagen-based scaffolds are widely utilized due to their inherent bioactivity. Their natural binding sites facilitate interactions with cells and extracellular proteins, enriching cell adhesion and proliferation. This characteristic offers a distinct clinical advantage over synthetic polymers, which are relatively inert and lack such bioactive motifs.[25] Degradable synthetic polymers attract substantial interest for bone graft

development as well. This interest is largely attributable to their tunable mechanical properties and the ease with which they can be fabricated into robust, complex structures. Notably, scaffolds made from polylactic acid (PLA) and poly(lactic-co-glycolic acid) (PLGA) have received regulatory approval as bone void fillers and autograft extenders, underscoring their clinical relevance.[5] In recent years, silicon and silicate-containing materials have garnered significant attention in bone tissue engineering, primarily due to their influence on osteogenesis at the molecular level. Silicon, the eighth most abundant element in the universe, typically exists in the form of oxides and silicates due to its high affinity for oxygen. These silicon compounds are recognized as essential micronutrients, playing critical roles in various biological processes, including the regulation of bone metabolism.[26], [27] Increasing evidence from both in vitro and in vivo investigations demonstrates that silicon positively affects bone structure and function, and participates in bone metabolism alongside calcium. Accumulating data indicate that silicon can stimulate bone formation. For instance, Gao et al. showed that silicon-containing scaffolds can upregulate the expression of key osteogenic genes, including bone morphogenetic protein 2 (BMP-2), collagen type I, and runt-related transcription factor 2 (Runx2). These findings collectively suggest that Si-based scaffolds hold significant promise for advancing the repair of large bone defects.[28]

1.2 Stem cells

Stem cells are undifferentiated cells characterized by their remarkable capacity for self-renewal and their potential to differentiate into specialized mature cells. Based on their differentiation potential, stem cells are classified into distinct categories:

- Totipotent stem cells have the highest differentiation potential. They can give rise to all embryonic cell types, including the three germ layers (ectoderm, mesoderm, and endoderm) as well as extra-embryonic structures such as the placenta. Totipotency is typically observed during the earliest stages of embryogenesis.
- Pluripotent stem cells (PSCs) originate from the inner cell mass of the blastocyst and have the capacity to differentiate into any cell type derived from the three primary germ layers; however, they lack the ability to generate extra-embryonic tissues. Induced pluripotent stem cells (iPSCs) are a type of pluripotent stem cell created in laboratory by reprogramming adult somatic cells. The initial generation of mouse iPSCs was achieved through the introduction of four critical

transcription factors (c-Myc, Oct3/4, Sox2, and Klf4) via retroviral vectors.[29] More recent studies have revealed that mouse embryonic fibroblasts can also be reprogrammed into iPSCs using specific combinations of chemical agents, providing innovative, non-viral approaches for cellular reprogramming.[29]

- Multipotent stem cells exhibit a more restricted differentiation capacity, limited to cell types within a particular germ layer or lineage. Mesenchymal stem cells (MSCs), for example, are multipotent cells capable of differentiating into mesodermal derivatives such as adipocytes, osteoblasts, and chondrocytes.[30]
- Unipotent stem cells have the most limited differentiation ability, being capable of producing only one specific cell type. Despite this restricted potency, they retain the capacity for extensive self-renewal, which is essential for their therapeutic potential in regenerative medicine.[31]

The differentiation of stem cells is governed by a complex interplay of signals. These include external cues, such as physical interactions with neighboring cells and chemical factors secreted by the surrounding microenvironment, and internal mechanisms, primarily regulated by genetic and epigenetic factors. Stem cell behavior and proliferative activity vary significantly depending on the tissue microenvironment. For instance, bone marrow stem cells continuously divide to maintain hematopoiesis, whereas in tissues like the pancreas, stem cell division is triggered predominantly under specific physiological conditions.

1.2.1 Mesenchymal Stem Cells (MSCs)

Somatic or adult stem cells are undifferentiated cells that persist within differentiated tissues throughout an organism's life. Their primary role involves tissue maintenance, repair, and regeneration by replacing cells lost due to injury, disease, or normal turnover. Adult stem cells typically demonstrate a limited differentiation spectrum compared to embryonic stem cells. Within the bone marrow niche, MSCs predominantly differentiate into cells of mesodermal origin, contributing to the formation of bone, cartilage, and adipose tissue (Figure 1.3).[32]

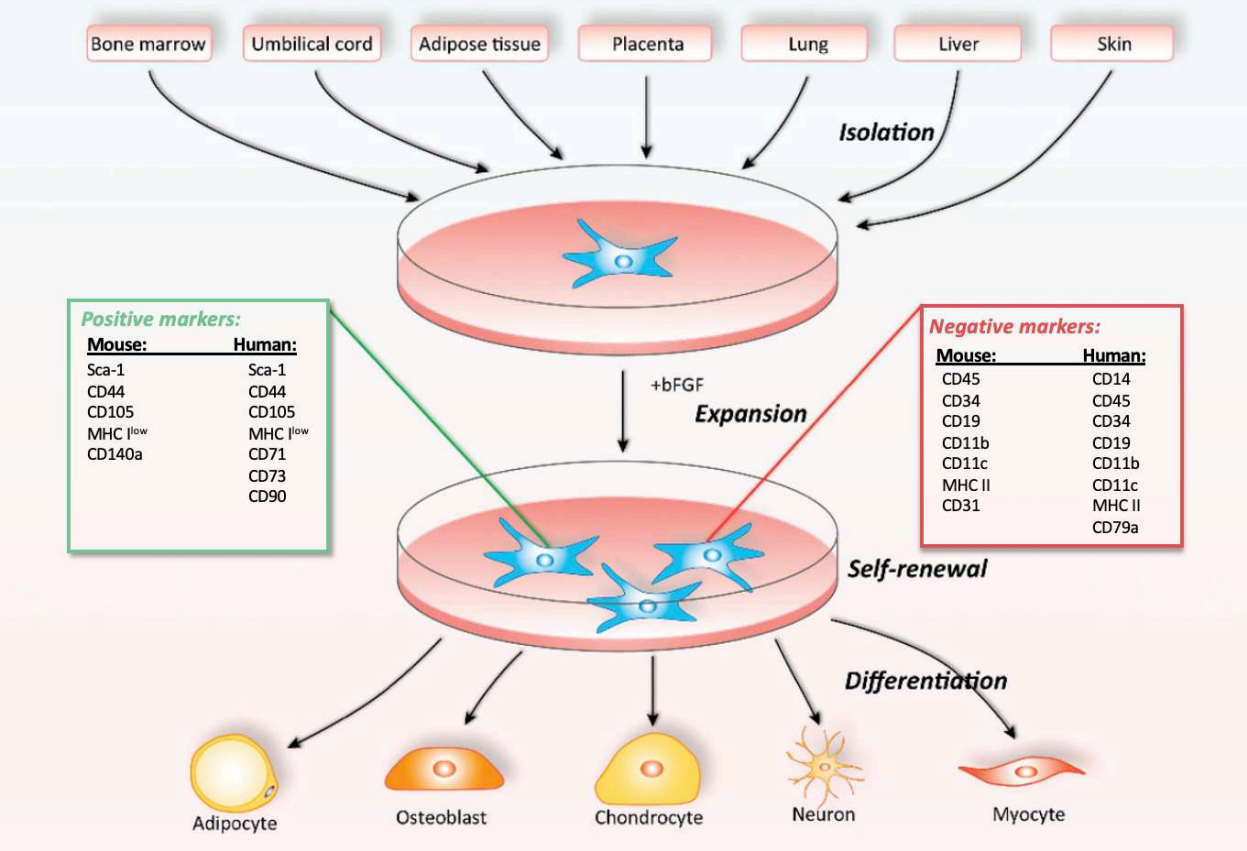


Figure 1.3. Differentiation potential of MSCs.[33]

MSCs are a population of non-hematopoietic stem cells characterized by their fusiform-shaped morphology and plastic-adherent properties.[31] First identified in the late 1960s originating from bone marrow, MSCs have since been isolated from a variety of tissues, including bone marrow, adipose tissue, umbilical cord blood, placenta, and others.[34] These cells exhibit remarkable multipotency, with the ability to differentiate into diverse phenotypes such as osteocytes, chondrocytes, adipocytes, fibroblasts, among others.[35]

The International Society for Cellular Therapy (ISCT) has proposed revised minimal criteria for the definition of human mesenchymal stromal cells (MSCs).[36] Accordingly, MSCs must:

- Express specific surface markers including CD73, CD90 and CD105
- Lack expression of other tissue-relevant markers such as CD45
- Demonstrate stemness and the capacity to differentiate into multiple mesodermal lineages in vitro

A key functional characteristic of MSCs is their inherent tropism toward sites of tissue injury, enabling them to migrate spontaneously to damaged areas where they can exert regenerative effects.[37] The therapeutic potential of MSCs largely stems from their paracrine activity, through which they secrete a variety of cytokines, soluble factors, and extracellular vesicles that modulate inflammation and promote tissue repair.[38]

From an immunological perspective, MSCs display low levels of major histocompatibility complex (MHC) class I molecules and lack expression of MHC class II. This profile confers a degree of immune privilege, allowing MSCs to evade immune detection. Consequently, they can survive longer after transplantation, which contributes to improved therapeutic outcomes by minimizing the risk of host immune-mediated rejection.[39]

MSCs have emerged as a promising alternative to conventional pharmaceutical treatments, owing to several advantages. Furthermore, they can be isolated easily and rapidly and expanded efficiently in vitro. Their selective migration to injured tissues, combined with low immunogenicity and a favorable safety profile that avoids ethical concerns, makes them highly attractive for regenerative medicine applications.[40]

Today MSCs are considered as one of the most promising cell types for cell therapy given their unique capacities for self-renewal and multipotent differentiation. Numerous studies have demonstrated their potential in regenerative medicine and tissue engineering, establishing MSC transplantation as a viable strategy for repairing damaged tissues.[41]

However, several challenges limit the clinical translation of MSCs. Among these, their relatively low proliferative capacity in vitro restricts large-scale expansion. Moreover, the proliferative and differentiation potential of MSCs declines with increasing donor age and passage number during culture, largely due to cellular senescence which impairs their functional properties.[40],[42]. Autologous MSC therapy is further limited by challenges such as the difficulty in harvesting sufficient healthy cells from patients suffering from systemic illnesses, as well as the prolonged time required for cell isolation and expansion, which restricts their timely use in emergency or critical conditions. Additionally, there are ongoing concerns about the longevity of MSCs after transplantation and the potential for unwanted or abnormal differentiation.[43]

Bone marrow-derived mesenchymal stem cells (BMSCs)

Bone marrow-derived mesenchymal stem cells (BMSCs) are non-hematopoietic stem cells located within the medullary stroma of bone marrow. Initially identified by Friedenstein et al. in 1976 as clonogenic fibroblast precursor cells, BMSCs have since been extensively characterized for their regenerative potential.[44] According to the International Society for Cellular Therapy (ISCT), bone marrow-derived mesenchymal stem cells (BMSCs) must fulfill several defining characteristics to ensure accurate identification and standardization across studies. These criteria include the capacity of the cells to adhere to plastic surfaces under conventional in vitro culture conditions. Additionally, the surface antigen profile requires that over 95% of the cell population express the mesenchymal markers CD73, CD90, and CD105, while simultaneously lacking expression of hematopoietic and endothelial markers such as CD14 or CD11b, CD79a or CD19, CD34, CD45, and human leukocyte antigen (HLA)-DR in more than 95% of the cells. Finally, BMSCs must demonstrate multipotency by differentiating in vitro into various mesenchymal lineages, including osteoblasts, adipocytes, chondroblasts, as well as neural and myogenic cells when subjected to appropriate differentiation conditions.[37]

While these foundational markers are critical for BMSC identification, additional stemness markers have been proposed to more comprehensively characterize their self-renewal ability, support of hematopoiesis, and multilineage differentiation potential. Such markers include STRO-1, CD146, CD106, platelet-derived growth factor receptor (PDGF-R), epidermal growth factor receptor (EGF-R), insulin-like growth factor receptor (IGF-R), integrins CD49a/CD29, nerve growth factor receptor (NGF-R), CD271, and CD44. These markers help refine the isolation and functional understanding of BMSC populations.[45] Beyond their classical differentiation into bone, cartilage, and adipose tissues, BMSCs have demonstrated the capacity to differentiate into tendon, myogenic, and neural lineages in vitro, and in certain contexts, in vivo, responding adaptively to environmental cues.[46] BMSCs demonstrate a range of advantageous properties that underlie their therapeutic promise in regenerative medicine. Their intrinsic multipotency enables differentiation into diverse cell types, while their immunomodulatory and anti-inflammatory properties contribute to a supportive healing environment. Moreover, BMSCs facilitate hematopoiesis and promote angiogenesis. Through the secretion of paracrine factors, BMSCs modulate the local microenvironment, a feature critically important for tissue repair and organ regeneration.[30] Due to these therapeutically desirable properties, BMSCs have been utilized and investigated in treating various diseases, including cardiac,

lung, neural, hematopoietic, graft-versus-host disease, and tendon, ligament, and musculoskeletal tissue repair[47].

Over the past decade, substantial progress has been made in elucidating the role of BMSCs in skeletal regeneration. While much of this knowledge stems from pre-clinical studies, several clinical trials have also explored BMSC-based therapies combined with ceramic, biodegradable synthetic, or matrix scaffolds for musculoskeletal tissue engineering. The growing clinical evidence underscores the translational potential of BMSC therapies in bone regeneration and repair.[47] Due to these compelling therapeutic advantages, BMSCs represent a highly promising cell source for regenerative approaches targeting bone defects.

1.2.2 Regenerative effects of MSCs-secreted paracrine factors

The mesenchymal stem cell secretome consists of a diverse collection of bioactive molecules released into the extracellular environment, encompassing a wide range of soluble molecules as well as different classes of extracellular vesicles (EVs). These EVs, which include membrane-enclosed entities such as exosomes and microvesicles, work synergistically with the soluble factors to mediate most MSCs' therapeutic properties, particularly their roles in tissue repair and immune regulation.[48]

Among the soluble molecules secreted by MSCs, a wide variety of growth factors (GFs) and cytokines are essential regulators of tissue repair mechanisms. Growth factors hold a central role in bone tissue engineering by directly interacting with bone progenitor cells through receptor binding, initiating intracellular signaling pathways that drive the differentiation and formation of new bone tissue. The concept of osteoinductive growth factors was first demonstrated by Levander et al., who first demonstrated ectopic bone formation by injecting bone extracts into muscle tissue.[16] Since then, several key growth factors have been identified and applied in the repair of bone defects. These include bone morphogenetic proteins (BMPs), fibroblast growth factor-2 (FGF-2), vascular endothelial growth factor (VEGF), growth differentiation factor 5 (GDF5), and transforming growth factor beta 1 (TGF-β1).

BMP-2, a member of the transforming growth factor-β superfamily, is well-known for its ability to induce osteoblastic differentiation in vitro and promote bone formation in vivo, while also enhancing angiogenesis within the defect site. Its efficacy and safety have been recognized with approval from regulatory agencies such as the FDA for clinical use as an osteoinductive agent.[49] Similarly, fibroblast growth factor-2 (FGF-2), a basic fibroblast growth factor belonging to the FGF-1 subfamily, plays a

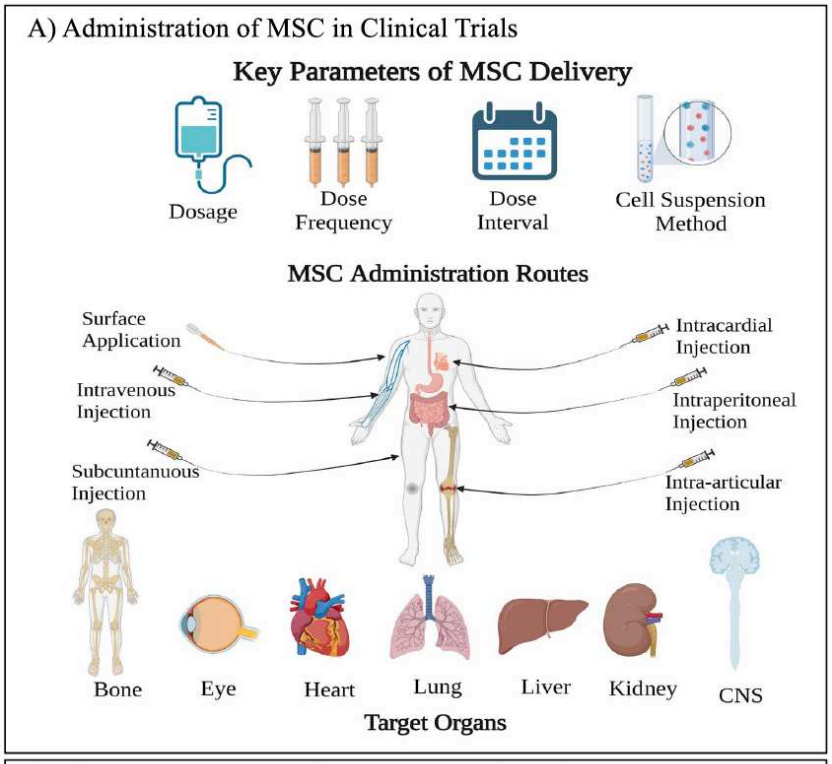
multifaceted role in bone regeneration by supporting osteoblast proliferation, differentiation, and vascular development, as well as mediating intracellular signaling pathways in bone progenitor cells. Interestingly, FGF-2 exhibits dose-dependent activity, whereby low concentrations enhance bone formation, whereas higher doses may inhibit osteogenesis. Vascular endothelial growth factor (VEGF), although primarily recognized for its pro-angiogenic properties, also contributes to bone regeneration by promoting the differentiation of mesenchymal stem cells (MSCs) into osteoblasts and suppressing their adipogenic differentiation. This dual function of osteoblast-derived VEGF is critical for maintaining bone homeostasis by balancing bone formation and fat cell development.[10] Growth differentiation factor 5 (GDF5) extends its influence beyond bone by promoting differentiation into cartilage, tendon, and ligament lineages, with numerous preclinical studies highlighting its positive effects on both bone formation and soft tissue repair. Furthermore, transforming growth factor beta 1 (TGF-β1) works synergistically with insulin-like growth factor-1 (IGF-1) to orchestrate bone remodeling processes. TGF-β1 facilitates the recruitment of bone marrow-derived mesenchymal stem cells (BMSCs) to sites of injury by regulating osteoclastogenesis, while IGF-1 enhances the differentiation of BMSCs into osteoblasts, collectively fostering new bone formation.[16]

1.2.3 Clinical Applications and Therapeutic Relevance of MSCs

Mesenchymal stem cells (MSCs) are multipotent stromal cells originally discovered within bone marrow stroma in the late 1960s by Friedenstein and colleagues. Their properties and nomenclature were later refined by Arnold Caplan. MSCs exhibit multipotency, defined by the well-characterized ability to differentiate into osteogenic, adipogenic, and chondrogenic lineages.[50], [51] They are now recognized as being ubiquitously present across various tissues and are notably responsive to cues from sites of tissue injury, making them essential to endogenous tissue repair and regeneration mechanisms.[52] MSCs can be isolated from a variety of sources including bone marrow, adipose tissue, synovium, umbilical cord blood, placenta, and dental pulp. The source of MSCs impacts their biological characteristics: bone marrow-derived MSCs are the most extensively researched and clinically utilized due to robust harvesting methodologies and scalability, whereas MSCs from umbilical cord blood show enhanced proliferative abilities, lower senescence rates, and pronounced anti-inflammatory properties.[53] Phenotypically, MSCs are often associated with perivascular regions and express surface markers such as CD10, CD13, CD44, CD73, CD90, CD105 and CD146. Rather than primarily relying on direct differentiation in vivo, their main therapeutic activity is attributed to

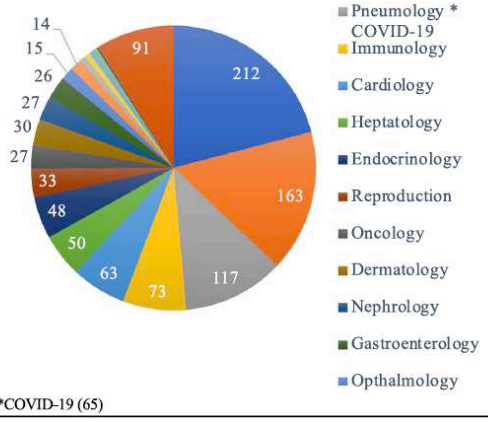
the secretion of immunomodulatory and trophic factors.[54], [55], [56]
The clinical benefits of MSCs lies in their broad capacity for tissue regeneration and immune modulation. Their secretome contains a diverse array of bioactive compounds such as cytokines, growth factors, chemokines, microRNAs, and extracellular vesicles, which coordinate vital processes such as immune regulation, inhibition of apoptosis and fibrosis, promotion of angiogenesis, tissue remodeling, and acceleration of wound repair.[57] MSCs exert immunomodulatory effects by suppressing the proliferation of both CD4+ and CD8+ T cells, facilitating the induction and expansion of regulatory T cells (Tregs), guiding macrophage polarization toward the anti-inflammatory M2 phenotype, and suppressing B cell, natural killer (NK) cell, and dendritic cell activity.[58], [59], [60] MSCs are able to modify their behavior based on the inflammatory conditions of their environment, which enables them to tailor their actions to the specific disease context. Additionally, they can actively migrate toward sites of tissue injury in response to chemical signals released during damage, further increasing their usefulness for clinical applications.[61]
Worldwide, over 1,700 clinical trials have been registered to investigate MSC therapies for a broad spectrum of degenerative, immune-mediated, and inflammatory disorders. (Figure 1.4).[62], [63] In neurological disorders, MSCs have demonstrated substantial therapeutic potential. For example, in multiple sclerosis (MS), a condition characterized by demyelination and chronic inflammation within the central nervous system, MSCs have exhibited capacity to suppress pro-inflammatory T helper cell populations, reduce proliferation of lymphocytes, and secrete anti-inflammatory mediators. Clinical studies administering MSCs, such as intrathecal delivery in progressive MS, have reported stabilization or modest improvements in disability and biomarker profiles indicative of neuronal preservation.[64], [65], [66], [67] Similarly, in amyotrophic lateral sclerosis (ALS), infusions of autologous bone marrow-derived MSCs have slowed progression and preserved respiratory function without serious side effects.[68] In Parkinson's disease (PD), preclinical animal studies have shown that MSCs grafts are capable of surviving, integrating into host brain tissue, and differentiating toward dopaminergic neuron-like phenotypes. These actions have resulted in significant improvements in motor function and neuroprotection of dopaminergic neurons, indicating a potential to modulate disease progression in experimental models.[69] Supporting these findings, clinical evidence also support the therapeutic potential of MSCs in Parkinsonian disorders. A phase I randomized controlled trial conducted on patients with progressive supranuclear palsy, which shares features with Parkinson's disease, found that intra-arterial delivery of autologous bone marrow-derived MSCs was well tolerated and associated with a slowing of disease progression.[70] Comparable positive effects have been demonstrated in

experimental stroke models, where MSCs and their extracellular vesicles promote angiogenesis, support neurogenesis, and enhance functional recovery. Several clinical trials are currently underway to evaluate these therapeutic benefits.[53], [71]



B) Clinical trials classified by medical specialty-disease category

Medical specialty	Number of CT
Musculoskeletal	212
Neurology	163
Pneumology *	117
Immunology	73
Cardiology	63
Heptatology	50
Endocrinology	48
Reproduction	33
Oncology	27
Dermatology	30
Nephrology	27
Gastroenterology	26
Opthalmology	15
Anal Disorders	14
Aging	7
Urology	6
Hematology	6
Psychiatry	4
HIV	2
Other	91
Total	1014



*COVID-19 (65)

Figure 1.4. Overview of the administration routes and targeted diseases for MSC-based clinical trials (as of July 14, 2021). Targeted diseases included musculoskeletal, neurological, pulmonary (notably COVID-19), cardiovascular, and immune disorders.[63]

Bone and cartilage regeneration represent key therapeutic targets for MSCs. Traditional autologous bone grafting, although widely used, is limited by issues such as donor site morbidity and inconsistent clinical results. In contrast, MSC-based therapies offer a promising regenerative alternative with the potential to improve healing outcomes.[72], [73], [74] Clinical studies involving implantation of autologous bone marrow-derived MSCs have reported enhanced fracture healing, pain reduction, and a favorable safety profile.[61] In patients with osteoarthritis (OA), particularly those with knee involvement, intra-articular or subchondral administration of both autologous and allogeneic bone marrow MSCs has led to significant improvements in pain relief, joint stiffness, overall function, and quality of life, alongside decreases in biomarkers indicative of cartilage degradation and reduction of synovial inflammation.[75], [76], [77], [78], [79] Additionally, MSCs derived from adipose tissue and synovium exhibit strong chondrogenic differentiation capacity and high proliferative potential, which are advantageous for musculoskeletal tissue repair. Furthermore, combining MSC treatment with biomaterial scaffolds or platelet-rich plasma has been shown to further augment clinical benefits.[80], [81], [82]

Mesenchymal stem cells enhance wound healing by actively engaging in and regulating all stages of the repair process. They migrate to injured tissues, reduce excessive inflammation, and promote the growth and proliferation of native keratinocytes, fibroblasts, and endothelial cells. Additionally, MSCs facilitate new blood vessel formation and extracellular matrix production, which are critical for tissue regeneration. Clinical studies employing both autologous bone marrow-derived and adipose-derived MSCs have demonstrated effective treatment outcomes in chronic wounds and diabetic foot ulcers, characterized by accelerated healing and a low incidence of adverse effects.[83] Emerging indications for MSC therapy include a variety of organ diseases. In liver pathologies such as acute-on-chronic injury and primary biliary cirrhosis, MSCs have produced reductions in hepatic enzyme levels, improved hepatic function, and enhanced survival in clinical research.[84] For renal diseases, particularly chronic kidney disease and polycystic kidney disease, MSCs and their secreted extracellular vesicles have shown antioxidative, anti-apoptotic, and anti-inflammatory activities, sometimes improving renal function in early-stage clinical evaluations.[85], [86] Cardiac models demonstrate that MSCs can transdifferentiate toward cardiomyocyte-like cells and aid in cardiac repair post-myocardial infarction via improved ejection fraction and reduced fibrotic scarring.[87]

Mesenchymal stem cell therapies have generally demonstrated favorable safety profiles, with only mild and temporary side effects such as low-grade fever or localized discomfort at the injection site reported in numerous clinical studies. Both autologous and allogeneic MSCs exhibit comparable safety and efficacy, although allogeneic cells present an advantage by enabling off-the-shelf, scalable treatment options. Despite these positive aspects, several obstacles remain, including intrinsic heterogeneity among MSC populations, variability dependent on the donor source, limited capacity for cell expansion, and a decline in functional properties during prolonged in vitro culture.[61], [62] These issues similarly affect MSC-derived extracellular vesicle products, which often experience inconsistencies in potency due to variability between production batches.[88] Therefore, it is crucial to establish standardized assays to accurately assess the potency of MSC therapies, along with uniform manufacturing procedures. Regulatory agencies highlight the importance of these standards to ensure that MSC-based treatments are consistently safe and effective for patients.

The inherent multipotency, immune-regulating properties, and paracrine functions of mesenchymal stem cells position them as a highly valuable tool in the field of regenerative medicine. Their therapeutic applications extend across a variety of disorders, including neurological and musculoskeletal diseases, chronic wounds, and the regeneration of vital organs. Ongoing research aims to improve MSCs effectiveness through genetic modification, preconditioning, and leveraging their secretome and extracellular vesicles while addressing challenges of heterogeneity, delivery, and regulatory standardization. As advancements continue in these domains, MSC-based therapies hold great promise to transform personalized regenerative treatments, offering new hope for numerous conditions that are currently difficult to treat.

1.3 Signaling Pathways controlling osteogenic Differentiation

Osteoblasts, which are the cells responsible for forming bone, develop through several specific stages in their lineage. This progression begins with mesenchymal progenitor cells, continues as these cells become pre-osteoblasts, then mature into fully functional osteoblasts. Eventually, some osteoblasts transform into osteocytes, which are embedded in the bone matrix, while others become bone-lining cells that cover the bone surface. The origin and classification of progenitor cells vary by developmental stage and bone environment, causing some debate. Skeletal stem and progenitor cells (SSPCs) are immature precursors in bone that can become bone-forming cells. This group includes

cartilage stem cells from growth plates, fetal perichondral cells involved in bone formation, periosteal progenitors important for fracture repair, and various bone marrow stromal cell subtypes with multiple differentiation potentials.[89] During skeletal development, osteoblasts are formed through two main processes: intramembranous ossification and endochondral ossification. Intramembranous ossification occurs mainly in flat bones, such as those in the skull, where mesenchymal stem cells directly turn into osteoblasts. In contrast, endochondral ossification is the process responsible for forming most other bones, including long bones. In this process, mesenchymal cells first become chondrocytes, creating a cartilage template. This cartilage is then gradually replaced by bone tissue. The tissue surrounding this cartilage, called the perichondrium, provides early osteoblast cells that help form bone structures like the periosteum.[11], [90]

Osteogenesis is regulated by a variety of signaling mechanisms that can be broadly classified into canonical and non-canonical pathways (Figure 1.5). These signaling networks coordinate the commitment of mesenchymal stem cells to the osteoblast lineage and control their progression through differentiation. Together, canonical and non-canonical pathways influence key cellular processes such as proliferation, maturation, survival, and the response to mechanical and environmental stimuli, ensuring proper bone formation and maintenance.[89] Wnt signaling plays a central role in regulating bone formation by controlling the proliferation, differentiation, and fate determination of MSCs into osteoblasts.[91] Activation of Wnt receptors, particularly the co-receptors LRP5 and LRP6, initiates the canonical Wnt/β-catenin pathway. This signaling cascade leads to the stabilization and accumulation of β-catenin in the cytoplasm, allowing its translocation into the nucleus where it activates transcription of genes important for osteogenic differentiation. Through this process, Wnt signaling not only enhances the expression of bone-forming genes but also suppresses alternative cell fates such as adipogenesis, thus ensuring MSCs preferentially become osteoblasts.[92] Various Wnt ligands engage this signaling network, with some activating the canonical pathway and others triggering non-canonical routes that also contribute to bone development. The pathway's activity is precisely modulated by several inhibitors, including sclerostin, a protein primarily secreted by osteocytes.[93]

Members of the TGF-β superfamily, including transforming growth factor-beta (TGF-β) and bone morphogenetic proteins (BMPs), are essential regulators of osteoblast differentiation.[94] Their signaling occurs mainly through two pathways, one that relies on Smad proteins and another that functions independently of them. The Smad-dependent pathway involves different types of Smads:

receptor-regulated Smads (R-Smads), which are activated by either BMPs (Smad1, Smad5, Smad8) or TGF-β (Smad2, Smad3); co-Smads like Smad4 that partner with R-Smads; and inhibitory Smads (Smad6, Smad7) that serve to suppress the signaling. Once activated, the R-Smad/co-Smad complexes translocate to the nucleus, where they regulate the expression osteoblastic genes. Beyond Smad pathways, BMPs, particularly BMP2, also influence osteoblast differentiation via alternative signaling pathways. For example, BMP2 activates the mitogen-activated protein kinase (MAPK) pathway to increase expression of markers such as alkaline phosphatase (ALP) and osteocalcin (OCN).[89] Through activation of DLX5 via the p38 MAPK pathway, BMP2 further facilitates the expression of Runx2 as well as Osterix (Osx), both critical transcription factors required for osteoblast development.[89], [90], [95]

The YAP/TAZ complex, key downstream effectors of the Hippo signaling pathway, functions primarily as transcriptional co-activators through interactions with partners such as TEAD family members.[96] YAP and TAZ critically regulate multiple stages of osteoblast lineage progression. Early in differentiation, YAP/TAZ promote mesenchymal stem cell commitment toward osteoblasts while inhibiting differentiation into adipocytes and chondrocytes. This process is modulated by extracellular matrix remodeling, cell-cell interactions, and mechanical forces.[97] YAP/TAZ also interact with other signaling pathways, notably forming complexes with β-catenin in the canonical Wnt pathway and cooperating with Smad proteins of the TGF-β/BMP pathways.[98] After BMP stimulation, YAP binds Smad1/5 to induce osteogenic target genes, while TAZ enhances BMP4 expression, facilitating osteoblast differentiation.[99] TAZ additionally acts as a coactivator of Runx2, the master regulator of osteoblastogenesis.[100] Growth factors such as FGF-2 stimulate TAZ expression and nuclear translocation via ERK signaling, further promoting osteoblast differentiation.[101] In mature osteocytes, YAP/TAZ regulate peri-lacunar/canalicular remodeling, essential for bone quality and mechanical integrity, and mediate responses to mechanical loading. Conditional deletion of YAP/TAZ in osteocytes impairs bone mass, collagen organization, and matrix remodeling by disrupting TGF-β-induced expression of matrix metalloproteinases.[102] YAP and TAZ act as key regulators that integrate both mechanical signals and molecular pathways to orchestrate the progression of osteoblast lineage commitment and maintain overall bone homeostasis.

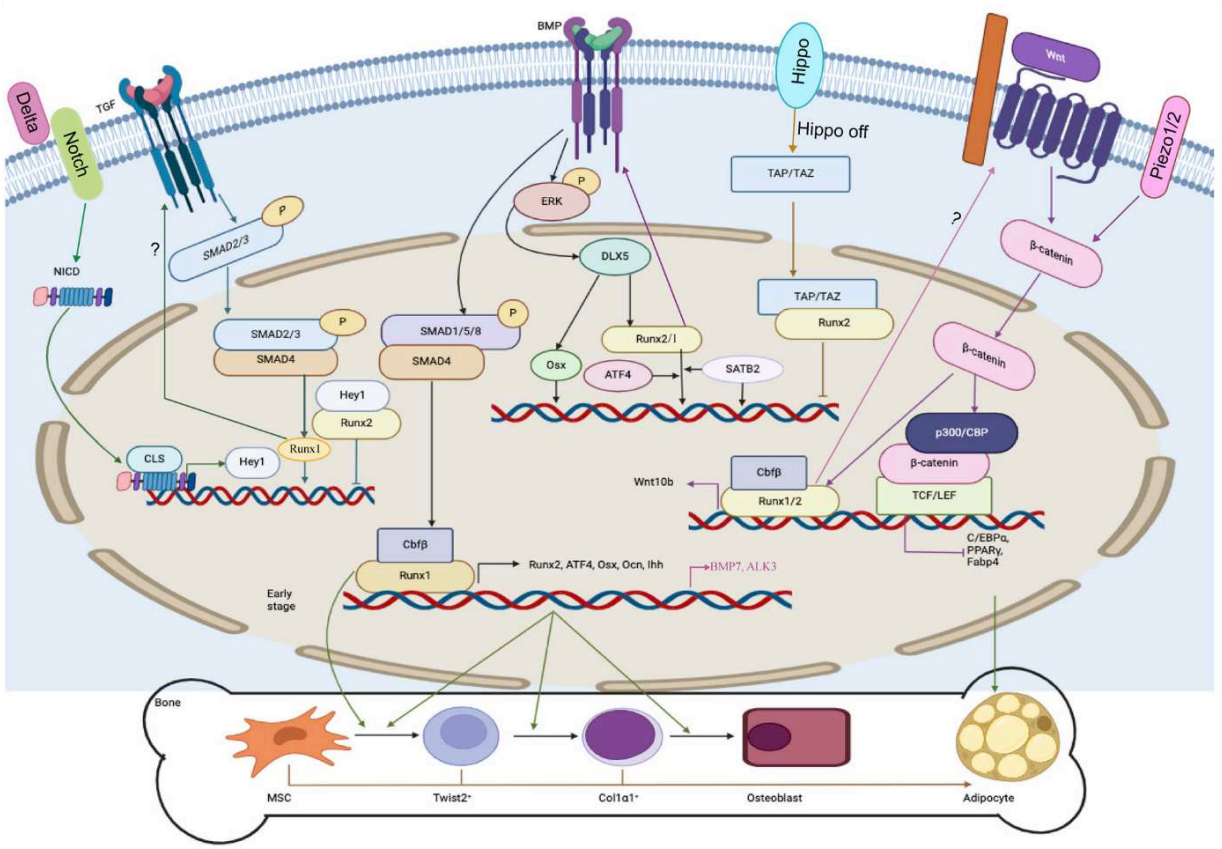


Figure 1.5. Signaling and transcriptional regulation of osteoblast cell lineage, commitment and differentiation.[89]

The osteoblast lineage arises from multipotent mesenchymal stem cells, progressing through several well-defined stages before giving rise to osteocytes, the most abundant cells in mature bone. MSCs, located within bone marrow and periosteum, possess self-renewal capacity and the potential to differentiate into osteoprogenitor cells under osteogenic stimuli. Osteoprogenitors lose their multipotency but retain high proliferative ability and begin expressing proteins such as type I collagen and alkaline phosphatase, which mark their commitment to the osteoblastic lineage. These progenitors develop into preosteoblasts, an intermediate cell type marked by strong proliferative potential and the expression of osteogenic markers including RUNX2, Osterix (SP7), type I collagen, and ALP. Morphologically, preosteoblasts reside between the more primitive fibroblastic progenitors and mature osteoblasts at sites of bone growth. Mature osteoblasts are polarized, cuboidal cells found at bone-forming surfaces. Characterized by abundant protein synthesis, mature osteoblasts secrete large quantities of type I collagen and other specialized proteins, such as osteocalcin, osteopontin, and bone sialoprotein, to form and mineralize

the bone matrix. After completing bone deposition, these osteoblasts either undergo apoptosis, become quiescent bone-lining cells that protect bone surfaces, or differentiate into osteocytes. Osteocytes, which account for roughly 95% of all bone cells, are former osteoblasts that become embedded within the mineralized matrix. These cells develop extensive networks with each other and with cells on the bone surface, acting as essential regulators of bone remodeling by responding to mechanical and hormonal signals, in part through the secretion of sclerostin.[89], [93], [103] The interplay between osteoblasts, osteocytes, and bone-lining cells forms a vital regulatory system that preserves bone integrity by coordinating bone deposition and resorption.

Chapter 2

Surface Modification Strategies for Biomaterial Functionalization

Mammalian cells in their natural environments continuously sense and respond to a wide range of external signals, including chemical, topographical, and mechanical cues, which regulate essential cellular activities such as proliferation, migration, differentiation, and apoptosis.[104] Recent advancements in materials engineering have facilitated the design of sophisticated in vitro models that replicate biochemical and biophysical signals with spatiotemporal complexity, enabling detailed investigations into how cells perceive and adapt to dynamic microenvironments. These models reveal how cells adapt to changes in their surroundings as conditions vary over time and space.[105], [106]

Surface modification of biomaterials plays a critical role in directing cellular behavior by precisely tuning the cell-material interface, where essential biological interactions occur. This targeted manipulation is particularly beneficial in tissue engineering contexts, providing cells with the necessary cues and support during early phases of tissue formation. Importantly, surface modifications can enhance the bioactivity of materials without compromising their bulk mechanical integrity, thereby preserving the fundamental structural properties of the scaffold or implant.

2.1 Influence of Surface Properties on Cell Behavior

Cellular interactions with biomaterials are primarily determined by surface characteristics. The nature of the biomaterial's surface, along with the types of bioactive agents and biomolecules used for functionalization, influences its performance once implanted in living tissues. Advanced surface coating technologies that incorporate bioactive molecules are widely employed to better replicate the

native tissue microenvironment, thereby enhancing the biological response to implants.[107] Several parameters must be carefully considered in the biomaterial design process, including surface chemistry, topography, chemical composition, wettability, mechanical stiffness and porosity. By systematically modifying surface properties such as surface charge, functional group composition, and micro- to nanoscale topography, initial cell attachment can be precisely controlled, enabling detailed studies of cell-material interactions.[108]

The surface chemistry of a biomaterial, especially the specific functional groups it presents, plays a decisive role in regulating cell–material interactions. Surface chemistry influences key factors such as wettability and surface charge, which in turn regulate cellular adhesion, morphology, proliferation, and differentiation. Studies employing self-assembled monolayers (SAMs) functionalized with different groups, including methyl, amino, carboxyl, and hydroxyl, have shown that each chemical modification can elicit distinct cellular behaviors.[107] For example, surfaces bearing amino ($-NH_2$) groups have been found to significantly enhance the attachment, proliferation, and osteocyte-like differentiation of human dental pulp stem cells, indicating their promise for improving osseointegration and biocompatibility in dental implants (Figure 2.1).[109] In contrast, neural stem cells cultured on surfaces modified with methyl ($-CH_3$) groups exhibited activation of genes associated with cell death, whereas those on amino-modified surfaces upregulated genes related to cell adhesion and axonal growth.[110]

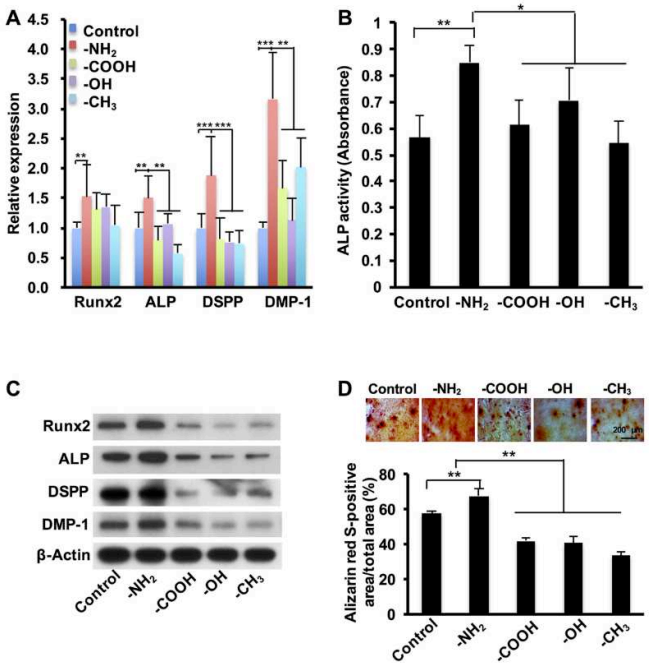


Figure 2.1. Effects of chemical functional groups on hDPSCs differentiation. (A) Expression levels of osteogenic-related genes. (B) Alkaline phosphatase (ALP) activity measured at day 7. (C) Western blot analysis of osteo/odontogenic marker proteins at day 7. (D) Alizarin Red staining showing mineralized matrix deposition at day 21.

Cells are highly responsive to the physical topography of a biomaterial's surface. The micro- and nanoscale architecture of the interface can guide cellular behaviors such as orientation, proliferation, cytoskeletal arrangement, and gene expression.[111], [112] Progress in nanofabrication and microfabrication techniques, including photolithography, electron beam lithography, electrospinning, and chemical etching, has made it possible to create precisely engineered surface patterns. Surface patterns can be broadly categorized into two types based on their orientation. Anisotropic patterns have a defined direction, such as grooves or ridges that are aligned uniformly, which can influence cells to grow or move along that specific direction. In contrast, isotropic patterns lack a preferred orientation and consist of features like evenly or randomly distributed pillars, pits, or protrusions. These non-directional patterns affect cell behavior differently by providing uniform cues from all directions.[113] Micropatterned surfaces often influence cell positioning and cytoskeletal organization, while nanopatterning tends to enhance protein adsorption, cell migration, and proliferation.[111], [114], [115], [116], [117], [118] One of the most important characteristics of surface topography is roughness, which describes the texture of the surface. Different cell types show preferences for specific roughness profiles. For example, osteoblasts tend to favor rough surfaces, while epithelial cells prefer smoother textures.[119] Surface roughness can be engineered through various techniques including plasma treatments, 3D printing, acid or ion etching, and electrospinning. These modifications have been demonstrated to influence not only cell attachment but also gene expression relevant to osteogenic differentiation.[120], [121] Additionally, hierarchical structures combining micro- and nanoscale features have been identified as particularly effective in enhancing bioactivity and accelerating tissue regeneration.[122], [123]

Surface charge is another key factor affecting cell-material interactions, mostly through its influence on protein adsorption and electrostatic interactions with the negatively charged cell membranes. Surfaces charge can be tailored to be positive, negative, or neutral through adsorption of ions, chemical group dissociation, or the application of external electric fields.[124] Positively charged surfaces generally enhance cell attachment by strengthening electrostatic attraction. For instance, cationic modifications on cellulose scaffolds or chitosan increase fibroblast adhesion significantly compared to

negatively charged counterparts.[125], [126] On the other hand, some studies have reported enhanced cell attachment on negatively charged hydroxyapatite surfaces, underscoring the complexity and context-dependent nature of charge effects.[127] Beyond cell adhesion, surface charge also influences the loading and cellular internalization of nanoparticles and drugs, making it an important factor in designing scaffolds for controlled delivery of bioactive molecules.[128]

Wettability, defined as the extent to which a surface interacts with water, is a key factor in regulating protein adsorption and subsequent cellular responses.[129] Generally, hydrophilic surfaces facilitate cell attachment and spreading compared to hydrophobic surfaces.[130] The type and number of proteins adsorbed onto a surface also depend on its wettability. For example, fibronectin preferentially adsorbs onto hydrophilic surfaces, while albumin tends to bind more to hydrophobic ones. Optimal cell adhesion is typically observed on surfaces with moderate contact angles, around 70 to 80 degrees. Surface wettability can be modulated by chemical functionalization and surface roughness, and these two parameters often act synergistically to enhance cellular responses.[129], [131] Although the importance of wettability in promoting cell adhesion and proliferation is well established, its specific effects on cell differentiation and other functional behaviors remain less understood and requires further investigation.

Surface free energy, closely linked to wettability, is defined as the increase in energy that occurs when an atom moves from the bulk material to its surface.[132] It reflects the energetic state of surface atoms compared to those within the bulk and plays a fundamental role in guiding interactions with water, proteins, and cells. Surfaces with higher free energy generally enhance cell attachment and promote tissue formation. For instance, increasing surface free energy has been shown to improve wettability, leading to greater osteoblastic cell adhesion and mineralization.[133] Biomaterials exhibiting surface energies in the range of about 100 to 130 erg/cm^2 are considered optimal for supporting cell adhesion and proliferation, whereas lower surface energies are usually less favorable for these processes.[107]

Mechanical cues, especially the stiffness of the substrate, are crucial factors that influence cell behavior and determine cell fate.[134] In the body, tissue stiffness varies significantly, ranging from very soft tissues like the brain, around 4 kPa, too much stiffer tissues such as bone, which can reach 15 to 20 GPa (Figure 2.2).[135] It has been recognized that growing cells on substrates with stiffness levels similar to their native tissue environment, helps maintain their natural phenotype and supports proper gene expression. For example, chondrocytes preserve their characteristic phenotype when cultured on

elastic materials that mimic the stiffness of cartilage, while mesenchymal stem cells tend to adopt an osteoblast-like shape when grown on stiffer surfaces.[136] Cells sense mechanical forces by converting physical stimuli into biochemical signals through mechanotransduction pathways.[137] These signals ultimately regulate gene expression, protein synthesis, and cellular phenotype.[138], [139], [140], [141], [142] Applied mechanical forces can alter protein conformations and trigger reorganization of the cytoskeleton, which activates signaling pathways including the mitogen-activated protein kinase (MAPK) cascade.[143] Consequently, controlling the mechanical properties of biomaterials is essential for optimizing cell-material interactions, promoting cell proliferation and differentiation, and supporting effective tissue regeneration that meets physiological requirements.

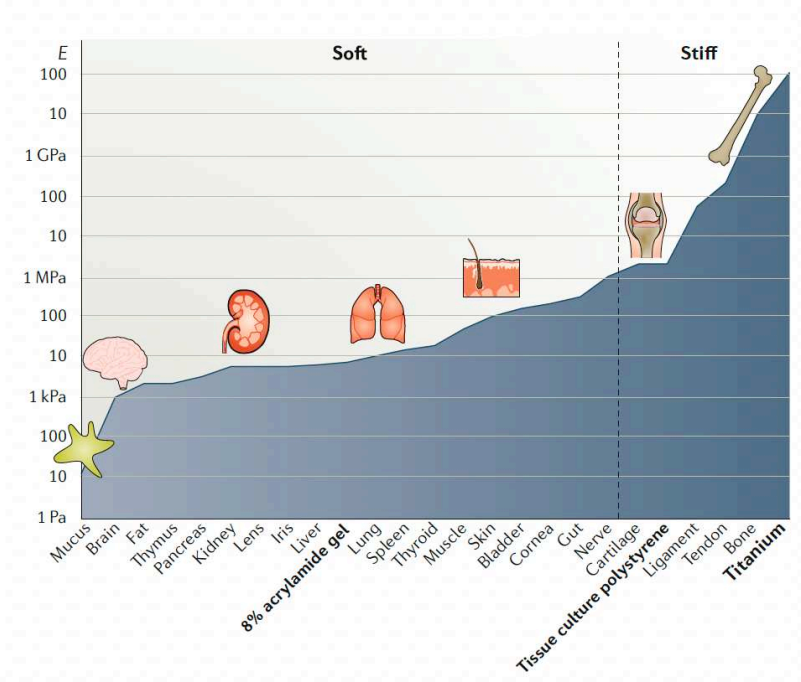


Figure 2.2. The stiffness of living tissues spans a wide range, from a few pascals to gigapascals.

This integrated overview highlights how the engineering of surface chemistry, topography, charge, wettability, energy, and mechanical stiffness enables the design of biomaterials that promote desirable cellular responses for tissue engineering and regenerative medicine. Understanding these complex and interrelated surface properties is fundamental for advancing the development of next-generation implants and scaffolds with enhanced biocompatibility and clinical performance.

2.2 Enhancing Biomaterial Interfaces through Functional Group Modification

Adding functional groups to biomaterial surfaces is essential for altering their interactions with biological environments. Although bare material surfaces may be biocompatible by not triggering strong immune reactions, they often lack the specific chemical groups needed to support targeted cellular interactions, protein adsorption, and effective tissue integration. Functional groups such as hydroxyl (-OH), carboxyl (-COOH), amine ($-NH_2$), or aldehyde (-CHO) serve as reactive sites on the surface that can directly affect surface energy, wettability, charge, and ultimately dictate the biological response.[144] These functional groups are critical because they allow covalent or strong non-covalent binding of biomolecules like proteins, peptides, or growth factors that activate specific biological pathways.[145] Functional group incorporation is achieved through chemical treatments that replace inert surface moieties with reactive groups. These controlled chemical modifications allow the introduction of various functionalities, including specific reactive groups, the attachment of biomolecules such as adhesion peptides or growth factors, and the modulation of surface properties like hydrophilicity and charge. These modifications are usually confined to the surface or near-surface layers of the material, ensuring that the bulk mechanical and structural properties remain unchanged while enhancing the biological activity at the interface with cell interactions.[146] Historically, wet chemical methods have been the most widely used and studied approaches. Among these, two main strategies are commonly employed: physical adsorption and covalent immobilization. Physical adsorption involves incubating the material in solutions containing biomolecules, allowing them to adhere to the surface primarily via non-covalent intermolecular forces such as electrostatic forces, van der Waals interactions, and hydrophobic effects. Due to its simplicity and cost-effectiveness, physical adsorption has served as a starting point for surface functionalization.[147], [148]

However, these methods have inherent limitations. Because the intermolecular forces involved are relatively weak (requiring only a few kilojoules per mole to break) the layer of adsorbed biomolecules can be quickly replaced by other proteins present in bodily fluids.[149] This process, known as the Vroman effect, reduces the stability and reliability of these coatings in the presence of biological fluids and cellular environments.[150], [151] The way biomolecules interact with a surface depends on both the chemical and physical properties of the surface and the biomolecules, as well as the surrounding environment.[152] For example, when in an aqueous environment, proteins typically adopt a

conformation where their hydrophobic amino acid residues are tucked into the protein's core, away from the aqueous surroundings, while the hydrophilic residues remain exposed on the exterior. Consequently, when proteins with hydrophilic surface residues encounter hydrophobic surfaces in water, they may unfold or become denatured, resulting in a loss of their original three-dimensional structure and, therefore, their biological function. To reduce protein unfolding during physical adsorption, surfaces are often made more hydrophilic by adding polar groups.[153] While a higher surface hydrophilicity can help preserve protein stability by preventing denaturation, it also tends to form a layer of water at the interface, making it less likely for proteins to adsorb onto the surface.

Covalent immobilization techniques on the other hand, allow to achieve more durable and efficient biofunctionalization. These methods rely on forming stable chemical bonds between biomolecules (primarily via reactive amino acid side chains) and suitably prepared surfaces. This stable anchoring prevents biomolecular detachment and displacement in physiological settings, maintaining biological function over the long term. To enable this bonding, the surface must first be chemically modified to present reactive groups such as amines, carboxyls, aldehydes, or hydroxyls. This functionalization can be done directly on the material's surface or indirectly by using bifunctional linker molecules like alkylsilanes or poly(ethylene glycol) derivatives, which act as bridges between the surface and the biomolecules.[154], [155]

Among the key chemical reactions widely employed for covalent immobilization of biomolecules onto biomaterial surfaces, carbodiimide-mediated coupling stands out as one of the most commonly used techniques due to its efficiency and mild reaction conditions. This method involves the activation of carboxyl (-COOH) groups on the surface or on biomolecules by carbodiimide reagents such as 1-ethyl-3-(3-dimethylaminopropyl) carbodiimide (EDC). The activated intermediate then readily reacts with primary amine ($-NH_2$) groups present in proteins, peptides, or other biomolecules to form stable amide bonds. Importantly, this amide linkage is robust under physiological conditions, preventing the detachment or displacement of bioactive molecules upon implantation or exposure to biological fluids. This strategy enables the covalent anchoring of a wide variety of biomolecules, including antibodies, growth factors, and adhesion peptides, providing the surface with specific biological functions tailored to the desired application.[156]

Another important covalent immobilization pathway involves Schiff-base chemistry, wherein aldehyde (-CHO) groups on surfaces react with primary amines of biomolecules to form reversible imine (Schiff base) linkages. Although imine bonds are typically unstable under physiological conditions, their

stability can be significantly improved through reductive amination, which chemically converts the imine into a more stable secondary amine bond. This technique enables gentle and relatively efficient conjugation of biomolecules, especially when maintaining protein function and orientation is crucial. The aldehyde groups needed for this chemistry are typically introduced onto surfaces by oxidation reactions or by employing chemical agents such as glutaraldehyde, which can both introduce reactive groups and act as a covalent linker to biomolecules.[157]

Thiol-disulfide exchange chemistry represents another valuable alternative approach. This method leverages cysteine residues naturally present in many proteins and peptides, which contain reactive thiol (-SH) groups. These thiols can participate in exchange reactions to form disulfide bonds (–S–S–) that link the biomolecule covalently to appropriately functionalized surfaces. The specificity of thiol chemistry allows site-selective immobilization and often preserves the bioactivity of the grafted molecules. Furthermore, disulfide bonds can be designed to be reversible under reducing environments, offering potential for controlled release applications or dynamic biointerfaces.[158]

Silanization is a powerful and versatile chemical surface modification technique that introduces reactive functional groups onto material surfaces, especially those rich in hydroxyl (-OH) groups, such as glass, silicon, and metals. This process involves the covalent attachment of organosilanes molecules to the surface through siloxane bonds (Si–O–Si), forming a stable, uniform, and densely packed silane layer. The silane molecules are typically composed of a hydrolyzable alkoxy group that reacts with surface hydroxyls, and an organofunctional group that provides a chemical handle for subsequent bio-functionalization.[159] Recent studies highlight that silanization not only enhances surface hydrophilicity and chemical reactivity but also offers precise control over surface characteristics, such as improved accessibility for biomolecule attachment, achieved by selecting appropriate silane chemistries and optimizing grafting conditions. This precise tunability optimizes biological responses including cell adhesion, proliferation, and differentiation, which are critical in tissue engineering and implant integration.[160] Pre-treatments like plasma or UV-ozone exposure, which increase surface hydroxyl density and provide effective cleaning, can significantly enhance the formation and efficiency of silane layer functionalization.[161] The robustness and versatility of silanization, along with its cost-effectiveness and straightforward processing steps, make it a widely used method for producing durable and functional biointerfaces where long-term stability and reliable performance are essential.

Plasma, known as the fourth state of the matter, is a partially ionized gas containing reactive species and it can modify surfaces at the nanoscale without solvents, high temperatures, or harsh chemicals.

Non-thermal plasmas are especially suitable for temperature-sensitive biomedical polymers, introducing polar groups (hydroxyl, carboxyl, amine) that increase surface energy and wettability, enhancing protein adsorption and cell interactions. Plasma can also etch surfaces, increasing roughness and biomolecular anchorage. By adjusting gas composition plasma treatments can selectively introduce functional groups, tailoring bioactivity.[162] Treatments can occur under vacuum or at atmospheric pressure, balancing control and cost. Plasma-generated surface radicals enable direct covalent grafting of biomolecules in simpler one-step processes, improving coating stability and reducing residual chemicals.[163] Despite its advantages, plasma modification has several drawbacks. The complex interactions between plasma species and surfaces make process control and reproducibility challenging. Maintaining precise tuning of parameters, such as gas composition, pressure, power, and exposure time, is crucial, as even small variations can lead to inconsistent outcomes. Although plasma treatments can introduce various functional groups, achieving high selectivity for specific desired moieties over other similar species is difficult, limiting precise control of surface chemistry. Overcoming these challenges is crucial to unlocking the full biomedical potential of plasma surface modification.

Together, these surface modification techniques offer different tools with distinct mechanisms, advantages, and uses. Choosing or combining methods depends on the nature of the base material, the biomolecule to be attached, the desired biological function, and the specific clinical or technological application.

2.3 Silanization strategies

Self-assembled monolayers (SAMs), first introduced by Jacob Sagiv in 1980, are organic assemblies formed by the adsorption of molecular components from solutions or the gas phase onto solid surfaces or orderly arrays on liquid surfaces. The adsorbed molecules spontaneously organize into crystalline or semicrystalline structures.[164], [165] These single-molecule-thick films form highly ordered arrangements on substrate surfaces and are composed of small organic molecules typically measuring between 1 and 5 nanometers in thickness, depending mainly on molecular size. This places them firmly within the category of nanoscale materials. Unlike polymeric or metallic films that attach through weaker physical forces, SAMs feature strong chemical bonds between their anchoring groups and the substrate, resulting in enhanced stability against detachment or dissolution in surrounding

environments.[166], [167], [168] The molecular architecture of a SAM-forming species generally consists of three fundamental components: the anchor (or head) group, the linker (or spacer), and the terminal functional group. The anchor group establishes a robust and specific interaction with the substrate, effectively dictating the choice of SAM molecules based on the nature of the surface (Figure 2.3).[164] For instance, sulfur-containing thiol groups can form covalent bonds with gold, but recent evidence suggests that self-assembled monolayers on gold are often stabilized by weaker, more dynamic interactions, making gold-thiol SAMs less robust than previously assumed.[169] By contrast, silane-based SAMs are commonly used on silicon, silicon oxide, and various metal oxide substrates. Additionally, phosphonic acids and carboxylic acids exhibit strong binding affinities towards metal oxides, expanding the toolkit for surface functionalization beyond thiols and silanes.

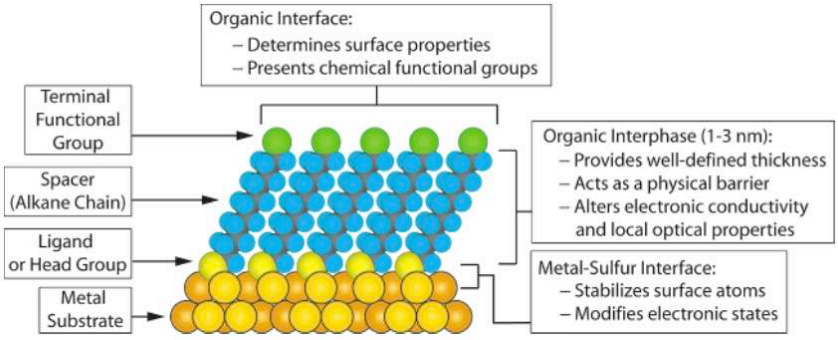


Figure 2.3. Schematic diagram of an ideal single-crystalline SAM of alkanethiolates on a gold surface.[164]

The length and configuration of the linker segment, most commonly an alkyl chain, significantly impact the monolayer's organization and stability by promoting molecular order and packing density. However, alternative linkers like aromatic rings or ethylene glycol oligomers may also be used depending on the desired structural and functional characteristics.[170] Meanwhile, the terminal group of the SAM is critical for defining the final surface properties after monolayer assembly. By varying this group, one can tailor surface wettability, chemical reactivity, charge, and other interfacial characteristics.[171] For instance, a hydrophobic surface can be achieved by incorporating alkyl terminal groups, whereas introducing polar groups such as amines or charged moieties imparts hydrophilicity or specific ionic functionality. Moreover, reactive terminal groups may be installed intentionally to facilitate further chemical reactions and surface modifications post-assembly.[164], [165], [172], [173]
Among the various types of SAMs, silane-based monolayers have emerged due to their high

versatility.[174] They are generated by the covalent attachment of silane molecules to hydroxylated surfaces, typically through trichloro-, trimethoxy-, or triethoxysilane head groups.[175] These silane anchoring units facilitate strong chemical bonding and, often due to their ability to form multiple covalent interactions, they yield highly stable and dense monolayers. The resultant layers not only serve as protective coatings but also provide a reactive platform for further chemical functionalization. This chemical stability sets silane-based SAMs apart from other commonly used systems, such as thiol-based monolayers on gold, which have been extensively studied and utilized for their ease of preparation but generally show less chemical stability.[166] Silane SAMs achieve their stability from covalent siloxane bonds (Si-O-Si) between the silane molecules and hydroxyl-terminated substrates. Among these, alkoxysilanes are generally more stable and easier to control under ambient conditions compared to chlorosilanes, which are highly sensitive to humidity. Additionally, silanes with longer alkyl chain tend to form more organized and densely packed monolayers, which results in enhanced protective and chemical stability properties. In contrast, shorter or branched chain silanes typically exhibit less ordered films that are more prone to instability.[176]

Surface modification using silane-based monolayers generally falls into two traditional categories: solution-phase and vapor-phase deposition. The solution-phase method involves immersing the substrate in a silane-containing solution, where factors like water content, solvent polarity and viscosity, temperature, and reaction duration play critical roles in dictating monolayer formation. In contrast, vapor-phase deposition exposes substrates to silane vapors at elevated temperatures (typically between 50 and 200°C), often resulting in denser films due to more controlled assembly conditions.[173]

In addition to the conventional solution-phase and vapor-phase deposition methods, the spin coating technique has emerged as a promising alternative for preparing silane-based self-assembled monolayers.[177] In contrast to solution and vapor-phase methods, which have been extensively used for grafting bioactive molecules and enabling further conjugation on surfaces, spin coating has mainly been applied for surface modification and multilayer deposition, but has not yet been utilized for subsequent bioactive molecule conjugation.[178], [179] Unlike the traditional solution immersion method, which requires strict controlled conditions and significant volumes of organic solvents that produce significant chemical waste, the spin coating technique is faster, simpler, and more environmentally friendly, using smaller amounts of solvent and functioning easily under ambient conditions. On the other hand, chemical vapor deposition (CVD), although solvent-free, typically

requires ultra-high vacuum or elevated temperatures that may not be suitable for substrates with sensitive organic functionalities, thereby restricting its practical use.[180], [181] Spin coating is a technique applied for depositing thin films and multilayers onto flat substrates. It involves dispensing a silane-containing solution onto the surface, followed by rapid spinning to evenly distribute the liquid and create a uniform, thin coating. This approach has been effectively utilized to produce monolayers from various silane precursors. Notably, recent advances demonstrated the preparation of functionalized SAMs, such as azide-terminated layers, via spin coating onto silica substrates, expanding the versatility of this technique.[182] A comprehensive study systematically evaluated spin coating as a general deposition strategy for silane-based SAMs by comparing it with the traditional solution immersion process. Four organotrimethoxysilanes with diverse molecular architectures were synthesized and grafted onto silica substrates using both spin coating and immersion techniques. Extensive material characterization indicated that the spin-coated self-assembled monolayers (SAMs) exhibited homogeneity and chemical quality comparable to those obtained through immersion (Figure 2.4). Additionally, the covalent grafting achieved via spin coating demonstrated robustness, with monolayer integrity preserved during subsequent chemical surface modifications.[177]

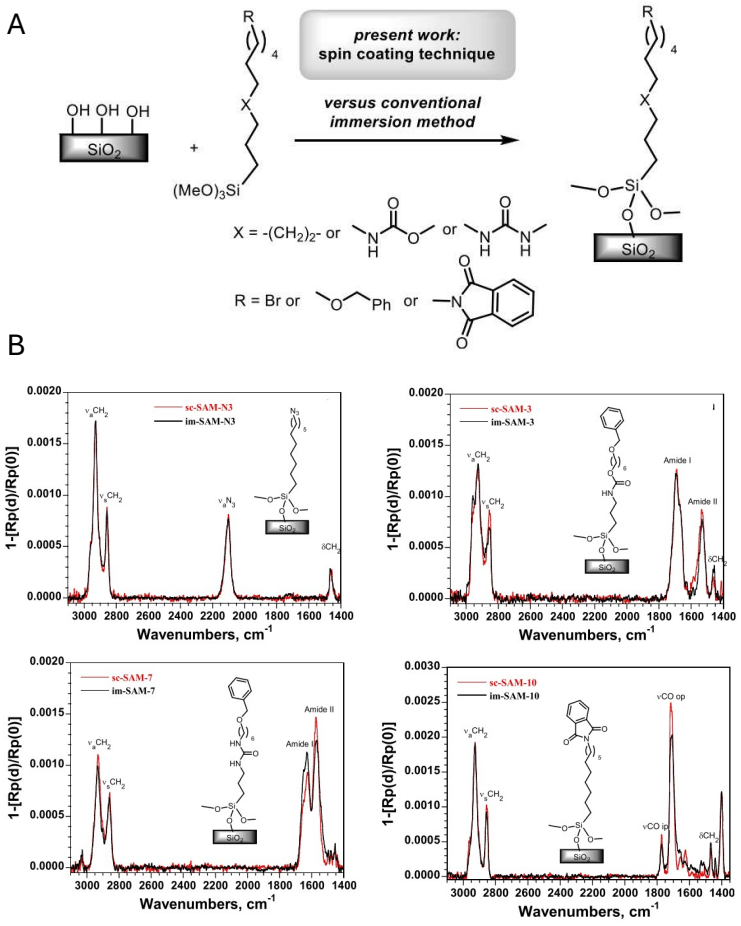


Figure 2.4. (A) Schematic illustration of the preparation of organosilane-based SAMs on silica substrates, including the chemical structures of the coupling agents utilized. (B) PM-IRRAS spectra comparing four different silane-coupled SAMs prepared by spin coating versus the conventional immersion method. Adapted from Rouvière et al.[177]

Amino-terminated self-assembled monolayers (SAMs) have garnered considerable interest due to their crucial role in surface biofunctionalization, enabling applications such as nanoparticle functionalization and cell adhesion studies.[183], [184] Commercially available aminosilanes like 3-aminopropyl-triethoxysilane (APTES), are commonly employed as coupling agents to introduce reactive amino groups onto various substrates.[185], [186], [187] However, despite their widespread use, achieving high-quality and reproducible amino-terminated monolayers remains a considerable challenge. This is due to the sensitivity of these systems to various experimental factors, including silane concentration, solvent properties, reaction time, temperature, and humidity, which all affect the molecular organization and uniformity of the resulting films. Moreover, the inherent chemical characteristics of these commercial aminosilanes can lead to

multilayer formation, film heterogeneity, and instability. The free amino end groups promote complex networks of hydrogen bonding and electrostatic interactions, driving disordered structures and limiting functional group accessibility. These challenges have driven the development of alternative molecular strategies aimed at minimizing noncovalent interactions and enhancing monolayer uniformity. For instance, the use of protecting groups such as phthalimide, to temporarily mask amino functionalities during deposition, has proven effective in limiting undesired interactions, thereby facilitating a more controlled and orderly assembly of silane molecules. This approach represents a significant advancement toward producing stable, homogeneous amino-terminated self-assembled monolayers with improved functional performance.[188]

The capacity to precisely engineer the terminal functional groups of silane-based monolayers has significantly expanded the potential for customizing surface properties to meet specific application needs. By selecting appropriate terminal groups, it is possible to finely tune a wide range of physical, chemical, biological, and optical characteristics, unlocking diverse functionalities and enabling the integration of self-assembled monolayers into numerous advanced technological and scientific applications.

Chapter 3

Mimicking the Extracellular Matrix: Peptide Functionalization for Osteogenic Platforms

3.1 Complexity and Biological Role of the Extracellular Matrix in Bone

The creation of effective tissue-engineered bone requires three fundamental components: scaffolds that encourage tissue and cell renewal, specific growth factors (or other bioactive molecules), and viable cell sources. Ideally, the scaffold should replicate the essential features of native bone, providing an environment that supports cell attachment, proliferation, differentiation into bone cells, and the formation of new blood vessels. Over time, the scaffolds should integrate with the surrounding tissue and develop the ability to bear normal mechanical stresses of the body.[189]
Cells secrete the extracellular matrix, a non-cellular structure composed of characteristic proteins and polysaccharides, which varies in composition and architecture depending on the tissue type and developmental stage.[190] By providing both strength and flexibility, the ECM supports tissue architecture and is constantly remodeled in response to variations in receptor expression, growth factor activity, local pH, ensuring proper development and physiological function, as well as preserving tissue homeostasis.[191]
The bone matrix is composed of approximately 40% organic and 60% inorganic material, with its precise composition influenced by factors such as sex, age, and overall health status. The inorganic portion mainly consists of calcium-deficient apatite along with trace minerals. In hard tissues such as bone and dentin, the predominant inorganic component is hydroxyapatite (HA, $Ca_5(PO_4)_3OH$). Its deposition takes place through biomineralization, a process where minerals ions interact with the extracellular matrix. During tissue mineralization, collagen fibers act as structural templates, guiding the organization and growth of hydroxyapatite crystals.[192]

The organic fraction is more complex, including about 90% type I collagen and roughly 10% non-collagenous proteins, most of which are produced by osteoblasts prior to mineral deposition.[193] The non-collagenous protein can be classified into four main categories: γ-carboxyglutamate-containing proteins, proteoglycans, glycoproteins, and the small integrin-binding ligand N-linked glycoprotein (SIBLING) family.[190]

Proteoglycans in bone are core proteins attached to glycosaminoglycan (GAG) chains, including keratan sulfate, chondroitin sulfate, heparan sulfate, hyaluronic acid, and dermatan sulfate. An important subgroup, the small leucine-rich proteoglycans (SLRPs), regulate cell behavior and participate in every stage of bone formation, from proliferation and differentiation to mineralization and remodeling, thus maintaining bone homeostasis.[194]

γ-Carboxyglutamic Acid-Containing Proteins are found in the bone matrix, dentin, and other calcified tissues. Major examples of γ-carboxyglutamic acid-containing proteins include osteocalcin (OCN) and matrix Gla protein (MGP). OCN is produced by osteoblasts and plays a dual role: it binds calcium within the bone matrix to support mineralization, and it also functions as a hormone influencing energy and glucose metabolism. MGP is synthesized by osteoblasts, osteocytes, and chondrocytes, and acts primarily as an inhibitor of pathological or excessive mineralization, ensuring that calcification occurs only where it is needed.[195]

Glycoproteins such as osteonectin and thrombospondins play crucial roles in the architecture, mineralization, and continuous remodeling of bone. Osteonectin is highly expressed by osteoblasts and is found in mineralized tissues. It binds both collagen fibers and hydroxyapatite crystals, acting as a molecular bridge and facilitating the proper deposition of mineral onto collagen during the bone formation process. Beyond mineralization, osteonectin influences cell-matrix interactions and can impact cell proliferation, migration, and survival within the bone microenvironment.[196]

Thrombospondins (TSPs) comprise a family of extracellular glycoproteins involved in angiogenesis and regulation of growth factor activity during skeletal development. They are secreted by osteoblasts and are present in both developing and mature bone. Animal models lacking specific TSPs exhibit pronounced skeletal abnormalities, underscoring their importance in coordinating bone cell differentiation, guiding proper tissue organization, and supporting vascularization in regenerating bone tissue.[197]

Small Integrin-Binding Ligand N-Linked Glycoproteins (SIBLINGs) includes bone sialoprotein (BSP), osteopontin (OPN), dentin matrix protein-1 (DMP1), dentin sialophosphoprotein (DSPP), and matrix extracellular phosphoglycoprotein (MEPE). These proteins constitute a distinctive family of

glycophosphoproteins predominantly found in fully mineralized tissues such as bone and dentin. These proteins share integrin-binding motifs, which enable them to mediate crucial interactions between cells and the mineralized matrix. Collectively, SIBLINGs regulate a range of essential processes, including osteoblast differentiation, the initiation and progression of mineralization, and phosphate metabolism, establishing them as central components in bone development and maintenance. BSP is highly expressed during the early stages of mineralization, where it promotes hydroxyapatite nucleation and assists in organizing the extracellular matrix necessary for bone growth.[198] OPN contributes to bone turnover by modulating osteoclast activity, maintaining the balance between new bone formation and resorption. Both DMP1 and MEPE serve as key regulators of mineral deposition and phosphate homeostasis, with DMP1 deficiency resulting in severe defects, such as hypomineralized bone and disrupted phosphate metabolism. Although DSPP is mainly present in dentin, it plays a critical role in mineralizing tissues and is believed to contribute to bone integrity as well.[190]

3.1.1 Cell-cell and cell-matrix interactions in bone microenvironment

The surrounding cellular microenvironment plays a key role in regulating cellular behavior. Through the formation of adhesion sites, cells sense and respond to physical and chemical signals, a process that is essential for guiding cellular functions. Membrane receptors translate mechanical and structural signals from the environment into intracellular signaling pathways, which regulate critical processes such as cell growth, migration, differentiation, and apoptosis. Through cell adhesion molecules, cells establish communication both with one another and with the extracellular matrix.[199] Cells maintain contact with one another through specialized adhesion molecules. Among these are cadherins, which link cells together in a calcium-dependent manner, and integrins, which mediate attachment between cells and the extracellular matrix (ECM). Cadherins are single-pass transmembrane glycoproteins that bind strongly to identical cadherin molecules on adjacent cells when calcium is present. Inside the cell, the cadherin cytoplasmic domain connects to actin filament bundles in the cytoskeleton via a protein complex that includes catenins (Figure 3.1A). Notably, one of these proteins, β-catenin, also plays a central role in the WNT signaling pathway, thereby linking cell adhesion with intracellular signaling. The cadherin family derives its name from the tissues in which its members were first discovered. For example, E-cadherin is predominantly found in epithelial tissues, while N-cadherin is mostly present in neural tissues.[200] Research has demonstrated that

osteoblasts predominantly express N-cadherin (cadherin-2, CDH2) and cadherin-11 (CDH11), both important regulators of bone formation and bone mass. Notably, the expression level of CDH2 influences the lineage commitment of precursor cells. Early in vivo studies showed that disrupting cadherin activity impairs osteoblast differentiation and indirectly promotes the commitment of bone marrow progenitors to the adipogenic lineage. A well-established mechanism through which cadherins regulate osteoblast precursor differentiation is cell-cell adhesion. This process is particularly relevant in bone tissue, as experimental inhibition of cell-cell adhesion has been shown to reduce osteoblast differentiation and bone mass in both in vitro and in vivo studies.[201]

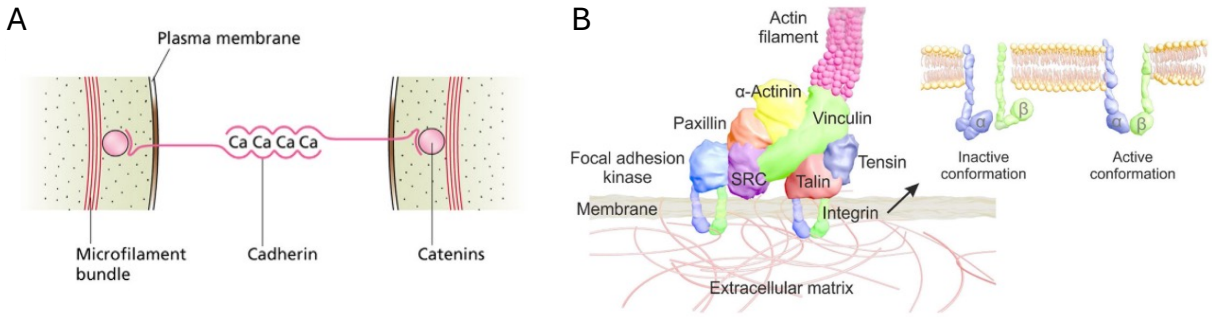


Figure 3.1. (A) Calcium-dependent cadherin cell-adhesion system. Adapted from Slack, J.M.W. [200] (B) Molecular structure of integrin adhesion complexes. Adapted from Luo et al.[199]

Cell-matrix interactions are mediated by integrins, which are cell-surface glycoproteins specialized in binding to extracellular matrix (ECM) components. Integrins are heterodimers composed of two distinct subunits, α and β, with their binding activity dependent on the presence of magnesium or calcium ions. The diversity of α and β subunits allows for numerous functional heterodimer combinations. On the intracellular side, integrins connect to cytoskeletal microfilaments, creating a physical and functional link between the external environment and the cell's internal cytoskeleton, similar to the role of cadherins. Beyond this structural function, integrins can also trigger intracellular signaling pathways and regulate gene transcription in response to specific ECM signals.[200] When a ligand binds to an integrin receptor, it triggers integrin clustering and the association of its cytoplasmic tail with cytoskeletal elements and other adaptor proteins (Figure 3.1B). This binding event also promotes the recruitment and phosphorylation of focal adhesion kinase (FAK), activating downstream signaling pathways. The α5β1 integrin, which serves as a fibronectin receptor, is critical for osteoblast formation in vitro. Suppression of the α5 subunit reduces osteoblast differentiation, whereas its overexpression enhances osteogenic differentiation in cultured mesenchymal skeletal cells

(MSCs). The β1 integrin subunit similarly supports osteoblast development through FAK/MAPK ERK1/2 signaling, which activates the transcription factor RUNX2. Moreover, α5β1 activation increases the production of insulin-like growth factor 2 (IGF2) and IGF-binding protein 2 (IGFBP2), stimulating their downstream signaling cascades and demonstrating crosstalk between integrins and local factors that drive osteogenesis. Meanwhile, α2β1 integrin, a principal receptor for type I collagen, has been shown to regulate collagen synthesis in osteoblasts in vivo. This integrin also influences MSC differentiation and survival by activating the ROCK, FAK, and MAPK-ERK1/2 pathways.[201], [202]

In addition to integrin-mediated adhesion, cell-matrix communication is also mediated by interactions involving heparin-binding domains (HBDs). These motifs, typically enriched in basic amino acids such as lysine and arginine, engage sulfated glycosaminoglycans (GAGs) including heparan sulfate and heparin, which are abundant both at the cell surface and within the extracellular matrix. Structurally, heparin is composed of repeating disaccharide building blocks made up of a uronic acid and glucosamine, whereas heparan sulfate contains the same fundamental units but features fewer sulfate groups and exhibits greater sequence variability in its chain structure.[203] The electrostatic attraction between the negatively charged sulfate and carboxyl groups on GAG chains and positively charged regions of proteins underlies the formation of highly specific and stable complexes. Through these interactions, heparan sulfate chains serve as essential molecular bridges that organize protein assemblies and regulate the localization, stability, and activity of signaling molecules. This, in turn, influences diverse cellular processes such as proliferation, migration, differentiation, and survival, while also contributing to matrix remodeling and tissue repair.[204] Many soluble signaling molecules depend on heparin- and heparan sulfate-mediated interactions to exert their biological effects. Several growth factor families, including fibroblast growth factors (FGFs), vascular endothelial growth factor (VEGF), hepatocyte growth factor (HGF), transforming growth factor-β (TGF-β), and platelet-derived growth factor (PDGF), require the presence of heparan sulfate proteoglycans (HSPGs) on the cell surface. The HSPGs act as essential co-receptors by stabilizing the growth factors, facilitating their presentation to specific transmembrane receptor tyrosine kinases, and promoting receptor dimerization. This cooperative binding between growth factors, HSPGs, and their receptors enhances signal transduction, which is critical for regulating proliferation, angiogenesis, and tissue morphogenesis. Chemokines represent another group of heparin-binding molecules. Their association with endothelial glycosaminoglycans not only protects them from degradation but also facilitates the

formation of haptotactic gradients that guide leukocyte recruitment during inflammation. In addition, annexins, a family of calcium-dependent phospholipid-binding proteins, can also interact with heparin and have been implicated in processes ranging from coagulation to inflammatory regulation.[205] Such interactions highlight the central role of heparan sulfate proteoglycans in localizing, stabilizing, and modulating the activity of diverse signaling proteins at the cell-matrix interface.

Besides their interactions with the extracellular matrix through integrins, bone cells also respond to a variety of hormonal and local factors signals via specific receptors, which play a crucial role skeletal development and homeostasis. The adult skeleton undergoes continual remodeling, and this activity is strongly influenced by hormones such as estrogens, parathyroid hormone (PTH), and 1,25-dihydroxyvitamin D_3 ($1,25D_3$). Estrogen is a major regulator of bone growth, turnover, and homeostasis. It supports the survival of osteoblasts and osteocytes, promotes apoptosis of osteoclasts, and suppresses pro-resorptive cytokines including IL-1, TNF, and IL-6. Loss of estrogen, as in menopause or following ovariectomy, is associated with increased bone resorption and consequent bone loss. Vitamin D, synthesized as the pro-hormones D_2 or D_3 and converted into the active form $1,25D_3$, acts through the vitamin D receptor (VDR) in bone, intestine, and kidney to regulate mineral metabolism. Evidence suggests that $1,25D_3$ can bind membrane-associated receptors to elicit rapid calcium transport and activating protein kinase C. PTH maintains systemic calcium balance through actions on bone, kidney, and indirectly the gut. Continuous PTH exposure favors bone resorption, whereas intermittent exposure can stimulate osteoblast activity and new bone formation.[202]

Within the extracellular microenvironment, growth factors act on osteogenic precursors, playing a critical role in directing their differentiation and function. One example is the bone morphogenetic proteins (BMPs), members of the TGF-β superfamily, originally identified for their ability to induce ectopic bone formation. There are over 20 bone morphogenetic proteins (BMPs), categorized into functional subgroups, that regulate the fate of mesenchymal stem cells by encouraging their differentiation into the osteoblastic lineage while suppressing alternative pathways like myoblast formation. BMPs also play a role in osteoclastogenesis, thus coordinating the balance between bone formation and resorption. They transmit signals through specific type I and type II serine/threonine kinase receptors on the cell surface, which form complexes even before binding to their ligands. Upon BMP engagement, these receptors activate intracellular pathways, most notably the Smad1/5/8 cascade, which forms complexes with Smad4 to regulate transcription in the nucleus. BMPs can also trigger Smad-independent signaling, such as p38 MAP kinase activation, linking them to functional

outcomes like alkaline phosphatase induction. Although related to TGF-β, BMPs often exert opposing effects on osteoblast maturation, with BMP2 stimulating osteogenic differentiation and TGF-β tending to inhibit terminal osteoblast maturation or diverting cells toward chondrogenic fates.[95], [206]

3.2 Biomimetic Surfaces: Bioactive Cues for Guiding Cell Responses

Several strategies in tissue engineering aim to tune the biochemical properties of materials to regulate the formation and maturation of focal adhesions (FAs) to promote initial cell attachment. A widely used method is surface functionalization with adhesion-promoting ligands. However, proteins or peptides involved in cell adhesion may adsorb unevenly or become inaccessible to cells, thereby disrupting FA dynamics.[207] As discussed in Chapter 2, chemical surface modification is a widely used strategy to enhance the bioactivity of biomaterials. By introducing specific functional groups, the surface can be tailored to support the immobilization of biologically active molecules that facilitate cell attachment. Techniques such as plasma deposition, wet chemical treatments, and chemical adsorption are widely applied for surface modification. While these treatments can directly influence cellular responses, they are more often used to create interfaces for biomolecule immobilization, one of the most advanced and versatile applications of surface engineering. The chosen functionalization strategy determines key parameters of immobilization, including the type of reactive groups available for cross-linking, their surface density, and their spatial distribution.[106]
Using full-length native proteins in biomaterial applications presents several challenges: they degrade rapidly limiting their functional lifespan, their stability is compromised by changes in temperature and pH, contamination with bacteria or endotoxins can occur during purification, and their production is generally costly and complicated due to poor solubility.[208], [209]
A promising strategy to overcome the limitations of full-length proteins is the use of synthetic peptides that represent specific functional domains of extracellular matrix proteins. Peptides are generally less expensive, structurally simpler, more stable than proteins, and they can be tailored for surface functionalization. In many cases, they can reproduce the biological activity of the complete protein toward a specific target.[210], [211] Mimicking the cellular microenvironment is essential for achieving effective biomaterial functionalization. This often involves incorporating biological signals that resemble those found in the tissue's native extracellular microenvironment to guide tissue

regeneration. The specific functionalization strategy varies depending on the target tissue. A variety of peptides derived from extracellular matrix proteins have demonstrated potential in bone tissue engineering due to their ability to modulate cell behavior and promote osteogenesis.[114], [212], [213], [214], [215], [216], [217], [218] These peptides can be generally grouped into functional categories such as integrin-binding sequences like RGD and PHSRN, peptides derived from collagen, bioactive peptides originating from growth factors including FGF-2, osteoinductive peptides based on bone morphogenetic proteins, heparin-binding peptides including KRSR and FHRRIKA, angiogenic peptides, osteoinductive peptides like osteopontin-derived sequences, as well as other bioactive peptides from non-collagenous matrix proteins such as laminin and fibronectin.[209], [210], [219] Their diverse signaling roles and biochemical interactions make them key molecular tools for enhancing cell adhesion, proliferation, differentiation, and matrix mineralization in engineered bone constructs.

Integrin-binding peptides

Materials with inherently low cell affinity can be functionally improved by incorporating adhesive peptides derived from key extracellular matrix (ECM) proteins such as fibronectin, vitronectin, or type I collagen. Among these, the RGD (Arg-Gly-Asp) sequence, first identified by Pierschbacher et al. in 1984, has been the most extensively studied.[220] RGD is present in multiple bone matrix proteins, including fibronectin (FN), vitronectin (VN), and collagen, and promotes cell attachment via binding to integrins. However, because several integrins can recognize RGD and related motifs, this can lead to non-specific cell adhesion across different cell types. Although several studies have noted RGD-associated increases in osteogenic differentiation and matrix mineralization, the literature remains inconsistent.[210], [211], [221] Pan et al., among others, have suggested that RGD requires additional biochemical cues to achieve consistent osteogenic outcomes.[222] Other studies reinforce this interpretation, for instance Moore et al. reported no hMSCs differentiation on RGD-modified self-assembled monolayers (SAMs) unless osteogenic supplements were present.[223] Collectively, these findings indicate that while RGD reliably enhances cell adhesion, it does not consistently induce osteogenic differentiation on its own. For bone tissue engineering applications, RGD should be combined with additional biochemical signals to achieve robust osteoinductive effects.

Collagen-derived peptides

GFOGER is a collagen-derived peptide motif located in the α1 chain of type I collagen. It has been widely applied to enhance stem cell adhesion, osteogenic differentiation, and matrix mineralization, and its efficacy has also been confirmed in in vivo bone healing models.[210] In one study, Shekaran et al. functionalized polyethylene glycol (PEG)-BMP-2 hydrogels with surface-immobilized GFOGER (Figure 3.2). Compared with RGD modification, the GFOGER-functionalized hydrogels supported greater bone marrow stromal cell (BMSC) spreading and osteogenic differentiation. Remarkably, in vivo experiments showed that GFOGER coatings could stimulate bone repair even without BMP-2, underscoring its strong osteoinductive potential.[224]

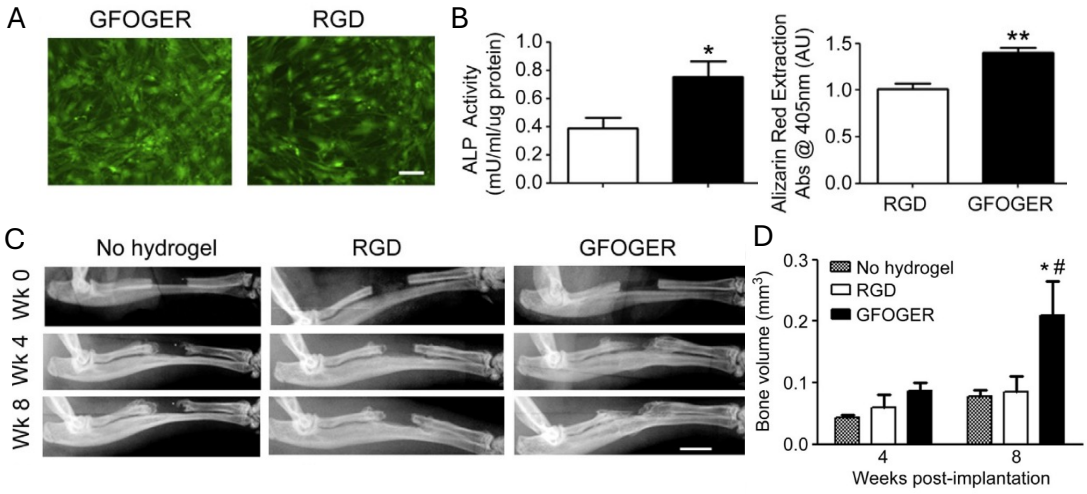


Figure 3.2. (A) Live/dead staining of hMSCs on GFOGER- and RGD-presenting hydrogels at day 3 of osteogenic induction. (B) ALP activity measured at day 14 and Alizarin Red staining for mineralization at day 21. (C) Radiographic images of radial defects treated with RGD- and GFOGER-presenting hydrogels. (D) Bone volume measurements for defects treated at weeks 4 and 8. Adapted from Shekaran et al.[224]

P15 is another collagen-inspired peptide, corresponding to residues 766–780 in the α1 helix of type I collagen. It binds specifically to the collagen-recognizing integrin α2β1, initiating growth factor and cytokine production that drives extracellular matrix synthesis and mineralization. Because this interaction is RGD-independent, P15 does not compete for binding with integrins that interact with fibronectin (αIIbβ3, α5β1) or vitronectin (αvβ3), making it a highly selective ligand.[210] Extensive in vitro and in vivo studies have demonstrated that P15 significantly enhances osteogenic

cell adhesion, proliferation, and mesenchymal stem cell differentiation. Liu et al. showed the potential of P15-modified titanium surfaces to improve implant integration, with Ti-P15 materials promoting increased attachment of osteogenic precursors and facilitating their differentiation (Figure 3.3).[225] Functionally, it can serve as a collagen type I substitute when immobilized on material surfaces.[226], [227] Its clinical relevance is highlighted by FDA approval for applications in periodontal regeneration (PepGen P-15®, Dentsply) and cervical disc reconstruction (i-Factor®, Cerapedics). Overall, these findings position P15 as a promising candidate for targeted, integrin-specific strategies in bone tissue engineering.

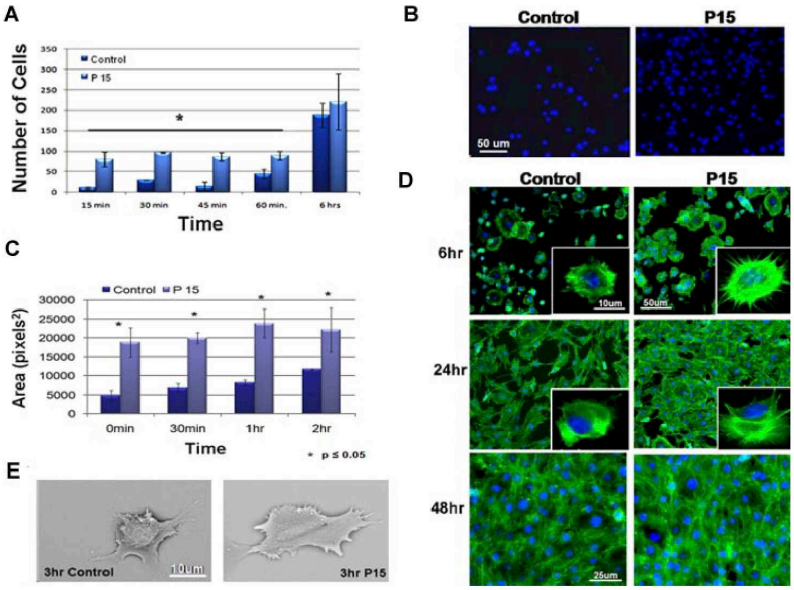


Figure 3.3. P15-functionalized Ti surfaces increase cell attachment and spreading. (A) Number of cells measured over 6 hours. (B) DAPI staining showing an increased number of cells on P15 material. (C) Cell spreading area. (D) Actin staining over 48 hours showing differences in cytoskeleton organization. (E) SEM analysis revealing increased cell area on P15 materials. Adapted from Liu et al.[225]

Growth factors-derived peptides

Alternatively, immobilizing growth factors mimetic peptides can provide necessary biochemical signals that drive stem cell differentiation toward specific lineages.[228] Notable examples include bone morphogenetic protein 2 (BMP-2), which promotes osteogenesis, and vascular endothelial growth factor (VEGF), a key inducer of blood vessel formation. Due to their powerful regulatory

effects, proteins and growth factors are widely employed in biomaterial functionalization to influence cell behavior and stimulate tissue repair and regeneration.[229] Vascular endothelial growth factor (VEGF) is a key signaling protein that stimulates angiogenesis. Guang et al. investigated VEGF-based surface coatings and found that they positively influenced bone regeneration. In vivo experiments in rats showed that VEGF enhanced the proliferation of both osteoblasts and endothelial cells. These effects were accompanied by increased levels of protein markers essential for bone tissue repair, including osteocalcin (OCN), an osteoblast-specific marker linked to bone formation, and CD31, a protein integral to angiogenesis, both of which showed higher expression compared to control samples. Complementary in vitro studies further revealed that VEGF promoted primary rat osteoblast proliferation, stimulated vasculogenesis, and elevated alkaline phosphatase (ALP) activity, all indicative of active bone remodeling.[230]

Bone morphogenetic proteins (BMPs), members of the TGF-β superfamily, are critical regulators of osteogenic differentiation. Among BMP isoforms, BMP-2 and BMP-7 (osteogenic protein-1, OP-1) stand out, having been approved by the FDA for clinical use in bone repair and spinal fusion. Bone morphogenetic proteins are crucial osteoinductive signaling molecules involved in skeletal development, bone formation, and remodeling. They exert their biological activity primarily through two specific sequences known as the "wrist" and "knuckle" epitopes, which preferentially bind to BMP type I and type II receptors on the cell surface.[231] Madl et al. showed that anchoring the BMP-2 knuckle epitope peptide to 3D alginate hydrogels accelerated osteogenic differentiation of mouse MSCs, increasing mineralization, osteopontin production, and SMAD 1/5/8 phosphorylation, underscoring the relevance of sustained peptide presentation in three-dimensional biomaterials.[232] BMP-2-derived peptides have demonstrated the ability to bind BMP type I and II receptors, activating similar downstream pathways as the full-length BMP-2 protein. For instance, Lukasova et al. showed that polycaprolactone nanofibrous scaffolds functionalized with a BMP-2 mimetic peptide enhanced osteogenic differentiation of porcine mesenchymal stem cells (pMSCs), evidenced by increased mRNA levels of osteocalcin (OCN) and collagen I, with no change in collagen II expression, indicating specificity toward osteogenic lineage.[233] Similarly, BMP-2 peptides immobilized on poly(lactic-co-glycolic acid) (PLGA) scaffolds boosted osteogenesis of human adipose-derived stem cells (hADSCs) and significantly enhanced bone regeneration in critical-size calvarial defects in vivo, as demonstrated by Ko et al. (Figure 3.4).[234]

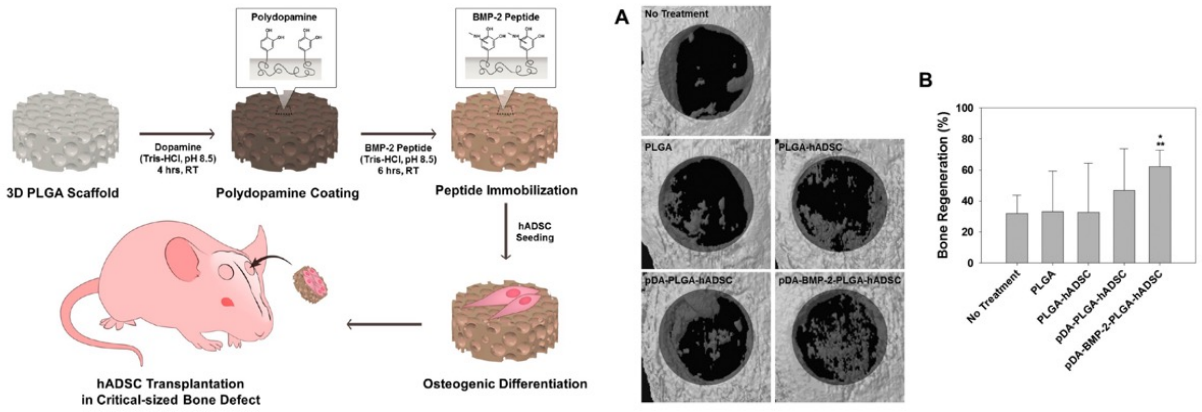


Figure 3.4. Schematic illustration of polydopamine coating combined with BMP-2 immobilization on 3D microporous PLGA scaffolds to promote osteogenic differentiation of hADSCs and bone formation. (A) Micro-CT images of calvarial bones from five experimental groups. (B) Quantification of regenerated bone tissue following hADSCs transplantation. Adapted from Ko et al.[234]

Each bioactive peptide possesses a distinct function determined by its amino acid sequence, three-dimensional conformation, and the specific biomolecule from which it is derived. Collectively, these studies underscore the therapeutic potential of protein-derived peptides, delivered via various scaffold materials and immobilization strategies, to enhance osteogenic differentiation and bone regeneration by mimicking native ECM signaling cues.
By selectively combining peptides with different biological roles, it is possible to activate complementary mechanisms of action, resulting in synergistic effects that surpass the activity of individual sequences alone.[209], [235] Such combinatorial functionalization strategies can more closely replicate the biochemical complexity of the native ECM, enhancing biomaterial bioactivity and potentially improving receptor specificity and binding affinity.

3.3 Synergistic Effects of Multi-Peptide Functionalization on Cell Differentiation

Combining peptides derived from different extracellular matrix (ECM) proteins can help replicate the complexity of the native cellular microenvironment. Many multifunctional strategies designed to enhance the adhesive properties of biomaterial surfaces involve pairing the widely recognized

integrin-binding tripeptide Arg-Gly-Asp (RGD) with additional bioactive motifs to expand their biological effects (Table 3.1). Among integrins, α5β1 and αvβ3 are two principal receptors that specifically recognize the RGD sequence. Although they perform distinct biological functions, their specific roles are not always fully understood. Both integrins bind to extracellular matrix proteins, but with different affinities. For example, α5β1 primarily interacts with fibronectin (FN), whereas αvβ3 can also recognize vitronectin (VN), FN, osteopontin, bone sialoprotein, and other ligands.[236] A well-described case of synergistic binding involves the PHSRN sequence within fibronectin in combination with RGD to enhance α5β1 binding . This interaction plays a central role in regulating cell adhesion, migration, and differentiation in multiple cell types, such as osteoblasts and mesenchymal stem cells. Consequently, biomaterial surfaces functionalized with RGD and PHSRN together have been shown to significantly improve in vitro cell attachment, spreading and differentiation.[237], [238]

Table 3.1 Overview of using combinatorial peptide-based surface modification to enhance biomaterials bioactivity.

Ref.	**Substrate**	**Biomolecules**	**Biological effect**
Hudalla et al.[239]	Gold	RGD + FGF-2	Increased *in vitro* cell spreading
Lee et al.[240]	HA	BMP-2 + OCN	Increased *in vitro* ALP activity, mineralization, BMP-2 and OCN gene expression
Kim et al.[241]	TCPS	RGD + BMP-2	Accelerated *in vitro* osteogenic differentiation of MSCs, increased ALP activity, calcium deposition, BMP-2 and OCN gene expression
Ma et al.[242]	Glass	RGD + BMP-2	Increased *in vitro* proliferation, Runx2 and BSP gene expression
Bilem et al.[215]	Glass	RGD + BMP-2	Increased *in vitro* Runx2 gene expression and decreased Stro-1 gene expression

Pan et al.[243]	Ti	RGD + OGP	Increased *in vitro* ALP activity, mineralization and induced bone formation *in vivo*
Padiolleau et al.[244]	PET	RGD + BMP-2 or OGP	Increased *in vitro* Coll-IA gene expression and ALP activity
Pan et al.[245]	PLGA	K_{16} + TGF-β	Increased *in vitro* differentiation and mineralization, and showed *in vivo* efficacy
Martino et al.[238]	PS	GRGD + PHSRN	Increased *in vitro* cell adhesion and differentiation
Benoit et al.[237]	PEG	RGD + PHSRN	Increased *in vitro* cell adhesion, spreading and differentiation
Moore et al.[223]	Glass	RGD + BMP-2	Upregulation of osteogenic markers
Shin et al.[246]	PLLA	RGD + BCP	Enhanced adhesion, spreading and ALP activity
Yang et al.[247]	Ti	BMP-2 + GDF-5	Upregulation of osteogenic markers and increased *in vitro* cell proliferation, enhanced *in vivo* bone formation and bone remodeling
Dee et al.[248]	Glass	RGD + KRSR	Increased *in vitro* cell attachment and cell spreading
Koepsel et al.[249]	Gold-coated glass	RGD + BMP-2 or heparin mimicking peptide	Increased osteogenic differentiation

Benoit et al. employed a combination of RGD and PHSRN peptides arranged to more closely replicate their natural spatial configuration, using an extended RGD sequence to allow greater spacing between

the two motifs. This biomimetic arrangement resulted in enhanced cell attachment, spreading, and differentiation compared to the use of RGD alone. The observed improvements in cellular behavior were attributed not only to the synergistic interaction between RGD and PHSRN but also to the extended RGD chain, which better mimics the native distance between these sequences in fibronectin. This study highlights the importance of precise biomimetic design in achieving more effective peptide-functionalized biomaterials, demonstrating that arranging peptides in a natural-like configuration can significantly boost their biological efficacy.[237]

In addition to integrin-binding motifs, growth factors (GFs) act as key signaling molecules, regulating cell migration, proliferation, and differentiation. While typically functioning as soluble mediators in paracrine signaling, many GFs can also bind to the ECM and remain biologically active. Moreover, certain GF receptors, such as those for BMP-2 (bone morphogenetic protein 2), can cooperate with integrins to enhance tissue repair.[250]. For instance, Bilem et al. functionalized glass coverslips with both integrin-binding RGD peptides and BMP-2 mimetic sequences using silanization (Figure 3.5). When combined, these peptides significantly enhanced cell attachment, in vitro spreading, and osteoblastic differentiation compared with surfaces grafted with either peptide alone. These results demonstrated a synergistic crosstalk between integrin and BMP receptors, highlighting a promising strategy for advanced surface functionalization to boost the bioactivity of biomaterials.[215]

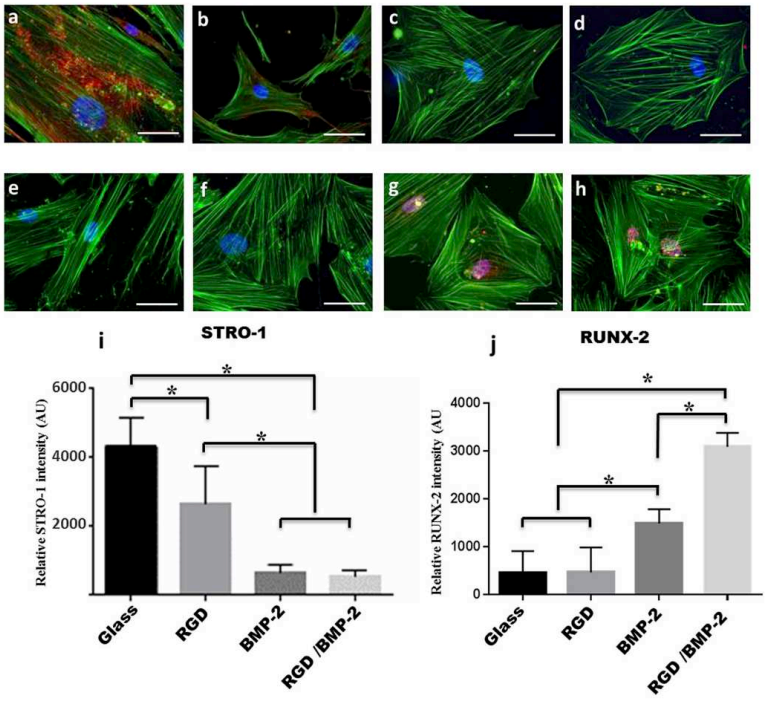


Figure 3.5. Osteogenic commitment of human bone marrow stromal cells (hBMSCs) after 4 weeks of culture on bare glass surfaces (a, e), RGD surfaces (b, f), BMP-2 surfaces (c, g), and RGD+BMP-2 surfaces (d, h). Expression of STRO-1 (i) and RUNX-2 (j) was assessed by immunofluorescence intensity. Adapted from Bilem et al.[215]

Another example of a BMP-2-coated surface is its application in combination with an additional growth factor, such as growth differentiation factor-5 (GDF-5). Yang et al. developed a multicomponent coating for titanium implants that incorporated both BMP-2 and GDF-5, separated by an intermediate heparin layer. This multilayer design enabled the controlled, sustained release of both growth factors from the implant surface. The biological effect of the Ti-BMP-2-GDF-5 coating was evaluated against bare titanium, Ti-BMP-2, and Ti-GDF-5 surfaces. In vitro experiments using MC3T3-E1 pre-osteoblasts showed that the dual coating significantly enhanced cell proliferation and alkaline phosphatase (ALP) activity, leading to increased calcium mineral deposition and upregulated expression of osteocalcin (OCN), type I collagen (COL1), and ALP mRNA compared with the control groups (Figure 3.6A). In vivo studies confirmed these findings, demonstrating greater bone formation at the bone-implant interface and enhanced bone remodeling and regeneration, with the most pronounced effects observed for the Ti-BMP-2-GDF-5 coating (Figure 3.6B).[247]

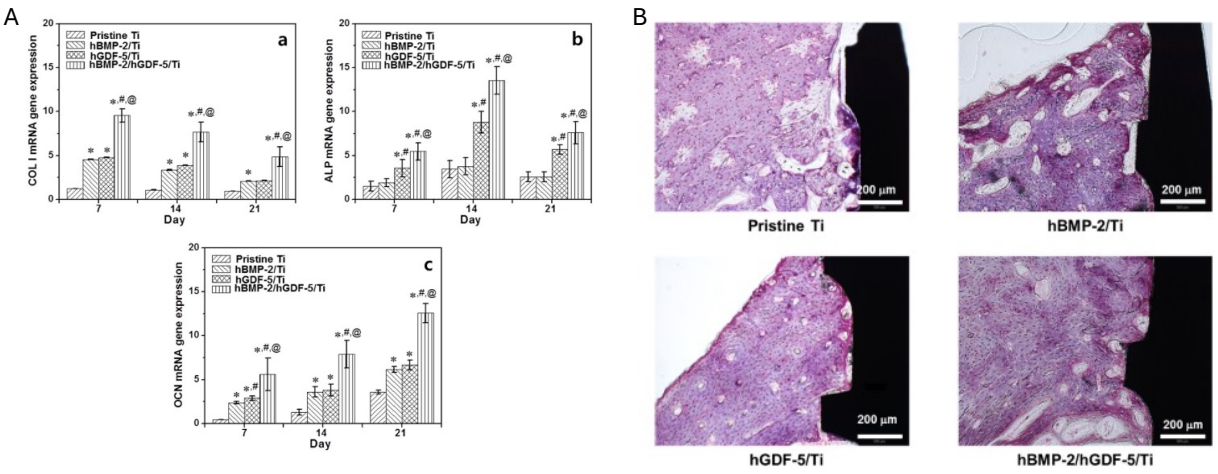


Figure 3.6. (A) Levels of COL1 (a), ALP (b), and OCN (c) mRNA expression at days 7, 14, and 21. (B) H&E-stained images of the surrounding tissue around the samples after implantation for four weeks. Adapted from Yang et al.[247]

Beyond integrin- and growth factor-binding motifs, certain peptides can interact with other cell surface receptors, such as proteoglycans, providing complementary biological effects. For instance, sequences like KRSR or FHRRIKA stimulate osteoblast activity through cell-proteoglycan interactions. Simultaneous targeting of integrin and proteoglycan pathways has been shown to further enhance cell adhesion. The RGD motif promotes anchorage via integrins, while KRSR facilitates attachment through proteoglycans. When used together, these mechanisms can act synergistically to improve cell binding. Dee et al. investigated osteoblast adhesion on glass substrates functionalized with RGD and KRSR peptides via silanization. Surfaces modified with RGD alone supported cell attachment but showed no improvement compared to unmodified glass. In contrast, KRSR alone increased adhesion, and the combination of RGD and KRSR produced the highest attachment levels, attributed to the synergistic effects of engaging both integrin- and proteoglycan-mediated binding.[248]

While most biochemical surface modifications to date have focused on single or dual peptide functionalization, this approach raises the question: are we genuinely replicating the complexity of the native extracellular matrix? The bone microenvironment is characterized by a sophisticated network of multiple, distinct biochemical cues that work synergistically to regulate cell behavior and tissue regeneration. Current strategies that incorporate only one or two bioactive peptides fall short of capturing this intricate interplay. Consequently, there is a clear gap in the development of

multifunctional biomaterial surfaces that integrate multiple peptides representing diverse ECM components. Addressing this gap through innovative multi-peptide functionalization strategies is essential to more faithfully mimic the native ECM and ultimately enhance the efficacy of biomaterials for bone regeneration.

Chapter 4

Project overview and research objectives

Strategies for bone tissue engineering often combine three key elements: biomaterials, stem cells, and bioactive molecules. Modifying materials using bioengineering techniques is one of the most explored fields in tissue engineering to enhance biological function, biocompatibility, and control of the cellular microenvironment. Specifically, incorporating peptides into biomaterial surfaces that mimic the native extracellular matrix (ECM) enhances cell recruitment and induces cell signaling pathways, promoting various modulatory biochemical responses.
This research project aimed to engineer biomaterial surfaces that closely mimicked the ECM to influence stem cell behavior and promote osteogenic differentiation. The project introduced an innovative surface functionalization method designed to create in vitro platforms capable of inducing rapid, effective, and reproducible osteogenic differentiation of human mesenchymal stem cells (hMSCs).

4.1 Comparative study on silanization techniques for surface modification

The first objective of this research was to develop and optimize a surface modification strategy based on silanization to facilitate the effective grafting of bioactive peptides. Specifically, a comprehensive comparative study was undertaken to evaluate various silanization techniques and silane molecules, including traditional methods such as the immersion method. This work proposed and validated spin coating as a novel and viable alternative for silanization, aiming to enhance the uniformity, reproducibility, and precision of peptide-functionalized surfaces. An innovative spin coating protocol was introduced employing a newly synthesized aminosilane molecule, Alk-Phtha, designed to challenge conventional silanes like APTES and AUTES (Figure 4.1). This approach targeted the

formation of well-defined self-assembled monolayers to improve subsequent bioactive molecule grafting essential to guide stem cell adhesion. The efficiency of surface modification at each step was systematically validated through a combination of characterization techniques. Water contact angle measurements assessed changes in surface hydrophilicity, while X-ray photoelectron spectroscopy (XPS) and polarization modulation-infrared reflection absorption spectroscopy (PM-IRRAS) provided detailed chemical composition and molecular bonding information. To assess the biological functionality of the modified surfaces, immunocytochemistry was employed to examine the behavior of mesenchymal stem cells cultured on these substrates. Differences in protein expression related to cell adhesion processes were analyzed to confirm the influence of surface functionalization on stem cell bioactivity.

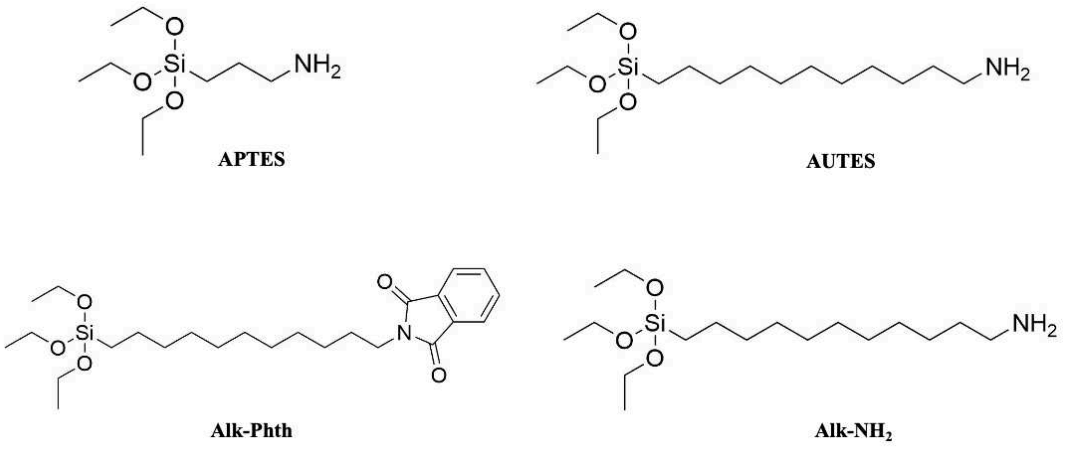


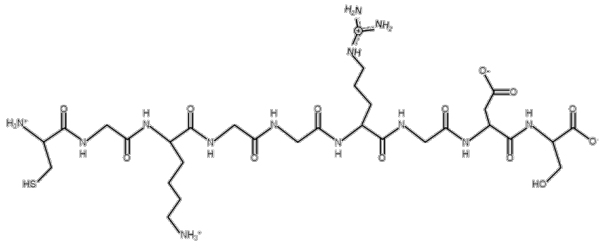
Figure 4.1. Chemical structures of the silane molecules utilized in this study: 3-aminopropyltriethoxysilane (APTES), 11-aminoundecyltriethoxysilane (AUTES), alkylsilane functionalized with a protective phthalimide group (Alk-Phtha), and the corresponding deprotected amino-terminated silane (Alk-NH_2).

4.2 Synergistic effect of multi-peptide functionalized interfaces

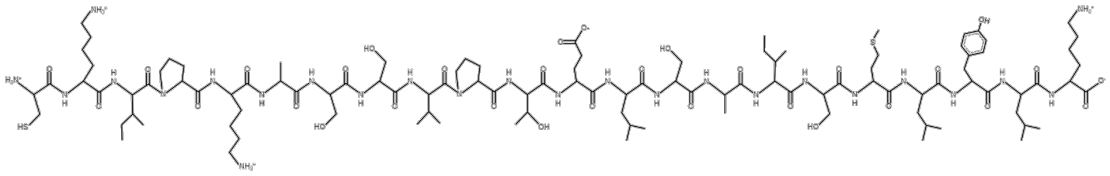
The second objective of this research focused on replicating the biochemical complexity of the native extracellular matrix to better influence mesenchymal stem cell behavior. Recognizing the ECM as a critical regulator of stem cell fate, this study explored the synergistic effects of co-immobilizing

multiple ECM-inspired peptides to more closely mimic the native cellular microenvironment. To achieve this, surfaces were functionalized simultaneously with three distinct peptides: adhesion-promoting peptide RGD, collagen-mimetic peptide P15, and growth factor mimetic-peptide BMP-2 (Figure 4.2). This tri-peptide functionalization strategy aimed to enhance adhesion, migration, and the early osteoblastic differentiation of human mesenchymal stem cells by leveraging the complementary biochemical signals provided by each peptide. Surface modification was primarily validated through PM-IRRAS analysis. Additionally, high-resolution fluorescence microscopy was utilized to confirm efficient and homogeneous grafting of multiple peptides, an essential consideration given the complexity of simultaneously immobilizing up to three different bioactive sequences. Biological responses of hMSCs cultured on the multi-peptide functionalized surfaces were extensively evaluated. Gene expression related to osteogenic differentiation was assessed at early and late time points using reverse transcription quantitative polymerase chain reaction (RT-qPCR), providing a quantitative measure of the differentiation process. Complementing this, immunocytochemistry offered detailed insights into protein expression at the single-cell level, allowing observation of heterogeneity within the cell population and precise localization of osteogenic markers.

(a)



(b)



(c)

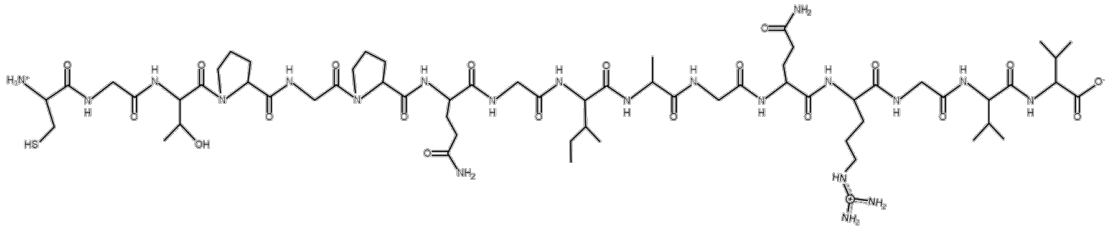


Figure 4.2. Molecular structures of the ECM-inspired peptides used in this study: (a) RGD, (b) BMP-2, (c) P15.

Results and Discussion

Chapter 5

Study 1: Silanization Strategies for Tailoring Peptide Functionalization on Silicon Surfaces: Implications for Enhancing Stem Cell Adhesion

Melissa Kosovari[1,2,3], Thierry Buffeteau[5], Laurent Thomas[5], Andrée-Anne Guay Bégin[2,3], Luc Vellutini[5], James D. McGettrick[4], Gaétan Laroche[2,3,□,*], Marie-Christine Durrieu[1,□,*]

[1]Univ. Bordeaux, CNRS, Bordeaux INP, CBMN, UMR 5248, F-33600 Pessac, France.

[2]Laboratoire d'Ingénierie de Surface, Centre de Recherche sur les Matériaux Avancés, Département de Génie des Mines, de la Métallurgie et des Matériaux, Université Laval, 1065 Avenue de la médecine, Québec G1V 0A6, Canada

[3]Axe médecine régénératrice, Centre de Recherche du Centre Hospitalier Universitaire de Québec, Hôpital St-François d'Assise, 10 rue de l'Espinay, Québec G1L 3L5, Canada

[4]College of Engineering, Swansea University Bay Campus, Swansea SA1 8EN, United Kingdom

[5]Univ. Bordeaux, CNRS, Bordeaux INP, ISM, UMR 5255, F-33400 Talence, France

□ Equally contributed.

* Corresponding authors:

Marie-Christine Durrieu: marie-christine.durrieu@inserm.fr

Gaétan Laroche: Gaetan.Laroche@gmn.ulaval.ca

This work has been published in the journal ACS Applied Materials and Interfaces.

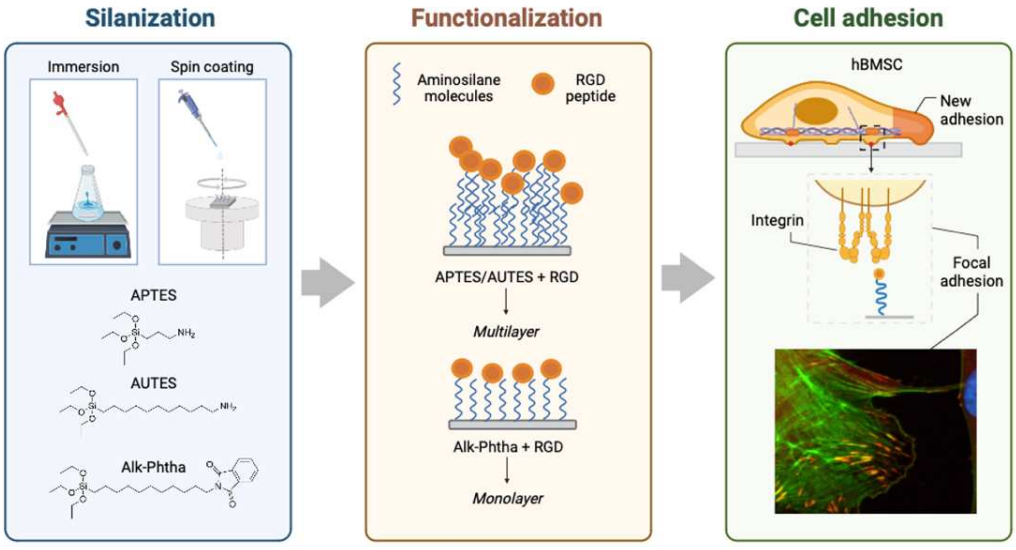
5.1 Résumé

L'ingénierie des surfaces de biomatériaux et l'intégration de ligands favorisant l'adhésion cellulaire jouent un rôle essentiel en recherche biologique et dans les applications biotechnologiques. L'interaction entre les cellules et leur microenvironnement, influencée par des signaux chimiques et physiques, impacte le comportement cellulaire. La modification de surface des biomatériaux influence profondément les réponses cellulaires, en particulier à l'interface cellule-surface. Ce travail se concentre sur l'amélioration des activités cellulaires par la manipulation des matériaux, en mettant l'accent sur la silanisation pour la fonctionnalisation ultérieure avec des molécules bioactives telles que les peptides RGD afin d'améliorer l'adhésion cellulaire. La greffe de trois silanes distincts sur des tranches de silicium a été étudiée en utilisant les méthodes de dépôt par spin coating et immersion. Cette étude éclaire les effets des différentes longueurs de chaînes alkyles et des groupes protecteurs sur le comportement cellulaire, apportant des connaissances précieuses pour l'optimisation des monocouches auto-assemblées (SAM) à base de silanes avant la greffe de peptides ou protéines, et ce pour la première fois. En particulier, elle remet en question l'usage courant des molécules APTES dans ce contexte. Ces résultats font progresser la compréhension des stratégies de modification de surface, ouvrant la voie à l'adaptation des surfaces de biomatériaux pour moduler le comportement cellulaire dans diverses applications biotechnologiques.

5.2 Abstract

Biomaterial surface engineering and integrating cell-adhesive ligands are crucial in biological research and biotechnological applications. The interplay between cells and their microenvironment, influenced by chemical and physical cues, impacts cellular behavior. Surface modification of biomaterials profoundly affects cellular responses, especially at the cell-surface interface. This work focuses on enhancing cellular activities through material manipulation, emphasizing silanization for further functionalization with bioactive molecules like RGD peptides to improve cell adhesion. The grafting of three distinct silanes onto silicon wafers using both spin coating and immersion methods was investigated. This study sheds light on the effects of different alkyl chain lengths and protecting groups on cellular behavior, providing valuable insights into optimizing silane-based self-assembled monolayers (SAMs) before peptide or protein grafting for the first time. Specifically, it challenges the common use of APTES molecules in this context. These findings advance our understanding of surface modification strategies, paving the way for tailoring biomaterial surfaces to modulate cellular behavior for diverse biotechnological applications.

Graphical abstract



5.3 Introduction

The field of biomaterial surface engineering and cell-adhesive ligands is expanding, representing a key area of biological investigation and a promising avenue for biotechnological applications[251]. In their natural environment, cells encounter different chemical and physical factors on various scales, from nanometers to hundreds of microns[252], [253].

Cellular behaviors are heavily influenced by the microenvironment in which they exist[254]. Indeed, cells can sense and respond to various physical and functional properties of their external environment through the formation of adhesions, a critical process for their decision-making and behavior[209], [255]. Cell membrane receptors, like integrins, play a significant role in transmitting physical information from the microenvironment into intracellular signaling pathways, ultimately leading to changes in cell proliferation, differentiation, migration, or apoptosis behaviors[256], [257]. Surface modification significantly affects the modulation of cellular activities because all functions are concentrated at the cell-surface interface[258]. Several strategies to control the biochemical properties of materials used in tissue engineering mainly influence focal adhesion (FA) formation and growth[259]. One of the most common is functionalization with ligands. However, various proteins or peptides involved in cell adhesion may adsorb unevenly or not be readily available to cells, thus impairing FA dynamics[260], [261]. Techniques used for chemical modification of a biomaterial aim to add a functional group, such as amines, carboxylic acids, or thiols, to the surface[107]. These groups allow for the covalent immobilization of polypeptides, whole proteins, glycosaminoglycans, or other selected molecules that can promote cell adhesion[262]. Creating robust and functional organic films as primary layers with controlled density is crucial in the field of biotechnological applications ranging from biosensors to tissue engineering. Silane-based self-assembled monolayers (SAMs) find diverse applications on silica substrates, leading to extensive research spanning several decades to refine fabrication techniques[161]. SAMs have been widely used to generate specific functional groups on oxide surfaces. The robustness of trialkoxysilanes-based SAMs comes from forming a siloxane bonds network by the horizontal polymerization between neighboring silanes and the free hydroxide groups on the silica surface[260].

Amino-terminated SAMs have been widely used for covalently immobilizing biomolecules to control cell behavior. In the intricate extracellular matrix (ECM) environment, where cells respond to dynamic cues, there is a crucial need to replicate the native microenvironment. This replication is designed to

facilitate the migration of stem cells while concurrently enhancing the microenvironment's capacity to attract cells on the surface. Conversely, when the surface remains untreated, immune cells often identify it as foreign, triggering an exaggerated inflammatory response[263]. When attaching organic molecules to inorganic surfaces, one common practice involves depositing self-assembled monolayers to modify these surfaces with reactive groups, such as amino groups achieved through the coupling of organosilanes. Subsequently, biomolecules can bind to these chemically altered surfaces by reacting with the introduced groups[264]. Chuah et al. observed significant transformations in the native surface properties of PDMS (polydimethylsiloxane), with a notable improvement in MSC (mesenchymal stem cells) adhesion evident upon APTES (3-aminopropyl-triethoxysilane) modification. This highlights the profound influence of silanization on PDMS surface characteristics, including decreased hydrophobicity, increased protein immobilization, and variations in nanotopography[184]. Furthermore, even the amine groups on APTMS-modified (3-aminopropyl-trimethoxysilane) surfaces exhibited a more efficient improvement in cell adhesion compared to the hydroxyl groups found on oxygen plasma-treated PDMS surfaces. The absorption of proteins emerges as an early in vivo occurrence in the interplay between implanted biomaterial and living tissue. Consequently, a surface featuring an organized arrangement of functional groups can serve as a conducive site for cell growth in the development of biomaterials[265]. The biological properties of silanized graphene oxide (SiGO) were explored in the context of material biomedical applications. Silanization using APTES enhanced the material in vitro cytocompatibility and mitigated its in vivo toxicity. The findings additionally indicated that SiGO exhibits superior biocompatibility compared to graphene oxide (GO), suggesting potential applications in the field of biomedical engineering [266].

Amino-terminated SAMs are generally prepared using commercially available organosilanes such as 3-aminopropyl-triethoxysilane (APTES) and 11-aminoundecyltriethoxysilane (AUTES). Silanization usually proceeds by immersing the material in an organosilane solution using an organic solvent. This so-called immersion silanization method is simple and easy to conduct. However, controlling the layer structure of amino-terminated SAMs is difficult, leading to the non-reproducibility of surface functionalization[267], [268]. The multiple possibilities of interactions of the amino-end group by hydrogen bonds and electrostatic attractions render the molecular organization in the organic layer difficult and, therefore, affect the accessibility and reactivity of the amine group[269]. A terminal amino protecting group such as N-phthalimide can be used to avoid multiple interactions[270] to prevent uncontrolled orientation of the amino silanes. Two prevalent methods for

surface modification involve silanes: solution-based reactions and vapor-phase deposition. The traditional solution immersion technique submerges clean substrates in a diluted solution of silylated coupling agents within a controlled environment. However, it generates significant chemical waste due to the use of organic solvents. In contrast, the chemical vapor deposition (CVD) method exposes clean substrates to silane vapor, eliminating the need for organic solvents but requiring ultra-high vacuum conditions and elevated temperatures. Less commonly used techniques, such as the Langmuir−Blodgett method and spin coating, have seen limited application and less extensive study than the primary methods[182], [271]. Here, we propose to employ spin coating for the first time as a methodology for rapidly and cost-effectively immobilizing silane molecules on silicon surfaces for bioactive molecule grafting. According to the literature, the fabrication of silane-based SAMs utilizing the spin coating technique was explored as an alternative, adaptable, and cost-effective approach in contrast to the traditional solution immersion method[272].

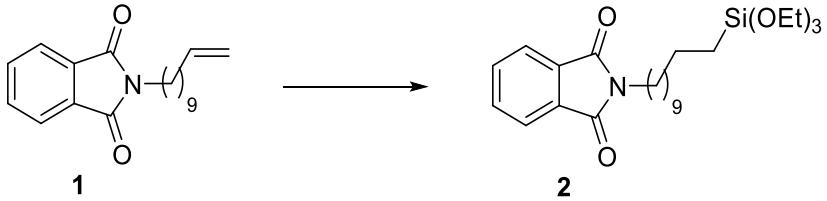
This study aimed to assess the influence of diverse silanization protocols (using conventional immersion method *vs* spin coating) using heterobifunctional silanes to obtain amino-functionalized silicon wafer surfaces for further RGD peptide conjugation and their impact on mesenchymal stem cell adhesion[12]. Organosilane molecules with identical trialkoxy anchoring groups but different alkyl chain lengths were investigated. On the other hand, a comparative analysis included molecules of identical chain lengths with or without N-phthalimide protecting groups opposite to the surface. This exploration aimed to evaluate the influence of the different alkyl chain lengths and the protecting group presence on the silane-based monolayer's distribution on the silicon surface, as well as its implications for the accessibility and subsequent efficacy of peptide grafting. This investigation enabled to highlight differences in surface functionalization using different silanization methods and their subsequent influence on cellular behavior, mainly focusing on adhesion dynamics and cell spreading tendencies. This study constitutes the first step toward the investigation of stem cell differentiation using fully optimized and controlled surface chemistries for further grafting of various bioactive molecules.

5.4 Materials and Methods

5.4.1 Materials

Silicon wafers (100 mm, thickness 500-550 μm) were obtained from Pure Wafer, San Jose, CA. The SiO_2/Au substrates used for PM-IRRAS experiments, specifically Goldflex mirrors with a SiO_2 protective layer (Goldflex PRO, reference 200785), were provided by Optics Balzers AG. Hydrogen peroxide (33 wt %), sulfuric acid (concentrated), acetone, ethanol, anhydrous toluene, dimethylsulfoxide (DMSO), 3-aminopropyltriethoxysilane (APTES), and succinimidyl-4-(p-maleimidophenyl) butyrate (SMPB) were all acquired from Sigma-Aldrich, France, while 11-aminoundecyltriethoxysilane (AUTES) was purchased from Gelest, Inc., Morrisville, PA. Alk-Phtha was synthesized in the Molecular Chemistry & Materials team at ISM, Bordeaux University, under the supervision of Prof. Luc Vellutini. GeneCust in Boynes, France, synthesized the fluorophore-tagged peptide CG-K(PEG3-TAMRA)-GGRGDS, referred to as RGD (molecular weight = 1437 g mol^{-1}). Bone marrow mesenchymal stem cells (hBMSCs), mesenchymal stem cell growth medium 2, and SupplementMix MSC growth medium 2 were procured from PromoCell GmbH, located in Heidelberg, Germany. Monoclonal Anti-Vinculin antibody (produced in mice) was obtained from Sigma-Aldrich, St. Louis, USA. Dulbecco's modified Eagle's medium (DMEM), Dulbecco's phosphate buffered saline (1×) (PBS), Trypsin-EDTA, fetal bovine serum (FBS), Alexa Fluoroshield™ 488 phalloidin, secondary antibodies (goat anti-mouse lgG (H + L) highly cross-adsorbed secondary antibody Alexa Fluoroshield™ 568 and DAPI were procured from Thermo Fisher Scientific (USA). Antibiotic/antimycotic solutions were obtained from GE Healthcare Life Sciences (USA).

Synthesis of phthalimide-terminated coupling agents



1 **2**

Scheme 1. Synthesis of phthalimide-terminated silylated coupling agent **2**: compound **1** was synthesized according to ref 17. Compound **2** was synthesized by a hydrosilylation reaction using $HSi(OEt)_3$ (5 eq.), MeCN, cat. Karstedt (0.0125 eq. Pt), 60 °C, 1 h.

The synthesis of coupling agents terminated with phthalimide (**2**) was performed to combine the same structure as AUTES but with the end amino group protected by a N-phthalimide group until deprotection and further grafting (Alk-NH_2). Phthalimide-terminated triethoxysilane **2** was synthesized by using the platinum-catalyzed hydrosilylation of alkene precursor **1**, as shown in Scheme 1. A dry Schlenk tube under inert atmosphere was filled with the alkene precursor **1** (1.014g, 3.4 mmol, 1eq) and 30 mL of anhydrous acetonitrile when needed. Triethoxysilane (2.33g, 14.2 mmol, 4 eq) was introduced in the Schlenk tube followed by Karstedt's catalyst (326 µl, 1 mmol, 0.3 eq). After 2 h under stirring at 60 °C, evaporation of the solvent occurred. The brown crude product underwent filtration on a silica pad with CH_2Cl_2, resulting in the acquisition of a colorless oil of compound **2** with an 85% yield after evaporation of CH_2Cl_2.

^{1}H NMR ($CDCl_3$, 300 MHz) δ (ppm): 7.86 (dd, J = 5.4, 3.0 Hz, 2H, 2 CH_{ar}), 7.72 (dd, J = 5.5, 3.1 Hz, 2H, CH_{ar}), 3.83 (q, 6H, 3 CH_2OSi), 3.70 (t, *J* = 7.2 Hz, 2H, CH_2N), 1.34 - 1.26 (m, 18H, 9 CH_2), 1.25 (t, 9H, 3 CH_3), 0.65 (m, 2H, CH_2Si).

^{13}C NMR ($CDCl_3$, 100 MHz) δ (ppm): 168.6 (2 CO), 134.0 (2 CH_{ar}), 132.3 (2 C_{ar}), 123.3 (2 CH_{ar}), 58.4 (3 CH_2OSi), 38.2 (CH_2N), 33.3 (CH_2), 29.7 (CH_2), 29.6 (2 CH_2), 29.4 (CH_2), 29.3 (CH_2), 28.7 (CH_2), 27.0 (CH_2), 22.7 (CH_2), 18.44 (CH_3), 10.5 (CH_2Si).

^{29}Si NMR ($CDCl_3$, 79 MHz) δ (ppm): -41.2. **HRMS** (ESI)**:** calculated for $C_{25}H_{41}O_5NSiNa^+$ ([M+Na^+]): 486.2646, found 486.2640.

5.4.2 Sample preparation

Activation. Silicon wafers were resized into appropriate dimensions, approximately 0.5 cm × 0.5 cm. The silicon slides underwent ultrasonic cleansing through successive immersions in acetone (10 min), deionized water (10 min), and methanol (10 min). Following this, the slides were activated by further immersion in a piranha solution (mixture of 10 mL of H_2O_2 (33% wt.) and 30 mL of concentrated H_2SO_4) for 15 min in an ultrasonic bath. Subsequently, the samples were subjected to three rounds of ultrasonic cleansing in water for 10 minutes and in methanol for 2 minutes. SiO_2/Au substrates were resized into suitable dimensions, approximately 2 cm × 2 cm. These substrates underwent thorough washing with Milli-Q water (18 MΩ cm), followed by a 15-minute sonication in chloroform and exposure to UV-ozone (185-254 nm) for 30 minutes. They were promptly utilized for silanization via either the spin-coating process or the immersion solution method.

Silanization by spin coating and immersion method. Two silanization techniques, spin coating and immersion, were investigated for efficient silanization, with three different silane molecules (Scheme 2): APTES (3-aminopropyltiethoxysilane) and AUTES (11-aminoundecyltriethoxysilane) commercial molecules, as well as a third silane molecule, Alk-Phtha (phthalimide-terminated undecyltriethoxysilane). The time of exposure to the silane solution was optimized according to Rouvière et al[270].

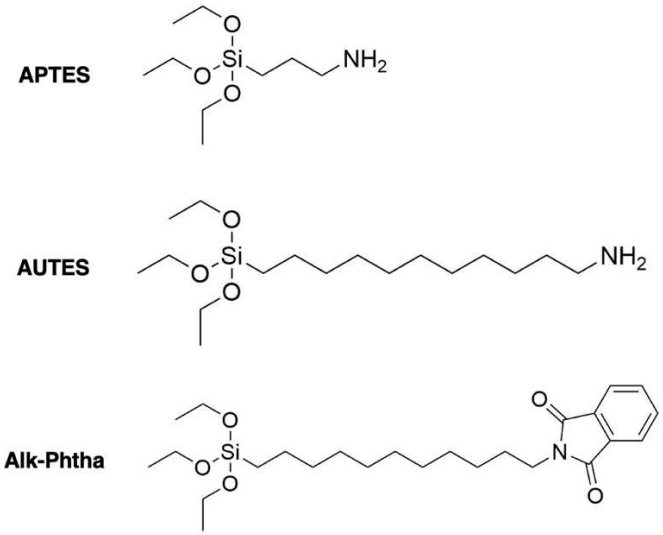
Silanization by immersion. After silicon surface activation, the cleaned surfaces were immediately functionalized with silane molecules. The specimens were soaked in a 2% v/v silane solution diluted in anhydrous toluene for a duration of 1 hour. The final volume of the silane solution ranges between 40 and 60 ml to adequately cover all surfaces of the immersed samples. The process was carried out with stirring and in an inert nitrogen environment. Following silanization, the substrates underwent outgassing at 120°C under vacuum for 1 h. Following this, the samples were treated to ultrasonic cleaning with anhydrous toluene, deionized water and methanol (2 sessions of 5 minutes each) to eliminate any unbound molecules.

Silanization by spin coating. Silane molecules were dissolved in absolute ethanol under an inert nitrogen atmosphere to achieve a final concentration of 2% v/v. 160 µL of the silane solution prepared just before was utilized to coat the silicon or SiO_2/Au substrates (2 cm^2 dimensions) at a rotation of 6000 rpm for 60 s. The samples underwent overnight drying at 120 °C under vacuum. Subsequently, they were subjected to sonication in ethanol, water and methanol (2 cycles of 5 minutes each) for washing.

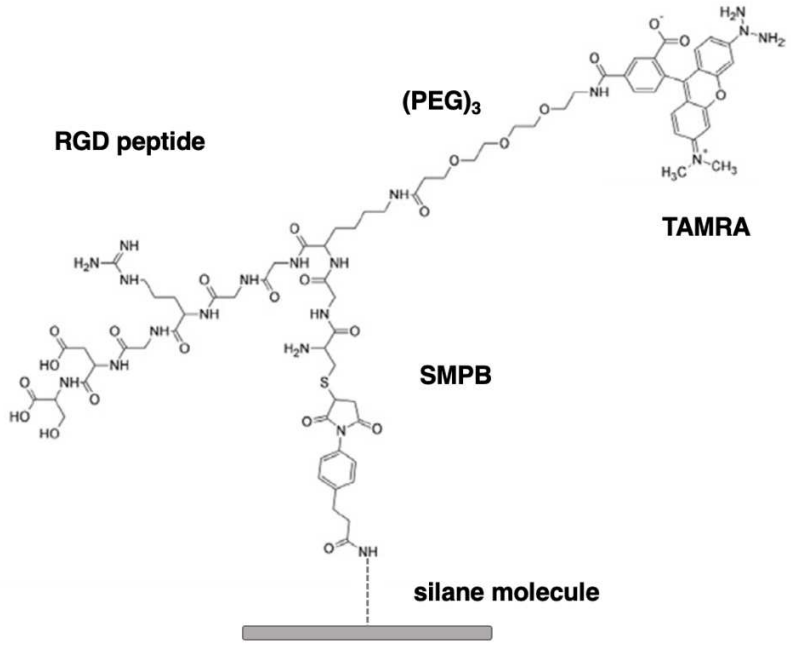
SMPB Crosslinker conjugation. Before peptide grafting, aminated silicon surfaces underwent conjugation with the heterobifunctional SMPB crosslinker. The succinimidyl functionality of this compound reacted with the surface amine groups, resulting in pendent maleimidyl moieties. These moieties subsequently reacted with thiol groups from the terminal cysteine of selected peptides. Initially, aminated surfaces were immersed in a solution of SMPB dissolved in DMSO at a concentration of 3 mg/mL for 2 hours in the dark. Following this, the substrates underwent a gentle washing with methanol and were rinsed in DMSO for 10 minutes using an ultrasonic bath. After the cleaning process, the substrates were air-dried and kept in the dark for 24 hours before peptide grafting.

RGD peptide grafting. SMPB-grafted surfaces were immersed in 300 µL of 0.1 mM CRGD-TAMRA PBS1X solution in a dark, moist chamber at room temperature to achieve anchoring of fluorescently labeled RGD mimetic peptides (Scheme 3). Samples were then cleaned by ultrasonication six times

for 15 min in nano-pure water to remove all non-covalently attached peptides. All reactions were performed under agitation at room temperature.



Scheme 2. Molecular structures of different silane molecules involved in the silanization process.



Scheme 3. Molecular structures of fluorophore labelled peptide anchored to SMPB crosslinker. [273]Adapted with permission from Hoesli C. et al.[273]

5.4.3 Surface Characterization

Water contact angle (WCA). The assessment of surface wettability involved measuring water contact angles after the deposition of nano pure water droplets of 3 µL at 20 °C in static mode on a Krüss DSA 100 goniometer. The reported contact angle values resulted from the mean of three drops on different surfaces (n between 2 and 6).

Atomic Force Microscopy (AFM). The measurements were performed on a Bruker Dimension Fastscan AFM in tapping mode in air using a Bruker SNL-C cantilever (resonant frequency around 56 kHz and nominal curvature radius of 2 nm) (Bruker, Billerica, USA). AFM images treatment and roughness analysis were performed with Gwyddion software.

X-Ray Photoelectron Spectroscopy (XPS). XPS analysis was performed on an Axis Supra instrument (Kratos Analytical, UK) using monochromated Al Kα x-rays at 15 mA, 225 W emission, with the electron lenses set in the 'Hybrid' mode. For every sample. ann initial survey scan of pass energy 160 eV was performed. High-resolution spectra were then obtained for each element identified in the survey scan with a pass energy of 40 eV, step size of 0.1 eV, and a minimum dwell time of 500 ms. Where atomic concentrations are low for a given element, extra sweeps and longer dwell times were introduced to improve signal-to-noise ratio. The integral charge neutralizer was used to limit differential charging. Analysis of the data was conducted utilizing CasaXPS (Version 2.3.24PR1.0, Casa Software Ltd, UK). Spectra were fitted with a Shirley baseline, and a synthetic component was used to model the data. The synthetic components utilized the mixed Gaussian-Lorentzian (GL (30)) line shape, and FWHM was kept constant for a given element. The spectra were charge-corrected to correct the C(1s) hydrocarbon component to 285.0 eV. The area of each peak was corrected using the Kratos sensitivity factor library. The expected theoretical values were calculated only based on the atomic composition of the silane molecules, without considering the composition of the surface on which they are anchored.

Polarization Modulation Infrared Reflection-Absorption Spectroscopy (PM-IRRAS). PM-IRRAS experiments utilized a ThermoNicolet Nexus 670 FTIR spectrometer equipped with a PM-IRRAS optical bench[28]. Spectra were acquired with a resolution of 4 cm^{-1} over a 5-hour acquisition period. Calibration was adjusted to present the PM-IRRAS spectra in IRRAS units[274], [275]. Data collection occurred in a dry-air atmosphere following a 1-hour incubation in the chamber.

5.4.4 Cell culture experiments

Commercially available Human Bone Marrow Mesenchymal Stem Cells (hBMSCs) were grown on culture flasks in DMEM medium enriched with 1% Pen Strep in serum-free conditions, subcultured using trypsin/EDTA 1x and sustained in a humidified atmosphere with 5% CO_2 at 37°C. RGD-grafted 1 × 1 cm silicon substrates were placed in 24-well cell culture plates. A density of 3000 cells/cm^2 of hBMSCs at the third passage were seeded onto surfaces grafted all with RGD but treated with different silanization methods. The cells were cultured for 24 h in serum-free DMEM medium. This condition enables interactions between grafted RGD peptides and their cell surface receptors without interference with serum proteins.

Immunocytochemical analysis. Following 24 h of cell culture, hBMSCs underwent PBS 1X rinsing and fixation in 4% paraformaldehyde at 4 °C for 20 min. Samples were then permeabilized with 0.5% Triton X-100 in PBS 1X for 5 min and blocked with 1% Bovine Serum Albumin (BSA) in PBS 1X for 30 min at 37 °C. Incubation with 1:200 primary antibodies mouse monoclonal anti-vinculin in 1% BSA in PBS was carried out for 1 h at room temperature. Next, samples were washed in PBS 1X, prior incubation with the secondary antibody Alexa Fluor 568 goat anti-mouse IgG (H + L) (1:200 dilution) for 30 min at room temperature. Incubation with Alexa Fluor 488 phalloidin (1:40 dilution) for 1 h at 37 °C was performed in order to detect the presence of cytoskeletal fibers of F-actin. Three rinsing cycles with 1X PBS and subsequent labeling of the cell nuclei with 20 ug/ml DAPI for 10 min at room temperature followed. Finally, surfaces were examined using a Leica DM5500B microscope equipped with a motorized and programmable stage and a CoolSnap HQ camera controlled by Metamorph 7.6. Image J freeware (NIH, http://rsb.info.nih.gov/ij) was used for quantification of vinculin and phalloidin expression. All stained marker images were acquired at the same exposure time, using a 40x objective. Image files were opened with Image J and converted to 16-bit files. The intensity detection of the green and red colour emitted by the label, was obtained taking into consideration the subtraction of the background signal from the RGD-TAMRA surfaces. The values of fluorescence intensity were obtained from the analyses performed on at least 80 cells for each surface type.

5.4.5 Statistics

Results are expressed as means ± SEM. Data were analyzed with Prism Software (GraphPad Software Inc.). Comparisons were made using ANOVA coupled with Tukey's multiple comparisons test. The statistical significance was defined for a P value of at least < 0.01.

5.5 Results

5.5.1 Characterization of the biochemical modification of silicon surfaces

Silanization experiments were performed for all three molecules (APTES, AUTES, Alk-Phtha) using both methodologies (spin coating and immersion). From these experiments, we decided to select the best technique for each silane molecule in terms of reproducibility based on XPS analyses (data not shown), with five experiments conducted for each method. It turned out that spin coating was selected for APTES and Alk-Phtha silanization, while the immersion method was chosen for AUTES silanization. Accordingly, we aimed to compare the three most efficient strategies to choose the best one above all, which could stand as the optimal solution for silanization processes for biological purposes. Of note, Rouvière et al.[272], have shown by PM-IRRAS experiments that the grafting of Alk-Phtha by spin coating and immersion methods give the same results by optimizing the experimental conditions of deposition.

5.5.2 Water Contact Angle and Atomic Force Microscopy

This technique provides a first indication that a change in the hydrophilic nature of the surface has occurred. Indeed, contact angle measurements made it possible to determine the hydrophobicity and hydrophilicity properties of the surface after each step of surface modification. After activation with piranha, the surface shows characteristic hydrophilicity ($< 10°$) due to the hydroxyl groups provided by the treatment. Following silanization, the increase in contact angle measurement confirms that wettability change has occurred, and the AUTES exhibited the highest hydrophobic character ($73 \pm 2°$) as compared to the APTES surface ($62 \pm 9°$) and deprotected Alk-NH_2 ($67 \pm 3°$). The observed transition from high hydrophilicity after piranha treatment to increased hydrophobicity underscores the effectiveness of silanization surface modification. AFM measurements were carried out to determine surface roughness and complement the evaluation of hydrophilicity. These data show that

the roughness of the various silane-conjugated surfaces ranges between 2.3 nm and 4.1 nm, meaning that the hydrophilicity differences between all investigated samples should be related to the chemical nature of the silane molecules as opposed to the surface roughness. These roughness measurements, as measured by AFM, are now provided along with the contact angle data in Table 5.1.

Table 5.1 Root mean square roughness (R rms) calculated by AFM measurements

Substrates	Water Contact Angle	Roughness RMS (nm)
Silicon	< 10°	0.3
APTES	62 ± 9°	3.4
AUTES	73 ± 2°	2.3
Alk-NH_2	67 ± 3°	4.1

5.5.3 X-Ray Photoelectron Spectroscopy

The efficiency of the silanization reaction with the three different silane molecules was confirmed by XPS analysis. Each surface exhibited the expected elements, with an increase in the percentage of carbon recorded and a decrease in oxygen and silicon, as expected from the chemical structure of APTES, AUTES, and Alk-NH_2 (Table 5.2). Contamination from carbonaceous species is always detected on any surface and cannot be removed entirely, even in an ultra-high vacuum. The appearance of nitrogen clearly showed the efficiency of aminosilanization since no nitrogen was observed on the piranha-activated surface (Table 5.2).

A high presence of silicon was observed when compared with the chemical structure of the molecules (scheme 1) under all conditions. This can be attributed to the silicon wafer to which these molecules are attached. In fact, chemical composition analysis with XPS also detects the substrate-derived silicon component and not only that of the grafted silanes.

Table 5.2 XPS survey analyses of silicon surfaces after activation, silanization, and RGD grafting.

	% C	% O	% Si	% N	N/C
Piranha	13 ± 1	38 ± 2	49 ± 1		
APTES	34 ± 2	31.2 ± 0.9	31 ± 2	4.2 ± 0.9	0.12
RGD	35 ± 2	28 ± 1	29 ± 1	5.2 ± 0.4	0.15
AUTES	65 ± 1	20 ± 1	12.2 ± 0.2	3.5 ± 0.3	0.05
RGD	55.2 ± 0.8	20.2 ± 0.3	14.7 ± 0.9	5.6 ± 0.2	0.1
Alk-NH_2	17.6 ± 0.2	32.9 ± 0.2	48.2 ± 0.1	1.0 ± 0.1	0.06
RGD	20 ± 3	32 ± 1	43 ± 2	2.2 ± 0.6	0.11

Figure 5.1 (left) represents XPS high-resolution spectra of silanized surfaces in the Si2p region for the three different silane molecules. The Si2p profile of the APTES-modified surface is identical to the one observed for the Alk-NH_2-modified surface. In contrast, the Si2p XPS spectrum obtained after the AUTES silanization is quite different from those of APTES and Alk-NH_2-modified surfaces, especially for AUTES and Alk-NH_2, which display the same molecular structure (Scheme 1). The Si2p XPS signal globally shows two distinct doublets, corresponding to bulk silicon (99.1 eV) and silicon bonded to oxygen (103.8 eV). On the APTES and Alk-NH_2-modified surfaces, the ratio of the Si peak to the SiO_2 peak is approximately 70/30, but for the AUTES-modified surface, the ratio is 10/90. This increase in the contribution of SiO_2 on the AUTES-modified Si surface may be due to two factors that are consistent with a higher surface loading of AUTES relative to APTES and Alk-NH_2-modified surfaces. First, the addition of AUTES on the surface could result in the deposition of a thicker layer on top of the silicon than the deposition of the other two silane compounds, thus leading to an attenuation of the XPS signal of the underlying bulk Si (elemental) and increasing the relative contribution of both the native SiO_2 oxide on the wafer and of the silane functional group. Second, the AUTES is grafted more densely on the surface, decreasing the relative XPS signal of the underlying Si (elemental).

The C1s high-resolution spectra after RGD grafting on the different silanized surfaces are shown in Figure 5.1 (right). All spectra were fitted to 3 peaks having different components assigned to C-C/C-H at 285 eV, C-O/C-N at 286.43 eV, and the peptide signature of N-C=O and N-C(=O)-O at 288.52 eV. These results agreed with the literature for peptide XPS spectra, revealing that a successful peptide grafting was achieved on all silanized surfaces[215], [276], [277].

Table 5.1 demonstrates varying presence of amine functions depending on the silanization method, but the amount of amine in the surface region sampled by XPS (<10 nm depth) may not correspond directly to the amines being available for surface functionalization with the RGD. All three silanized surfaces showed increased nitrogen consistent with the increased proportion of nitrogen present in the RGD. The single sulfur atom present in the SMPB linking arm was not observed, XPS has a relatively low sensitivity of ~0.1 At%, so the relatively low number of sulfur atoms likely render sulfur below the detection limit. However, the SMPB linker arm and TAMRA fluorophore both contain a significant number of sp2 hybridized carbon atoms. The sp2 and sp3 C(1s) photoelectron peaks would be expected to overlap, but sp2 hybridized carbon atoms also display a distinct shake-up peak due to electron $\pi \rightarrow \pi^*$ transitions[278]. In this case a small feature corresponding to possible presence of the $\pi \rightarrow \pi^*$ is observed for only one of the RGD-modified films: Alk-NH_2.

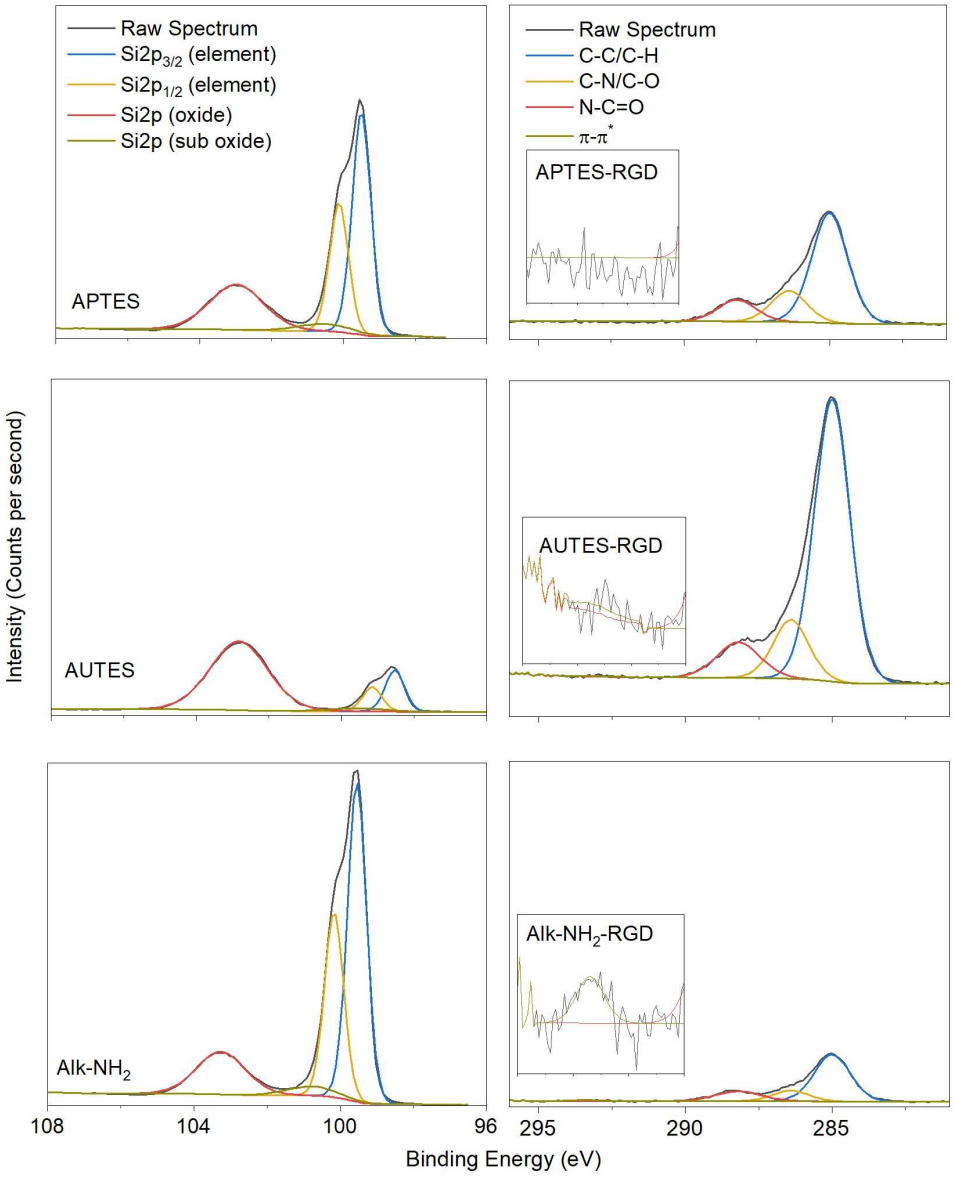
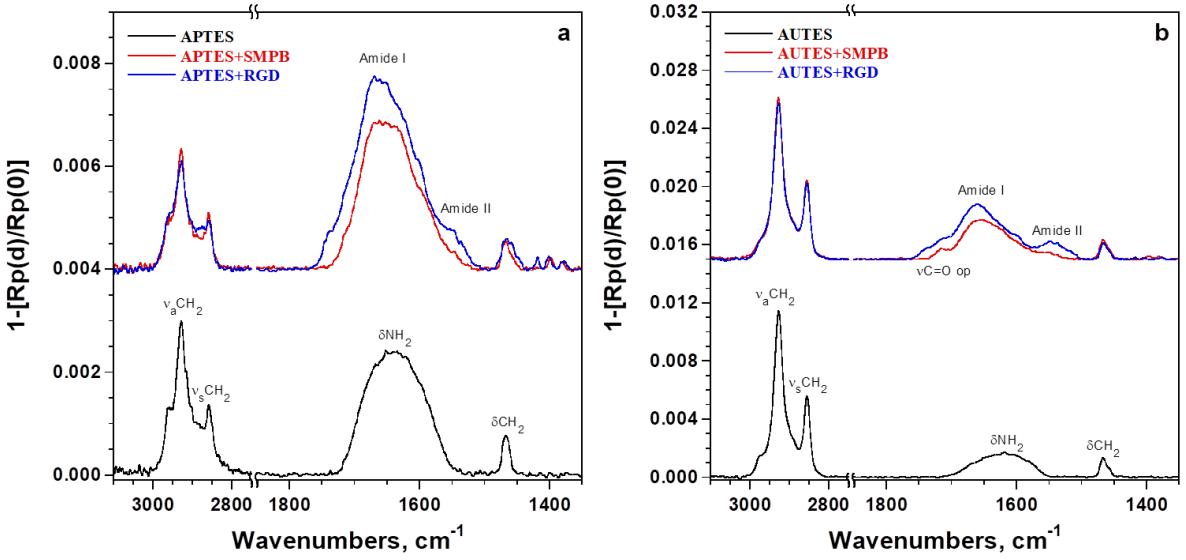


Figure 5.1. XPS high-resolution spectra of Si2p after silanization with APTES, AUTES, and Alk-NH_2 (left) and C1s after RGD grafting (right). Silanization of APTES and Alk-Phtha was achieved through spin coating using a 2% v/v solution in absolute ethanol, while AUTES silanization was conducted via immersion in a 2% v/v solution in anhydrous toluene.

5.5.4 Polarization Modulation Infrared Reflection-Absorption Spectroscopy (PM-IRRAS)

Silane-based self-assembled monolayers (SAMs) are fabricated by chemically attaching silane layers that offer a prime opportunity for probing interactions at interfaces[279]. After their deposition, the self-assembled monolayers of silane molecules on the surface were also characterized by PM-IRRAS. The PM-IRRAS spectra of amine or phthalimide-terminated silane layers, prepared via spin coating (APTES, Alk-Phtha) and immersion (AUTES) are presented in Figure 5.2. The effectiveness of the grafting process was confirmed for all compounds by identifying distinct IR bands on the PM-IRRAS spectra (black spectra in Figure 5.2). First, the disorderly nature of the alkyl chains was revealed by the positioning of the antisymmetric (ν_aCH_2) and symmetric (ν_sCH_2) stretching vibrations of the methylene groups at 2927 and 2855 cm^{-1}, respectively. This aligns with the findings in existing literature[272], [280]. From the intensity of the ν_aCH_2 feature (0.0025), it can be deduced that the thickness of the Alk-Phtha layer is 15 Å, which is in agreement with the presence of a single monolayer[271]. For APTES and AUTES layers, the broad peak around 1625 cm^{-1} was assigned to the bending mode (δNH_2) of the amino groups. The conversion of phthalimide groups into amine groups was performed by immersion in a methylamine solution.[33] This deprotection was confirmed in Figure 5.2c, by the complete disappearance of the bands at 1773 and 1715 cm^{-1}, assigned respectively to the in-phase and out-of-phase carbonyl stretching vibrations of the phthalimide terminal. Additionally, a new band appeared at 1625 cm^{-1} due to the bending vibration of NH_2 groups.



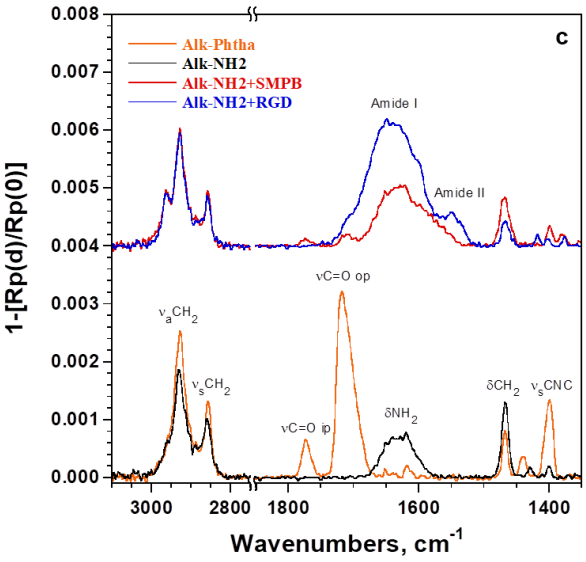


Figure 5.2. PM-IRRAS spectra after silanization with APTES (a), AUTES (b), and Alk-Phtha (c) onto SiO_2/Au substrates and after RGD peptide grafting. Silanization of APTES and Alk-Phtha was achieved through spin coating using a 2% v/v solution in absolute ethanol, while AUTES silanization was conducted via immersion in a 2% v/v solution in anhydrous toluene.

The three amino-terminated surfaces were immersed in the heterobifunctional SMPB crosslinker solution to afford the corresponding maleimide-terminated surface. The characteristic band at 1715 cm^{-1} assigned to the out-of-phase carbonyl stretching vibrations of the maleimide moiety appeared clearly on the PM-IRRAS spectra of Alk-NH_2+SMPB and AUTES+SMPB[281], [282]. In addition, the new amide bond was revealed by the presence of the corresponding amide I and amide II bands around 1650 cm^{-1} and 1545 cm^{-1}, respectively, that confirm the covalent grafting of SMPB. For APTES+SMPB, the broad band of amino group centered at 1650 cm^{-1} masks the corresponding bands of SMPB, which renders the extent of the reaction with SMPB difficult to evaluate. The cell-adhesive peptide RGD bearing a sulfydryl group was immobilized on the maleimide pendent surface through a stable covalent thioether bond. The PM-IRRAS spectra after the peptide grafting show that the intensities of amide I and amide II bands for Alk-NH_2+RGD increased significantly more than for APTES+RGD and AUTES+RGD.

5.5.5 Silanization impacts cell adhesion

Silanization is a critical step in surface functionalization with protein mimetic peptides derived from ECM proteins[280]. Different silanization strategies were explored to assess the impact not only on the density of surface-immobilized peptides but also on their accessibility, bioactivity, and how this consequently impacts cell behavior. Cell adhesion tests were conducted on silicon surfaces functionalized with APTES+RGD, AUTES+RGD, and Alk-NH_2+RGD.

Cell morphology, dimensions, and arrangement are pivotal in optimally operating natural tissues and organs. In our investigation, we focused on quantifying the average area of individual cells (cell area, μm^2). Figure 5.3 illustrates how human bone marrow-derived mesenchymal stem cells (hBMSCs) exhibit diverse adhesion behaviors when adhering to our RGD-modified surfaces through various silane molecules and silanization techniques. Cells exhibited a pronounced spread morphology when cultured on surfaces functionalized with AUTES+RGD and Alk-NH_2+RGD. The characteristic elongation of cell bodies evidenced this. In contrast, cells appeared quiescent on control substrates with a rounded shape.

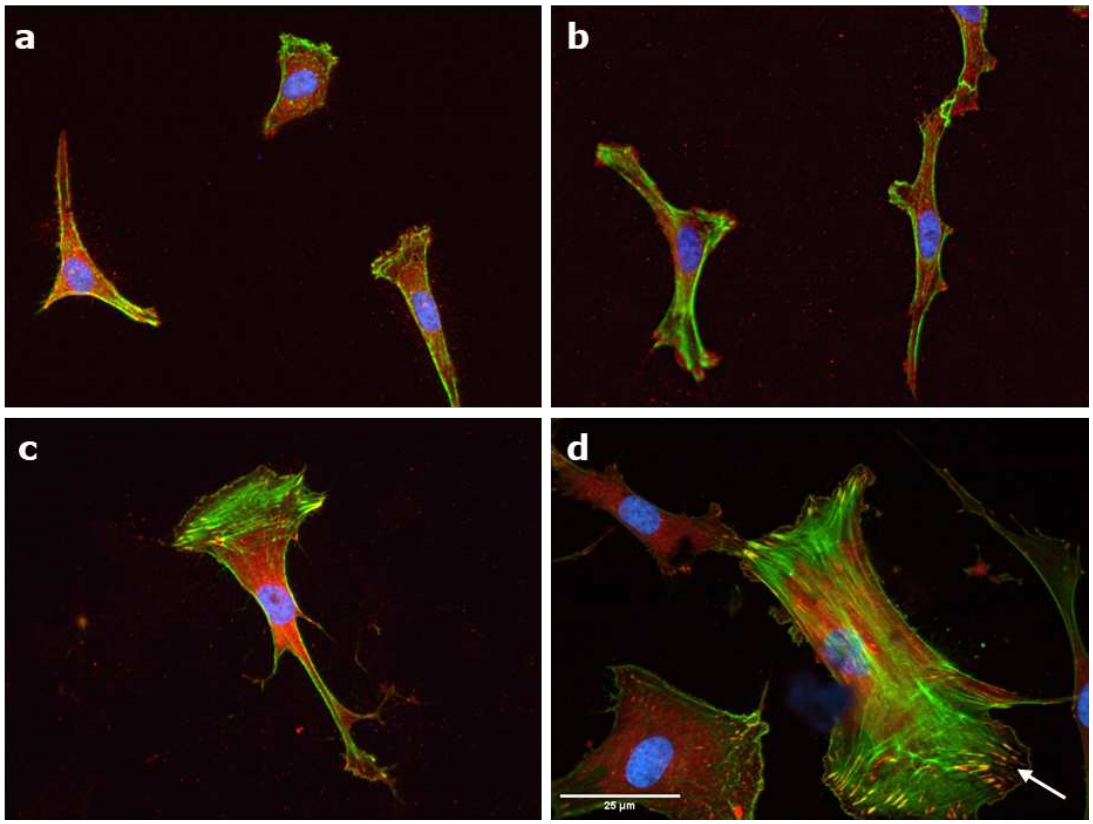


Figure 5.3. Representative fluorescence images of hBMSCs were seeded for 24 h in a DMEM medium on control (a), APTES+RGD (b), AUTES+RGD (c), and Alk-NH_2+RGD (d) substrates in serum-free conditions. Nucleus (Blue), F-actin (Green), and Vinculin (Red). The scale bar is 25 μm.

The measured cell area was 2566, 4069, 5051, and 5425 μm^2 for control, APTES+RGD, AUTES+RGD, and Alk-NH_2+RGD, respectively (Figure 5.4A). The cellular area of hBMSCs is significantly larger on all surfaces functionalized with RGD peptides compared to the control (virgin silicon). The cell area is lower after 24 h of culture for cells seeded on control and functionalized materials with APTES+RGD than those with AUTES+RGD and Alk-NH_2+RGD.

For this reason, F-actin and vinculin expressions were investigated to ascertain whether different silanized RGD-grafted surfaces may directly affect cytoskeletal changes and focal adhesion formation. Quantification of fluorescence intensity in F-actin showed that hBMSCs adherent to the Alk-NH_2+RGD substrate had a significantly higher fluorescence intensity than the other conditions, whose intensity was comparable to that found in the control samples (Figure 5.4B). Variations in the arrangement of the actin cytoskeleton were observed as well. hBMSCs cultured on surfaces treated with Alk-NH_2+RGD (Figure 5.3d) and AUTES+RGD substrates (Figure 5.3c) displayed large and well-organized actin stress fibers, whereas cells on the APTES+RGD surfaces exhibited a more disorganized actin cytoskeleton consisting of thin fibers and individual filaments extending outward from the cell's main body (Figure 5.3b). Lastly, hBMSCs cultivated on the control surfaces resulted in having a highly disorganized actin cytoskeleton (Figure 5.3a).

Next, we assessed the expression of vinculin, an essential element in forming focal adhesions crucial for cell adhesion and spreading. First, it was evident that vinculin exhibited varying distribution patterns across the different substrates. On both the control and APTES+RGD substrates, vinculin appeared prominently near the nucleus, with a dispersed presence throughout the cytoplasm. Conversely, on the AUTES+RGD and especially on the Alk-NH_2+RGD surfaces, vinculin expression is primarily localized to the cell peripheries, precisely at the tips of cytoplasmic filopodia, forming characteristic dash-like structures (white arrow Figure 5.3d).

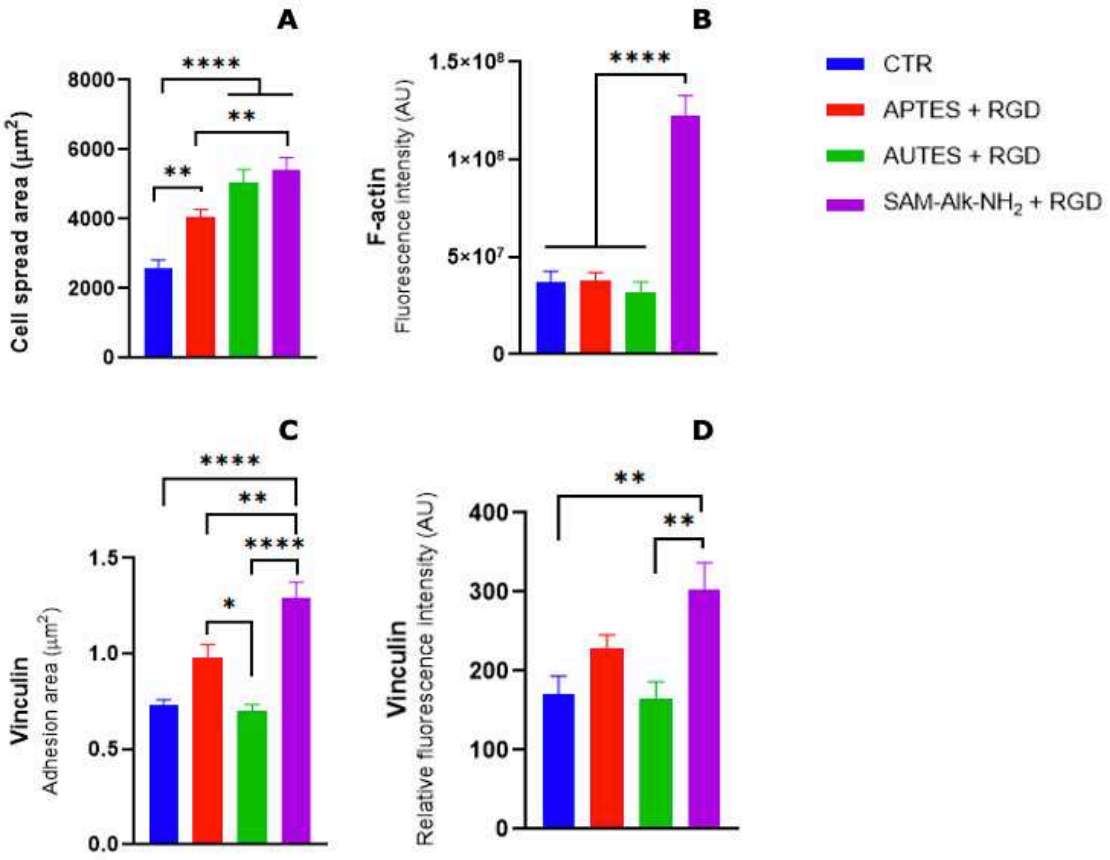


Figure 5.4. Histograms showing the change in cell spreading area of hBMSCs in response to RGD-substrates functionalized with different silanization strategies (A), F-actin expression (B), vinculin-containing focal adhesion area (C) and relative vinculin expression within focal adhesions (D). Statistical data are based on more than 80 cells in each group in two independent experiments ($n > 80$). Values are expressed as mean ± SEM. The statistically significant differences were determined by one-way ANOVA (**** $P < 0.0001$, *** $P < 0.001$, ** $P < 0.01$).

Therefore, the presence of focal adhesion points having an area within this range was assessed. Figure 5.4C shows that the substrate functionalized with Alk-NH_2+RGD had focal adhesion significantly more extensive than those that appeared on the control, APTES+RGD, and AUTES+RGD substrates. In addition, the fluorescence intensity in the focal adhesion sites was evaluated, revealing significantly elevated protein expression within the focal adhesion points of cells adhered to the Alk-NH_2+RGD, demonstrating a markedly higher vinculin expression compared to the other functionalized substrates (Figure 5.4D).

5.6 Discussion

The results presented in this study shed light on the critical role of silanization in surface functionalization with protein mimetic peptides derived from ECM proteins and its consequential impact on cell behavior. The comprehensive surface characterization aimed to elucidate the effects of silanization on the subsequent functionalization of biomaterials, specifically silicon wafers modified with different silane molecules and further grafted with the adhesive peptide RGD. An extensive understanding of the chemical and structural transformations at each surface modification stage was attained through the application of diverse analytical methodologies.

Most scientific literature reports APTES as the most used molecule for surface silanization to ensure subsequent grafting of biomolecules[283], [284]. Consistent trends in elemental composition and surface distribution resulting from silanization through 3-aminopropyltriethoxysilane (APTES) were observed in X-ray photoelectron spectroscopy (XPS) analysis, aligning with existing literature[285]. However, a lack of reproducibility in APTES-based silanization was identified and attributed to the influence of numerous uncontrollable variables. To address this, we introduced an analogue molecule of APTES, 11-aminoundecyltriethoxysilane (AUTES), possessing an extended alkyl chain with 11 carbon atoms. Discrepancies in the existing literature regarding the efficacy of silanization methods prompted a comparative investigation by Liu et al. In their study, they explored the surface modification of silicon using APTES and AUTES. The findings revealed that AUTES-modified silicon surfaces effectively regulated ligand orientation, while APTES-modified surfaces exhibited heightened sensitivity in IgG adherence, particularly demonstrating a higher detection limit for anti-IgG. Consequently, APTES was identified as the more suitable candidate for biosensor applications[286]. However, Taylor et al. reported contrasting results, noting enhanced support for cell adhesion, proliferation, and viability on plain glass coverslips modified with AUTES, thereby introducing a conflicting perspective in the literature[287].

Previous studies have addressed the relationship between diverse chain lengths of aminosilanes and the behavior of human mesenchymal stem cells (hMSCs). Chen et al. carried out an investigation focused on elucidating the influence of C_3 and C_{11} alkyl chain length in silane molecules, specifically assessing the modified deposition pattern of NH_2 groups on the substrate surface[285]. Their investigation resulted in the identification of the C_{11} chain length to increase the roughness at the

nanoscale, providing further osteoinductive properties of the modified material, which was lacking in the other chain lengths tested.

In a similar investigation, Taylor et al. observed that silanization with a longer carbon chain molecule (C_{11}) produced significantly superior results for neuronal cells in terms of adhesion and differentiation. In particular, the average length of neurites extending from primary neurons was significantly longer when grown on long-chain aminosilanes than when grown on short-chain aminosilanes (C_3). This study shows how the choice of a long-chain silane increases hydrophobicity and surface roughness, impacting cell differentiation[288].

The present study not only investigated the effects of different lengths (C_3 *vs* C_{11}) of silane chains but also made a distinctive contribution by employing a silane molecule, Alk-Phtha, with the same chemical structure as AUTES but presenting a protecting N-phthalimide group on the terminal amine. This comparative study drew attention to a possible direct correlation between surface modification induced by silane molecules with a protecting group and subsequent alterations in cell behavior.

Indeed, XPS results obtained in the present study, showed a consistency with what is found in the literature concerning the chemical elemental distribution on the surface upon AUTES silanization[285], [287]. However, XPS survey analysis revealed a different chemical composition after Alk-Phtha deposition, although after deprotection, the resulting molecule (Alk-NH_2) has the same chemical structure as AUTES. The observed differences were particularly pronounced in the high-resolution spectra, with AUTES showing a higher concentration on the surface than Alk-NH_2. The substantial differences observed in the high-resolution Si2p spectrum after the silanization process reveal pronounced variations that can be attributed to the distinctive molecular characteristics of the silanes. The hypothesis of multilayer formation during AUTES silanization was supported by the increased presence of C and N percentages, together with a decrease in the Si metal peak, which, on the other hand, in the case of monolayers should still be well detectable by XPS analysis. Indeed, the apparent correlation between the presence of free NH_2 groups in AUTES-modified substrates and the appearance of silanol bonds suggests potential multilayer formation explained by the observed changes in the Si spectrum.

This proposition was further validated by PM-IRRAS analysis. The intensity of the νaCH2 and νsCH2 bands at 2927 and 2855 cm-1, respectively, seems to be influenced by the total amount of silane molecules. Despite sharing the same chemical structure, AUTES and Alk-NH2 yielded distinct PM-

IRRAS spectra. Notably, in the AUTES spectrum, the methylene band IRRAS intensity was significantly higher than that of the Alk-Phtha spectrum. This disparity may be attributed to the presence of a multilayer in the case of AUTES deposition. Conversely, when comparing APTES and Alk-Phtha modified surfaces, one would expect a lower contribution of the methylene bands in the APTES spectrum due to its alkyl chain consisting of only three carbon atoms, as opposed to the Alk-Phtha with 11 carbon atoms in its alkyl chain. Nevertheless, the two spectra displayed comparable peak intensities, suggesting that APTES deposition likely results in the creation of multilayers on the SiO2/Au surface. It is interesting to note that the general spectrum intensity of Alk-Phtha was consistent with the existence of the monolayer in the literature[270]. All in all, this study clearly shows the unfavorable impact of the terminal free amine group on the formation of a monolayer whatever the deposition method. The multiple possible interactions of the amine group during silanization lead to a disorganized film and therefore favor 3D polymerization (multilayers). Conversely, when Alk-Phtha interacts with the surface, after hydrolysis only trisilanol can establish H-bonding interactions with the silanols groups of the silica surface, enabling molecule orientation and 2D polymerization (monolayer). In addition, the analyses using XPS and PM-IRRAS techniques have provided consistent results, demonstrating the presence of either monolayers or multilayers depending on deposition conditions and silanes utilized. Accordingly, the complexity of assessing the density of accessible amine functions on the surface may be difficult due to the intricate nature of molecular compactness of the layers.

Interestingly, despite the seemingly lower concentration on the surface, Alk-NH_2 demonstrated potential advantages, likely attributable to the protecting phthalimide group. This group, shielding the NH_2 moiety, facilitated a more homogeneous distribution on the surface. The subsequent deprotection of the phthalimide group, confirmed by PM-IRRAS, resulted in enhanced accessibility for peptide grafting. These results clearly show the advantage of using the phthalimide protecting group as a strategy to prepare amino-terminated SAMs, which allows more accessible amino groups on the surface, unlike commercial aminosilanes which led to disordered layers with unavailable amines engaged in multiple interactions. These findings emphasize the critical role of functional group protection and molecular organization in controlling surface reactions during silanization[279]. Silane molecules have conventionally served as agents for silanization through traditional immersion or vapor deposition techniques. In this investigation, a novel approach was presented: silanization employing spin coating, which, to the best of our knowledge, is the first time it has been used for

subsequent grafting of biomolecules. Prior research has established spin coating as an effective silanization method, comparable to conventional approaches[272]. The distinctive advantages of this methodology are twofold. Firstly, it facilitates the use of fewer solvents, thereby mitigating the generation of chemical waste that would otherwise ensue with methods such as immersion silanization. Simultaneously, it substantially diminishes the duration of the silanization process, enhancing productivity within a shorter timeframe, a pivotal consideration, particularly in the context of industrial-scale processes.

A cell adhesion study was carried out, where hBMSCs cultured on differently silanized materials yet grafted with the same RGD peptide displayed distinct behavior. The observed variations in cell spreading led to exploring cytoskeletal changes and focal adhesion formation. Our findings align with previous studies observations on the impact of cell shape alterations on focal adhesion (FA) organization and orientation relative to cytoskeletal structures[289], [290], [291], [292], [293], [294], [295]. Specifically, mesenchymal stem cells (MSCs) respond to extracellular cues by forming cellular adhesive organelles (FAs)[296], connecting with radial stress fibers[297], and bridging with transverse fibers to establish a dynamic cytoskeletal network, indicative of early commitment[298]. Our investigation expanded on these dynamics by noting significant differences in F-actin expression and organization across various substrates. Cells adhering to control and APTES+RGD substrates demonstrated reduced cell area, correlating with diminished F-actin fluorescence intensity. Conversely, cells cultured on Alk-NH_2+RGD displayed larger cell areas and notably higher fluorescence intensity in relation to F-actin protein expression. This might imply a correlation between cell area and cytoskeletal rearrangement, as evidenced by altered F-actin expression levels. Focal adhesion analysis further supported these findings. These formations represent structured clusters of specialized proteins, such as cytoskeletal, signalling, and regulatory proteins, distributed along the basal surface of adherent cells[259], [299]. They establish physical connections between the extracellular matrix and the actin cytoskeleton through transmembrane receptor integrins, facilitating signal transduction between the cell and its environment [300], [301], [302]. Based on a previous study[290], [298], emphasis was placed on vinculin-containing focal adhesions formed within 24 h with a total area ranging from 0.5 – 5 μm^2. The focal adhesion sites area and fluorescence intensity were notably higher for Alk-NH_2+RGD. This suggests that the silanization method plays a crucial role in the accessibility of NH_2 groups and therefore how the peptides are distributed onto the surface. Alk-NH_2+RGD facilitated a substantially more significant expansion of adhesion site area and vinculin protein

expression within focal adhesion sites. These findings contribute valuable insights into the interplay between substrate-induced alterations in cell morphology and associated cytoskeletal dynamics.

In the context of biomaterial surface functionalization, APTES in immersion has been widely recognized as a well-established and effective silanization method, often considered the first choice due to its ability to allow stable grafting of biomolecules by creating stable and high-density covalent bonds on the surface[156], [303], [304]. However, the density of molecules on the surface does not necessarily correlate directly with effectiveness. Indeed, a higher density may not necessarily lead to increased bioactivity following bioactive molecule grafting[305]. Aligned with these findings, it was demonstrated that a lower density on the surface, confirmed by XPS analysis, yielded the most favorable results in cell adhesion. To further explore and compare with the conventional APTES with a short alkyl chain (C_3), two other molecules were introduced, AUTES, with a longer alkyl chain (C_{11}), and Alk-Phtha, capable of creating a self-assembled monolayer with a steric hindrance effect due to the N-protecting phthalimide group.

Exploration of the standard silanization methods was also undertaken. While widely used, solution-based reactions present challenges such as substantial solvent use and chemical waste generation. On the other hand, vapor-phase deposition eliminates the need for organic solvents but requires ultra-high vacuum conditions and elevated temperatures[272], [306]. A novel approach was introduced with this work, by implementing spin coating as a silanization method, a technique utilized for other purposes[307] but was never used to immobilized biomolecules. Surprisingly, our comparison revealed that, once deprotected, Alk-NH_2 exhibited the best cell adhesion behavior, potentially due to better accessibility of the amino groups, even at a lower density, allowing for improved grafting and enhanced interaction with cell receptors.

The present study challenges the conventional silanization techniques and introduces spin coating as a versatile and effective alternative. Different silanization processes provided a further distribution of the peptide that has been perceived differently by cells, which reacted very differently to the same RGD peptide grafted on the surface just because it was grafted on different silanized surfaces. This study demonstrated that silanization constitutes a critical step in the functionalization of biomaterials, as evidenced by the cell adhesion study. The molecule Alk-Phtha, emerged as a promising candidate for achieving better grafting orientation and enhanced accessibility for peptide grafting.

This work introduces a novel method and molecule for biological purposes, challenging conventional approaches and demonstrating that comparable, if not superior, results can be attained through a

simpler, more cost-effective, and environmentally sustainable methodology. This novel perspective on biomaterial surface functionalization opens the door to re-evaluating the initial layer of modification, which plays a pivotal role in determining the success of subsequent layers and overall outcomes. These results collectively validate the sequential and successful alteration of surface properties, showing the intricate control achieved in tailoring surface properties. The study demonstrates that the functionalization strategy is very important and can determine the quality of functionalization in terms of accessibility of terminal functions and thus responsiveness and homogeneity, as well as having a strong influence on cells. This deviation from conventional protocols gives researchers greater autonomy in modeling biomaterial fabrication processes, paving the way for the creation of more efficient and customized techniques to address biomedical challenges.

5.7 Conclusion

In conclusion, this study provides valuable insights into the interplay between substrate-induced alterations in cell morphology and associated cytoskeletal dynamics. We challenge conventional techniques by exploring novel silanization methodologies and introducing silanization by spin coating as a versatile and effective alternative for grafting bioactive molecules onto the surface. The functionalization strategy using a protected aminosilane provides a better controlled surface functionalization, resulting in a homogeneous SAM. The findings demonstrate that different silanization processes result in varied peptide distributions, leading to distinct cellular responses. Silanization emerges as a critical step in the functionalization of biomaterials, influencing surface characteristics that, in turn, impact cell adhesion. The sequential alteration of surface properties showcases the intricate control achieved in tailoring biomaterial surfaces.

This deviation from conventional protocols allows for refining surface engineering methodologies and achieving tailored surface properties, offering increased autonomy in shaping biomaterial fabrication processes for addressing diverse biomedical challenges. This research highlights the fundamental importance of silanization as a foundational stage, unveiling its significant impact on the subsequent functionality of biomaterials and the effectiveness of interactions at the cell-surface interface.

Acknowledgements

The authors thank Anthony Vial and Michael Molinari from the VibrAFM platform at CBMN for the AFM experiments. This work was supported by the Natural Science and Engineering Research Council of Canada (G.L), as well as the Centre Québécois sur les Matériaux Fonctionnels (G.L). M.K is the recipient of a scholarship from the Fondation du CHU de Québec-Université Laval. M.C.D would like to thank the French National Research Agency (ANR-21-CE06-0031-02) for its support, as well as the Nouvelle Aquitaine Region (contract n° 2017-1R30109-00013176) and the Department of Health Sciences and Technologies from the University of Bordeaux for their support.

Chapter 6

Study 2: Synergistic Multi-Peptide Interfaces Enhance Early Osteogenic Differentiation of Mesenchymal Stem Cells

Melissa Kosovari[1,2,3], Marc Dussauze[4], Claire Petuya[4], Thierry Buffeteau[4], Murielle Remy[1], Luc Vellutini[4], Artem Zibarov[1], Gaétan Laroche[2,3,□,*], Marie-Christine Durrieu[1,□,*]

[1]Univ. Bordeaux, CNRS, Bordeaux INP, CBMN, UMR 5248, F-33600 Pessac, France.

[2]Laboratoire d'Ingénierie de Surface, Centre de Recherche sur les Matériaux Avancés, Département de Génie des Mines, de la Métallurgie et des Matériaux, Université Laval, 1065 Avenue de la médecine, Québec G1V 0A6, Canada

[3]Axe médecine régénératrice, Centre de Recherche du Centre Hospitalier Universitaire de Québec, Hôpital St-François d'Assise, 10 rue de l'Espinay, Québec G1L 3L5, Canada

[4]Univ. Bordeaux, CNRS, Bordeaux INP, ISM, UMR 5255, F-33400 Talence, France

□ Equally contributed.

* Corresponding authors

* Corresponding authors:

Marie-Christine Durrieu: marie-christine.durrieu@inserm.fr

Gaétan Laroche: Gaetan.Laroche@gmn.ulaval.ca

This work has been submitted for publication on September, 2025.

6.1 Résumé

La matrice extracellulaire (MEC) orchestre le destin des cellules souches par une interaction sophistiquée de signaux biochimiques et biophysiques. Alors que les approches biomatériaux antérieures ont généralement fait appel à un ou deux peptides bioactifs, ces stratégies reproduisent rarement la complexité de l'environnement signalétique de la MEC native. Dans cette étude, nous présentons une surface co-fonctionnalisée avec trois peptides distincts — BMP2, RGD et P15 — au moyen d'une nouvelle stratégie de silanisation par spin-coating, offrant un niveau avancé de biomimétisme de la MEC. La fonctionnalisation de surface a été confirmée par spectroscopie d'absorption infrarouge en modulation de polarisation-réflexion (PM-IRRAS) et par microscopie à fluorescence. Des cellules souches mésenchymateuses humaines (hMSCs) cultivées sur ces surfaces multi-peptides ont été évaluées de manière systématique par RT-qPCR et immunocytochimie, afin d'analyser l'expression des marqueurs ostéogéniques aux niveaux génique et protéique. Nos résultats démontrent que la présentation simultanée de BMP2, RGD et P15 accélère significativement l'expression précoce des gènes ostéogéniques et renforce la différenciation durable des hMSCs par rapport aux surfaces fonctionnalisées avec un ou deux peptides seulement. Ces observations soulignent l'importance des signaux multifactoriels dans l'orientation du destin cellulaire et positionnent les surfaces multi-fonctionnalisées comme des plateformes prometteuses pour améliorer les performances des biomatériaux en médecine régénérative.

6.2 Abstract

The extracellular matrix (ECM) orchestrates stem cell fate through a sophisticated interplay of biochemical and biophysical cues. While prior biomaterial strategies have typically employed one or two bioactive peptides, such approaches rarely replicate the multifaceted signaling environment of native ECM. Here, we present a biomaterial surface co-functionalized with three distinct peptides—BMP2, RGD, and P15—through a novel spin-coating silanization strategy, providing an advanced level of ECM biomimicry. Surface functionalization was confirmed via polarization modulation-infrared reflection-absorption spectroscopy (PM-IRRAS) and fluorescence microscopy. Human mesenchymal stem cells (hMSCs) cultured on these multi-peptide surfaces were systematically evaluated by RT-qPCR and immunocytochemistry to assess the expression of osteogenic markers at

the gene and protein levels. Our results demonstrate that the concurrent presentation of BMP2, RGD, and P15 significantly accelerates early osteogenic gene expression and enhances the sustained differentiation of hMSCs compared to single- or dual-peptide modifications. These findings highlight the importance of multifactorial signaling for directing stem cell fate and establish multi-functionalized surfaces as promising platforms for improving biomaterial performance in regenerative medicine.

6.3 Introduction

The extracellular matrix (ECM) is a highly organized and dynamic network secreted by cells, offering structural support and spatial organization to tissues and organs.[258] Beyond its mechanical role, the ECM establishes a bioactive microenvironment, composed of structural proteins, adhesion molecules, and glycans, that delivers essential biochemical and biophysical cues to regulate key cellular processes.[308] This environment facilitates nutrient diffusion and cellular communication and is characterized by a dynamic reciprocity: the ECM influences cell morphology and phenotype, while cells actively remodel the matrix in response to environmental cues.[309] Given its central role in orchestrating cell behavior, the ECM has long served as the natural scaffold that ultimately inspires the design of biomaterials. A major objective in this field is to recreate the native ECM environment to guide cellular processes, particularly stem cell differentiation. Stem cells, such as human mesenchymal stem cells (hMSCs), possess the capacity for self-renewal and the potential to differentiate into specialized cell types, including cartilage, bone, and adipose tissue.[33],[310] Although spontaneous differentiation can occur in vitro, it is generally inefficient and produces heterogeneous cell populations, which complicates both therapeutic applications and fundamental studies of differentiation mechanisms.[311]

To overcome these limitations, stem cell expansion and differentiation are typically directed using combinations of growth factors, signaling molecules, or genetic modifications. Osteogenic differentiation of hMSCs is known as a process tightly regulated by biochemical cues present in the cellular microenvironment. Functionalizing the interface of a biomaterial with specific sequences of factors that target the desired pathway is crucial for guiding hMSCs behaviour. A wide range of research has focused on leveraging peptides to enhance osteogenic differentiation. Notably, the most widely explored are RGD, OGP, PHSRN, FHRRIKA, KRSR, GFOGER, P15, and various BMP-mimetic sequences, which have consistently demonstrated strong relevance in both research and

clinical applications. Among these, the RGD motif, commonly found in ECM proteins like fibronectin and vitronectin, is well known for facilitating cell adhesion.[312] The RGD sequence specifically interacts with cellular integrins, most notably α5β1, αIIbβ3, and αvβ3, mediating key cell adhesion and signaling processes.[313] Studies have demonstrated that RGD, especially when used in conjunction with other peptides, can significantly improve cell attachment, spreading, viability, and support osteogenic differentiation.[246], [314] Additionally, the BMP2 mimetic peptide, which is derived from bone morphogenetic protein, is widely applied to stimulate osteogenesis.[114], [138], [140], [141], [212], [218], [315], [316], [317] BMP2-derived peptides have been shown to bind BMP type I and II receptors, effectively activating downstream signaling pathways analogous to those triggered by the full-length BMP2 protein, thereby enhancing osteogenic differentiation in cells.[231], [232], [233] Importantly, several investigations report that combining RGD with BMP2 peptides produces a greater enhancement of osteogenic differentiation than either peptide alone.[121], [138], [139], [142], [212], [213], [215], [216], [217], [223], [242], [318] Another key peptide is P15, a synthetic peptide that replicates the cell-binding domain of collagen type I, the primary structural protein in bone ECM.[319] It has been extensively demonstrated, both in vitro and in vivo, to enhance osteogenic cell attachment, proliferation, and differentiation, as well as to promote matrix mineralization and new bone formation.[320], [321] Despite its commercial availability and proven efficacy, P15 has so far only been utilized as a single functionalization in biomaterial coatings, and its use in combination with other bioactive peptides has not been explored.[319], [322]
P15 exerts its effects primarily through high-affinity interactions with the α2β1 integrin, which is specific for collagen. This mechanism of action is independent of the RGD-mediated pathways utilized by fibronectin and vitronectin, which interact with integrins such as αIIbβ3 and α5β1 for fibronectin, and αvβ3 for vitronectin.[313] As a result, it is believed that P15 does not compete with these cell surface integrins for binding to fibronectin or vitronectin, allowing for distinct and potentially complementary cellular interactions.
To date, the functionalization of biomaterial surfaces has largely relied on the presentation of single peptides or, less commonly, simple combinations of two bioactive motifs. Approaches that integrate more than two peptides remain rare considering the difficulties in precisely controlling their spatial distribution and maintaining consistent ratios, despite the fact that the extracellular matrix (ECM) naturally presents a rich and diverse array of biochemical signals. Mono- and bi-functionalized surfaces provide valuable insights but may not fully capture the complexity of the native ECM environment, potentially limiting the regenerative potential of engineered biomaterials.

While engineered surfaces incorporating ECM-derived mimetic peptides have yielded promising results, the development of truly multifunctional biomaterial interfaces, capable of synergistically engaging multiple signaling pathways, remains limited. There is a pressing need for advanced strategies that enable the integration of diverse cues on material surfaces, thereby providing more physiologically relevant microenvironments for precise regulation of stem cell fate and, ultimately, enhancing regenerative outcomes.

In response to these challenges, this study introduces multifunctional biomaterial surfaces designed to better replicate the complex biochemical landscape of the native ECM and thereby promote osteogenic differentiation of hMSCs. A novel silanization strategy using spin coating was developed, departing from the conventional reliance on APTES, and has demonstrated strong potential for enhancing hMSCs adhesion.[160] Here, surfaces were functionalized with up to three distinct peptides (BMP2, RGD and P15), marking, to our knowledge, the first attempt to present such a combination on a single substrate and enabling unprecedented insights into their synergistic effects. This design enables P15 to function in parallel with RGD-containing peptides, as they target different integrin receptors, allowing simultaneous and complementary interactions with cells. In addition, BMP2 activates distinct osteogenic pathways, completing the synergistic effect of the three peptides. Surface characterization by PM-IRRAS and fluorescence microscopy provided semi-quantitative evaluation of peptide immobilization. Notably, the concurrent quantification of more than two surface-bound peptides as a means to direct cell differentiation has, to date, not been reported. Surfaces functionalized with one, two, or all three peptides were prepared and compared through comprehensive cellular analyses. Osteogenic commitment was assessed at both the gene (RT-qPCR) and protein (immunocytochemistry) levels to investigate the influence of distinct peptide assemblies on hMSCs behavior and to identify the most effective configuration for inducing osteogenesis within a shortened timeframe, an issue that has seen limited investigation in the international literature. By incorporating three peptides with complementary biological activities, this work establishes an advanced in vitro platform for rapid and scalable osteogenic differentiation, addressing a significant gap in biomaterial design. These findings also pave the way for novel strategies in implant surface functionalization and the broader development of next-generation regenerative therapies.

6.4 Materials and Methods

6.4.1 Materials

Silicon wafers (100 mm, thickness 500−550 μm) were acquired from Pure Wafer, San Jose, CA. The SiO_2/Au substrates used for PM-IRRAS experiments, specifically Goldflex mirrors with a SiO_2 protective layer (Goldflex PRO, reference 200,785), were provided by Optics Balzers AG. All solvents and surfactants were purchased from Sigma-Aldrich, unless stated otherwise. The synthesis of phthalimide-terminated coupling agents was performed as previously described in a previous publication from our group.[160] GeneCust in Boynes, France, synthesized the fluorophore-tagged peptides: CG-K(PEG3-TAMRA)- GGRGDS, referred to as RGD (molecular weight = 1437 g mol−1), CGTPGPQGIAGQRGVV-K(Cy5) and CGTPGPQGIAGQRGVV-K(AMC), referred to as P15 (molecular weight (Cy5) = 2263.66 g mol−1, (AMC) = 1653.86 g mol-1), CKIPKASSVPTELSAISMLYLK-FITC[323], referred to as BMP2 (molecular weight = 2769.26 g mol−1). Bone marrow mesenchymal stem cells (hMSCs), mesenchymal stem cell growth medium 2, and SupplementMix MSC growth medium 2 were procured from PromoCell GmbH, located in Heidelberg, Germany. Monoclonal Anti-SATB2 (ab92446), Anti-COL1A1 (ab255809), Anti-OCN (ab133612) antibodies (produced in rabbit) were obtained from Abcam, United Kingdom. Dulbecco's modified Eagle's medium (DMEM), Dulbecco's phosphate buffered saline (1×) (PBS), Trypsin−EDTA, fetal bovine serum (FBS), Alexa Fluoroshield 488 phalloidin, secondary antibodies (goat anti-mouse IgG (H + L) highly cross-adsorbed secondary antibody Alexa Fluoroshield 568 and DAPI were procured from Thermo Fisher Scientific (USA). Mouse monoclonal Anti-osteopontin was obtained from Santa Cruz Biotechnology (USA). RNA extraction and genomic DNA removal was done using the RNeasy Plus Mini Kit (QIAGEN). All the reagents used in DNA digestion and RNA retro-transcription were acquired from Thermo Fisher Scientific. The primers used for RT-qPCR were acquired at Eurofins, whereas SsoAdvanced Universal SYBR Green Supermix was purchased from Bio-Rad. The synthesis of phthalimide-terminated coupling agents was performed as previously described in our previous work.[160]

6.4.2 Sample Preparation

Activation. Silicon wafers and SiO_2/Au substrates were cut into 2 cm x 2 cm dimensions. These substrates underwent ultrasonic cleaning through successive immersions in acetone, deionized water, and methanol (10 min each). Subsequently, the slides were activated by exposure to UV-ozone (185−254 nm) for 30 min. They were promptly utilized for silanization via spin-coating method. *Silanization.* Alk-Phtha silane molecules were dissolved in anhydrous chloroform under an inert nitrogen atmosphere to achieve a final concentration of 15 mM. 160 µL of the silane solution freshly prepared was used to coat the Si and SiO_2/Au substrates (4 cm^2 dimensions) during rotation at 6000 rpm for 60 s. The samples were then dried overnight at 120 °C under vacuum. They were after subjected to an intensive washing by sonication in chloroform, Milli-Q water, and methanol (2 cycles of 5 min each). Then, the monolayers were deprotected to give amino-terminated silane molecules by immersion in a solution of $MeNH_2$ 40% in water for a minimum of 4 min at room temperature. Then, amino-silanized substrate were washed using an ultrasonic bath for 5 min successively with Milli-Q water, DMF/Milli-Q water (1:1, v/v), 2-propanol, and CHCl3, and dried under nitrogen flow.[324] *SMPB Cross-Linker Conjugation.* Silanized silicon substrates were functionalized with the heterobifunctional cross-linker SMPB prior to peptide immobilization. The succinimidyl group of SMPB reacted with surface amine functionalities, resulting in the formation of accessible maleimide groups. These maleimide moieties were subsequently employed to couple with thiol groups present on the terminal cysteine residues of the selected peptides. Specifically, aminated surfaces were incubated in a 3 mg/mL SMPB solution in DMSO for 2 hours in the dark. After incubation, the substrates were rinsed in DMSO for 10 minutes using an ultrasonic bath, followed by gentle washing with methanol. The cleaned substrates were then air-dried and stored in the dark until peptide grafting was performed. *Peptide Grafting.* To achieve peptide grafting of different combinations, PBS1X solutions were prepared containing either a single peptide (RGD, BMP2 or P15), a mixture of two peptides in equal parts (BMP2 and RGD), or a mixture of three peptides in equal parts (BMP2, RGD, and P15). The surfaces were incubated overnight in the dark with a peptide solution to allow the anchoring of fluorescently labeled mimetic peptides at a total concentration of 0.1 mM, whether one, two, or three different peptides were used. The final reaction volume was set to 1.5 mL. Samples were then cleaned by ultrasonication six times for 15 min in nanopure water to remove all non-covalently attached peptides. All reactions were performed under agitation at room temperature.

6.4.3 Polarization Modulation Infrared Reflection-Absorption Spectroscopy

PM-IRRAS experiments were performed on a ThermoNicolet Nexus 670 FTIR spectrometer with a PM-IRRAS optical bench.[274] The PM-IRRAS spectra were recorded at a resolution of 4 cm^{-1} during 5h acquisition time. The PM-IRRAS spectra were calibrated to be presented in IRRAS units.[275] All spectra were collected in a dry-air atmosphere after 1h of incubation in the chamber.

6.4.4 Fluorescence Microscopy

Fluorescence emission spectra were recorded using a Labram microspectrometer (Horiba Jobin Yvon, Villeneuve d'Ascq, France) with three different wavelengths of laser acting as the excitation source, depending on the chromophore: 405 nm for BMP2 (single-peptide FITC), 532 nm for RGD (single-peptide TAMRA) and 633 nm for P15 (single peptide-Cy5). Only a wavelength of 405 nm was used for substrates containing a mixture of two peptides (BMP2 and RGD) or a mixture of three peptides (BMP2, RGD, and P15) in equal parts. 0.01 % and 0.1 % of the laser power was sent to samples with containing one peptide and to the mixtures, respectively to prevent damaging samples. A 100X objective allowed focusing the incident laser beam and collecting the fluorescence response. The fluorescence was dispersed by a resolution holographic grating of 150 lines/mm and analyzed using a Peltier-cooled CCD detector (Andor, Belfast, UK). The calibration of the spectrometer was done using the 520.7 cm^{-1} Raman mode of a silicon sample.

6.4.5 Cell Culture

Human bone marrow-derived mesenchymal stem cells (hMSCs) were seeded onto both unmodified silicon wafers (control, CTR) and various functionalized substrates: BMP2, P15, BMP2+RGD, and BMP2+RGD+P15. To minimize the influence of serum proteins on initial cell attachment and behavior, cells were first incubated for 6 hours in serum-free DMEM basal medium. Following this period, the culture medium was supplemented with 10% fetal bovine serum (FBS). At 24 hours post-seeding, the culture medium was replaced with osteogenic differentiation medium, consisting of DMEM basal medium supplemented with ascorbic acid (50 μg/mL), dexamethasone (100 nM), β-glycerophosphate (10 mM), and 10% FBS.

6.4.6 Immunocytochemistry assays

On day 5, hMSCs were rinsed with 1× PBS and fixed in 4% paraformaldehyde at 4 °C for 20 minutes. The cells were then permeabilized using 0.5% Triton X-100 in 1× PBS for 5 minutes, followed by blocking with 1% bovine serum albumin (BSA) in 1× PBS for 30 minutes at 37 °C. For osteopontin detection, samples were incubated for 1 hour at room temperature with a mouse monoclonal anti-osteopontin primary antibody (diluted 1:200 in 1% BSA/PBS). After washing with 1× PBS, cells were exposed to Alexa Fluor 568-conjugated rabbit anti-mouse IgG (H+L) secondary antibody (diluted 1:200 dilution in 1% BSA/PBS) for 30 minutes at room temperature. For F-actin visualization, samples were treated with Alexa Fluor 488 phalloidin (diluted 1:400) for 1 hour at 37 °C. This was followed by three washes with 1× PBS, and nuclei were counterstained with DAPI at 20 μg/mL for 10 minutes at room temperature. Imaging was performed using a Leica DM5500B microscope equipped with a motorized, programmable stage and a CoolSnap HQ camera, with image acquisition managed by Metamorph 7.6 software. Quantitative analysis of osteopontin and phalloidin staining was conducted using ImageJ (NIH, https://imagej.nih.gov/ij/). All fluorescent images were captured at identical exposure settings using a 63× objective lens, and fluorescence intensity measurements were obtained from 20 cells per sample.

6.4.7 Real-Time Quantitative Polymerase Chain Reaction.

Total RNA was extracted, and genomic DNA was eliminated using the RNeasy Plus Mini Kit (QIAGEN). RNA purity was assessed by measuring absorbance ratios at A260/A280 and A260/A230 using a NanoDrop 1000 spectrophotometer (Thermo Fisher Scientific). RNA integrity was evaluated using the RNA ScreenTape Assay on an Agilent TapeStation 4150 system. cDNA was synthesized from 2 μg of total RNA using random primers and Maxima Reverse Transcriptase (Thermofisher). PCR primers were either selected from PrimerBank (Harvard University) or designed de novo using Primer3Plus software, utilizing gene sequences obtained in FASTA format from genomic databases (Table 6.1). This dual strategy ensured optimal coverage and specificity for all target regions.

Table 6.1 RT-qPCR primer sequences and functions for genes analyzed.

Gene symbol	Primer Sequence 5'-3'	mRNA accession number	Function
SMAD1	CTCATGTCATTTACTGCCGTGT	NM_005900.3	Transduces bone morphogenetic protein (BMP) signals to regulate gene expression for cell growth, development, and apoptosis.
SMAD5	TCTCCAAACAGCCCTTATCCC	NM_001001420.3	Transduces bone morphogenetic protein (BMP) and TGF-β signals by acting as a transcription factor, regulating genes involved in cell growth and differentiation. Activated via phosphorylation by BMP type I receptor kinases.
RUNX2	TCAACGATCTGAGATTTGTGGG	NM_001015051.4	Master transcription factor required for osteoblast differentiation and skeletal morphogenesis; regulates bone-specific gene expression and acts as a scaffold for regulatory factors.
ALPL	AACATCAGGGACATTGACGTG	NM_001127501.4	Encodes a tissue-nonspecific alkaline phosphatase enzyme, crucial for bone and tooth mineralization by hydrolyzing phosphate groups.
COL1A1	GAGGGCCAAGACGAAGACATC	NM_000088.4	Encodes the pro-alpha1 chain of type I collagen, a fibril-forming protein abundant in bone, cornea, dermis, tendon, and most connective tissues.
BGLAP	GGCGCTACCTGTATCAATGG	NM_199173.6	Encodes osteocalcin, a calcium-binding bone protein secreted by osteoblasts that regulates bone remodeling and energy metabolism.
SATB2	GACAGTGGCCGACATGCTAC	NM_001172509.2	Binds DNA at matrix/scaffold regions to regulate gene expression and chromatin structure in neural and skeletal development.

The cDNA synthesis reaction was performed by sequentially incubating at 25 °C for 10 minutes, 50 °C for 60 minutes, and 70 °C for 15 minutes. The resulting cDNA was used for dye-based RT-qPCR to assess the expression of the target genes (primer sequences provided in Table 6.1). RT-qPCR reactions were prepared in a final volume of 10 μL, containing 2 ng of cDNA and 500 nM of each primer. Amplification was performed on a CFX Connect Real-Time PCR System (Bio-Rad). For normalization, RPL13A was chosen as the reference gene from a panel of six housekeeping genes evaluated for stability (primer sequences provided in Table 6.2). The PCR cycling conditions comprised 40 cycles of denaturation at 95 °C for 3 seconds and annealing/extension at 60 °C for 30 seconds. Quantification cycle (Cq) values for each target gene were normalized to RPL13A, and relative gene expression was calculated using the comparative ΔΔCq method, with silicon (Si) samples as the control group. In addition, we note that the Y-axis values shown in the figures correspond to the raw GOI/RPL13A (ΔCt) normalization, without further normalization to a specific day or condition. Each experimental condition was analyzed in duplicate (two independent experiments). Primer efficiency was validated by standard curve analysis in duplicate, and product specificity was verified by melting curve analysis.

Table 6.2 Panel of 7 candidate housekeeping genes evaluated.

Gene symbol	Primer Sequence 5'-3'	mRNA accession number	Function
RPL13A	GCCCTACGACAAGAAAAAGCG	NM_012423.4	RPL13A encodes a 60S ribosomal protein involved in protein synthesis and regulation of inflammation.
PPIA	TCTGCACTGCCAAGACTGAG	NM_021130.5	Catalyzes the cis-trans isomerization of proline residues to accelerate protein folding.
TBP	CCCGAAACGCCGAATATAATCC	NM_003194.5	Binds to the TATA box in gene promoters, enabling RNA polymerase II to initiate transcription.
GAPDH	ACAACTTTGGTATCGTGGAAGG	NM_001256799.3	Catalyzes a key step in glycolysis and performs diverse roles including DNA repair and antimicrobial activity.
RPC53	GGCCGTCCAGAAGTGATCC	NM_001722.3	Essential subunit of RNA polymerase III required for tRNA and small RNA synthesis, enabling protein biosynthesis.
GUSB	TGCAGGGTTTCACCAGGATC	NM_000181.4	Lysosomal enzyme that degrades glycosaminoglycans, including heparan sulfate, dermatan sulfate, and chondroitin sulfate.

6.4.8 Statistical Analysis

Data are expressed as mean ± standard deviation (SD), unless otherwise specified. Statistical analyses for RT-qPCR and immunocytochemistry were performed using Prism Software (GraphPad Software Inc.). Group comparisons were made using one-way ANOVA followed by Tukey's post hoc test. Statistical significance was set at $p < 0.05$.

6.5 Results

6.5.1 Polarization Modulation Infrared Reflection-Absorption Spectroscopy

Surface functionalization was first investigated by polarization modulation infrared reflection-absorption spectroscopy (PM-IRRAS). The PM-IRRAS spectrum of phthalimide-terminated silane layers (C_{11}-Phtha), prepared via spin-coating method and dried overnight at 120 °C under vacuum is presented in Figure 6.1 (black spectrum) in the 3100-1350 cm^{-1} spectral range. The characteristic bands of C_{11}-Phtha are observed: the antisymmetric (ν_aCH_2) and symmetric (ν_sCH_2) stretching modes of methylene groups at 2928 and 2856 cm^{-1}, respectively, the in-plane ($\nu C{=}O_{ip}$) and out-of-plane ($\nu C{=}O_{op}$) stretching modes of the carbonyl groups of the phthalimide moiety at 1771 and 1710 cm^{-1}, respectively. The wavenumbers of ν_aCH_2 and ν_sCH_2 are sensitive to both the conformation (*trans* and *gauche*) and the order of the alkyl chains. The position of methylene bands reveals the presence of gauche defects related to the disorder of the alkyl chains in the monolayers. The IRRAS intensities

around 0.002 for the $\nu_a CH_2$ and $\nu C{=}O_{op}$ bands are consistent with the thickness of a single monolayer.[324]

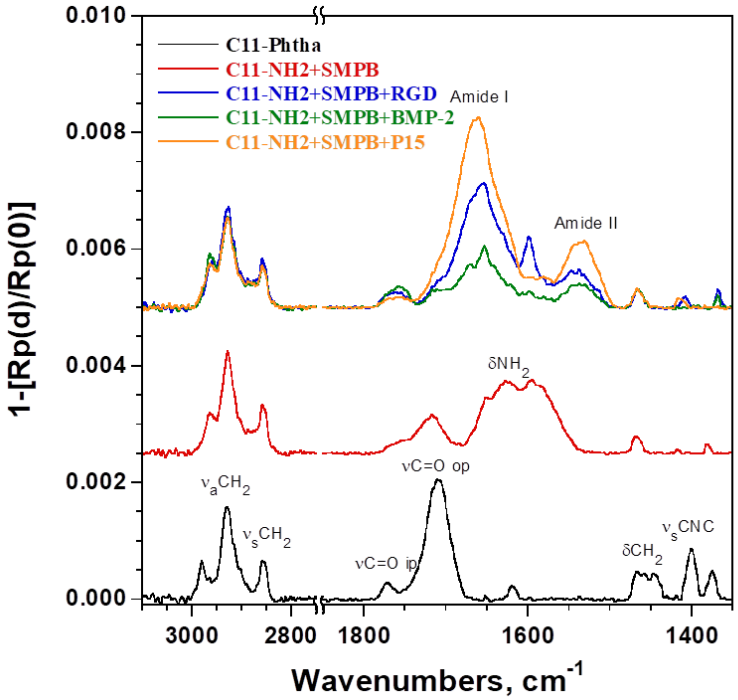


Figure 6.1. PM-IRRAS spectra after silanization with C_{11}-Phtha onto SiO_2/Au substrate (black spectrum), SMPB cross-linker conjugation onto deprotected amino surface (red spectrum) and after RGD (blue spectrum), BMP2 (green spectrum) or P15 (orange spectrum) peptide grafting.

The conversion of phthalimide groups into amine groups was performed by immersion in a methylamine solution.[188] This deprotection was confirmed in previous papers,[160], [177], [188] by the complete disappearance of the bands related to the in-phase and out-of-phase carbonyl stretching vibrations of the phthalimide terminal at 1771 and 1710 cm^{-1}, respectively. Additionally, a new band appeared around 1625 cm^{-1} due to the bending vibration of NH_2 groups. The SMPB cross-linker conjugation onto deprotected amino surface was performed to produce the formation of accessible maleimide groups. The characteristic band at 1717 cm^{-1} assigned to the out-of-phase carbonyl stretching vibrations of the maleimide moiety appeared clearly on the PM-IRRAS spectra of C_{11}-NH_2+SMPB (red spectrum in Figure 6.1). In addition, the new amide bond was revealed by the presence of the corresponding amide I and amide II bands in the 1650 - 1550 cm^{-1} spectral range, that confirm the covalent grafting of SMPB. The broad band centered at 1625 cm^{-1} reveals the presence of unreacted amino groups.

The cell-adhesive peptide RGD, P15 and BMP2 were immobilized on the maleimide pendent surface through a stable covalent thioether bond. The PM-IRRAS spectra after the peptide grafting are presented in Figure 6.1 (blue spectrum for RGD, orange spectrum for P15 and green spectrum for BMP2). These spectra show variable intensities for amide I and amide II bands with a maximum intensity for the P15 peptide. Since the PM-IRRAS spectra of the three peptides are similar (except the presence of the 1597 cm^{-1} band for the RGD peptide) in the amide I and amide II region, the mixture of two or three peptides was investigated by fluorescence microscopy.

6.5.2 Fluorescence Microscopy

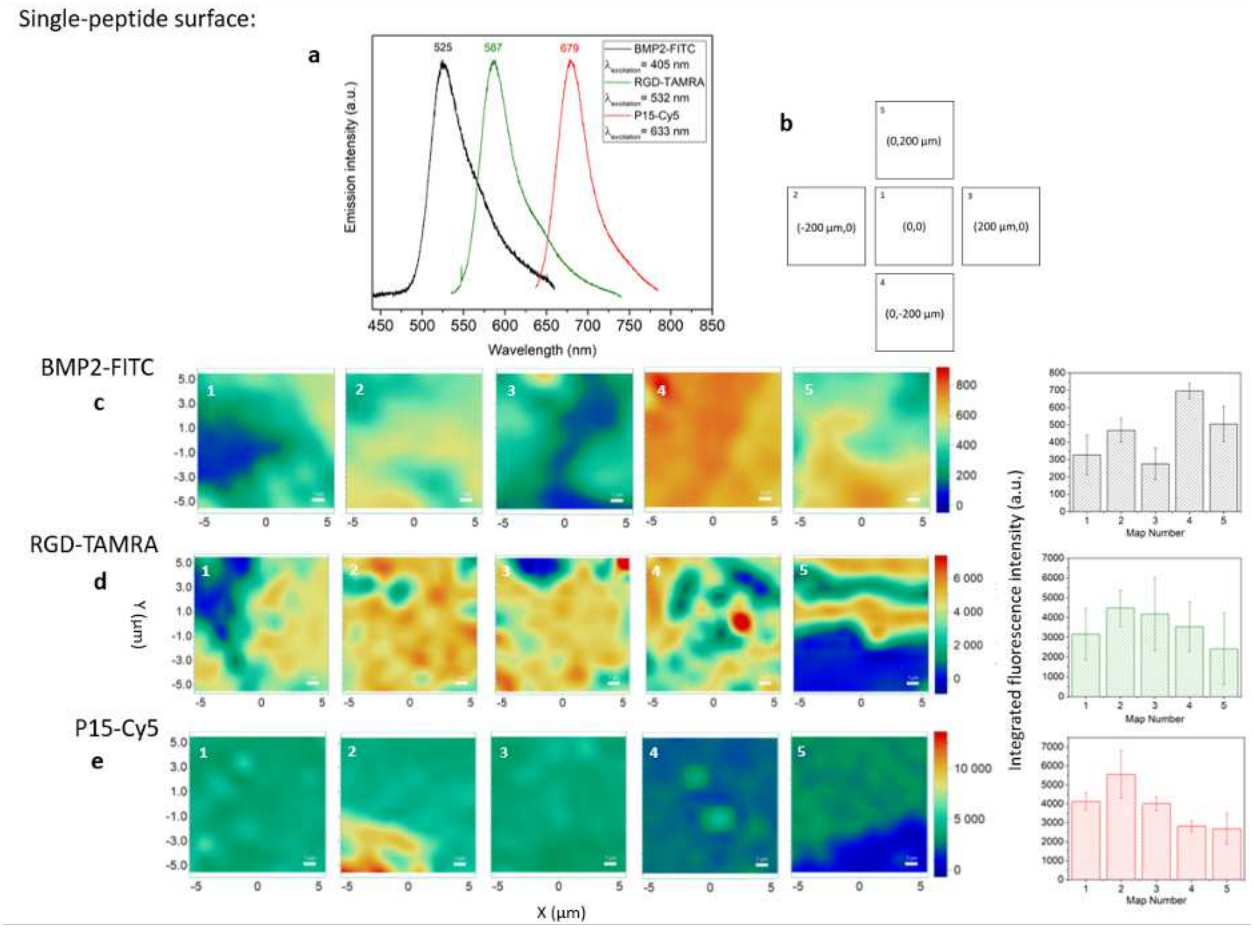


Figure 6.2. Characterization of single peptide surfaces via fluorescence spectroscopy. (a) Averaged emission spectra for each single peptide surface, recorded using three excitation wavelengths tailored to the respective fluorophores. (b) Schematic illustrating the five characterized zones (labeled 1–5) on each peptide surface. (c–e) Fluorescence intensity maps for each single peptide surface, with on the

right side corresponding averaged fluorescence intensities and standard deviations (error bars) for the five zones. The scale bar in white corresponds to a distance of 1μm.

Initially, we focused on single-peptide functionalized surfaces with two primary objectives: (i) Confirming the presence of peptides on each surface and (ii) Characterizing the homogeneity of peptide distribution at scales ranging from 1 to 100 micrometers.

Fluorescence microscopy was performed using a micro-Raman setup, enabling the acquisition of a full emission spectrum for each measurement. Excitation was achieved using continuous-wave (CW) lasers at wavelengths of 405 nm, 532 nm, and 633 nm, selected based on the specific fluorophores associated with each peptide: FITC for BMP2, TAMRA for RGD, and Cy5 for P15.

As shown in Figure 6.2a, the emission spectra measured on each single-peptide surface align perfectly with the expected fluorescence spectra of these well-characterized fluorophores.

To assess the homogeneity of peptide surface coverage, we analyzed five 10 × 10 μm^2 zones with micrometer resolution (one spectrum measured every micrometer). These zones were spaced 200 μm apart, following the schematic depicted in Figure 6.2b.

Fluorescence maps, obtained by integrating the fluorescent emission for BMP2-FITC, RGD-TAMRA, and P15-Cy5, are presented in Figure 6.2c, d, and e, respectively. These results confirm the presence of peptides in all analyzed zones, consistent with observations made using PM-IRRAS in the previous section.

At the micrometer scale, peptide distribution is not perfectly homogeneous: a few micrometer-sized domains exhibit weaker—but non-zero—fluorescence signals (blue-colored areas). For each map, the average fluorescence intensity and standard deviation were calculated (values shown on the right side of Figure 6.2). These data indicate a relatively homogeneous distribution across the five analyzed zones.

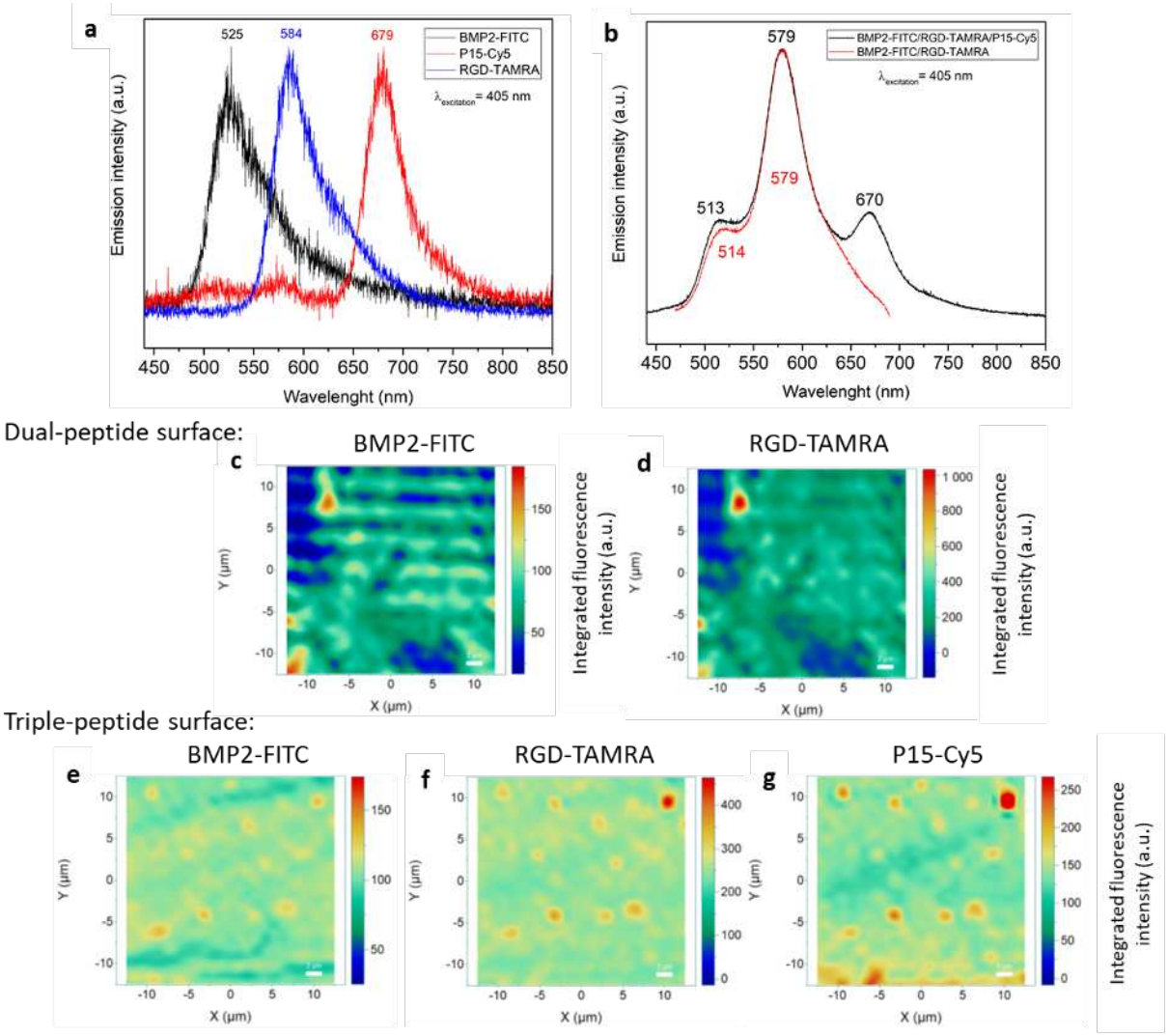


Figure 6.3. Fluorescence spectroscopy characterization of dual and triple peptide surfaces. (a) Emission spectra of individual peptide surfaces recorded using a fixed excitation wavelength of 405 nm. (b) Averaged emission spectra of dual and triple peptide surfaces (excitation at 405 nm). (c–d) Fluorescence intensity maps of a dual peptide surface, generated by integrating the fluorescent bands corresponding to each fluorophore. (e–g) Fluorescence intensity maps of a triple peptide surface, generated by integrating the fluorescent bands corresponding to each fluorophore. The scale bar in white corresponds to a distance of 2 µm.

To investigate dual- and triple-peptide surfaces using fluorescence microscopy, we employed a methodology based on a single excitation wavelength (405 nm) capable of inducing emission from all three fluorophores (FITC, TAMRA, and Cy5). We first validated this approach on single-peptide surfaces, confirming that the emission spectra obtained at 405 nm exhibited the same spectral profile and peak emission wavelengths as those acquired using fluorophore-specific excitation wavelengths. This is demonstrated in Figure 6.3a, where the emission spectra are compared with those in Figure 6.2a. The results confirm that 405 nm excitation is suitable not only for probing BMP2-FITC but also for RGD-TAMRA and P15-Cy5. This has also been confirmed by testing the single, dual and triple peptide solutions as provided in the Supplementary Section.

Concerning the emission cross sections of single-peptide surfaces excited at 405 nm, unnormalized emission spectra are provided in the Supplementary Section. These spectra reveal that the emission intensities of FITC and TAMRA are comparable, while Cy5 emission is approximately three times weaker. Since the emission intensities for all single-peptide surfaces fall within the same order of magnitude under 405 nm excitation, this methodology enables the simultaneous detection of all three fluorophores on multi-peptide surfaces using a single measurement.

In Figure 6.3b, the averaged emission spectra of dual- and triple-peptide surfaces are compared. The triple-peptide surface exhibits a spectral profile composed of three distinct peaks at 513 nm, 579 nm, and 670 nm, corresponding to FITC, TAMRA, and Cy5, respectively. For the dual-peptide surface, only two peaks are observed at 514 nm and 579 nm. While the emission maxima of the multi-peptide surfaces show slight shifts toward lower wavelengths compared to single-peptide surfaces, these components can still be confidently attributed to the presence of the respective peptides. This confirms the effectiveness of the surface functionalization protocol used to prepare multi-peptide surfaces.

The observed spectral shifts can be explained by energy transfer between fluorophores, which is expected due to the spectral overlap between their excitation and emission profiles.

Next, we examined the spatial distribution of each peptide on the functionalized surfaces. This was achieved by mapping the integrated emission intensities of the spectral components corresponding to each fluorophore. For the dual-peptide surface (Figure 6.2c and d), the surface concentration variations and homogeneity are comparable to those observed for single-peptide surfaces. Additionally, the fluorescence maps obtained by integrating the emission intensities of BMP2-FITC

and RGD-TAMRA indicate that the relative surface concentration of the two peptides remains consistent across all pixels. Similarly, for the triple-peptide surface, three fluorescence maps were generated, corresponding to the integrated emission of BMP2-FITC, RGD-TAMRA, and P15-Cy5. The observed variations in relative intensity are consistent across all three peptides, suggesting a uniform peptide mixture throughout the probed surface. In both dual- and triple-peptide cases, these findings indicate that the peptide composition is homogeneous across the entire surface.

Finally, a comparison of the averaged spectra for dual- and triple-peptide surfaces (Figure 6.3b) reveals that the relative emission intensities of the FITC and TAMRA markers are similar. This further supports the conclusion that the relative concentrations of BMP2 and RGD are consistent between dual- and triple-peptide surfaces.

It is important to note that quantitative conclusions cannot be drawn due to the lack of critical parameters, such as the emission cross-sections of each fluorophore on the surface and the extent of energy transfer effects on emission intensities. However, the relative comparisons conducted in this study provide compelling evidence of homogeneous peptide mixing on the surfaces.

6.5.3 Gene Expression Analysis of Osteogenic Differentiation by RT-qPCR

To evaluate the impact of peptide-functionalized surfaces on the osteogenic differentiation of human mesenchymal stem cells (hMSCs), quantitative RT-PCR was performed at days 3 and 10 for five key markers: RUNX2 and ALPL (early-stage), COL1A1 (intermediate-stage), and BGLAP (OCN) and SATB2 (late-stage).

6.5.3.1 Early Time Point Analysis of Differentiation Markers

Interestingly, after only 3 days of culture, hMSCs cultured on the triple-peptide-functionalized surface (BMP2+RGD+P15) exhibited significantly increased expression of BGLAP (OCN) compared to both the control (virgin silicon; $p < 0.05$) and all other peptide-functionalized groups ($p < 0.01$) (Figure 6.4d). SATB2 expression was also markedly overexpressed on the triple-peptide surface relative to the control and P15-functionalized conditions ($p < 0.001$), as well as versus BMP2 and BMP2+RGD surfaces ($p < 0.01$) (Figure 6.4e). COL1A1 expression was markedly upregulated on the triple-peptide surface versus all other conditions, including the control ($p < 0.0001$). Notably, COL1A1 expression was highest on the triple-peptide surface, significantly upregulated relative to all other conditions,

including control ($p < 0.0001$) (Figure 6.4c). ALPL expression was increased across all peptide-functionalized groups compared to control at day 3, except for the P15 condition. Specifically, the BMP2+RGD+P15 group showed a significant increase versus control ($p < 0.01$), While the increases in the BMP2 and BMP2+RGD groups were lower than those observed for the BMP2+RGD+P15 group, they were still significantly higher compared to control ($p < 0.05$). However, no significant differences were observed among single-, dual-, or triple-peptide surfaces ($p > 0.05$) (Figure 6.4b). RUNX2 expression did not significantly differ among groups at this time point ($p > 0.05$) (Figure 6.4a).

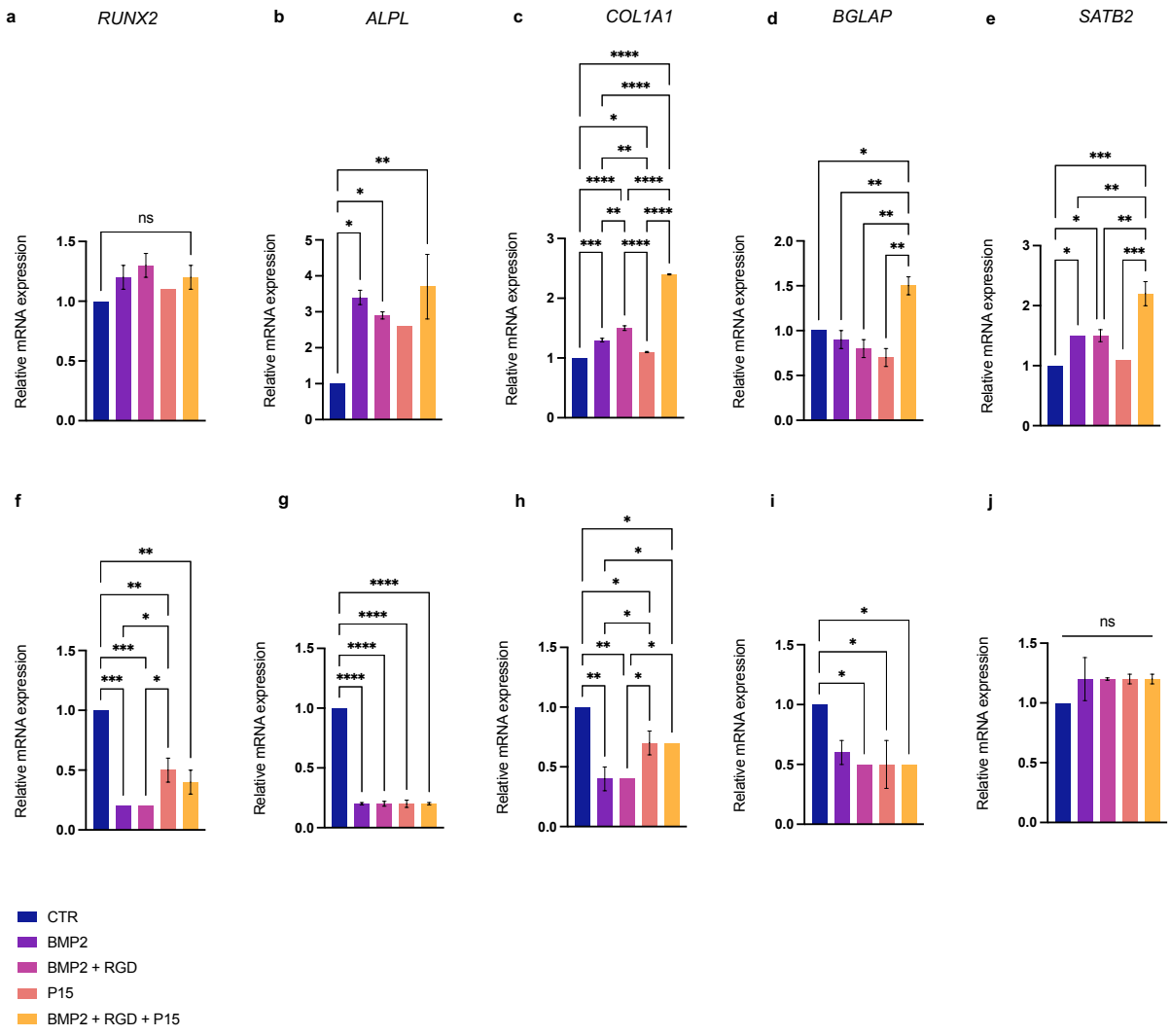


Figure 6.4. Gene expression analysis of early osteogenic markers (RUNX2, ALPL), mid-stage marker (COL1A1), and late-stage markers (BGLAP, SATB2) in hMSCs cultured on control and peptide-functionalized surfaces for 3 days (a, b, c, d, e) and 10 days (f, g, h, i, j) in osteogenic medium. All gene

expression measurements were normalized to the reference gene RPL13A (n = 2). Differences between experimental groups were analyzed by one-way ANOVA; significance values are represented as follows: **** $p < 0.0001$, *** $p < 0.001$, ** $p < 0.01$, * $p < 0.05$. In cases where error bars are not visible, the replicate values were identical.

6.5.3.2 Late Time Point Analysis of Differentiation Markers

By day 10, gene expression patterns had shifted. hMSCs on the control surface displayed significantly higher levels of RUNX2 ($p < 0.001$ vs BMP2 and BMP2+RGD; $p < 0.01$ vs P15 and BMP2+RGD+P15), ALPL ($p < 0.0001$ vs all conditions), BGLAP ($p < 0.05$ vs all conditions, except for BMP2), and COL1A1 ($p < 0.01$ vs BMP2 and BMP2+RGD; $p < 0.05$ vs P15 and BMP2+RGD+P15) compared to all peptide-functionalized surfaces (Figure 6.4f, g, h, and i). In contrast, cells on peptide-functionalized substrates exhibited stable or decreased expression of these markers relative to day 3, with significant downregulation of ALPL and COL1A1 (Figure 6.4g and h). SATB2 remained the only marker with slightly higher expression on all peptide-functionalized surfaces than on control at day 10 (Figure 6.4l), though these differences did not reach statistical significance ($p > 0.05$).

6.5.3.3 BMP/Smad Pathway Activation in Early Osteogenic Induction

To explore possible involvement of the BMP/Smad signaling pathway, SMAD1 and SMAD5 expression was assessed at days 3 and 10. At day 3, SMAD1 was significantly upregulated in BMP2, BMP2+RGD, and P15 conditions compared to control. Both BMP2 and P15 surfaces presented higher SMAD1 expression than control and the triple-peptide group ($p < 0.01$), while BMP2+RGD exhibited the greatest increase versus both control and triple-peptide conditions ($p < 0.001$). Interestingly, no significant difference was observed between the control and the triple-peptide group. (Figure 6.5a) At day 10, SMAD1 remained elevated in BMP2 and P15 groups compared to control ($p < 0.05$), whereas SMAD5 was downregulated in all peptide-functionalized conditions, most notably in the BMP2+RGD sample compared to control (Figure 6.5c).

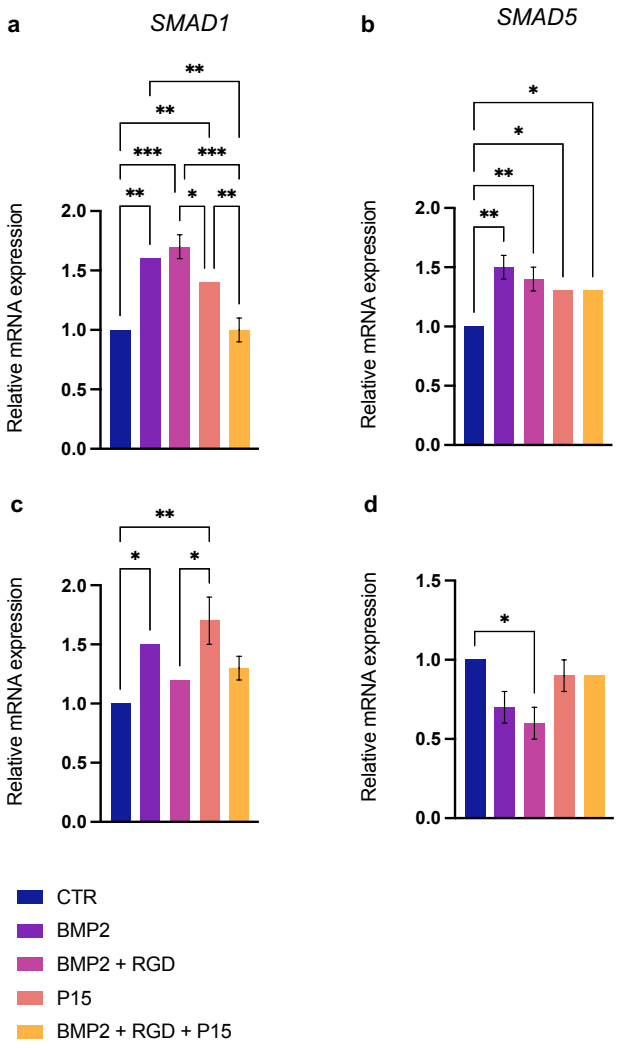


Figure 6.5. Analysis of SMAD1 and SMAD5 mRNA expression in hMSCs cultured under osteogenic conditions on control or peptide-functionalized substrates for 3 days (a, b) and 10 days (c, d). Data represent fold changes calculated after normalization to the RPL13A housekeeping gene (n = 2 replicates per group). One-way ANOVA was used to compare the groups; levels of statistical significance are represented as follows: * $p < 0.05$, ** $p < 0.01$, *** $p < 0.001$, **** $p < 0.0001$. In cases where error bars are not visible, the replicate values were identical.

6.5.4 Immunocytochemistry

Immunocytochemistry analyses were performed to validate the significant influence of peptide functionalization on the differentiation of hMSCs into the osteogenic lineage. Since RT-qPCR results demonstrated that both single-peptide and dual-peptide surfaces possess similar osteogenic potential

in inducing the gene expression of key osteogenic markers, the comparison here focused on the BMP2+RGD+P15 substrate, the control, and the dual-peptide condition BMP2+RGD. Representative images of hMSCs at the 5-day time point are shown in Figure S3 (see Supporting Information), illustrating the overall cell morphology and distribution on the control and peptide-functionalized substrates.

Figure 6.6 presents osteopontin expression, a key osteoblastic marker. Quantification of fluorescence intensity revealed that hMSCs cultured on the BMP2+RGD+P15 substrate exhibited significantly higher osteopontin fluorescence compared to the control, but not when compared to the BMP2+RGD condition (Figure 6.6d). No significant difference was observed between the BMP2+RGD and BMP2+RGD+P15 materials. It is important to note that these data were collected after 5 days of culture, a time point at which not all cells are expected to be at the same stage of osteogenic differentiation. To provide a more comprehensive understanding of osteogenic commitment, the distribution of osteopontin fluorescence intensity among cells in the control and peptide-functionalized conditions was analyzed (Figure 6.6e). Most cells in the control group displayed OPN intensity between 0.5 and 1 A.U., representing the lowest detectable range. This proportion decreased in the BMP2+RGD group and was nearly absent in the BMP2+RGD+P15 group. Intensities between 1 and 1.5 A.U. were observed in a greater number of cells from the BMP2+RGD and BMP2+RGD+P15 conditions compared to the control, where such cells were fewer. Similarly, the proportion of cells with intensities between 1.5 and 2 A.U. was higher in the peptide-functionalized groups, particularly in the BMP2+RGD condition. Notably, the highest number of cells with osteopontin intensity between 2 and 2.5 A.U. was observed in the triple-peptide (BMP2+RGD+P15) condition, followed by the dual-peptide group, with the control displaying the lowest count. Cells with fluorescence intensities between 2.5 and 3 A.U. were present only on the peptide-functionalized substrates and were completely absent in the control. Most remarkably, only the BMP2+RGD+P15 condition showed a substantial population of cells with osteopontin expression exceeding 3 A.U., highlighting a pronounced effect of the triple-peptide functionalization on osteogenic differentiation.

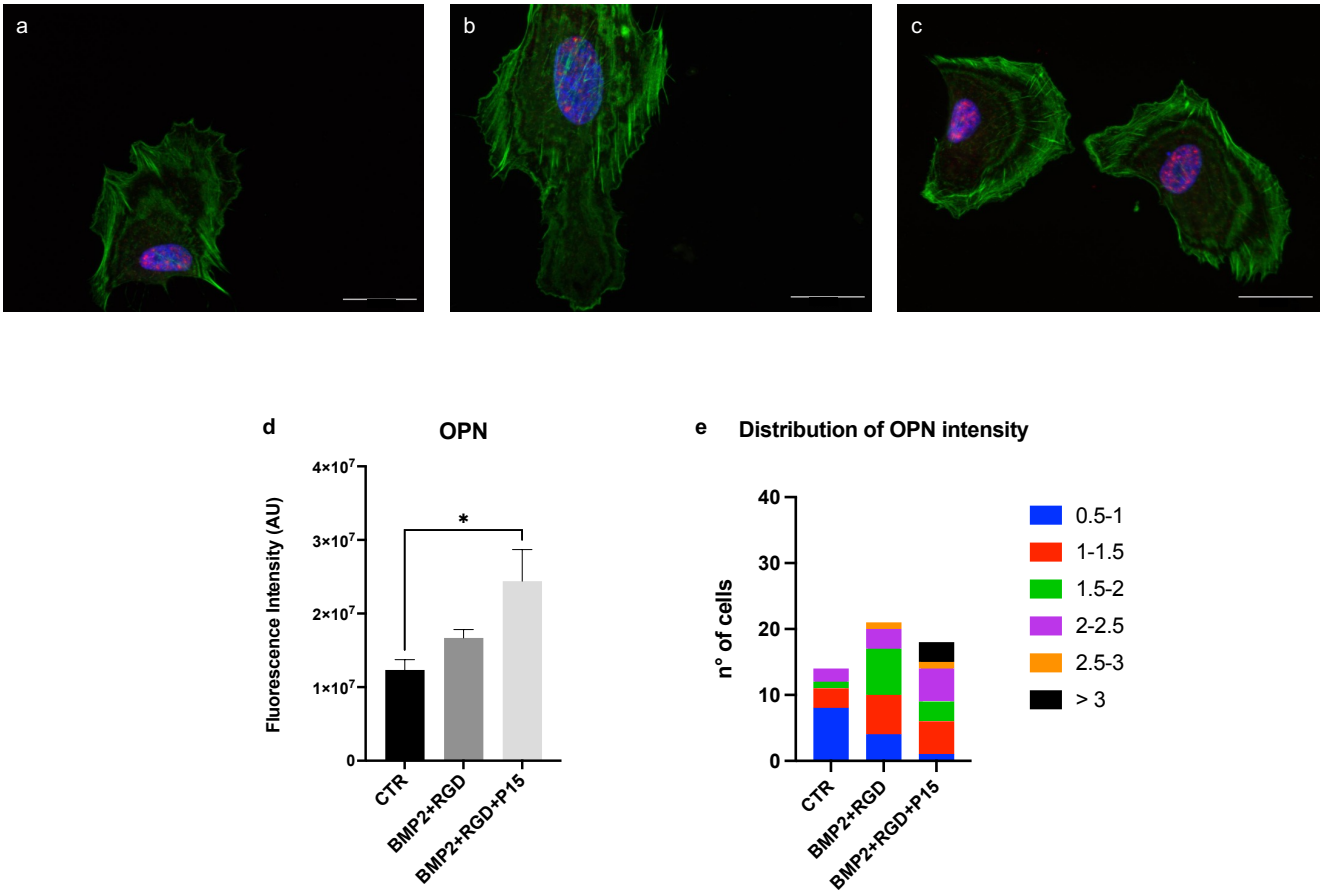


Figure 6.6. Representative immunofluorescence images of hMSCs showing OPN expression on control (a), BMP2+RGD (b), and BMP2+RGD+P15 (c) conditions at day 5. Nucleus (blue), F-actin (green), and osteopontin (red). Histograms showing OPN expression of hMSCs in response to Si-substrates functionalized with different peptide combinations (d) and distribution of OPN fluorescence intensity (e). Values are expressed as mean ± SD. The statistically significant differences were determined by one-way ANOVA (**** $p < 0.0001$, *** $p < 0.001$, ** $p < 0.01$, * $p < 0.05$). (n = 2 independent experiments). Scale bar, 25 μm.

6.6 Discussion

Advances in bone tissue engineering have increasingly highlighted the potential of bioactive peptides as key agents for bone repair and regeneration. Peptides offer several advantages over conventional protein-based therapies, including precise control over their molecular composition, enhanced stability under varying environmental conditions, and straightforward integration into biomaterial surfaces.[231], [325] These molecules are typically classified as either extracellular matrix (ECM)-derived, which contain functional domains that interact with cell receptors to influence processes like adhesion and differentiation, or as bone morphogenetic protein (BMP)-derived, known for their strong osteoinductive activity.[49], [308], [326] Still, achieving rapid and consistent osteogenic differentiation as observed in native bone tissue remains a significant challenge. The bone microenvironment is shaped by a complex interplay of physical, chemical, and biological cues, making it difficult to recreate using synthetic materials.[107], [258], [327] In response, research is increasingly focused on developing biomimetic and multifunctional surfaces that can deliver a combination of osteoinductive signals, aiming to better replicate the natural conditions required for effective bone regeneration. However, despite these advances, there remains a notable lack of studies that employ truly multi-functionalized strategies capable of recapitulating the full complexity of the bone extracellular matrix (ECM). Most existing approaches rely on single or dual bioactive modifications, which may not sufficiently replicate the synergistic interactions present in native bone tissue. This gap highlights the need for innovative surface engineering strategies that integrate multiple signaling domains to more accurately mimic the dynamic and multifaceted nature of the ECM. Within this context, the present study focuses on the multi-peptide functionalization of biomaterial surfaces by combining BMP2, RGD, and P15 mimetic peptides. This strategy is designed to more closely mimic the synergistic signaling environment of the native extracellular matrix and to provide a robust platform for accelerating and enhancing the osteogenic differentiation of human mesenchymal stem cells with at least three peptides. Each one contributes a distinct biological function: BMP2 is a potent osteoinductive factor that activates intracellular signaling pathways critical for osteoblast differentiation;[94] RGD is a well-characterized cell-adhesion motif, which promotes integrin-mediated attachment and spreading of stem cells on the material surface;[328], [329] and P15 is a synthetic peptide that mimics the cell-binding domain of type I collagen, further supporting cell adhesion and providing additional osteogenic cues.[226], [227] By integrating these multiple bioactive motifs, this approach aims not only to drive early osteogenic commitment but also to sustain the

differentiation process, ultimately improving the efficacy of bone regeneration strategies through a truly multifunctional and biomimetic surface.

In recent years, a wide range of biomaterial surface modification strategies have been developed to direct stem cell differentiation toward the osteoblastic lineage, a crucial step for successful bone tissue regeneration. Both physical and chemical modifications have been explored to enhance the osteogenic potential of implant surfaces.[107] For example, Mangano et al. compared laser-sintered and acid-etched titanium implants, finding that significant upregulation of osteogenic markers such as osteocalcin occurred only at later time points, highlighting the challenge of promoting early osteogenic commitment.[330] In contrast, our approach of simultaneously grafting three different bioactive peptides, demonstrated a marked acceleration of osteoblastic differentiation. Notably, we observed significant upregulation of both OCN and COL1A1 as early as day 3 on the triple-peptide surface, outperforming both single- and dual-peptide modifications. This rapid response stands out when compared with recent work by Yang et al.[331], who reported increased expression of key osteogenic markers (COL1A1, OCN, RUNX2) at day 14 on PEEK materials functionalized with metal element-fusion peptide nano-coatings. In our system, similar or greater upregulation was observed much earlier, and ALP expression at day 3 was nearly double that reported by Yang et al. at day 14.[331] Other investigations have highlighted how surface chemistry influences osteogenic differentiation. Tamaño-Machiavello et al., for instance, observed that gelatin-functionalized substrates significantly enhanced COL1A1 expression in hMSCs, while heparin-functionalized surfaces did not produce this effect.[332] Consistent with these findings, our triple-peptide functionalized surface led to a robust increase in COL1A1 expression, and notably, this upregulation occurred at an even earlier stage. Moreover, both our study and that of Tamaño-Machiavello et al. reported relatively low levels of RUNX2 expression, suggesting that the orchestration of osteogenic gene expression is highly dependent on the precise timing and interplay of bioactive cues presented to the cells. RUNX2 is widely recognized as a key transcription factor involved the early stages of osteogenic differentiation, directing mesenchymal stem cells toward the osteoblast lineage.[333] Its expression typically peaks during the initial commitment phase and subsequently declines as cells mature, while the expression of late-stage markers increases.[334], [335] This tightly regulated temporal pattern is essential, as persistently high levels of RUNX2 can actually impede osteoblast maturation, whereas its downregulation is necessary to maintain proper osteoblast function.[336], [337] In this study, no significant differences in RUNX2 expression were observed at day 3 among the tested conditions, including both control and peptide-functionalized surfaces. This observation likely reflects the fact

that, by this early time point, cells, particularly those on the triple-peptide surface, had already initiated commitment to the osteoblastic lineage, as evidenced by the pronounced upregulation of late and mid-stage markers. The subsequent marked decrease in RUNX2 expression observed by day 10 in all peptide-functionalized groups further supports the hypothesis that these cells had advanced along the differentiation pathway, in contrast to the control group where sustained RUNX2 levels suggested a delay in maturation. These findings highlight the strong osteoinductive potential of our multi-peptide functionalization strategy in promoting early osteogenic commitment and facilitating timely progression through the differentiation process.

There is growing consensus that closely replicating the essential features of the native ECM is key to providing cells with the complex array of biochemical and biophysical cues required for effective osteogenesis. The ECM is a highly complex and dynamic environment that orchestrates cell behavior through an interplay of structural, adhesive, and signaling molecules. Our findings with the BMP2+RGD+P15 triple-peptide functionalization reinforce the importance of designing multi-functionalized biomaterials that better emulate this intricate environment. By presenting cells with a synergistic combination of bioactive signals, such biomimetic surfaces appear to more effectively drive osteogenic differentiation. The interplay between RGD and BMP2 peptides in osteogenesis has been widely explored, with studies reporting both encouraging results and challenges in achieving consistent synergy. While several studies have demonstrated enhanced osteoinductive responses when both peptides are co-presented,[138], [139], [140], [213], [215], [223], [240], [338] the results are not always consistent. For example, Kim and co-workers found that BMP2 alone was more effective than its combination with RGD in upregulating osteogenic markers such as RUNX2 and COL1A1,[241] while Ma et al. similarly reported no clear synergistic benefit from co-presenting GRGDS and BMP2.[242] In contrast, Oliver-Cervelló et al. reported that titanium surfaces functionalized with RGD and DWIVA peptides induced a twofold increase in COL1A1 and a threefold increase in ALP expression by day 4, demonstrating the benefits of dual-peptide functionalization for promoting osteogenic differentiation.[339] Similarly, Bilem et al. functionalized glass coverslips with both integrin-binding RGD peptides and BMP2 mimetic sequences, demonstrating that their combination significantly enhanced cell attachment, in vitro spreading, and osteoblastic differentiation compared to surfaces grafted with either peptide alone.[215]

Building on these insights, our study shows that incorporating a third peptide, P15, alongside BMP2 and RGD leads to an even greater enhancement, COL1A1 expression increased 2.4-fold and ALP nearly 4-fold within just 3 days. This marked enhancement compared to the dual-peptide system

underscores the superior osteoinductive capacity of our triple-peptide approach and further supports the value of incorporating multiple bioactive cues to enhance and accelerate hMSCs osteogenic differentiation.

P15 recognized for its osteogenic potential as a biomimetic of the cell-binding domain of type I collagen,[319] has traditionally been studied either on its own or in conjunction with substrates like hydroxyapatite[340], titanium[225], [341] or anorganic bone matrix.[342] However, its effects in combination with other grafted bioactive peptides has not been explored. In our study, integrating P15 with BMP2 and RGD resulted in a notably strong upregulation of late-stage osteogenic markers as early as day 3, exceeding the effects observed with either single- or dual-peptide modifications and the unmodified control. This early gene activation indicates that cells receive a stronger and faster osteogenic stimulus than what is usually achieved with P15 or other peptides alone. Interestingly, the control surfaces did not achieve comparable levels of osteogenic marker expression until day 10, indicating a slower and less efficient differentiation process. By contrast, on the triple-peptide surface, gene expression had already peaked and begun to stabilize or decrease by day 10, suggesting that the cells had reached a more advanced stage of osteogenic maturation much earlier. Overall, these results highlight the advantage of presenting multiple adhesion and osteogenic cues simultaneously, supporting a synergistic effect that accelerates and enhances osteodifferentiation beyond what is achievable with single-peptide or unmodified substrates.

To date, only three other studies have explored the use of a triple-peptide functionalized materials to induce osteogenic differentiation. This limited number of studies may be attributed to challenges in precisely controlling the amount and ratio of multiples peptides grafted onto the surface, which is critical for ensuring reproducible and effective multi-functionalization. For instance, Liu et al. investigated titanium surfaces modified with RGD, osteogenic growth peptide (OGP), and a pro-angiogenic peptide (Ang), reporting ALP expression at day 7 that was comparable to the levels we observed as early as day 3 with our BMP2+RGD+P15 system. While regarding late-stage osteogenic differentiation, Liu et al. found a higher OCN expression at day 7 than what we detected at day 3.[343] Moreover, the compared study uses UV–vis spectroscopy for bulk quantification of adsorbed peptides, supported by fluorescence microscopy confirming overall distribution. In contrast, our high-resolution fluorescence microscopy approach not only visualizes different peptides simultaneously on the same surface but also provides detailed spatial distribution and homogeneity information, revealing micro-scale localization and peptide co-grafting patterns that UV–vis cannot capture.[66] Importantly, another key distinction of our study is the use of human bone marrow-derived stem cells, whereas all

previous studies investigating triple-peptide functionalization have relied on mouse or rat bone marrow-derived cells. To our knowledge, this is the first evaluation of the osteogenic potential of triple-peptide functionalized materials using human stem cells, highlighting the innovation and potential translational impact of our work.

SATB2 is a crucial transcription factor that orchestrates the expression of osteogenic markers and plays a critical role in skeletal development.[344] In our study, we observed a marked upregulation of SATB2 mRNA expression at day 3, particularly in the triple-peptide condition. Notably, SATB2 expression level remained elevated even at day 10 in all peptide-functionalized conditions, suggesting a sustained osteogenic differentiation process, potentially reflecting the presence of later-stage osteoblastic cells. SATB2 has been extensively studied as a key regulator of skeletal development. It promotes the transcription of key osteogenic genes and is essential for proper skeletogenesis. Previous studies have shown that SATB2 deficiency results in significant bone loss and craniofacial abnormalities, highlighting its function as a central molecular node in the transcriptional network that regulates osteoblast differentiation and skeletal development.[345] SATB2 regulates the expression and function of key osteogenic genes, including Runx2 and Osterix, which in turn promotes osteoblast differentiation and maturation.[346], [347]
A well-established mechanism for SATB2 activation is the BMP signaling pathway. Upon binding of BMP2, BMP4, or BMP7 to their membrane receptors, Smad1/5 proteins become phosphorylated and can directly bind to the SATB2 promoter, thereby inducing its transcription and promoting osteoblast differentiation.[348]
Our RT-qPCR analysis aimed to elucidate the involvement of key signaling pathways in SATB2 regulation. We observed upregulation of Smad1 and Smad5, particularly in conditions containing BMP2 alone or in combination with RGD. Interestingly, the triple-peptide condition (BMP2+RGD+P15) did not show the same increase in Smad1/5 expression. Despite this, SATB2 expression was most strongly upregulated in the triple-peptide group. These findings are consistent with the established role of BMP proteins in activating the Smad pathway, as the most pronounced upregulation of Smad1 and Smad5 was observed in the BMP2 and BMP2+RGD conditions during early differentiation.[89] In contrast, the triple-peptide group, despite exhibiting robust early SATB2 expression, did not show comparable Smad1/5 induction. This suggests that the enhanced osteogenic response in the triple-peptide condition may involve additional signaling mechanisms beyond canonical BMP/Smad activation. In particular, pathways activated by P15, which mimics the cell-

binding domain of collagen I and engages integrin-mediated signaling, may synergistically enhance SATB2 expression in conjunction with BMP signaling.[89], [319] Our results indicate that SATB2 serves as a key regulator of osteogenic differentiation, and its expression can be influenced by both BMP/Smad-dependent mechanisms and additional signaling pathways. The sustained high levels of SATB2 expression observed in the triple-peptide group highlight the potential for combinatorial biomaterial strategies to optimize osteogenic differentiation by targeting multiple signaling axes simultaneously.

Osteopontin (OPN) is another key late osteogenic marker whose expression reflects the maturation stage of osteogenic differentiation.[89], [90] Immunocytochemistry for OPN revealed that the triple-peptide functionalized surface significantly enhanced osteogenic commitment compared to the control. Although the overall fluorescence intensity of OPN expression was not significantly different between cells on the dual-peptide and triple-peptide surfaces, a closer single-cell analysis revealed important distinctions. Examining OPN expression on a cell-by-cell basis showed a markedly different distribution between the two groups. Specifically, the triple-peptide functionalization led to a clear shift toward higher OPN expression levels at the individual cell level, with almost no low-expressing cells and a substantial population of cells exhibiting strong OPN fluorescence (above 3 A.U.), which was absent in the dual-peptide and control groups. This single-cell insight complements molecular approaches by revealing cell-to-cell variability in protein expression and highlighting the enhanced osteoinductive potential of multifunctional coatings on individual cells. These findings align with our gene expression data and reinforce that triple-peptide presentation synergistically promotes advanced osteogenic differentiation.

6.7 Conclusions

This study demonstrates the significant advantages of multi-peptide functionalization in biomaterial design for bone tissue engineering. By integrating BMP2, RGD, and P15 peptides onto a single surface, we created a biomimetic interface that more closely mimic the complexity of the native extracellular matrix. Through comprehensive surface characterization and biological evaluation, we demonstrated that these multi-functionalized surfaces strongly promote osteogenic differentiation of human mesenchymal stem cells. Notably, the triple-peptide approach led to a marked upregulation of key osteogenic markers, including late-stage factors such as SATB2 and OCN, at much earlier time

points than observed with conventional single- or dual-peptide modifications. These results underscore the potential of combining multiple complementary bioactive cues to substantially accelerate the osteogenic differentiation process. This strategy offers a promising avenue for the development of next-generation biomaterials capable of enhancing the speed and effectiveness of bone regeneration in clinical applications.

Supporting Information

Normalized emission spectra of single, dual-, and triple-peptide solutions (Figure S1); unnormalized emission spectra of single-peptide functionalized surfaces (Figure S2); representative hMSCs images at 5-day time point on control and peptide-functionalized materials (Figure S3).

Acknowledgements

This work was supported by the Natural Science and Engineering Research Council of Canada (G.L), as well as the Centre Québécois sur les Matériaux Fonctionnels (G.L). M.K is the recipient of a scholarship from the Fondation du CHU de Québec-Université Laval. M.C.D would like to thank the French National Research Agency (ANR-21-CE06-0031-02) for its support, as well as the Nouvelle Aquitaine Region (contract n° 2017-1R30109-00013176) and the Department of Health Sciences and Technologies from the University of Bordeaux for their support.

6.8 Supporting Information

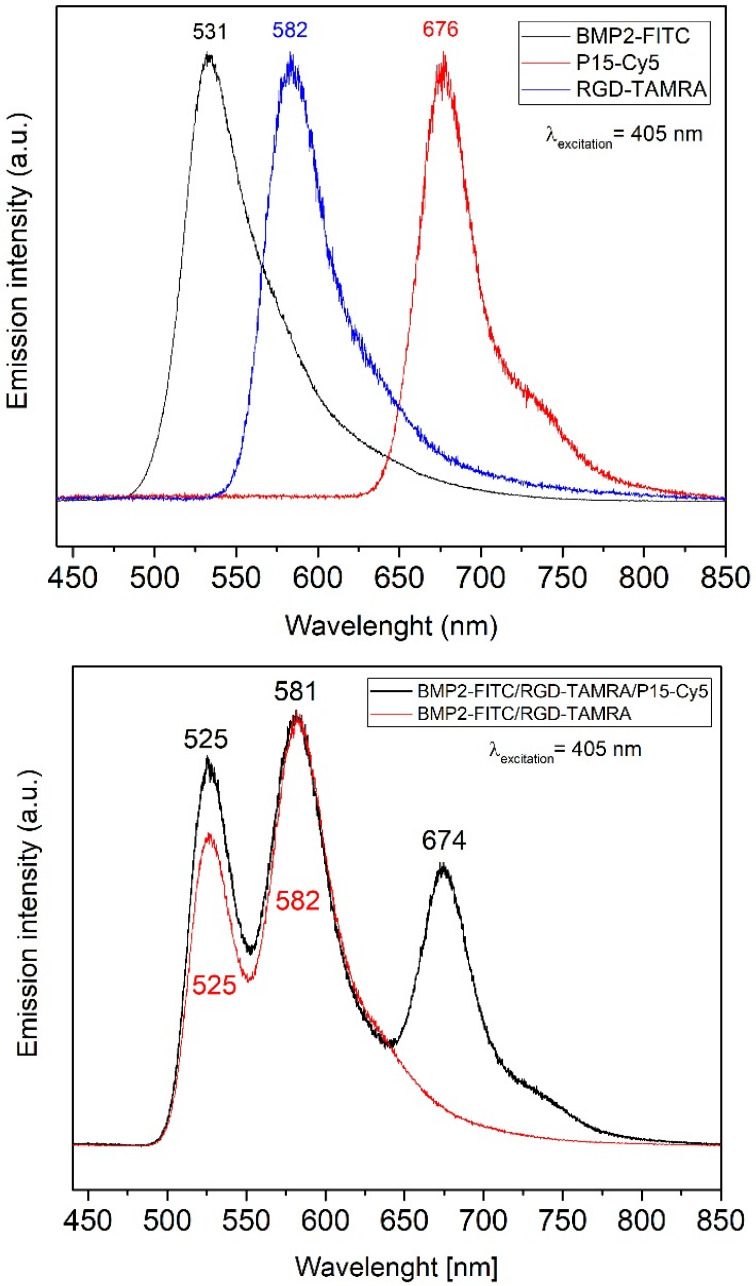


Figure 6.7. Normalized emission spectra of single peptides (left), dual-peptide and triple-peptide (right) in solution, excited at 405 nm.

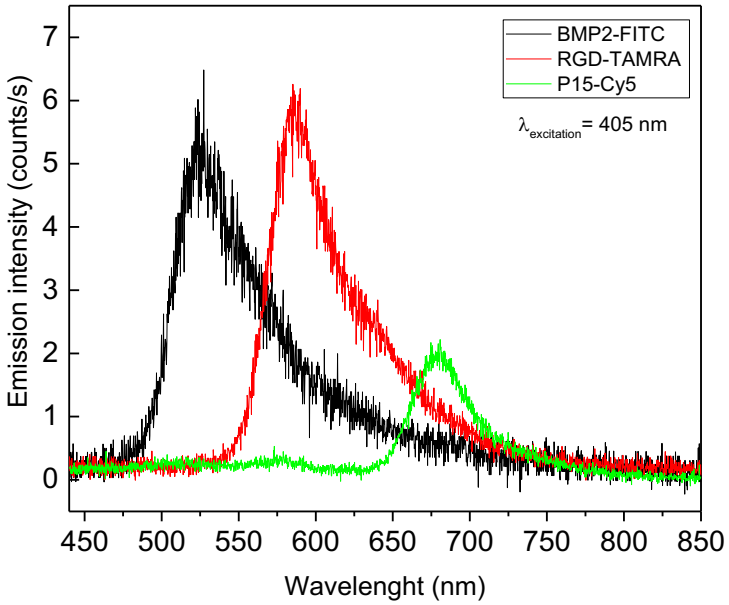


Figure 6.8. Unnormalized emission spectra of single peptide surfaces excited at 405 nm.

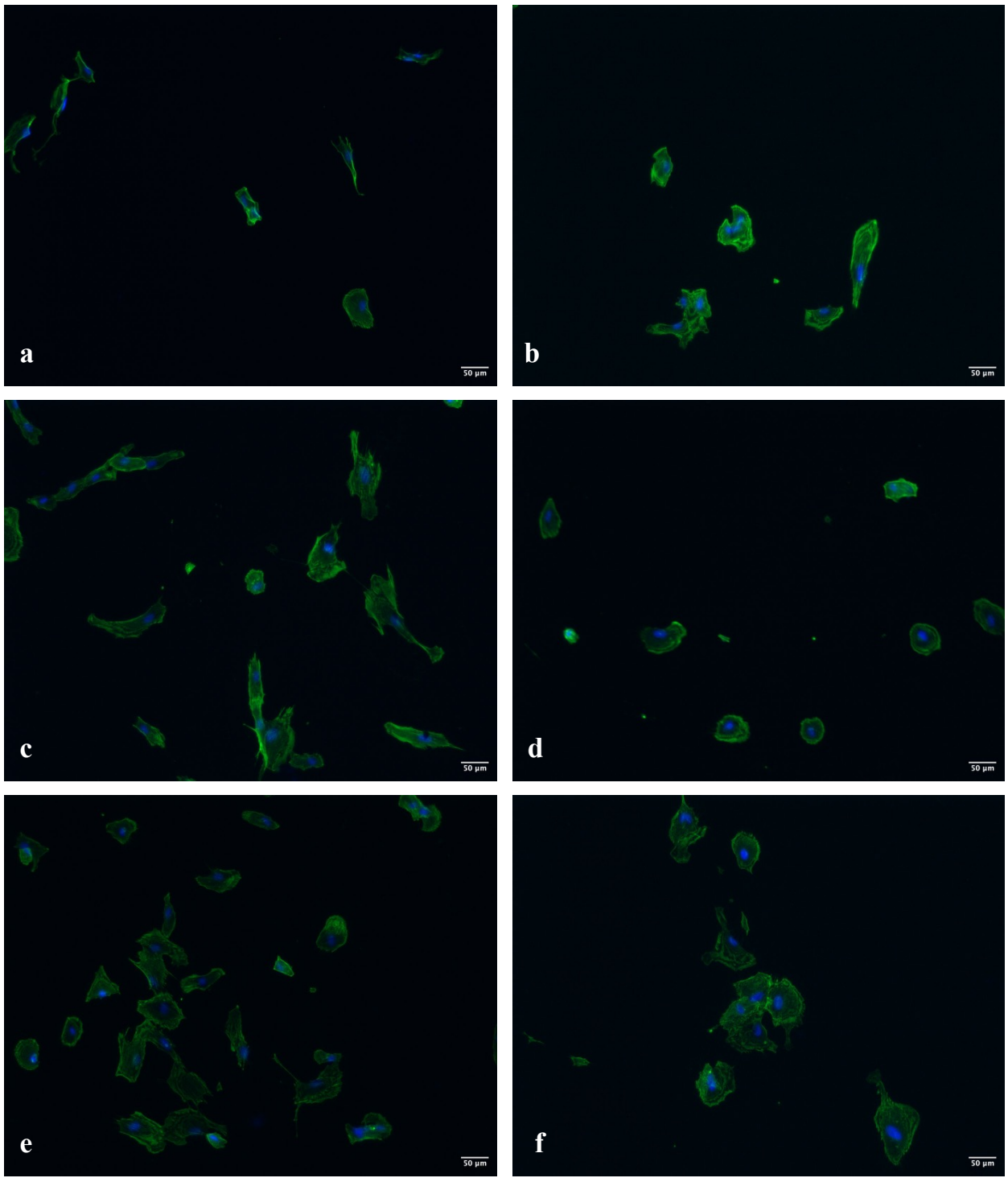


Figure 6.9. Representative images of hMSCs at the 5-day time point, acquired at 10× magnification (n = 2 biologically independent experiments). (a–b) Cells on the control material (silicon without peptides); (c–d) cells on material functionalized with BMP-2 + RGD peptides; (e–f) cells on material functionalized with BMP-2 + RGD + P15 peptides. Scale bar, 50 µm.

Conclusion

General discussion

This study focused on the design and development of in vitro platforms capable of inducing rapid and efficient differentiation of hMSCs towards the osteogenic lineage. The work lies within the field of biomaterials for tissue engineering, at the intersection of biology and materials science. The main objective of this research project was to functionalize silicon wafers with ECM-derived mimetic peptides to enhance both cell–cell and cell–material interactions, thereby inducing osteogenic differentiation.

The following general discussion will highlight the main conclusions, key achievements, and address the limitations observed in this study, framing them within the current state of the art. Finally, future perspectives and possible directions that emerge from this work will be outlined.

1. Silanization strategies and impact on biomaterial functionalization

In the first part of this work, presented in Chapter 4, attention was devoted to investigating and characterizing the effect of silanization on the subsequent anchoring of biomolecules. An extensive and comparative study was carried out, challenging the conventional use of silane molecules that have been traditionally employed for this procedure. The results presented in this study highlight the critical role of silanization as the initial step in the functionalization of biomaterials, exerting a profound influence both on peptide immobilization efficiency and on the cellular response to the modified surfaces. APTES has traditionally been the most commonly used silane for surface modification, facilitating subsequent grafting of biomolecules.[283], [284] However, our findings, in agreement with recent reports, underline important limitations of this approach.[285], [288] In particular, APTES silanization demonstrated a lack of reproducibility, mainly attributed to its tendency to form disorganized multilayers under variable and hardly controllable conditions. Moreover, a high density of amine groups on the surface did not necessarily correlate with improved bioactivity, indicating that

surface chemistry must be viewed not only in terms of quantity but also accessibility and organization of functional groups.

A central contribution of this work was the comparative analysis of alternative silanization strategies. Longer-chain silanes, such as AUTES, were found to increase nanoscale roughness and hydrophobicity, properties previously associated with enhanced osteoinductive potential and improved cell differentiation.[285] More importantly, the introduction of a protected silane molecule, Alk-Phtha, provided further insights into the critical relationship between molecular organization and biological outcomes. Although structurally analogous to AUTES after deprotection, the Alk-Phtha generated more homogeneous and ordered monolayers. Following deprotection, the resulting Alk-NH_2 substrate, despite its lower overall density of amine groups, offered superior accessibility for peptide grafting. This resulted in enhanced biological responses, particularly in terms of cell adhesion, cytoskeletal organization, and focal adhesion maturation. These findings emphasize that protecting group strategies represent a powerful tool to regulate the orientation and accessibility of reactive moieties during surface modification, overcoming the inherent limitations of commercial aminosilanes.

Equally significant is the methodological innovation introduced in this work. For the first time, spin coating was employed as a silanization technique prior to biomolecule immobilization. Compared with conventional immersion or vapor-phase processes, spin coating demonstrated multiple advantages, including reduced solvent consumption, lower chemical waste generation, and a substantial reduction in processing time. Remarkably, this optimized and low-cost approach produced surfaces with biological performance comparable to, and in some instances superior to, that of traditional employed methods. Thus, spin coating emerges as a sustainable and technically appealing alternative for large-scale or industrial applications of biomaterial functionalization.

The biological relevance of these surface modifications was demonstrated in adhesion studies with hBMSCs cultured on differently silanized substrates functionalized with the same RGD peptide. Clear differences were observed in cell spreading, organization of the actin cytoskeleton, and focal adhesion formation. In particular, Alk-NH_2-modified surfaces supported more extensive cell spreading, along with stronger F-actin expression and more robust focal adhesions.

The silanization step is critically important as the foundation of surface modification, given its substantial influence on all subsequent layers. These findings clearly demonstrate that even when biochemical signals remain the same, the nature of the silanization chemistry profoundly shapes the cellular responses that follow. This emphasizes that the initial silanization chemistry doesn't just

prepare the surface, it fundamentally dictates the behavior of all subsequent grafted biomolecules, making it a decisive factor in the overall performance of the modified surface. Altogether, these results challenge conventional assumptions about silanization and propose a paradigm shift in biomaterial surface functionalization. Rather than focusing solely on achieving the highest grafting density, effective strategies should prioritize control, orientation, and accessibility of functional groups. The use of protecting groups and the implementation of spin coating provide a higher degree of precision in tailoring surface properties, ultimately enabling superior cellular outcomes. This work therefore introduces both a novel molecule and a novel method, offering a cost-effective, sustainable, and biologically advantageous pathway for biomaterial design.

2. Multi-peptide functionalization enhances osteogenic differentiation

Building on the findings presented in the first part of this thesis, which demonstrated the critical role of silanization in biomaterial surface modification by enhancing peptide accessibility and promoting stem cell adhesion, the second part of this work, detailed in Chapter 5, extends this foundation to focus on osteogenic differentiation. Specifically, an optimized silanization strategy was developed to immobilize three ECM-derived mimetic peptides, RGD, BMP-2, and P15, each targeting distinct cellular pathways in human mesenchymal stem cells. While the adhesion-promoting RGD peptide was previously utilized, the incorporation of BMP-2 and P15 introduces osteogenic signals, resulting in a multifunctional surface designed to support cell attachment and actively promote differentiation toward the osteoblastic lineage.

The osteoinductive effects of these peptides were evaluated individually as well as in dual and triple combinations. This combinatorial approach demonstrated strong synergistic interactions, significantly enhancing and accelerating early osteogenic differentiation in vitro.

Advances in bone tissue engineering increasingly recognize bioactive peptides as effective agents for bone regeneration due to their precise molecular control, stability, and effective surface immobilization. These peptides, typically derived from extracellular matrix proteins or bone morphogenetic proteins (BMPs), play distinct roles in promoting osteogenic differentiation. However, achieving rapid and consistent osteogenesis comparable to native bone remains challenging due to the complexity of the bone microenvironment. This study developed a multi-peptide functionalized biomaterial surface combining BMP-2, RGD, and P15 peptides to better emulate the native extracellular matrix's synergistic signaling. The triple-peptide approach significantly accelerated

osteogenic differentiation of hMSCs, with early and marked upregulation of key osteogenic markers such as OCN, COL1A1, ALP, and SATB2, compared to single- and dual-peptide modifications. Notably, osteogenic commitment was induced at an unusually early time point (as soon as 3 days), along with robust expression of late-stage and fully committed osteoblast markers, indicating both rapid initiation and progression of differentiation.

This multi-peptide functionalization strategy builds on previous dual-peptide systems by adding a third component, more closely resembling the complex and active environment of the native extracellular matrix. The three peptides (BMP-2, RGD, and P15) were carefully selected to target independent cellular pathways, thereby activating multiple signaling mechanisms simultaneously to maximize the osteogenic response. The inclusion of this third complementary peptide represents a significant advancement toward better mimicking the multifaceted signaling characteristic of the natural ECM, which is critical for effective osteogenic differentiation.

This study represents the first reported use of this specific triple-peptide combination immobilized on a biomaterial surface with the objective of enhancing osteoinductive effects through their synergistic interplay. Moreover, while multi-peptide strategies involving more than two peptides for osteogenic differentiation are still rarely explored, the few existing studies have been limited to rodent-derived bone marrow stem cells (rats or mice).[343], [349] In contrast, this work pioneers the application of this triple-peptide functionalization to human bone marrow-derived mesenchymal stem cells, marking a significant advancement that enhances the translational potential for clinical bone regeneration therapies.

These findings were reinforced through high-resolution spatial mapping, which revealed a uniform and homogeneous distribution of the three peptides across the surface. This consistent co-localization supports the hypothesis that all three peptides are positioned optimally to interact concurrently with cellular receptors, thereby facilitating synergistic cellular responses. Such an even distribution is critical for mimicking the complex architecture of the native extracellular matrix, ensuring that multiple signaling pathways are engaged simultaneously.

Overall, these findings underscore the critical importance of designing biomimetic multifunctional surfaces that recreate the complex native extracellular matrix environment through multiple signaling domains, efficiently guiding stem cell differentiation towards osteogenic lineage.

3. Importance of silane molecule in optimizing multi-peptide immobilization

As previously discussed in this section, the first part of this thesis focused on the importance of silanization as a fundamental initial step in biomaterial modification. We demonstrated how silanization impacts not only the biomolecules that are subsequently immobilized but also the cellular behavior that arises from the interaction with these molecules and their presentation to the cells. Building on this understanding, we developed a new silanization strategy using the innovative Alk-Phtha molecule, which allows deprotection at the very last stage prior grafting, ensuring greater accessibility of amino groups for biomolecule conjugation. This advancement formed the foundation for the second phase of our research.

The impressive results obtained from the triple-peptide immobilization on surfaces silanized with this novel method revealed a significant potential to induce osteogenic differentiation. This effect is attributed to the multifactorial contribution of different peptides acting synergistically and complementarily, activating diverse cellular mechanisms that further amplify the osteoinductive response. Furthermore, it is crucial to emphasize the hypothesis that the optimization of the silanization process played an essential role in the highly positive outcomes achieved with the triple-peptide functionalization. The combination of the Alk-Phtha molecule with the spin coating technique significantly optimized subsequent peptide grafting, ensuring improved accessibility and a more efficient presentation of the functional domains to the cells in contact with the modified surfaces. Based on the conclusions of comparative studies between commercial silanes and the proposed Alk-Phtha molecule, along with previous evidence from cellular adhesion assays involving the RGD peptide, there is substantial evidence to suggest that the remarkable outcomes observed with silanization in RGD immobilization are likewise achieved and potentially enhanced when applied to multi-peptide functionalization strategies. This highlights the critical role of tailored silanization in advancing the performance and bioactivity of peptide-modified biomaterial surfaces.

4. Unraveling peptide spatial distribution through fluorescence imaging

A critical and challenging aspect of biomaterial functionalization involving peptide immobilization on surfaces is the precise determination of peptide presence and density. This issue becomes particularly complex given that, to date, no methodology exists that can provide absolute quantification of grafted peptides per unit area. The challenge deepens further when simultaneous quantification of multiple peptides on the same surface is required. One widely used technique to confirm peptide layer

formation after functionalization is X-ray Photoelectron Spectroscopy (XPS). By analyzing significant changes in both C1s and N1s spectra relative to the silanized surface for instance, the presence of a peptide layer can be detected. Specifically, pronounced peaks corresponding to amide bonds appear in these spectra, serving as a signature of peptide linkages.[114], [350] Although XPS unequivocally confirms peptide presence, it fails to discriminate peptide identities or provide spatial information on their distribution.

Contact mode Atomic Force Microscopy (AFM) complements this by revealing the uniformity of the peptide layer through surface roughness measurements. An increase in roughness compared to the unmodified substrate indicates the formation of a homogeneous peptide monolayer. Likewise, contact angle measurements typically show decreased values following peptide conjugation, providing indirect but useful evidence of surface modification.[351]

Further validation of peptide attachment is achieved with Time-of-Flight Secondary Ion Mass Spectrometry (ToF-SIMS), which detects characteristic "immonium ions", small fragment ions unique to amino acid side chains. These serve as diagnostic markers for peptides and enable identification of amino acid residues such as glycine, arginine, leucine, and methionine on the surface.[114], [351] Despite their value, these methods collectively confirm grafting success but do not enable differentiation between peptides or detailed spatial mapping of their distribution.

Bulk quantification techniques such as UV-vis spectroscopy estimate peptide density indirectly by measuring the concentration difference of peptide solutions before and after surface grafting, attributing this difference to immobilized peptides.[343]

Fluorescence microscopy remains the closest approach to semi-quantitative peptide density analysis on surfaces. This technique involves functionalizing surfaces with peptides tagged with distinct fluorophores. Fluorescence intensities measured at specific wavelengths are correlated with calibration curves, allowing estimation of peptide surface densities in picomoles per square millimeter ($pmol/mm^2$).[140], [214], [215] This strategy enables more precise quantification and simultaneous differentiation of multiple peptides grafted on biomaterial surfaces.

Building on this, we employed high-resolution fluorescence microscopy by tagging three peptides with fluorophores emitting at distinct wavelengths, permitting independent detection. This approach allowed us to determine fluorescence intensities in single-peptide functionalized surfaces, as well as simultaneously detect all three peptides on the triple-modified material, confirming successful co-functionalization and discrimination of peptides.

Furthermore, we performed mapping analysis to evaluate the homogeneity of peptide distribution on

surfaces functionalized with dual and triple peptide combinations. These mappings not only visualized peptides simultaneously but also facilitated semi-quantitative comparisons by correlating peak intensities from single-, dual-, and triple-functionalized surfaces, estimating relative peptide concentration. Critically, spatial distribution observations confirmed precise localization and homogeneous co-grafting of peptides, offering qualitative and semi-quantitative insights into multi-peptide functionalization with spatial resolution, enhancing our understanding of surface grafting efficiency and peptide distribution.

However, although various analytical techniques confirm peptide immobilization, achieving precise, spatially resolved, and absolute quantification of grafted peptides remains a significant challenge in biomaterials research.

Future Perspectives

This work has contributed significant advances in the functionalization of biomaterials to induce the osteogenic differentiation of stem cells, aiming to fill some of the existing gaps in the current scientific literature. Nevertheless, several aspects remain open for further investigation, which could expand and complete the discoveries presented here.

Regarding silanization, this study has challenged both the conventional methods traditionally employed and the commercial molecules commonly used for this process, opening new research perspectives on the fundamental importance of the very first modification layer, which determines the success of subsequent processing steps and the overall performance of engineered biomaterials. It would therefore be highly relevant to evaluate the effects of the proposed silanization strategies on substrates other than silicon wafers, such as glass and silica-based materials, metal oxides, ceramic materials, in order to optimize biofunctionalization across different types of biomaterials. This is particularly important considering the significant impact that silanization exerts not only on the surface chemistry but also on subsequent cell behavior.

A major innovation of this work is the first demonstration of the simultaneous use of three peptides in the biofunctionalization of substrates with human stem cells. While a few previous studies have explored tri-peptide functionalization, none had applied this approach to human stem cells until now.[343], [349] This work represents indeed the first evaluation of triple-peptide functionalization using human stem cells, emphasizing its strong translational potential for next-generation bone repair biomaterials. The evidence presented here opens unprecedented opportunities to enhance the biomimicry of the extracellular matrix. Future investigations could extend this approach to the use of more than three peptides simultaneously, targeting different signaling pathways to influence cell fate decisions through synergistic and multi-level modulation.

An especially promising avenue is the use of multifunctional peptides, in which a shared backbone anchors the molecule to the substrate while exposing multiple bioactive domains on its surface. For instance, multifunctional peptides could combine RGD and BMP-2 sequences within the same structure.[260], [352] This approach could better reproduce the functional diversity of the ECM and

more faithfully mimic the spatial proximity of different epitopes naturally present in the extracellular environment.

Considering the importance of replicating native cell-cell and cell-matrix communication, future work could also explore combining multi-peptide biofunctionalization with the incorporation of soluble factors that mediate paracrine signaling. In physiological microenvironments, it is precisely the synergy of multiple communication modalities that drives the activation of complex cellular processes, rather than single isolated signals.[353], [354]

From the standpoint of surface characterization, this study introduced the combined use of high-resolution fluorescence microscopy and Raman spectroscopy achieving a semi-quantitative estimation and precise localization of peptides on biomaterial surfaces. However, the absolute quantification of peptide density remains an open challenge. This methodology could be developed further by introducing calibration curves correlating fluorescence intensities with known concentrations, thereby enabling absolute quantification alongside spatial distribution mapping. This integrated approach would provide complementary and unprecedented information on peptide functionalization.

With respect to the cell models employed, this work relied on hMSCs derived from a 61-year-old male donor. However, physiological variables such as age and sex are known to influence stem cell behavior.[355], [356], [357] Future studies should therefore assess donor-dependent variability by systematically comparing stem cells from younger and older individuals and from both sexes. Within the emerging framework of personalized medicine, the ideal approach would involve isolating and evaluating stem cells directly from individual patients to assess their regenerative potential in a patient-specific manner.

Finally, a crucial perspective concerns the investigation of complete osteogenic differentiation. This study successfully demonstrated accelerated and efficient osteoblastic differentiation in vitro using multi-peptide functionalized platforms. However, future developments should focus on the progression toward osteocyte maturation and matrix mineralization, which are still challenging to achieve under in vitro conditions, particularly for fully mature human osteocytes. Long-term studies would therefore be essential to assess the stability and mineralization capacity of osteogenically differentiated cells, providing valuable insight into the ability of multi-functionalized platforms to sustain late-stage osteogenic processes.

This work demonstrates that effective biomimetic surface design depends on both assembling multiple bioactive cues and precisely controlling their chemical presentation. By introducing an innovative silanization method and showing the unique benefits of triple-peptide functionalization in human stem cell differentiation, this work pushes bone tissue engineering closer to truly biomimetic solutions. The approaches developed here pave the way for advanced biomaterials aimed at driving complex cellular responses and supporting future regenerative therapies.

Appendix A

Scientific communications

A.1 Publications

Silanization Strategies for Tailoring Peptide Functionalization on Silicon Surfaces: Implications for Enhancing Stem Cell Adhesion, Kosovari, Melissa; Buffeteau, Thierry; Thomas, Laurent; Guay-Bégin, Andrée-Anne; Vellutini, Luc; McGettrick, James; Laroche, Gaetan; Durrieu, Marie-Christine, ACS Appl. Mater. Interfaces 2024, 16, 23, 29770–29782

Synergistic Multi-Peptide Interfaces Enhance Early Osteogenic Differentiation of Mesenchymal Stem Cells, Kosovari, Melissa; Dussauze, Marc; Petuya, Claire; Buffeteau, Thierry; Remy Murielle; Vellutini, Luc; Zibarov, Artem; Laroche, Gaetan; Durrieu, Marie-Christine. Submitted for publication on September, 2025.

A.2 Oral Communications

Melissa Kosovari, Murielle Remy, Luc Vellutini, Gaétan Laroche, Marie-Christine Durrieu, Engineering **Multi-Peptide Biointerfaces to Enhance Osteogenic Differentiation**, CBMN day, Bordeaux, France, 2025, 30 June

Melissa Kosovari, Thierry Buffeteau, Murielle Remy, Luc Vellutini, Gaétan Laroche, Marie-Christine Durrieu, **Advanced Silanization and Multi-Peptide Functionalization of Biomaterials for Stem Cell Osteodifferentiation**, Journées BIOMAT 2025, Arcachon, France, 2025, June 23-25

Melissa Kosovari, Thierry Buffeteau, Murielle Remy, Luc Vellutini, Gaétan Laroche, Marie-Christine Durrieu, **In Vitro Strategies for Bone Tissue Engineering: Biomaterial Functionalization with Mimetic Peptides and Silanization Approaches**, 13th Young Scientists Symposium, Université de Bordeaux, Bordeaux, France, 2025, May 16

Melissa Kosovari, Thierry Buffeteau, Mariam Taha, Luc Vellutini, Hesham Abdelbary, Gaétan Laroche, Marie-Christine Durrieu, **Biomaterial Surface Modifications: Enhancing Cell Adhesion for Successful Implant Osteointegration**, Journée scientifique annuelle du Département Sciences et Technologies pour la Santé, 2024, November 25

Melissa Kosovari, Thierry Buffeteau, Luc Vellutini, James McGettrick, Gaétan Laroche, Marie-Christine Durrieu, **In vitro systems for bone tissue engineering: Biochemical functionalization with mimetic peptides**, Doctoral Seminar II, Université Laval, Québec, Canada, 2024, July 9

Melissa Kosovari, Thierry Buffeteau, Luc Vellutini, Gaétan Laroche, Marie-Christine Durrieu, **Impact of Silanization on Peptide Presentation and Stem Cell Behavior on Silicon Surface,** 8e colloque CQMF/QCAM, Université Laval, Québec, Canada, 2024, May 22-23

Melissa Kosovari, Thierry Buffeteau, Luc Vellutini, James McGettrick, Gaétan Laroche, Marie-Christine Durrieu, **Impact of Silanization on Peptide Presentation and Stem Cell Behavior on Silicon Surface**, Séminaire Axe Médecine Régénératrice du CRCHU de Québec - Université Laval, Québec, Canada, 2024, May 16

Melissa Kosovari, Thierry Buffeteau, Luc Vellutini, James McGettrick, Gaétan Laroche, Marie-Christine Durrieu, **Silanization affects peptide functionalization of silicon surfaces: impact on stem cell adhesion**, STS Department Scientific Day 5th edition, Université de Bordeaux, Bordeaux, France, 2023, November 23

Melissa Kosovari, Thierry Buffeteau, Luc Vellutini, Gaétan Laroche, Marie-Christine Durrieu, Surface structuring at the nano and micrometric scale for cell differentiation, Seminar at ISM - Institut des Sciences Moléculaires, Université de Bordeaux, Bordeaux, France, 2023, November 7

Melissa Kosovari, Thierry Buffeteau, Luc Vellutini, James McGettrick, Gaétan Laroche, Marie-Christine Durrieu, **Effect of different silanization strategies on silicon substrates to enhance peptide grafting for osteogenic differentiation**, CBSC day, Université de Bordeaux, Bordeaux, France, 2023, July 12

Melissa Kosovari, Andrée-Anne Guay-Bégin, Gaétan Laroche, Marie-Christine Durrieu, **Surface structuring at the nano and micrometric scale for cell differentiation**, Session CBMN internal seminar for 1st year Ph.D. students, Université de Bordeaux, Bordeaux, France, 2023, February 2

Melissa Kosovari, Andrée-Anne Guay-Bégin, Marie-Christine Durrieu, Gaétan Laroche, **Surface structuring at the nano and micrometric scale for cell differentiation**, European Tissue Repair Society Annual Meeting 2022 - ETRS 2022, Lyon, France, 2022, September 15-17

Melissa Kosovari, Andrée-Anne Guay-Bégin, Marie-Christine Durrieu, Gaétan Laroche, **Surface structuring at the nano and micrometric scale for cell differentiation**, Doctoral Seminar I, Université Laval, Québec, Canada, 2022, June 15

A.3 Poster presentation

Melissa Kosovari, Thierry Buffeteau, Murielle Remy, Luc Vellutini, Gaétan Laroche, Marie-Christine Durrieu, **Cocktail Chemistry Meets Biomaterials: Advanced Functionalization for Regenerative Medicine**, ISSCR 2025 Annual Meeting - The Global Stem Cell Event, Hong Kong, 2025, June 11-14

Melissa Kosovari, Thierry Buffeteau, Mariam Taha, Luc Vellutini, Hesham Abdelbary, Gaétan Laroche, Marie-Christine Durrieu, **Biomaterial Surface Modifications: Enhancing Cell Adhesion**

for Successful Implant Osteointegration, Chemistry Biology Interface Day (CBID 2024), Université de Bordeaux, Bordeaux, France, 2024, November 26

Melissa Kosovari, Thierry Buffeteau, Laurent Thomas, Andrée-Anne Guay-Bégin, Luc Vellutini, James McGettrick, Gaétan Laroche, Marie-Christine Durrieu, **Silanization-induced changes in peptide presentation on silicon surfaces and their effects on stem cell behavior**, World Biomaterial Congress 2024, Daegu, South Korea, 2024, May 21-26

Melissa Kosovari, Thierry Buffeteau, Laurent Thomas, Andrée-Anne Guay-Bégin, Luc Vellutini, James McGettrick, Gaétan Laroche, Marie-Christine Durrieu, **Silanization-induced changes in peptide presentation on silicon surfaces and their effects on stem cell behavior**, Colloque du CERMA 2024, Université Laval, Québec, Canada, 2024, February 14

Melissa Kosovari, Andrée-Anne Guay-Bégin, Murielle Remy, Artem Zibarov, James McGettrick, Luc Vellutini, Gaétan Laroche, Marie-Christine Durrieu, **Silanization affects peptide functionalization of silicon surfaces: impact on stem cell adhesion**, STS Department Scientific Day 5th edition, Université de Bordeaux, Bordeaux, France, 2023, November 23

Melissa Kosovari, Andrée-Anne Guay-Bégin, Gaétan Laroche, Marie-Christine Durrieu, **Optimizing silanization for biomedical applications**, 25eme Journée de l'École Doctoral de Sciences Chimiques, Université de Bordeaux, Bordeaux, France, 2023, April 13

Melissa Kosovari, Andrée-Anne Guay-Bégin, Marie-Christine Durrieu, Gaétan Laroche, **Surface structuring at the nano and micrometric scale for cell differentiation**, École Thématique SNOSCELLS, Les Houches, 2023, January 22-27

Bibliography

[1] N. Xue, X. Ding, R. Huang, R. Jiang, H. Huang, X. Pan, W. Min, J. Chen, J.-A. Duan, P. Liu, and Y. Wang, "Bone Tissue Engineering in the Treatment of Bone Defects," 2022, doi: 10.3390/ph15070879.

[2] M. R. Urist, "Bone: Formation by Autoinduction," *New Series*, vol. 150, no. 3698, pp. 893–899, 1965.

[3] X. Lin, S. Patil, Y. G. Gao, and A. Qian, "The Bone Extracellular Matrix in Bone Formation and Regeneration," *Front Pharmacol*, vol. 11, May 2020, doi: 10.3389/FPHAR.2020.00757/FULL.

[4] T. F. Day, X. Guo, L. Garrett-Beal, and Y. Yang, "Wnt/β-catenin signaling in mesenchymal progenitors controls osteoblast and chondrocyte differentiation during vertebrate skeletogenesis," *Dev Cell*, vol. 8, no. 5, pp. 739–750, May 2005, doi: 10.1016/J.DEVCEL.2005.03.016.

[5] A. Stahl and Y. P. Yang, "Regenerative Approaches for the Treatment of Large Bone Defects," Dec. 01, 2021, *Mary Ann Liebert Inc.* doi: 10.1089/ten.teb.2020.0281.

[6] J. Caetano-Lopes, H. Canhão, and J. E. Fonseca, "Osteoblasts and bone formation," 2007.

[7] R. Florencio-Silva, G. R. D. S. Sasso, E. Sasso-Cerri, M. J. Simões, and P. S. Cerri, "Biology of Bone Tissue: Structure, Function, and Factors That Influence Bone Cells," 2015, *Hindawi Publishing Corporation*. doi: 10.1155/2015/421746.

[8] M. R. Urist, R. J. Delange, and G. A. M. Finerman, "Bone Cell Differentiation and Growth Factors," *New Series*, vol. 220, no. 4598, pp. 680–686, 1983.

[9] S. Christakos, P. Dhawan, B. Benn, A. Porta, M. Hediger, G. T. Oh, E. B. Jeung, Y. Zhong, D. Ajibade, K. Dhawan, and S. Joshi, "Vitamin D," *Ann N Y Acad Sci*, vol. 1116, no. 1, pp. 340–348, Nov. 2007, doi: 10.1196/ANNALS.1402.070.

[10] N. Xue, X. Ding, R. Huang, R. Jiang, H. Huang, X. Pan, W. Min, J. Chen, J.-A. Duan, P. Liu, and Y. Wang, "Bone Tissue Engineering in the Treatment of Bone Defects," 2022, doi: 10.3390/ph15070879.

[11] R. M. Klar, "The induction of bone formation: The translation enigma," *Front Bioeng Biotechnol*, vol. 9, no. JUN, Jun. 2018, doi: 10.3389/FBIOE.2018.00074/FULL.

[12] M. D. Ryser, N. Nigam, and S. V Komarova, "Mathematical Modeling of Spatio-Temporal Dynamics of a Single Bone Multicellular Unit," *JOURNAL OF BONE AND MINERAL RESEARCH*, vol. 24, no. 5, pp. 860–870, 2009, doi: 10.1359/JBMR.081229.

[13] K. N. Weilbaecher, T. A. Guise, and L. K. McCauley, "Cancer to bone: A fatal attraction," *Nat Rev Cancer*, vol. 11, no. 6, pp. 411–425, Jun. 2011, doi: 10.1038/NRC3055.

[14] P. R. Buenzli, P. Pivonka, and D. W. Smith, "Spatio-temporal structure of cell distribution in cortical Bone Multicellular Units: A mathematical model Mathematical modeling," 2010, doi: 10.1016/j.bone.2010.12.009.

[15] M. D. Ryser, N. Nigam, and S. V Komarova, "Mathematical Modeling of Spatio-Temporal Dynamics of a Single Bone Multicellular Unit," *JOURNAL OF BONE AND MINERAL RESEARCH*, vol. 24, no. 5, pp. 860–870, 2009, doi: 10.1359/JBMR.081229.

[16] L. Y. Zhang, Q. Bi, C. Zhao, J. Y. Chen, M. H. Cai, and X. Y. Chen, "Recent Advances in Biomaterials for the Treatment of Bone Defects," 2020, *Bellwether Publishing, Ltd.* doi: 10.1080/15476278.2020.1808428.

[17] M. Alonzo, F. A. Primo, S. A. Kumar, J. A. Mudloff, E. Dominguez, G. Fregoso, N. Ortiz, W. M. Weiss, B. Joddar, A. Boccaccini, H. S. Nanda, S. Nukavarapu, and V. Thomas, "Bone tissue engineering techniques, advances, and scaffolds for treatment of bone defects," 2020, doi: 10.1016/j.cobme.2020.100248.

[18] P.-I. Brinemark, R. Adell, T. Albrektsson, U. Lekholm, S. Lundkvist, and B. Rockier, "Osseointegrated titanium fixtures in the treatment of edentulousness," 1981.

[19] P. Bialek, B. Kern, X. Yang, M. Schrock, D. Sosic, N. Hong, H. Wu, K. Yu, D. M. Ornitz, E. N. Olson, M. J. Justice, and G. Karsenty, "A twist code determines the onset of osteoblast differentiation," *Dev Cell*, vol. 6, no. 3, pp. 423–435, Mar. 2004, doi: 10.1016/S1534-5807(04)00058-9.

[20] M. K. Bergenstock and N. C. Partridge, "Parathyroid Hormone Stimulation of Noncanonical Wnt Signaling in Bone," *Ann N Y Acad Sci*, vol. 1116, no. 1, pp. 354–359, Nov. 2007, doi: 10.1196/ANNALS.1402.047.

[21] Y. Su, I. Cockerill, Y. Zheng, L. Tang, Y. X. Qin, and D. Zhu, "Biofunctionalization of metallic implants by calcium phosphate coatings," *Bioact Mater*, vol. 4, pp. 196–206, Dec. 2019, doi: 10.1016/J.BIOACTMAT.2019.05.001.

[22] C. Wang, D. Xu, S. Li, C. Yi, X. Zhang, Y. He, and D. Yu, "Effect of Pore Size on the Physicochemical Properties and Osteogenesis of Ti6Al4V Porous Scaffolds with Bionic Structure," 2020, doi: 10.1021/acsomega.0c03824.

[23] Y. Yang, C. He, Dianyu E, W. Yang, F. Qi, D. Xie, L. Shen, S. Peng, and C. Shuai, "Mg bone implant: Features, developments and perspectives," *Mater Des*, vol. 185, Jan. 2020, doi: 10.1016/J.MATDES.2019.108259.

[24] H. Qin, Y. Wei, J. Han, | Xiaojian Jiang, X. Yang, Y. Wu, Z. Gou, | Lili Chen, and Z. -California, "3D printed bioceramic scaffolds: Adjusting pore dimension is beneficial for mandibular bone defects repair," 2022, doi: 10.1002/term.3287.

[25] G. Montalbano, G. Borciani, C. Pontremoli, G. Ciapetti, M. Mattioli-Belmonte, S. Fiorilli, and C. Vitale-Brovarone, "materials Development and Biocompatibility of Collagen-Based Composites Enriched with Nanoparticles of Strontium Containing Mesoporous Glass," 2019, doi: 10.3390/ma12223719.

[26] W. Götz, E. Tobiasch, S. Witzleben, and M. Schulze, "Effects of silicon compounds on biomineralization, osteogenesis, and hard tissue formation," Mar. 01, 2019, *MDPI AG*. doi: 10.3390/pharmaceutics11030117.

[27] J. R. Henstock, L. T. Canham, and S. I. Anderson, "Silicon: The evolution of its use in biomaterials," 2015, *Elsevier Ltd.* doi: 10.1016/j.actbio.2014.09.025.

[28] T. Gao, H. T. Aro, H. Ylak, and E. Vuorio, "Silica-based bioactive glasses modulate expression of bone morphogenetic protein-2 mRNA in Saos-2 osteoblasts in vitro," 2001.

[29] K. Takahashi and S. Yamanaka, "Induction of Pluripotent Stem Cells from Mouse Embryonic and Adult Fibroblast Cultures by Defined Factors," *Cell*, vol. 126, no. 4, pp. 663–676, 2006, doi: https://doi.org/10.1016/j.cell.2006.07.024.

[30] R. A. Musina, E. S. Bekchanova, A. V Belyavskii, and G. T. Sukhikh, "Differentiation potential of mesenchymal stem cells of different origin," *Bull Exp Biol Med*, vol. 141, no. 1, pp. 147–151, 2006, doi: 10.1007/s10517-006-0115-2.

[31] M. Dominici, K. Le Blanc, I. Mueller, I. Slaper-Cortenbach, F. C. Marini, D. S. Krause, R. J. Deans, A. Keating, D. J. Prockop, and E. M. Horwitz, "Minimal criteria for defining multipotent mesenchymal stromal cells. The International Society for Cellular Therapy position statement", doi: 10.1080/14653240600855905.

[32] M. Al-Nbaheen, R. vishnubalaji, D. Ali, A. Bouslimi, F. Al-Jassir, M. Megges, A. Prigione, J. Adjaye, M. Kassem, and A. Aldahmash, "Human Stromal (Mesenchymal) Stem Cells from Bone Marrow, Adipose Tissue and Skin Exhibit Differences in Molecular Phenotype and Differentiation Potential," *Stem Cell Rev Rep*, vol. 9, no. 1, pp. 32–43, Feb. 2013, doi: 10.1007/S12015-012-9365-8.

[33] Q. Chen, P. Shou, C. Zheng, M. Jiang, G. Cao, Q. Yang, J. Cao, N. Xie, T. Velletri, X. Zhang, C. Xu, L. Zhang, H. Yang, J. Hou, Y. Wang, and Y. Shi, "Fate decision of

mesenchymal stem cells: adipocytes or osteoblasts?," *Cell Death Differ*, vol. 23, pp. 1128–1139, 2016, doi: 10.1038/cdd.2015.168.

[34] K. Sinclair, S. T. Yerkovich, and D. C. Chambers, "Mesenchymal stem cells and the lung," *Respirology*, vol. 18, no. 3, pp. 397–411, Apr. 2013, doi: https://doi.org/10.1111/resp.12050.

[35] D. Cook and P. Genever, "Regulation of Mesenchymal Stem Cell Differentiation BT - Transcriptional and Translational Regulation of Stem Cells," G. Hime and H. Abud, Eds., Dordrecht: Springer Netherlands, 2013, pp. 213–229. doi: 10.1007/978-94-007-6621-1_12.

[36] E. F. Wiest, "Advancing mesenchymal stromal cell therapy: The crucial role of updated guidelines," *Cytotherapy*, vol. 27, no. 5, pp. 565–566, May 2025, doi: 10.1016/j.jcyt.2025.01.014.

[37] R. M. Samsonraj, M. Raghunath, V. Nurcombe, J. H. Hui, A. J. van Wijnen, and S. M. Cool, "Concise Review: Multifaceted Characterization of Human Mesenchymal Stem Cells for Use in Regenerative Medicine," *Stem Cells Transl Med*, vol. 6, no. 12, pp. 2173–2185, Dec. 2017, doi: 10.1002/sctm.17-0129.

[38] I. Linero and O. Chaparro, "Paracrine Effect of Mesenchymal Stem Cells Derived from Human Adipose Tissue in Bone Regeneration," *PLoS One*, vol. 9, Sep. 2014, doi: 10.1371/journal.pone.0107001.

[39] J. M. Ryan, F. P. Barry, J. M. Murphy, and B. P. Mahon, "Mesenchymal stem cells avoid allogeneic rejection," *J Inflamm*, vol. 2, no. 1, p. 8, 2005, doi: 10.1186/1476-9255-2-8.

[40] K. A. Payne, D. M. Didiano, and C. R. Chu, "Donor sex and age influence the chondrogenic potential of human femoral bone marrow stem cells," *Osteoarthritis Cartilage*, vol. 18, no. 5, pp. 705–713, 2010, doi: https://doi.org/10.1016/j.joca.2010.01.011.

[41] Y. Zhu, J. Ge, C. Huang, H. Liu, and H. Jiang, "Application of mesenchymal stem cell therapy for aging frailty: from mechanisms to therapeutics," *Issue 12 Theranostics*, vol. 11, no. 12, pp. 5675–5685, 2021, doi: 10.7150/thno.46436.

[42] P. Ganguly, J. J. El-Jawhari, P. V Giannoudis, A. N. Burska, F. Ponchel, and E. A. Jones, "Age-related Changes in Bone Marrow Mesenchymal Stromal Cells: A Potential Impact on Osteoporosis and Osteoarthritis Development," *Cell Transplant*, vol. 26, no. 9, pp. 1520–1529, Sep. 2017, doi: 10.1177/0963689717721201.

[43] J. Yang, X. Zhang, H. Zhang, T. Zhang, S. Zhao, P. Zheng, J. Huo, and H. Wu, "Gastric cancer-derived mesenchymal stem cells prompt gastric cancer progression

through secretion of interleukin-8," *J Exp Clin Cancer Res*, vol. 34, no. 1, p. 52, May 2015, doi: 10.1186/s13046-015-0172-3.

[44] D. T. Chu, T. N. T. Phuong, N. L. B. Tien, D. K. Tran, V. Van Thanh, T. L. Quang, D. T. Truong, V. H. Pham, V. T. N. Ngoc, T. Chu-Dinh, and K. Kushekhar, "An update on the progress of isolation, culture, storage, and clinical application of human bone marrow mesenchymal stem/stromal cells," *Int J Mol Sci*, vol. 21, no. 3, 2020, doi: 10.3390/ijms21030708.

[45] I. Martin, J. De Boer, and L. Sensebe, "A relativity concept in mesenchymal stromal cell manufacturing," *Cytotherapy*, vol. 18, no. 5, pp. 613–620, 2016, doi: https://doi.org/10.1016/j.jcyt.2016.02.004.

[46] F. Soldner, J. Laganière, A. W. Cheng, D. Hockemeyer, Q. Gao, R. Alagappan, V. Khurana, L. I. Golbe, R. H. Myers, S. Lindquist, L. Zhang, D. Guschin, L. K. Fong, B. J. Vu, X. Meng, F. D. Urnov, E. J. Rebar, P. D. Gregory, H. S. Zhang, *et al.*, "Generation of Isogenic Pluripotent Stem Cells Differing Exclusively at Two Early Onset Parkinson Point Mutations," *Cell*, vol. 146, no. 2, pp. 318–331, 2011, doi: https://doi.org/10.1016/j.cell.2011.06.019.

[47] A. Arthur and S. Gronthos, "Clinical application of bone marrow mesenchymal stem/stromal cells to repair skeletal tissue," *Int J Mol Sci*, vol. 21, no. 24, pp. 1–27, 2020, doi: 10.3390/ijms21249759.

[48] X. Wang and P. Thomsen, "Mesenchymal stem cell–derived small extracellular vesicles and bone regeneration," *Basic Clin Pharmacol Toxicol*, vol. 128, no. 1, pp. 18–36, 2021, doi: 10.1111/bcpt.13478.

[49] L. Zhu, Y. Liu, A. Wang, Z. Zhu, Y. Li, C. Zhu, Z. Che, T. Liu, H. Liu, and L. Huang, "Application of BMP in Bone Tissue Engineering," *Front Bioeng Biotechnol*, vol. 10, Mar. 2022, doi: 10.3389/FBIOE.2022.810880/FULL.

[50] A. J. K. V. A. I. G. P. FRIEDENSTEIN, "HETEROTOPIC TRANSPLANTS OF BONE MARROW," *Transplantation*, no. 2, pp. 230–247, Mar. 1968.

[51] A. I. Caplan, "Mesenchymal stem cells," *Journal of Orthopaedic Research*, vol. 9, no. 5, pp. 641–650, 1991, doi: 10.1002/jor.1100090504.

[52] J. Zhou and Y. Shi, "Mesenchymal stem/stromal cells (MSCs): origin, immune regulation, and clinical applications," Jun. 01, 2023, *Springer Nature*. doi: 10.1038/s41423-023-01034-9.

[53] J. Pharoun, J. Berro, J. Sobh, M. M. Abou-Younes, L. Nasr, A. Majed, A. Khalil, Joseph, Stephan, and W. H. Faour, "Mesenchymal stem cells biological and biotechnological advances: Implications for clinical applications," *Eur J Pharmacol*, vol. 977, Aug. 2024, doi: 10.1016/j.ejphar.2024.176719.

[54] N. Guimarães-Camboa, P. Cattaneo, Y. Sun, T. Moore-Morris, Y. Gu, N. D. Dalton, E. Rockenstein, E. Masliah, K. L. Peterson, W. B. Stallcup, J. Chen, and S. M. Evans, "Pericytes of Multiple Organs Do Not Behave as Mesenchymal Stem Cells In Vivo," *Cell Stem Cell*, vol. 20, no. 3, pp. 345-359.e5, Mar. 2017, doi: 10.1016/j.stem.2016.12.006.

[55] M. Crisan, S. Yap, L. Casteilla, C. W. Chen, M. Corselli, T. S. Park, G. Andriolo, B. Sun, B. Zheng, L. Zhang, C. Norotte, P. N. Teng, J. Traas, R. Schugar, B. M. Deasy, S. Badylak, H. J. Buhring, J. P. Giacobino, L. Lazzari, *et al.*, "A Perivascular Origin for Mesenchymal Stem Cells in Multiple Human Organs," *Cell Stem Cell*, vol. 3, no. 3, pp. 301–313, Sep. 2008, doi: 10.1016/j.stem.2008.07.003.

[56] A. I. Caplan and D. Correa, "The MSC: An injury drugstore," Jul. 08, 2011, *Cell Press*. doi: 10.1016/j.stem.2011.06.008.

[57] M. Rao, "Stem cells and regenerative medicine," *Stem Cell Res Ther*, Jul. 2012, doi: 10.1038/nmeth0110-81.

[58] A. Bartholomew, M. Siatskas, K. Ferrer, K. Mcintosh, S. Patil, W. Hardy, S. Devine, D. Ucker, R. Deans, A. Moseley, and R. Hoffman, "Mesenchymal stem cells suppress lymphocyte proliferation in vitro and prolong skin graft survival in vivo," 2002.

[59] M. Di Nicola, C. Carlo-Stella, M. Magni, M. Milanesi, P. D. Longoni, P. Matteucci, S. Grisanti, and A. M. Gianni, "Human bone marrow stromal cells suppress T-lymphocyte proliferation induced by cellular or nonspecific mitogenic stimuli," 2002. [Online]. Available: http://ashpublications.org/blood/article-pdf/99/10/3838/1684678/h81002003838.pdf

[60] F. Djouad, P. Plence, C. Bony, P. Tropel, F. Apparailly, J. Sany, D. Noël, and C. Jorgensen, "Immunosuppressive effect of mesenchymal stem cells favors tumor growth in allogeneic animals," *Blood*, vol. 102, no. 10, pp. 3837–3844, Nov. 2003, doi: 10.1182/blood-2003-04-1193.

[61] R. Margiana, A. Markov, A. O. Zekiy, M. U. Hamza, K. A. Al-Dabbagh, S. H. Al-Zubaidi, N. M. Hameed, I. Ahmad, R. Sivaraman, H. H. Kzar, M. E. Al-Gazally, Y. F. Mustafa, and H. Siahmansouri, "Clinical application of mesenchymal stem cell in regenerative medicine: a narrative review," Dec. 01, 2022, *BioMed Central Ltd.* doi: 10.1186/s13287-022-03054-0.

[62] B. Giebel, "A milestone for the therapeutic EV field: FDA approves Ryoncil, an allogeneic bone marrow-derived mesenchymal stromal cell therapy," *Extracell Vesicles Circ Nucl Acids*, vol. 6, no. 1, pp. 183–190, Mar. 2025, doi: 10.20517/evcna.2025.02.

[63] D. Jovic, Y. Yu, D. Wang, K. Wang, H. Li, F. Xu, C. Liu, J. Liu, and Y. Luo, "A Brief Overview of Global Trends in MSC-Based Cell Therapy," Jun. 01, 2022, *Springer*. doi: 10.1007/s12015-022-10369-1.

[64] Y. Dong, C. D'Mello, W. Pinsky, B. M. Lozinski, D. K. Kaushik, S. Ghorbani, D. Moezzi, D. Brown, F. C. Melo, S. Zandee, T. Vo, A. Prat, S. N. Whitehead, and V. W. Yong, "Oxidized phosphatidylcholines found in multiple sclerosis lesions mediate neurodegeneration and are neutralized by microglia," *Nat Neurosci*, vol. 24, no. 4, pp. 489–503, Apr. 2021, doi: 10.1038/s41593-021-00801-z.

[65] F. Yousefi, F. Lavi Arab, K. Saeidi, H. Amiri, and M. Mahmoudi, "Various strategies to improve efficacy of stem cell transplantation in multiple sclerosis: Focus on mesenchymal stem cells and neuroprotection," Mar. 15, 2019, *Elsevier B.V.* doi: 10.1016/j.jneuroim.2018.11.015.

[66] S. Dadfar, E. Yazdanpanah, A. Pazoki, M. H. Nemati, M. Eslami, D. Haghmorad, and V. Oksenych, "The Role of Mesenchymal Stem Cells in Modulating Adaptive Immune Responses in Multiple Sclerosis," Sep. 01, 2024, *Multidisciplinary Digital Publishing Institute (MDPI)*. doi: 10.3390/cells13181556.

[67] M. J. Bejargafshe, M. Hedayati, S. Zahabiasli, E. Tahmasbpour, S. Rahmanzadeh, and A. Nejad-Moghaddam, "Safety and efficacy of stem cell therapy for treatment of neural damage in patients with multiple sclerosis," 2019, *AME Publishing Company*. doi: 10.21037/sci.2019.10.06.

[68] O. Hardiman, A. Al-Chalabi, A. Chio, E. M. Corr, G. Logroscino, W. Robberecht, P. J. Shaw, Z. Simmons, and L. H. Van Den Berg, "Amyotrophic lateral sclerosis," Oct. 05, 2017, *Nature Publishing Group*. doi: 10.1038/nrdp.2017.71.

[69] P. V. Torres-Ortega, R. Del Campo-Montoya, D. Plano, J. Paredes, J. Aldazabal, M. R. Luquin, E. Santamaría, C. Sanmartín, M. J. Blanco-Prieto, and E. Garbayo, "Encapsulation of MSCs and GDNF in an Injectable Nanoreinforced Supramolecular Hydrogel for Brain Tissue Engineering," *Biomacromolecules*, vol. 23, no. 11, pp. 4629–4644, Nov. 2022, doi: 10.1021/acs.biomac.2c00853.

[70] R. Giordano, M. Canesi, M. Isalberti, I. U. Isaias, T. Montemurro, M. Viganò, E. Montelatici, V. Boldrin, R. Benti, A. Cortelezzi, N. Fracchiolla, L. Lazzari, and G. Pezzoli, "Autologous mesenchymal stem cell therapy for progressive supranuclear palsy: Translation into a phase I controlled, randomized clinical study," *J Transl Med*, vol. 12, no. 1, Jan. 2014, doi: 10.1186/1479-5876-12-14.

[71] S. Wu, B. Wu, M. Liu, X. Wu Hospital, S. Wales, S. Wu, B. Wu, M. Liu, Z. Chen, W. Wang, C. S. Anderson, P. Sandercock, Y. Wang, Y. Huang, L. Cui, C. Pu, J. Jia, T. Zhang, X. Liu, *et al.*, "Neurological diseases in China 2 Stroke in China: advances and

challenges in epidemiology, prevention, and management," 2019. [Online]. Available: http://ghdx.healthdata.org/

[72] A. R. Amini, C. T. Laurencin, and S. P. Nukavarapu, "Bone Tissue Engineering: Recent Advances and Challenges," 2012.

[73] G. M. Raghoebar, R. S. B. Liem, R. R. M. Bos, J. E. Van Der Wal, and A. Vissink, "Resorbable screws for fixation of autologous bone grafts," *Clin Oral Implants Res*, vol. 17, no. 3, pp. 288–293, Jun. 2006, doi: 10.1111/j.1600-0501.2005.01200.x.

[74] P. Felice, R. Pistilli, G. Lizio, G. Pellegrino, A. Nisii, and C. Marchetti, "Inlay versus onlay iliac bone grafting in atrophic posterior mandible: A prospective controlled clinical trial for the comparison of two techniques," *Clin Implant Dent Relat Res*, vol. 11, no. SUPPL. 1, Oct. 2009, doi: 10.1111/j.1708-8208.2009.00212.x.

[75] J. Chahal, A. Gómez-Aristizábal, K. Shestopaloff, S. Bhatt, A. Chaboureau, A. Fazio, J. Chisholm, A. Weston, J. Chiovitti, A. Keating, M. Kapoor, D. J. Ogilvie-Harris, K. A. Syed, R. Gandhi, N. N. Mahomed, K. W. Marshall, M. S. Sussman, A. M. Naraghi, and S. Viswanathan, "Bone Marrow Mesenchymal Stromal Cell Treatment in Patients with Osteoarthritis Results in Overall Improvement in Pain and Symptoms and Reduces Synovial Inflammation," *Stem Cells Transl Med*, vol. 8, no. 8, pp. 746–757, Aug. 2019, doi: 10.1002/sctm.18-0183.

[76] P. Hernigou, J. Delambre, S. Quiennec, and A. Poignard, "Human bone marrow mesenchymal stem cell injection in subchondral lesions of knee osteoarthritis: a prospective randomized study versus contralateral arthroplasty at a mean fifteen year follow-up," *Int Orthop*, vol. 45, no. 2, pp. 365–373, Feb. 2021, doi: 10.1007/s00264-020-04571-4.

[77] S. Muthu, S. C. Patil, N. Jeyaraman, M. Jeyaraman, P. Gangadaran, R. L. Rajendran, E. J. Oh, M. Khanna, H. Y. Chung, and B. C. Ahn, "Comparative effectiveness of adipose-derived mesenchymal stromal cells in the management of knee osteoarthritis: A meta-analysis," *World J Orthop*, vol. 14, no. 1, pp. 23–41, 2023, doi: 10.5312/wjo.v14.i1.23.

[78] A. Vega, M. A. Martín-Ferrero, F. Del Canto, M. Alberca, V. García, A. Munar, L. Orozco, R. Soler, J. J. Fuertes, M. Huguet, A. Sánchez, and J. García-Sancho, "Treatment of knee osteoarthritis with allogeneic bone marrow mesenchymal stem cells: A randomized controlled trial," *Transplantation*, vol. 99, no. 8, pp. 1681–1690, Aug. 2015, doi: 10.1097/TP.0000000000000678.

[79] L. Orozco, A. Munar, R. Soler, M. Alberca, F. Soler, M. Huguet, J. Sentís, A. Sánchez, and J. García-Sancho, "Treatment of knee osteoarthritis with autologous mesenchymal stem cells: A pilot study," *Transplantation*, vol. 95, no. 12, pp. 1535–1541, Jun. 2013, doi: 10.1097/TP.0b013e318291a2da.

[80] R. Bastos, M. Mathias, R. Andrade, R. Bastos, A. Balduino, V. Schott, S. Rodeo, and J. Espregueira-Mendes, "Intra-articular injections of expanded mesenchymal stem cells with and without addition of platelet-rich plasma are safe and effective for knee osteoarthritis," *Knee Surgery, Sports Traumatology, Arthroscopy*, vol. 26, no. 11, pp. 3342–3350, Nov. 2018, doi: 10.1007/s00167-018-4883-9.

[81] A. Hatakeyama, S. Uchida, H. Utsunomiya, M. Tsukamoto, H. Nakashima, E. Nakamura, C. Pascual-Garrido, I. Sekiya, and A. Sakai, "Isolation and Characterization of Synovial Mesenchymal Stem Cell Derived from Hip Joints: A Comparative Analysis with a Matched Control Knee Group," *Stem Cells Int*, vol. 2017, 2017, doi: 10.1155/2017/9312329.

[82] H. Lin, J. Sohn, H. Shen, M. T. Langhans, and R. S. Tuan, "Bone marrow mesenchymal stem cells: Aging and tissue engineering applications to enhance bone healing," *Biomaterials*, vol. 203, pp. 96–110, May 2019, doi: 10.1016/j.biomaterials.2018.06.026.

[83] V. Falanga, S. Iwamoto, M. Chartier, T. Yufit, J. Butmarc, N. Kouttab, D. Shrayer, and P. Carson, "Autologous bone marrow-derived cultured mesenchymal stem cells delivered in a fibrin spray accelerate healing in murine and human cutaneous wounds," *Tissue Eng*, vol. 13, no. 6, pp. 1299–1312, Jun. 2007, doi: 10.1089/ten.2006.0278.

[84] W. xiong Xu, H. liang He, S. wen Pan, Y. li Chen, M. ling Zhang, S. Zhu, Z. liang Gao, L. Peng, and J. guo Li, "Combination treatments of plasma exchange and umbilical cord-derived mesenchymal stem cell transplantation for patients with hepatitis B virus-related acute-on-chronic liver failure: A clinical trial in China," *Stem Cells Int*, vol. 2019, 2019, doi: 10.1155/2019/4130757.

[85] F. T. Chebib and V. E. Torres, "Autosomal Dominant Polycystic Kidney Disease: Core Curriculum 2016," *American Journal of Kidney Diseases*, vol. 67, no. 5, pp. 792–810, May 2016, doi: 10.1053/j.ajkd.2015.07.037.

[86] A. Makhlough, S. Shekarchian, R. Moghadasali, B. Einollahi, S. E. Hosseini, N. Jaroughi, T. Bolurieh, H. Baharvand, and N. Aghdami, "Safety and tolerability of autologous bone marrow mesenchymal stromal cells in ADPKD patients," *Stem Cell Res Ther*, vol. 8, no. 1, May 2017, doi: 10.1186/s13287-017-0557-7.

[87] E. B. Lushaj, E. Anstadt, R. Haworth, D. Roenneburg, J. Kim, P. Hematti, and T. Kohmoto, "Mesenchymal stromal cells are present in the heart and promote growth of adult stem cells in vitro," *Cytotherapy*, vol. 13, no. 4, pp. 400–406, 2011, doi: 10.3109/14653249.2010.529890.

[88] L. A. Costa, N. Eiro, M. Fraile, L. O. Gonzalez, J. Saá, P. Garcia-Portabella, B. Vega, J. Schneider, and F. J. Vizoso, "Functional heterogeneity of mesenchymal stem cells from natural niches to culture conditions: implications for further clinical uses," Jan.

01, 2021, *Springer Science and Business Media Deutschland GmbH*. doi: 10.1007/s00018-020-03600-0.

[89] S. Zhu, W. Chen, A. Masson, and Y.-P. Li, "Cell Discovery Cell signaling and transcriptional regulation of osteoblast lineage commitment, differentiation, bone formation, and homeostasis," *Cell Discov*, vol. 10, p. 71, 2024, doi: 10.1038/s41421-024-00689-6.

[90] W. Huang, S. Yang, J. Shao, and Y.-P. Li, "Signaling and transcriptional regulation in osteoblast commitment and differentiation," 2007.

[91] T. F. Day, X. Guo, L. Garrett-Beal, and Y. Yang, "Wnt/β-catenin signaling in mesenchymal progenitors controls osteoblast and chondrocyte differentiation during vertebrate skeletogenesis," *Dev Cell*, vol. 8, no. 5, pp. 739–750, May 2005, doi: 10.1016/J.DEVCEL.2005.03.016.

[92] T. Gaur, C. J. Lengner, H. Hovhannisyan, R. A. Bhat, P. V. N. Bodine, B. S. Komm, A. Javed, A. J. Van Wijnen, J. L. Stein, G. S. Stein, and J. B. Lian, "Canonical WNT signaling promotes osteogenesis by directly stimulating Runx2 gene expression," *Journal of Biological Chemistry*, vol. 280, no. 39, pp. 33132–33140, Sep. 2005, doi: 10.1074/JBC.M500608200.

[93] S. Thomas, · Bithiah, and G. Jaganathan, "Signaling network regulating osteogenesis in mesenchymal stem cells," *J Cell Commun Signal*, vol. 16, no. 3, pp. 47–61, Jul. 2021, doi: 10.1007/s12079-021-00635-1.

[94] X. Wu, W. Shi, and X. Cao, "Multiplicity of BMP Signaling in Skeletal Development," *Ann N Y Acad Sci*, vol. 1116, no. 1, pp. 29–49, Nov. 2007, doi: 10.1196/ANNALS.1402.053.

[95] D. Yadin, P. Knaus, and T. D. Mueller, "Structural insights into BMP receptors: Specificity, activation and inhibition," 2015, doi: 10.1016/j.cytogfr.2015.11.005.

[96] A. Zhou, H. Yu, J. Liu, J. Zheng, Y. Jia, B. Wu, and L. Xiang, "Role of Hippo-YAP Signaling in Osseointegration by Regulating Osteogenesis, Angiogenesis, and Osteoimmunology," Aug. 19, 2020, *Frontiers Media S.A.* doi: 10.3389/fcell.2020.00780.

[97] C. Lorthongpanich, K. Thumanu, K. Tangkiettrakul, N. Jiamvoraphong, C. Laowtammathron, N. Damkham, Y. U-Pratya, and S. Issaragrisil, "YAP as a key regulator of adipo-osteogenic differentiation in human MSCs," *Stem Cell Res Ther*, vol. 10, no. 1, Dec. 2019, doi: 10.1186/s13287-019-1494-4.

[98] Q. Wei, A. Holle, J. Li, F. Posa, F. Biagioni, O. Croci, A. S. Benk, J. Young, F. Noureddine, J. Deng, M. Zhang, G. J. Inman, J. P. Spatz, S. Campaner, and E. A. Cavalcanti-Adam, "BMP-2 Signaling and Mechanotransduction Synergize to Drive

Osteogenic Differentiation via YAP/TAZ," *Advanced Science*, vol. 7, no. 15, Aug. 2020, doi: 10.1002/advs.201902931.

[99] M. Zarka, E. Haÿ, and M. Cohen-Solal, "YAP/TAZ in Bone and Cartilage Biology," Jan. 04, 2022, *Frontiers Media S.A.* doi: 10.3389/fcell.2021.788773.

[100] C. Bin Cui, L. F. Cooper, X. Yang, G. Karsenty, and I. Aukhil, "Transcriptional Coactivation of Bone-Specific Transcription Factor Cbfa1 by TAZ," *Mol Cell Biol*, vol. 23, no. 3, pp. 1004–1013, Feb. 2003, doi: 10.1128/mcb.23.3.1004-1013.2003.

[101] M. R. Byun, A. R. Kim, J. H. Hwang, K. M. Kim, E. S. Hwang, and J. H. Hong, "FGF2 stimulates osteogenic differentiation through ERK induced TAZ expression," *Bone*, vol. 58, pp. 72–80, 2014, doi: 10.1016/j.bone.2013.09.024.

[102] C. D. Kegelman, J. C. Coulombe, K. M. Jordan, D. J. Horan, L. Qin, A. G. Robling, V. L. Ferguson, T. M. Bellido, and J. D. Boerckel, "YAP and TAZ Mediate Osteocyte Perilacunar/Canalicular Remodeling," *Journal of Bone and Mineral Research*, vol. 35, no. 1, pp. 196–210, Jan. 2020, doi: 10.1002/jbmr.3876.

[103] F. Long, "Building strong bones: Molecular regulation of the osteoblast lineage," Jan. 2012. doi: 10.1038/nrm3254.

[104] P. Y. Wang, W. T. Li, J. Yu, and W. B. Tsai, "Modulation of osteogenic, adipogenic and myogenic differentiation of mesenchymal stem cells by submicron grooved topography," *J Mater Sci Mater Med*, vol. 23, no. 12, pp. 3015–3028, Dec. 2012, doi: 10.1007/s10856-012-4748-6.

[105] C. Cimmino, L. Rossano, P. A. Netti, and M. Ventre, "Spatio-temporal control of cell adhesion: Toward programmable platforms to manipulate cell functions and fate," Dec. 04, 2018, *Frontiers Media S.A.* doi: 10.3389/fbioe.2018.00190.

[106] N. R. Richbourg, N. A. Peppas, and V. I. Sikavitsas, "Tuning the biomimetic behavior of scaffolds for regenerative medicine through surface modifications," *J Tissue Eng Regen Med*, vol. 13, no. 8, pp. 1275–1293, Aug. 2019, doi: 10.1002/TERM.2859.

[107] H. Amani, H. Arzaghi, M. Bayandori, A. S. Dezfuli, H. Pazoki-Toroudi, A. Shafiee, and L. Moradi, "Controlling Cell Behavior through the Design of Biomaterial Surfaces: A Focus on Surface Modification Techniques," *Adv Mater Interfaces*, vol. 6, no. 13, pp. 1–30, 2019, doi: 10.1002/admi.201900572.

[108] P. Roach, D. Eglin, K. Rohde, and C. C. Perry, "Modern biomaterials: A review - Bulk properties and implications of surface modifications," Jul. 2007. doi: 10.1007/s10856-006-0064-3.

[109] T. T. Yu, F. Z. Cui, Q. Y. Meng, J. Wang, D. C. Wu, J. Zhang, X. X. Kou, R. L. Yang, Y. Liu, Y. S. Zhang, F. Yang, and Y. H. Zhou, "Influence of Surface Chemistry on

Adhesion and Osteo/Odontogenic Differentiation of Dental Pulp Stem Cells," *ACS Biomater Sci Eng*, vol. 3, no. 6, pp. 1119–1128, Jun. 2017, doi: 10.1021/acsbiomaterials.7b00274.

[110] Y. Wang, S. Yao, Q. Meng, X. Yu, X. Wang, and F. Cui, "Gene expression profiling and mechanism study of neural stem cells response to surface chemistry," *Regen Biomater*, vol. 1, no. 1, pp. 37–47, Nov. 2014, doi: 10.1093/rb/rbu012.

[111] S. Nasrollahi, S. Banerjee, B. Qayum, P. Banerjee, and A. Pathak, "Nanoscale Matrix Topography Influences Microscale Cell Motility through Adhesions, Actin Organization, and Cell Shape," *ACS Biomater Sci Eng*, vol. 3, no. 11, pp. 2980–2986, Nov. 2017, doi: 10.1021/acsbiomaterials.6b00554.

[112] A. Cunha, O. F. Zouani, L. Plawinski, A. M. Botelho Do Rego, A. Almeida, R. Vilar, and M. C. Durrieu, "Human mesenchymal stem cell behavior on femtosecond laser-textured Ti-6Al-4V surfaces," *Nanomedicine*, vol. 10, no. 5, pp. 725–739, Mar. 2015, doi: 10.2217/nnm.15.19.

[113] K. Von Der Mark, J. Park, S. Bauer, and P. Schmuki, "Nanoscale engineering of biomimetic surfaces: Cues from the extracellular matrix," Jan. 2010. doi: 10.1007/s00441-009-0896-5.

[114] I. Bilem, L. Plawinski, P. Chevallier, C. Ayela, E. D. Sone, G. Laroche, and M. C. Durrieu, "The spatial patterning of RGD and BMP-2 mimetic peptides at the subcellular scale modulates human mesenchymal stem cells osteogenesis," 2017, doi: 10.1002/jbm.a.36296.

[115] O. F. Zouani, C. Chanseau, B. Brouillaud, R. Bareille, F. Deliane, M. P. Foulc, A. Mehdi, and M. C. Durrieu, "Altered nanofeature size dictates stem cell differentiation," *J Cell Sci*, vol. 125, no. 5, pp. 1217–1224, Mar. 2012, doi: 10.1242/jcs.093229.

[116] Z. A. Cheng, O. F. Zouani, K. Glinel, A. M. Jonas, and M. C. Durrieu, "Bioactive chemical nanopatterns impact human mesenchymal stem cell fate," *Nano Lett*, vol. 13, no. 8, pp. 3923–3929, Aug. 2013, doi: 10.1021/nl4020149.

[117] R. K. Das, O. F. Zouani, C. Labrugère, R. Oda, and M. C. Durrieu, "Influence of nanohelical shape and periodicity on stem cell fate," *ACS Nano*, vol. 7, no. 4, pp. 3351–3361, Apr. 2013, doi: 10.1021/nn4001325.

[118] C. Royer, A. A. Guay-Bégin, C. Chanseau, P. Chevallier, L. Bordenave, G. Laroche, and M. C. Durrieu, "Bioactive micropatterning of biomaterials for induction of endothelial progenitor cell differentiation: Acceleration of in situ endothelialization," *J Biomed Mater Res A*, vol. 108, no. 7, pp. 1479–1492, May 2020, doi: 10.1002/jbm.a.36918.

[119] C. Xu, F. Yang, S. Wang, and S. Ramakrishna, "In vitro study of human vascular endothelial cell function on materials with various surface roughness," *J Biomed Mater Res A*, vol. 71, no. 1, pp. 154–161, Oct. 2004, doi: 10.1002/jbm.a.30143.

[120] C. R. Pedrosa, D. Arl, P. Grysan, I. Khan, ¶ Stéphanie, S. Durrieu, S. Krishnamoorthy, and M.-C. Durrieu, "Controlled Nanoscale Topographies for Osteogenic Differentiation of Mesenchymal Stem Cells," 2019, doi: 10.1021/acsami.8b21393.

[121] C. R. Pedrosa, C. Chanseau, C. Labrugère, S. Krishnamoorthy, M.-C. Durrieu, and K. Anselme, "Mesenchymal Stem Cell Differentiation Driven by Osteoinductive Bioactive Nanoscale Topographies," 2021, doi: 10.3390/app112311209.

[122] C. Dhand, S. T. Ong, N. Dwivedi, S. M. Diaz, J. R. Venugopal, B. Navaneethan, M. H. U. T. Fazil, S. Liu, V. Seitz, E. Wintermantel, R. W. Beuerman, S. Ramakrishna, N. K. Verma, and R. Lakshminarayanan, "Bio-inspired in situ crosslinking and mineralization of electrospun collagen scaffolds for bone tissue engineering," *Biomaterials*, vol. 104, pp. 323–338, Oct. 2016, doi: 10.1016/j.biomaterials.2016.07.007.

[123] H. Xu, F. Lv, Y. Zhang, Z. Yi, Q. Ke, C. Wu, M. Liu, and J. Chang, "Hierarchically micro-patterned nanofibrous scaffolds with a nanosized bio-glass surface for accelerating wound healing," *Nanoscale*, vol. 7, no. 44, pp. 18446–18452, Nov. 2015, doi: 10.1039/c5nr04802h.

[124] D. Jing and B. Bhushan, "Quantification of surface charge density and its effect on boundary slip," *Langmuir*, vol. 29, no. 23, pp. 6953–6963, Jun. 2013, doi: 10.1021/la401168w.

[125] J. C. Courtenay, C. Deneke, E. M. Lanzoni, C. A. Costa, Y. Bae, J. L. Scott, and R. I. Sharma, "Modulating cell response on cellulose surfaces; tunable attachment and scaffold mechanics," *Cellulose*, vol. 25, no. 2, pp. 925–940, Feb. 2018, doi: 10.1007/s10570-017-1612-3.

[126] A. P. Zhu and N. Fang, "Adhesion dynamics, morphology, and organization of 3T3 fibroblast on chitosan and its derivative: The effect of O-carboxymethylation," *Biomacromolecules*, vol. 6, no. 5, pp. 2607–2614, Sep. 2005, doi: 10.1021/bm050328q.

[127] H. H. K. Xu, J. B. Quinn, S. Takagi, L. C. Chow, and F. C. Eichmiller, "Strong and macroporous calcium phosphate cement: Effects of porosity and fiber reinforcement on mechanical properties," 2001.

[128] A. Villanueva, M. Cãete, A. G. Roca, M. Calero, S. Veintemillas-Verdaguer, C. J. Serna, M. Del Puerto Morales, and R. Miranda, "The influence of surface functionalization on the enhanced internalization of magnetic nanoparticles in cancer cells," *Nanotechnology*, vol. 20, no. 11, 2009, doi: 10.1088/0957-4484/20/11/115103.

[129] Y. Lai, F. Pan, C. Xu, H. Fuchs, and L. Chi, "In situ surface-modification-induced superhydrophobic patterns with reversible wettability and adhesion," *Advanced Materials*, vol. 25, no. 12, pp. 1682–1686, Mar. 2013, doi: 10.1002/adma.201203797.

[130] Y. Arima and H. Iwata, "Effect of wettability and surface functional groups on protein adsorption and cell adhesion using well-defined mixed self-assembled monolayers," *Biomaterials*, vol. 28, no. 20, pp. 3074–3082, Jul. 2007, doi: 10.1016/j.biomaterials.2007.03.013.

[131] E. Ueda and P. A. Levkin, "Micropatterning hydrophobic liquid on a porous polymer surface for long-term selective cell-repellency," *Adv Healthc Mater*, vol. 2, no. 11, pp. 1425–1429, 2013, doi: 10.1002/adhm.201300073.

[132] M. M. Gentleman and E. Gentleman, "The role of surface free energy in osteoblast-biomaterial interactions," Nov. 01, 2014, *Maney Publishing*. doi: 10.1179/1743280414Y.0000000038.

[133] M. Nakamura, N. Hori, S. Namba, T. Toyama, N. Nishimiya, and K. Yamashita, "Wettability and surface free energy of polarised ceramic biomaterials," *Biomedical Materials (Bristol)*, vol. 10, no. 1, Feb. 2015, doi: 10.1088/1748-6041/10/1/011001.

[134] R. Kummala, W. Xu, C. Xu, and M. Toivakka, "Stiffness and swelling characteristics of nanocellulose films in cell culture media," *Cellulose*, vol. 25, no. 9, pp. 4969–4978, Sep. 2018, doi: 10.1007/s10570-018-1940-y.

[135] C. F. Guimarães, L. Gasperini, A. P. Marques, and R. L. Reis, "The stiffness of living tissues and its implications for tissue engineering," May 01, 2020, *Nature Research*. doi: 10.1038/s41578-019-0169-1.

[136] E. Schuh, S. Hofmann, K. Stok, H. Notbohm, R. Müller, and N. Rotter, "Chondrocyte redifferentiation in 3D: The effect of adhesion site density and substrate elasticity," *J Biomed Mater Res A*, vol. 100 A, no. 1, pp. 38–47, Jan. 2012, doi: 10.1002/jbm.a.33226.

[137] D. E. Ingber, "From cellular mechanotransduction to biologically inspired engineering: 2009 pritzker award lecture, BMES annual meeting October 10, 2009," in *Annals of Biomedical Engineering*, Mar. 2010, pp. 1148–1161. doi: 10.1007/s10439-010-9946-0.

[138] O. F. Zouani, J. Kalisky, E. Ibarboure, and M. C. Durrieu, "Effect of BMP-2 from matrices of different stiffnesses for the modulation of stem cell fate," *Biomaterials*, vol. 34, no. 9, pp. 2157–2166, Mar. 2013, doi: 10.1016/j.biomaterials.2012.12.007.

[139] C. López-Serrano, M. Rémy, T. Leste-Lasserre, G. Laroche, and M. C. Durrieu, "Unravelling the synergies: effects of hydrogel mechanics and biofunctionalization on mesenchymal stem cell osteogenic differentiation," *Mater Adv*, 2025, doi: 10.1039/d5ma00165j.

[140] C. López-Serrano, Y. Côté-Paradis, B. Habenstein, A. Loquet, C. Le Coz, J. Ruel, G. Laroche, and M. C. Durrieu, "Integrating Mechanics and Bioactivity: A Detailed Assessment of Elasticity and Viscoelasticity at Different Scales in 2D Biofunctionalized PEGDA Hydrogels for Targeted Bone Regeneration," *ACS Appl Mater Interfaces*, Jul. 2024, doi: 10.1021/acsami.4c10755.

[141] E. Prouvé, B. Drouin, P. Chevallier, M. Rémy, M. C. Durrieu, and G. Laroche, "Evaluating Poly(Acrylamide-co-Acrylic Acid) Hydrogels Stress Relaxation to Direct the Osteogenic Differentiation of Mesenchymal Stem Cells," *Macromol Biosci*, vol. 21, no. 6, Jun. 2021, doi: 10.1002/mabi.202100069.

[142] E. Prouvé, M. Rémy, C. Feuillie, M. Molinari, P. Chevallier, B. Drouin, G. Laroche, and M. C. Durrieu, "Interplay of matrix stiffness and stress relaxation in directing osteogenic differentiation of mesenchymal stem cells," *Biomater Sci*, vol. 10, no. 17, pp. 4978–4996, Jul. 2022, doi: 10.1039/d2bm00485b.

[143] B. D. Hoffman, C. Grashoff, and M. A. Schwartz, "Dynamic molecular processes mediate cellular mechanotransduction," Jul. 21, 2011. doi: 10.1038/nature10316.

[144] U. Hersel, C. Dahmen, and H. Kessler, "RGD modified polymers: Biomaterials for stimulated cell adhesion and beyond," *Biomaterials*, vol. 24, no. 24, pp. 4385–4415, 2003, doi: 10.1016/S0142-9612(03)00343-0.

[145] M. Zhianmanesh, A. Gilmour, M. M. M. Bilek, and B. Akhavan, "Plasma surface functionalization: A comprehensive review of advances in the quest for bioinstructive materials and interfaces," Jun. 01, 2023, *American Institute of Physics Inc.* doi: 10.1063/5.0130829.

[146] G. Wu, P. Li, H. Feng, X. Zhang, and P. K. Chu, "Engineering and functionalization of biomaterials via surface modification," Mar. 14, 2015, *Royal Society of Chemistry*. doi: 10.1039/c4tb01934b.

[147] E. Steen Redeker, D. T. Ta, D. Cortens, B. Billen, W. Guedens, and P. Adriaensens, "Protein engineering for directed immobilization," Nov. 20, 2013, *American Chemical Society*. doi: 10.1021/bc4002823.

[148] F. Rusmini, Z. Zhong, and J. Feijen, "Protein immobilization strategies for protein biochips," Jun. 2007. doi: 10.1021/bm061197b.

[149] S. Jacob, A. A. Shirwaikar, K. K. Srinivasan, J. Alex, S. L. Prabu, R. Mahalaxmi, and R. Kumar, "Stability of Proteins in Aqueous Solution and Solid State." [Online]. Available: www.ijpsonline.com

[150] L. Vroman, A. L. Adams, G. C. Fischer, and P. C. Munoz, "Interaction of High Molecular Weight Kininogen, Factor XII, and Fibrinogen in Plasma at Interfaces,"

1980. [Online]. Available: http://ashpublications.org/blood/article-pdf/55/1/156/1713989/156.pdf

[151] S. L. Hirsh, D. R. McKenzie, N. J. Nosworthy, J. A. Denman, O. U. Sezerman, and M. M. M. Bilek, "The Vroman effect: Competitive protein exchange with dynamic multilayer protein aggregates," *Colloids Surf B Biointerfaces*, vol. 103, pp. 395–404, Mar. 2013, doi: 10.1016/j.colsurfb.2012.10.039.

[152] V. Hlady and J. Buijs, "Protein adsorption on solid surfaces," *Curr Opin Biotechnol*, vol. 7, pp. 72–77, 1996.

[153] M. Iqbal, D. K. Dinh, Q. Abbas, M. Imran, H. Sattar, and A. Ul Ahmad, "Controlled Surface Wettability by Plasma Polymer Surface Modification," Jun. 01, 2019, *Multidisciplinary Digital Publishing Institute (MDPI)*. doi: 10.3390/surfaces2020026.

[154] F. Kong and Y. F. Hu, "Biomolecule immobilization techniques for bioactive paper fabrication," *Anal Bioanal Chem*, vol. 403, no. 1, pp. 7–13, Apr. 2012, doi: 10.1007/s00216-012-5821-1.

[155] A. W. G. Nijhuis, S. C. G. Leeuwenburgh, and J. A. Jansen, "Wet-Chemical Deposition of Functional Coatings for Bone Implantology," Nov. 10, 2010. doi: 10.1002/mabi.201000142.

[156] D. Rother, T. Sen, D. East, and I. J. Bruce, "Silicon, silica and its surface patterning/activation with alkoxy-and amino-silanes for nanomedical applications," Feb. 2011. doi: 10.2217/nnm.10.159.

[157] E. H. Cordes, W. P. Jencks, E. H. Cordes, and W. P. Jencks, "On the Mechanism of Schiff Base Formation and Hydrolysis1." [Online]. Available: https://pubs.acs.org/sharingguidelines

[158] C. Stewart, B. Akhavan, S. G. Wise, and M. M. M. Bilek, "A review of biomimetic surface functionalization for bone-integrating orthopedic implants: Mechanisms, current approaches, and future directions," Dec. 01, 2019, *Elsevier Ltd*. doi: 10.1016/j.pmatsci.2019.100588.

[159] L. Rouvière, A. Hachin, S. Shinkaruk, J. Hunel, C. Aupetit, T. Buffeteau, E. Genin, and L. Vellutini, "Self-assembly of amino-terminated monolayers depending on the chemical structure," *New Journal of Chemistry*, vol. 47, no. 20, pp. 9661–9668, Apr. 2023, doi: 10.1039/d3nj01312j.

[160] M. Kosovari, T. Buffeteau, L. Thomas, A. A. Guay Bégin, L. Vellutini, J. D. McGettrick, G. Laroche, and M. C. Durrieu, "Silanization Strategies for Tailoring Peptide Functionalization on Silicon Surfaces: Implications for Enhancing Stem Cell Adhesion," *ACS Applied Materials and Interfaces* , vol. 16, no. 23, pp. 29770–29782, Jun. 2024, doi: 10.1021/acsami.4c03727.

[161] L. Wang, U. S. Schubert, and S. Hoeppener, "Surface chemical reactions on self-assembled silane based monolayers," Jun. 07, 2021, *Royal Society of Chemistry*. doi: 10.1039/d0cs01220c.

[162] W. Caceres, A. Destrieux, J. Profili, A. A. Guay-Bégin, S. Ravichandran, M. Laurent, A. Smith, and G. Laroche, "Homogeneity study of fluoropolymer films modified by atmospheric pressure nitrogen plasma discharges," *Polymer-Plastics Technology and Materials*, vol. 63, no. 2, pp. 120–133, 2023, doi: 10.1080/25740881.2023.2277388.

[163] H. Tanaka, K. Ishikawa, M. Mizuno, S. Toyokuni, H. Kajiyama, F. Kikkawa, H. R. Metelmann, and M. Hori, "State of the art in medical applications using non-thermal atmospheric pressure plasma," Dec. 01, 2017, *Springer*. doi: 10.1007/s41614-017-0004-3.

[164] J. C. Love, L. A. Estroff, J. K. Kriebel, R. G. Nuzzo, and G. M. Whitesides, "Self-assembled monolayers of thiolates on metals as a form of nanotechnology," Apr. 2005. doi: 10.1021/cr0300789.

[165] Sagiv J., "Organized Monolayers by Adsorption. 1. Formation and Structure of Oleophobic Mixed Monolayers on Solid Surfaces," Plenum Press, 1980. [Online]. Available: https://pubs.acs.org/sharingguidelines

[166] S. Casalini, C. A. Bortolotti, F. Leonardi, and F. Biscarini, "Self-assembled monolayers in organic electronics," Jan. 01, 2017, *Royal Society of Chemistry*. doi: 10.1039/c6cs00509h.

[167] C. Nicosia and J. Huskens, "Reactive self-assembled monolayers: From surface functionalization to gradient formation," Jan. 01, 2014, *Royal Society of Chemistry*. doi: 10.1039/c3mh00046j.

[168] A. Ulman, "Formation and Structure of Self-Assembled Monolayers," 1996. [Online]. Available: https://pubs.acs.org/sharingguidelines

[169] M. S. Inkpen, Z. –F Liu, H. Li, L. M. Campos, J. B. Neaton, and L. Venkataraman, "Non-chemisorbed gold–sulfur binding prevails in self-assembled monolayers," *Nat Chem*, vol. 11, no. 4, pp. 351–358, Apr. 2019, doi: 10.1038/s41557-019-0216-y.

[170] P. M. Lundin, B. L. Fiser, M. S. Blackledge, H. L. Pickett, and A. L. Copeland, "Functionalized Self-Assembled Monolayers: Versatile Strategies to Combat Bacterial Biofilm Formation," Aug. 01, 2022, *MDPI*. doi: 10.3390/pharmaceutics14081613.

[171] O. Seitz, P. G. Fernandes, R. Tian, N. Karnik, H. C. Wen, H. Stiegler, R. A. Chapman, E. M. Vogel, and Y. J. Chabal, "Control and stability of self-assembled monolayers under biosensing conditions," *J Mater Chem*, vol. 21, no. 12, pp. 4384–4392, Mar. 2011, doi: 10.1039/c1jm10132c.

[172] R. G. Nuzzo and D. L. Allara, "Adsorption of Bifunctional Organic Disulfides on Gold Surfaces".

[173] S. P. Pujari, L. Scheres, A. T. M. Marcelis, and H. Zuilhof, "Covalent surface modification of oxide surfaces," Jun. 16, 2014, *Wiley-VCH Verlag*. doi: 10.1002/anie.201306709.

[174] J. Sánchez-Bodón, J. A. Del Olmo, J. M. Alonso, I. Moreno-Benítez, J. L. Vilas-Vilela, and L. Pérez-Álvarez, "Bioactive Coatings on Titanium: A Review on Hydroxylation, Self-Assembled Monolayers (SAMs) and Surface Modification Strategies," *Polymers (Basel)*, vol. 14, no. 1, Jan. 2022, doi: 10.3390/polym14010165.

[175] C. Haensch, S. Hoeppener, and U. S. Schubert, "Chemical modification of self-assembled silane based monolayers by surface reactions," *Chem Soc Rev*, vol. 39, no. 6, pp. 2323–2334, May 2010, doi: 10.1039/b920491a.

[176] Y. Yang, A. M. Bittner, S. Baldelli, and K. Kern, "Study of self-assembled triethoxysilane thin films made by casting neat reagents in ambient atmosphere," *Thin Solid Films*, vol. 516, no. 12, pp. 3948–3956, Apr. 2008, doi: 10.1016/j.tsf.2007.07.208.

[177] L. Rouvière, N. Al-Hajj, J. Hunel, C. Aupetit, T. Buffeteau, L. Vellutini, and E. Genin, "Silane-Based SAMs Deposited by Spin Coating as a Versatile Alternative Process to Solution Immersion," *Langmuir*, vol. 38, no. 20, pp. 6464–6471, May 2022, doi: 10.1021/acs.langmuir.2c00668.

[178] Z. Wu, D. Wang, and P. Yang, "A facile bifunctional strategy for fabrication of bioactive or bioinert functionalized organic surfaces via amides-initiated photochemical reactions," *Ind Eng Chem Res*, vol. 53, no. 22, pp. 9401–9410, Jun. 2014, doi: 10.1021/ie501058f.

[179] T. B. Donadt and R. Yang, "Vapor-Deposited Biointerfaces and Bacteria: An Evolving Conversation," *ACS Biomater Sci Eng*, vol. 6, no. 1, pp. 182–197, Jan. 2020, doi: 10.1021/acsbiomaterials.9b01496.

[180] R. Vos, C. Rolin, J. Rip, T. Conard, T. Steylaerts, M. V. Cabanilles, K. Levrie, K. Jans, and T. Stakenborg, "Chemical Vapor Deposition of Azidoalkylsilane Monolayer Films," *Langmuir*, vol. 34, no. 4, pp. 1400–1409, Jan. 2018, doi: 10.1021/acs.langmuir.7b04011.

[181] R. D. Lowe, M. A. Pellow, T. D. P. Stack, and C. E. D. Chidsey, "Deposition of dense siloxane monolayers from water and trimethoxyorganosilane vapor," *Langmuir*, vol. 27, no. 16, pp. 9928–9935, Aug. 2011, doi: 10.1021/la201333y.

[182] Y. Mousli, L. Rouvière, I. Traboulsi, J. Hunel, T. Buffeteau, K. Heuzé, L. Vellutini, and E. Genin, "Hydrosilylation of Azide-Containing Olefins as a Convenient Access to Azidoorganotrialkoxysilanes for Self-Assembled Monolayer Elaboration onto Silica by

Spin Coating," *ChemistrySelect*, vol. 3, no. 25, pp. 7333–7339, Jul. 2018, doi: 10.1002/SLCT.201800858.

[183] Y. C. Chang, M. Chandra Sil, Y. P. Zhang, S. C. Chou, Y. X. Liu, S. Y. Li, and C. M. Chen, "Surface co-silanization engineering to enhance amine functionality for adhesive heterojunction and antimicrobial application," *Compos Sci Technol*, vol. 218, Feb. 2022, doi: 10.1016/j.compscitech.2021.109196.

[184] Y. J. Chuah, S. Kuddannaya, M. Hui, A. Lee, Y. Zhang, and Y. Kang, "The effects of poly(dimethylsiloxane) surface silanization on the mesenchymal stem cell fate," *Biomater Sci*, vol. 3, p. 383, 2015, doi: 10.1039/c4bm00268g.

[185] S. K. Vashist, E. Lam, S. Hrapovic, K. B. Male, and J. H. T. Luong, "Immobilization of antibodies and enzymes on 3-aminopropyltriethoxysilane-functionalized bioanalytical platforms for biosensors and diagnostics," Nov. 12, 2014, *American Chemical Society*. doi: 10.1021/cr5000943.

[186] A. Hasan, S. K. Pattanayek, and L. M. Pandey, "Effect of Functional Groups of Self-Assembled Monolayers on Protein Adsorption and Initial Cell Adhesion," *ACS Biomater Sci Eng*, vol. 4, no. 9, pp. 3224–3233, Sep. 2018, doi: 10.1021/acsbiomaterials.8b00795.

[187] E. Siurdyban, T. Brotin, D. Talaga, K. Heuzé, L. Vellutini, and T. Buffeteau, "Immobilization of Cryptophane Derivatives onto γ-Fe2O3 Core-Shell Magnetic Nanoparticles," *Journal of Physical Chemistry C*, vol. 120, no. 12, pp. 6583–6590, Mar. 2016, doi: 10.1021/acs.jpcc.5b12514.

[188] L. Rouvière, A. Hachin, S. Shinkaruk, J. Hunel, C. Aupetit, T. Buffeteau, E. Genin, and L. Vellutini, "Self-assembly of amino-terminated monolayers depending on the chemical structure," *New Journal of Chemistry*, vol. 47, no. 20, pp. 9661–9668, Apr. 2023, doi: 10.1039/d3nj01312j.

[189] R. Mishra, T. Bishop, I. L. Valerio, J. P. Fisher, and D. Dean, "The potential impact of bone tissue engineering in the clinic," Sep. 01, 2016, *Future Medicine Ltd.* doi: 10.2217/rme-2016-0042.

[190] X. Lin, S. Patil, Y. G. Gao, and A. Qian, "The Bone Extracellular Matrix in Bone Formation and Regeneration," May 26, 2020, *Frontiers Media S.A.* doi: 10.3389/fphar.2020.00757.

[191] C. Bonnans, J. Chou, and Z. Werb, "Remodelling the extracellular matrix in development and disease," Dec. 11, 2014, *Nature Publishing Group*. doi: 10.1038/nrm3904.

[192] M. Tavafoghi and M. Cerruti, "The role of amino acids in hydroxyapatite mineralization," Oct. 01, 2016, *Royal Society of London*. doi: 10.1098/rsif.2016.0462.

[193] A. Mansour, M. A. Mezour, Z. Badran, and F. Tamimi, "Extracellular matrices for bone regeneration: A literature review," Dec. 01, 2017, *Mary Ann Liebert Inc.* doi: 10.1089/ten.tea.2017.0026.

[194] D. Nikitovic, J. Aggelidakis, M. F. Young, R. V. Iozzo, N. K. Karamanos, and G. N. Tzanakakis, "The biology of small leucine-rich proteoglycans in bone pathophysiology," Oct. 05, 2012. doi: 10.1074/jbc.R112.379602.

[195] L. Wen, J. Chen, L. Duan, and S. Li, "Vitamin K-dependent proteins involved in bone and cardiovascular health (Review)," Jul. 01, 2018, *Spandidos Publications*. doi: 10.3892/mmr.2018.8940.

[196] E. M. Rosset and A. D. Bradshaw, "SPARC/osteonectin in mineralized tissue," May 01, 2016, *Elsevier B.V.* doi: 10.1016/j.matbio.2016.02.001.

[197] A. M. Delany and K. D. Hankenson, "Thrombospondin-2 and SPARC/osteonectin are critical regulators of bone remodeling," 2009. doi: 10.1007/s12079-009-0076-0.

[198] R. Marinovich, Y. Soenjaya, G. Q. Wallace, A. Zuskov, A. Dunkman, B. L. Foster, M. Ao, K. Bartman, V. Lam, A. Rizkalla, F. Beier, M. J. Somerman, D. W. Holdsworth, L. J. Soslowsky, F. Lagugné-Labarthet, and H. A. Goldberg, "The role of bone sialoprotein in the tendon-bone insertion," *Matrix Biology*, vol. 52–54, pp. 325–338, May 2016, doi: 10.1016/j.matbio.2016.01.016.

[199] J. Luo, M. Walker, Y. Xiao, H. Donnelly, M. J. Dalby, and M. Salmeron-Sanchez, "The influence of nanotopography on cell behaviour through interactions with the extracellular matrix – A review," Sep. 01, 2022, *KeAi Communications Co.* doi: 10.1016/j.bioactmat.2021.11.024.

[200] J. M. W. Slack, "Molecular biology of the cell," in *Principles of Tissue Engineering*, Elsevier, 2020, pp. 65–78. doi: 10.1016/B978-0-12-818422-6.00005-8.

[201] P. J. Marie, E. Haÿ, and Z. Saidak, "Integrin and cadherin signaling in bone: Role and potential therapeutic targets," 2014, *Elsevier Inc.* doi: 10.1016/j.tem.2014.06.009.

[202] Lynda F. Bonewald, "Cell–Cell and Cell–Matrix Interactions in Bone," in *Handbook of Cell Signaling, Second Edition*, vol. 1, Elsevier, 2010, pp. 1–4. doi: 10.1016/B978-0-12-374145-5.00001-2.

[203] M. C. Z. Meneghetti, A. J. Hughes, T. R. Rudd, H. B. Nader, A. K. Powell, E. A. Yates, and M. A. Lima, "Heparan sulfate and heparin interactions with proteins," Sep. 06, 2015, *Royal Society of London*. doi: 10.1098/rsif.2015.0589.

[204] F. Heide, M. Koch, and J. Stetefeld, "Heparin Mimetics and Their Impact on Extracellular Matrix Protein Assemblies," *Pharmaceuticals*, vol. 16, no. 3, Mar. 2023, doi: 10.3390/ph16030471.

[205] I. Capila and R. J. Linhardt, "Heparin - Protein interactions," Feb. 01, 2002. doi: 10.1002/1521-3773(20020201)41:3<390::AID-ANIE390>3.0.CO;2-B.

[206] X. Wu, W. Shi, and X. Cao, "Multiplicity of BMP signaling in skeletal development," in *Annals of the New York Academy of Sciences*, Blackwell Publishing Inc., 2007, pp. 29–49. doi: 10.1196/annals.1402.053.

[207] C. Cimmino, L. Rossano, P. A. Netti, and M. Ventre, "Spatio-temporal control of cell adhesion: Toward programmable platforms to manipulate cell functions and fate," Dec. 04, 2018, *Frontiers Media S.A.* doi: 10.3389/fbioe.2018.00190.

[208] D. Yadin, P. Knaus, and T. D. Mueller, "Structural insights into BMP receptors: Specificity, activation and inhibition," 2015, doi: 10.1016/j.cytogfr.2015.11.005.

[209] R. Visser, G. A. Rico-Llanos, H. Pulkkinen, and J. Becerra, "Peptides for bone tissue engineering," 2016, doi: 10.1016/j.jconrel.2016.10.024.

[210] G. Bullock, J. Atkinson, P. Gentile, P. Hatton, and C. Miller, "Osteogenic peptides and attachment methods determine tissue regeneration in modified bone graft substitutes," Jun. 01, 2021, *MDPI*. doi: 10.3390/jfb12020022.

[211] C. Mas-Moruno, "Surface functionalization of biomaterials for bone tissue regeneration and repair," in *Peptides and Proteins as Biomaterials for Tissue Regeneration and Repair*, Elsevier Inc., 2018, pp. 73–100. doi: 10.1016/B978-0-08-100803-4.00003-6.

[212] O. F. Zouani, L. Rami, Y. Lei, and M. C. Durrieu, "Insights into the osteoblast precursor differentiation towards mature osteoblasts induced by continuous BMP-2 signaling," *Biol Open*, vol. 2, no. 9, pp. 872–881, Sep. 2013, doi: 10.1242/bio.20134986.

[213] Y. Zhang, M. Remy, T. Leste-Lasserre, and M.-C. Durrieu, "Manipulating Stem Cell Fate with Disordered Bioactive Cues on Surfaces: The Role of Bioactive Ligand Selection," *Cite This: ACS Appl. Mater. Interfaces*, vol. 16, pp. 18474–18489, 2024, doi: 10.1021/acsami.4c00262.

[214] Y. Zhang, M. Rémy, E. Apartsin, E. Prouvé, C. Feuillie, C. Labrugère, N. Cam, and M. C. Durrieu, "Controlling differentiation of stem cells via bioactive disordered cues," *Biomater Sci*, vol. 11, no. 18, pp. 6116–6134, Aug. 2023, doi: 10.1039/d3bm00605k.

[215] I. Bilem, P. Chevallier, L. Plawinski, E. D. Sone, M. C. Durrieu, and G. Laroche, "RGD and BMP-2 mimetic peptide crosstalk enhances osteogenic commitment of human bone marrow stem cells," *Acta Biomater*, vol. 36, pp. 132–142, May 2016, doi: 10.1016/j.actbio.2016.03.032.

[216] I. Bilem, P. Chevallier, L. Plawinski, E. D. Sone, M. C. Durrieu, and G. Laroche, "Interplay of Geometric Cues and RGD/BMP-2 Crosstalk in Directing Stem Cell

Fate," *ACS Biomater Sci Eng*, vol. 3, no. 10, pp. 2514–2523, Oct. 2017, doi: 10.1021/acsbiomaterials.7b00279.

[217] L. Padiolleau, C. Chanseau, S. Durrieu, P. Chevallier, G. Laroche, and M. C. Durrieu, "Single or Mixed Tethered Peptides to Promote hMSC Differentiation toward Osteoblastic Lineage," *ACS Appl Bio Mater*, vol. 1, no. 6, pp. 1800–1809, Dec. 2018, doi: 10.1021/acsabm.8b00236.

[218] L. Padiolleau, C. Chanseau, S. Durrieu, C. Ayela, G. Laroche, and M.-C. Durrieu, "Directing hMSCs fate through geometrical cues and mimetics peptides," 2019, doi: 10.1002/jbm.a.36804.

[219] I. Pountos, M. Panteli, A. Lampropoulos, E. Jones, G. M. Calori, and P. V. Giannoudis, "The role of peptides in bone healing and regeneration: A systematic review," *BMC Med*, vol. 14, no. 1, Jul. 2016, doi: 10.1186/s12916-016-0646-y.

[220] M. D. Pierschbacher and E. Ruoslahti, "Cell attachment activity of fibronectin can be duplicated by small synthetic fragments of the molecule".

[221] L. Oliver-Cervelló, H. Martin-Gómez, and C. Mas-Moruno, "New trends in the development of multifunctional peptides to functionalize biomaterials," Jan. 01, 2022, *John Wiley and Sons Ltd.* doi: 10.1002/psc.3335.

[222] H. Pan, Q. Zheng, S. Yang, X. Guo, B. Wu, Z. Zou, and Z. Duan, "A novel peptide-modified and gene-activated biomimetic bone matrix accelerating bone regeneration," *J Biomed Mater Res A*, vol. 102, no. 8, pp. 2864–2874, 2014, doi: 10.1002/jbm.a.34961.

[223] N. M. Moore, N. J. Lin, N. D. Gallant, and M. L. Becker, "Synergistic enhancement of human bone marrow stromal cell proliferation and osteogenic differentiation on BMP-2-derived and RGD peptide concentration gradients", doi: 10.1016/j.actbio.2011.01.019.

[224] A. Shekaran, J. R. García, A. Y. Clark, T. E. Kavanaugh, A. S. Lin, R. E. Guldberg, and A. J. García, "Bone regeneration using an alpha 2 beta 1 integrin-specific hydrogel as a BMP-2 delivery vehicle," *Biomaterials*, vol. 35, no. 21, pp. 5453–5461, 2014, doi: 10.1016/j.biomaterials.2014.03.055.

[225] Q. Liu, W. Limthongkul, G. Sidhu, J. Zhang, A. Vaccaro, R. Shenck, N. Hickok, I. Shapiro, and T. Freeman, "Covalent attachment of P15 peptide to titanium surfaces enhances cell attachment, spreading, and osteogenic gene expression," *Journal of Orthopaedic Research*, vol. 30, no. 10, pp. 1626–1633, 2012, doi: 10.1002/jor.22116.

[226] V. Sollazzo, A. Palmieri, A. Girardi, F. Farinella, and F. Carinci, "Early effects of P-15 on human bone marrow stem cells," *J Oral Maxillofac Res*, vol. 1, no. 1, 2010, doi: 10.5037/jomr.2010.1104.

[227] H. Krenzlin, A. Foelger, V. Mailänder, C. Blase, M. Brockmann, C. Düber, F. Ringel, N. Keric, W. Kämmerer, and B. Al-Nawas, "Novel Biodegradable Composite of Calcium Phosphate Cement and the Collagen I Mimetic P-15 for Pedicle Screw Augmentation in Osteoporotic Bone," 2021, doi: 10.3390/biomedicines9101392.

[228] A. W. James, "Review of Signaling Pathways Governing MSC Osteogenic and Adipogenic Differentiation," *Scientifica (Cairo)*, vol. 2013, pp. 1–17, 2013, doi: 10.1155/2013/684736.

[229] C. Mas-Moruno, "Surface functionalization of biomaterials for bone tissue regeneration and repair," in *Peptides and Proteins as Biomaterials for Tissue Regeneration and Repair*, Elsevier Inc., 2018, pp. 73–100. doi: 10.1016/B978-0-08-100803-4.00003-6.

[230] M. Guang, B. Huang, Y. Yao, L. Zhang, B. Yang, and P. Gong, "Effects of vascular endothelial growth factor on osteoblasts around dental implants in vitro and in vivo," *J Oral Sci*, vol. 59, no. 2, pp. 215–223, 2017, doi: 10.2334/josnusd.16-0406.

[231] P. Jurczak, J. Witkowska, S. Rodziewicz-Motowidło, and S. Lach, "Proteins, peptides and peptidomimetics as active agents in implant surface functionalization," Feb. 01, 2020, *Elsevier B.V.* doi: 10.1016/j.cis.2019.102083.

[232] C. M. Madl, M. Mehta, G. N. Duda, S. C. Heilshorn, and D. J. Mooney, "Presentation of BMP-2 mimicking peptides in 3D hydrogels directs cell fate commitment in osteoblasts and mesenchymal stem cells," *Biomacromolecules*, vol. 15, no. 2, pp. 445–455, Feb. 2014, doi: 10.1021/bm401726u.

[233] V. Lukasova, M. Buzgo, V. Sovkova, J. Dankova, M. Rampichova, and E. Amler, "Osteogenic differentiation of 3D cultured mesenchymal stem cells induced by bioactive peptides," *Cell Prolif*, vol. 50, no. 4, Aug. 2017, doi: 10.1111/cpr.12357.

[234] E. Ko, K. Yang, J. Shin, and S. W. Cho, "Polydopamine-assisted osteoinductive peptide immobilization of polymer scaffolds for enhanced bone regeneration by human adipose-derived stem cells," *Biomacromolecules*, vol. 14, no. 9, pp. 3202–3213, Sep. 2013, doi: 10.1021/bm4008343.

[235] A. E. Rodda, L. Meagher, D. R. Nisbet, and J. S. Forsythe, "Specific control of cell-material interactions: Targeting cell receptors using ligand-functionalized polymer substrates," *Prog Polym Sci*, vol. 39, pp. 1312–1347, 2014, doi: 10.1016/j.progpolymsci.2013.11.006.

[236] C. Mas-Moruno, "Surface functionalization of biomaterials for bone tissue regeneration and repair," in *Peptides and Proteins as Biomaterials for Tissue Regeneration and Repair*, Elsevier Inc., 2018, pp. 73–100. doi: 10.1016/B978-0-08-100803-4.00003-6.

[237] D. S. W. Benoit and K. S. Anseth, "The effect on osteoblast function of colocalized RGD and PHSRN epitopes on PEG surfaces," *Biomaterials*, vol. 26, no. 25, pp. 5209–5220, Sep. 2005, doi: 10.1016/j.biomaterials.2005.01.045.

[238] M. M. Martino, M. Mochizuki, D. A. Rothenfluh, S. A. Rempel, J. A. Hubbell, and T. H. Barker, "Controlling integrin specificity and stem cell differentiation in 2D and 3D environments through regulation of fibronectin domain stability," 2008, doi: 10.1016/j.biomaterials.2008.10.047.

[239] / Langmuir, G. A. Hudalla, and W. L. Murphy, "Immobilization of Peptides with Distinct Biological Activities onto Stem Cell Culture Substrates Using Orthogonal Chemistries," *Langmuir*, vol. 26, no. 9, pp. 6449–6456, 2010, doi: 10.1021/la1008208.

[240] J. Sam Lee, J. Sung Lee, A. Wagoner-Johnson, W. L. Murphy, J. S. Lee, W. L. Murphy, and A. Wagoner-Johnson, "Modular Peptide Growth Factor Modular Peptide Growth Factors for Substrate-Mediated Stem Cell Differentiation**", doi: 10.1002/anie.200901618.

[241] Y. Kim, J. N. Renner, and J. C. Liu, "Incorporating the BMP-2 peptide in genetically-engineered biomaterials accelerates osteogenic differentiation †," *Cite this: Biomater. Sci*, vol. 2, p. 1110, 2014, doi: 10.1039/c3bm60333d.

[242] Y. Ma, G. M. Policastro, Q. Li, J. Zheng, R. Jacquet, W. J. Landis, and M. L. Becker, "Concentration-Dependent hMSC Differentiation on Orthogonal Concentration Gradients of GRGDS and BMP-2 Peptides," 2016, doi: 10.1021/acs.biomac.6b00088.

[243] G. Pan, S. Sun, W. Zhang, R. Zhao, W. Cui, F. He, L. Huang, S.-H. Lee, K. J. Shea, Q. Shi, and H. Yang, "Biomimetic Design of Mussel-Derived Bioactive Peptides for Dual-Functionalization of Titanium-Based Biomaterials," 2016, doi: 10.1021/jacs.6b09770.

[244] L. Citation Padiolleau, C. Chanseau, S. Durrieu, P. Chevallier, G. Laroche, and M. C. Durrieu, "Single or Mixed Tethered Peptides To Promote hMSC Differentiation toward Osteoblastic Lineage," *ACS Appl Bio Mater*, vol. 1, no. 6, pp. 1800–1809, 2018, doi: 10.1021/acsabm.8b00236.

[245] H. Pan, Q. Zheng, S. Yang, X. Guo, B. Wu, Z. Zou, and Z. Duan, "A novel peptide-modified and gene-activated biomimetic bone matrix accelerating bone regeneration," 2013, doi: 10.1002/jbm.a.34961.

[246] Y. M. Shin, S. Y. Jo, J. S. Park, H. J. Gwon, S. I. Jeong, and Y. M. Lim, "Synergistic effect of dual-functionalized fibrous scaffold with BCP and RGD containing peptide for improved osteogenic differentiation," *Macromol Biosci*, vol. 14, no. 8, pp. 1190–1198, 2014, doi: 10.1002/mabi.201400023.

[247] D. H. Yang, S. W. Moon, and D. W. Lee, "Surface modification of titanium with BMP-2/GDF-5 by a heparin linker and its efficacy as a dental implant," *Int J Mol Sci*, vol. 18, no. 1, Jan. 2017, doi: 10.3390/ijms18010229.

[248] K. C. Dee, T. T. Andersen, and R. Bizios, "Design and function of novel osteoblast-adhesive peptides for chemical modification of biomaterials," *J Biomed Mater Res*, vol. 40, no. 3, pp. 371–377, Jun. 1998, doi: 10.1002/(SICI)1097-4636(19980605)40:3<371::AID-JBM5>3.0.CO;2-C.

[249] J. T. Koepsel, P. T. Brown, S. G. Loveland, ab Wan-Ju Li ab, and W. L. Murphy, "Combinatorial screening of chemically defined human mesenchymal stem cell culture substrates †", doi: 10.1039/c2jm32242k.

[250] G. Bullock, J. Atkinson, P. Gentile, P. Hatton, and C. Miller, "Osteogenic peptides and attachment methods determine tissue regeneration in modified bone graft substitutes," Jun. 01, 2021, *MDPI*. doi: 10.3390/jfb12020022.

[251] M. P. Lutolf and J. A. Hubbell, "Synthetic biomaterials as instructive extracellular microenvironments for morphogenesis in tissue engineering," 2005. doi: 10.1038/nbt1055.

[252] C. Cimmino, L. Rossano, P. A. Netti, and M. Ventre, "Spatio-temporal control of cell adhesion: Toward programmable platforms to manipulate cell functions and fate," Dec. 04, 2018, *Frontiers Media S.A.* doi: 10.3389/fbioe.2018.00190.

[253] R. A. S. and D. V. S. Barbara L. Ekerdt, "Spatial organization of cell-adhesive ligands for advanced cell culture," 2013, doi: 10.1002/biot.201300302.

[254] "Differentiation potential of mesenchymal stem cells of different origin | Enhanced Reader."

[255] A. Higuchi, Q. D. Ling, Y. Chang, S. T. Hsu, and A. Umezawa, "Physical cues of biomaterials guide stem cell differentiation fate," May 08, 2013. doi: 10.1021/cr300426x.

[256] J. Luo, M. Walker, Y. Xiao, H. Donnelly, M. J. Dalby, and M. Salmeron-Sanchez, "The influence of nanotopography on cell behaviour through interactions with the extracellular matrix – A review," *Bioact Mater*, vol. 15, pp. 145–159, Sep. 2022, doi: 10.1016/J.BIOACTMAT.2021.11.024.

[257] G. Hime and H. Abud, "Transcriptional and Translational Regulation of Stem Cells." [Online]. Available: http://www.springer.com/series/5584

[258] A. S. Mertgen, V. T. Trossmann, A. G. Guex, K. Maniura-Weber, T. Scheibel, and M. Rottmar, "Multifunctional Biomaterials: Combining Material Modification Strategies

for Engineering of Cell-Contacting Surfaces," May 13, 2020, *American Chemical Society*. doi: 10.1021/acsami.0c01893.

[259] H. Chen, D. M. Cohen, D. M. Choudhury, N. Kioka, and S. W. Craig, "Spatial distribution and functional significance of activated vinculin in living cells," *Journal of Cell Biology*, vol. 169, no. 3, pp. 459–470, May 2005, doi: 10.1083/jcb.200410100.

[260] L. Oliver-Cervelló, H. Martin-Gómez, and C. Mas-Moruno, "New trends in the development of multifunctional peptides to functionalize biomaterials," Jan. 01, 2022, *John Wiley and Sons Ltd*. doi: 10.1002/psc.3335.

[261] K. M. Sawicka, M. Seeliger, T. Musaev, L. K. Macri, and R. A. F. Clark, "CRITICAL REVIEWS Fibronectin Interaction and Enhancement of Growth Factors: Importance for Wound Healing TRANSLATIONAL RELEVANCE Disturbances in GFs and the ex-tracellular matrix (ECM) account for," *Adv Wound Care (New Rochelle)*, vol. 4, no. 8, doi: 10.1089/wound.2014.0616.

[262] N. R. Richbourg, N. A. Peppas, and V. I. Sikavitsas, "Tuning the biomimetic behavior of scaffolds for regenerative medicine through surface modifications," *J Tissue Eng Regen Med*, vol. 13, no. 8, pp. 1275–1293, Aug. 2019, doi: 10.1002/TERM.2859.

[263] S. Bauer, P. Schmuki, K. Von Der Mark, J. Park, and J. Park, "Engineering biocompatible implant surfaces Part I: Materials and surfaces," *Prog Mater Sci*, vol. 58, pp. 261–326, 2013, doi: 10.1016/j.pmatsci.2012.09.001.

[264] H.-S. Hung, A. Yang-Hao Yu, S.-C. Hsieh, M.-L. Kung, H.-Y. Huang, R.-H. Fu, C.-A. Yeh, and S. Hsu, "Enhanced Biocompatibility and Differentiation Capacity of Mesenchymal Stem Cells on Poly(dimethylsiloxane) by Topographically Patterned Dopamine," *Cite This: ACS Appl. Mater. Interfaces*, vol. 12, pp. 44393–44406, 2020, doi: 10.1021/acsami.0c05747.

[265] C.-C. Wu, C.-Y. Yuan, and S.-J. Ding, "Effect of polydimethylsiloxane surfaces silanized with different nitrogen-containing groups on the adhesion progress of epithelial cells," 2010, doi: 10.1016/j.surfcoat.2010.11.036.

[266] S. Sharan, R. Vuppaladadium, T. Agarwal, S. Kulanthaivel, B. Mohanty, C. Sekhar Barik, T. K. Maiti, S. Pal, K. Pal, and I. Banerjee, "Silanization improves biocompatibility of graphene oxide," 2020, doi: 10.1016/j.msec.2020.110647.

[267] J. Böhmler, L. Ploux, V. Ball, K. Anselme, and A. Ponche, "Necessity of a Thorough Characterization of Functionalized Silicon Wafers before Biointerface Studies," *J. Phys. Chem. C*, vol. 115, pp. 11102–11111, 2011, doi: 10.1021/jp201377n.

[268] A. Álvarez-López, L. Colchero, M. Elices, G. V Guinea, J. Pérez-Rigueiro, and D. González-Nieto, "Improved cell adhesion to activated vapor silanization-

biofunctionalized Ti-6Al-4V surfaces with ECM-derived oligopeptides," 2021, doi: 10.1016/j.msec.2021.112614.

[269] W. Wang, M. W. Vaughn, and M. W. Vaughn, "Morphology and Amine Accessibility of (3-Aminopropyl) Triethoxysilane Films on Glass Surfaces," vol. 30, pp. 65–77, 2008, doi: 10.1002/sca.20097.

[270] L. Rouviè, A. Hachin, S. Shinkaruk, J. Hunel, C. Aupetit, T. Buffeteau, E. Genin, and L. Vellutini, "Self-assembly of amino-terminated monolayers depending on the chemical structure †," *New J. Chem*, vol. 47, p. 9661, 2023, doi: 10.1039/d3nj01312j.

[271] N. Al-Hajj, Y. Mousli, A. Miche, V. Humblot, J. Hunel, K. Heuzé, T. Buffeteau, E. Genin, and L. Vellutini, "Influence of the grafting process on the orientation and the reactivity of azide-terminated monolayers onto silica surface," 2020, doi: 10.1016/j.apsusc.2020.146778.

[272] L. Rouvière, N. Al-Hajj, J. Hunel, C. Aupetit, T. Buffeteau, L. Vellutini, and E. Genin, "Silane-Based SAMs Deposited by Spin Coating as a Versatile Alternative Process to Solution Immersion," *Langmuir*, 2022, doi: 10.1021/acs.langmuir.2c00668.

[273] C. A. Hoesli, A. Garnier, P. M. Juneau, P. Chevallier, C. Duchesne, and G. Laroche, "A fluorophore-tagged RGD peptide to control endothelial cell adhesion to micropatterned surfaces," *Biomaterials*, vol. 35, no. 3, pp. 879–890, Jan. 2014, doi: 10.1016/j.biomaterials.2013.09.076.

[274] M. A. Ramin, G. Le Bourdon, N. Daugey, B. Bennetau, L. Vellutini, and T. Buffeteau, "PM-IRRAS investigation of self-assembled monolayers grafted onto SiO 2/Au substrates," *Langmuir*, vol. 27, no. 10, pp. 6076–6084, Jun. 2011, doi: 10.1021/la2006293.

[275] T. Buffeteau, B. Desbat, D. Blaudez, and J. M. Turlet, "Calibration procedure to derive IRRAS spectra from PM-IRRAS spectra," *Appl Spectrosc*, vol. 54, no. 11, pp. 1646–1650, Nov. 2000, doi: 10.1366/0003702001948673.

[276] G. Polzonetti, C. Battocchio, M. Dettin, R. Gambaretto, C. Di Bello, V. Carravetta, S. Monti, and G. Iucci, "Self-assembling peptides: A combined XPS and NEXAFS investigation on the structure of two dipeptides Ala-Glu, Ala-Lys," *Materials Science and Engineering C*, vol. 28, no. 2, pp. 309–315, Mar. 2008, doi: 10.1016/j.msec.2007.02.004.

[277] F. Shamsi, "Investigation of human cell response to covalently attached RADA16-I peptide on silicon surfaces," *Colloids Surf B Biointerfaces*, vol. 145, pp. 470–478, 2016, doi: 10.1016/j.colsurfb.2016.05.030.

[278] J. F. Watts, "High resolution XPS of organic polymers: The Scienta ESCA 300 database. G. Beamson and D. Briggs. 280pp., £65. John Wiley & Sons, Chichester,

ISBN 0471 935921, (1992)," *Surface and Interface Analysis*, vol. 20, no. 3, pp. 267–267, Mar. 1993, doi: 10.1002/SIA.740200310.

[279] L. Rouvière, A. Hachin, S. Shinkaruk, J. Hunel, C. Aupetit, T. Buffeteau, E. Genin, and L. Vellutini, "Self-assembly of amino-terminated monolayers depending on the chemical structure," *New Journal of Chemistry*, vol. 47, no. 20, pp. 9661–9668, Apr. 2023, doi: 10.1039/d3nj01312j.

[280] N. Al-Hajj, Y. Mousli, A. Miche, V. Humblot, J. Hunel, K. Heuzé, T. Buffeteau, E. Genin, and L. Vellutini, "Influence of the grafting process on the orientation and the reactivity of azide-terminated monolayers onto silica surface," *Appl Surf Sci*, vol. 527, Oct. 2020, doi: 10.1016/j.apsusc.2020.146778.

[281] S.-J. Xiao, M. Textor, N. D. Spencer, and H. Sigrist, "Covalent Attachment of Cell-Adhesive, (Arg-Gly-Asp)-Containing Peptides to Titanium Surfaces," 1998, Accessed: Jan. 25, 2024. [Online]. Available: https://pubs.acs.org/sharingguidelines

[282] S.-J. Xiao, S. Brunner, and M. Wieland, "Reactions of Surface Amines with Heterobifunctional Cross-Linkers Bearing Both Succinimidyl Ester and Maleimide for Grafting Biomolecules," 2004, doi: 10.1021/jp047726s.

[283] M. Nicolas, B. Beito, M. Oliveira, M. T. Martins, B. Gallas, M. Salmain, S. Boujday, and V. Humblot, "Strategies for antimicrobial peptides immobilization on surfaces to prevent biofilm growth on biomedical devices," *Antibiotics*, vol. 11, no. 1, Jan. 2022, doi: 10.3390/antibiotics11010013.

[284] L. Stillger and D. Müller, "Peptide-coating combating antimicrobial contaminations: a review of covalent immobilization strategies for industrial applications," Jun. 01, 2022, *Springer*. doi: 10.1007/s10853-022-07266-w.

[285] R. Chen, J. A. Hunt, S. Fawcett, R. D'sa, R. Akhtar, and J. M. Curran, "The optimization and production of stable homogeneous amine enriched surfaces with characterized nanotopographical properties for enhanced osteoinduction of mesenchymal stem cells," *J Biomed Mater Res A*, vol. 106, no. 7, pp. 1862–1877, Jul. 2018, doi: 10.1002/jbm.a.36383.

[286] H. Liu and G. Jin, "Comparison of modified molecules 3-aminopropyltriethoxysilane and 11-aminoundecyltriethoxysilane in orientation angle and interaction with protein by sum frequency vibration spectrum and imaging ellipsometry biosensor," *Thin Solid Films*, vol. 769, p. 139738, 2023, doi: 10.1016/j.tsf.2023.139738.

[287] C. S. Taylor, J. Barnes, M. Prasad Koduri, S. Haq, D. A. Gregory, I. Roy, R. A. D'Sa, J. Curran, and J. W. Haycock, "Aminosilane Functionalized Aligned Fiber PCL Scaffolds for Peripheral Nerve Repair," *Macromol Biosci*, vol. 23, no. 11, Nov. 2023, doi: 10.1002/mabi.202300226.

[288] C. S. Taylor, R. Chen, R. D'Sa, J. A. Hunt, J. M. Curran, and J. W. Haycock, "Cost effective optimised synthetic surface modification strategies for enhanced control of neuronal cell differentiation and supporting neuronal and Schwann cell viability," *J Biomed Mater Res B Appl Biomater*, vol. 109, no. 11, pp. 1713–1723, Nov. 2021, doi: 10.1002/jbm.b.34829.

[289] M.-C. Wu, H. W. Yu, Y.-Q. Chen, M.-H. Ou, R. Serrano, G.-L. Huang, Y.-K. Wang, K.-H. Lin, Y.-J. Fan, C.-C. Wu, J. C. Del Álamo, A. Chiou, S. Chien, J.-C. Kuo, M.-C. Wu, H. W. Yu, and Y.-Q. Chen, "Early committed polarization of intracellular tension in response to cell shape determines the osteogenic differentiation of mesenchymal stromal cells ☆-NC-ND license (http://creativecommons.org/licenses/by-nc-nd/4.0/)," *Acta Biomater*, vol. 163, pp. 287–301, 2023, doi: 10.1016/j.actbio.2022.10.052.

[290] D. H. Kim and D. Wirtz, "Focal adhesion size uniquely predicts cell migration," *FASEB Journal*, vol. 27, no. 4, pp. 1351–1361, Apr. 2013, doi: 10.1096/fj.12-220160.

[291] E. Filova, J. Fojt, M. Kryslova, H. Moravec, L. Joska, and L. Bacakova, "The diameter of nanotubes formed on Ti-6Al-4V alloy controls the adhesion and differentiation of Saos-2 cells," *Int J Nanomedicine*, vol. 10, pp. 7145–7163, Nov. 2015, doi: 10.2147/IJN.S87474.

[292] Y. Yu, Y. Suryo Rahmanto, M. H. Lee, P. H. Wu, J. M. Phillip, C. H. Huang, M. I. Vitolo, S. Gaillard, S. S. Martin, D. Wirtz, I. M. Shih, and T. L. Wang, "Inhibition of ovarian tumor cell invasiveness by targeting SYK in the tyrosine kinase signaling pathway," *Oncogene*, vol. 37, no. 28, pp. 3778–3789, Jul. 2018, doi: 10.1038/s41388-018-0241-0.

[293] M. Izdebska, M. Gagat, and A. Grzanka, "Overexpression of lamin B1 induces mitotic catastrophe in colon cancer lovo cells and is associated with worse clinical outcomes," *Int J Oncol*, vol. 52, no. 1, pp. 89–102, Jan. 2018, doi: 10.3892/ijo.2017.4182.

[294] M. N. Medina-Rosales, M. H. Muñoz-Ortega, M. H. García-Hernández, P. Talamás-Rohana, I. E. Medina-Ramírez, L. G. Salas-Morón, S. L. Martínez-Hernández, M. E. Ávila-Blanco, B. Medina-Rosales, and J. Ventura-Juárez, "Acetylcholine Upregulates Entamoeba histolytica Virulence Factors, Enhancing Parasite Pathogenicity in Experimental Liver Amebiasis," *Front Cell Infect Microbiol*, vol. 10, Jan. 2021, doi: 10.3389/fcimb.2020.586354.

[295] G. Le Saux, M.-C. Wu, E. Toledo, Y.-Q. Chen, Y.-J. Fan, J.-C. Kuo, and M. Schvartzman, "Cell−Cell Adhesion-Driven Contact Guidance and Its Effect on Human Mesenchymal Stem Cell Differentiation," *Cite This: ACS Appl. Mater. Interfaces*, vol. 12, pp. 22399–22409, 2020, doi: 10.1021/acsami.9b20939.

[296] J. Golji and M. R. K. Mofrad, "The Interaction of Vinculin with Actin," *PLoS Comput Biol*, vol. 9, no. 4, 2013, doi: 10.1371/journal.pcbi.1002995.

[297] I. Lauria, M. Kramer, T. Schröder, S. Kant, A. Hausmann, F. Böke, R. Leube, R. Telle, and H. Fischer, "Inkjet printed periodical micropatterns made of inert alumina ceramics induce contact guidance and stimulate osteogenic differentiation of mesenchymal stromal cells," *Acta Biomater*, vol. 44, pp. 85–96, Oct. 2016, doi: 10.1016/j.actbio.2016.08.004.

[298] L. B. Case, M. A. Baird, G. Shtengel, S. L. Campbell, H. F. Hess, M. W. Davidson, and C. M. Waterman, "Molecular mechanism of vinculin activation and nanoscale spatial organization in focal adhesions," *Nat Cell Biol*, vol. 17, no. 7, pp. 880–892, Jul. 2015, doi: 10.1038/ncb3180.

[299] J. L. Bays and K. A. DeMali, "Vinculin in cell–cell and cell–matrix adhesions," Aug. 01, 2017, *Birkhauser Verlag AG*. doi: 10.1007/s00018-017-2511-3.

[300] C. Mas-Moruno, R. Fraioli, F. Rechenmacher, S. Neubauer, T. G. Kapp, and H. Kessler, "αvβ3- or α5β1-Integrin-Selective Peptidomimetics for Surface Coating," *Angewandte Chemie - International Edition*, vol. 55, no. 25, pp. 7048–7067, Jun. 2016, doi: 10.1002/ANIE.201509782.

[301] L. Fourel, A. Valat, E. Faurobert, R. Guillot, I. Bourrin-Reynard, K. Ren, L. Lafanechère, E. Planus, C. Picart, and C. Albiges-Rizo, "β3 integrin-mediated spreading induced by matrix-bound BMP-2 controls Smad signaling in a stiffness-independent manner," *Journal of Cell Biology*, vol. 212, no. 6, pp. 693–706, Mar. 2016, doi: 10.1083/jcb.201508018.

[302] E. A. Cavalcanti-Adam, A. Micoulet, J. Blu¨mmelblu¨mmel, J. J. Auernheimer, H. Kessler, and J. P. Spatz, "Lateral spacing of integrin ligands influences cell spreading and focal adhesion assembly," *Eur J Cell Biol*, vol. 85, pp. 219–224, 2006, doi: 10.1016/j.ejcb.2005.09.011.

[303] M. Nicolas, B. Beito, M. Oliveira, M. T. Martins, B. Gallas, M. Salmain, S. Boujday, and V. Humblot, "Strategies for antimicrobial peptides immobilization on surfaces to prevent biofilm growth on biomedical devices," *Antibiotics*, vol. 11, no. 1, Jan. 2022, doi: 10.3390/antibiotics11010013.

[304] R. G. Acres, A. V. Ellis, J. Alvino, C. E. Lenahan, D. A. Khodakov, G. F. Metha, and G. G. Andersson, "Molecular structure of 3-aminopropyltriethoxysilane layers formed on silanol-terminated silicon surfaces," *Journal of Physical Chemistry C*, vol. 116, no. 10, pp. 6289–6297, Mar. 2012, doi: 10.1021/jp212056s.

[305] J. Martin, J. Martinez, A. Mehdi, and G. Subra, "Silicone grafted bioactive peptides and their applications," Oct. 01, 2019, *Elsevier Ltd.* doi: 10.1016/j.cbpa.2019.06.012.

[306] N. R. Glass, R. Tjeung, P. Chan, L. Y. Yeo, and J. R. Friend, "Organosilane deposition for microfluidic applications," *Biomicrofluidics*, vol. 5, no. 3, 2011, doi: 10.1063/1.3625605.

[307] Y. Zhang, C. A. D'Ambra, R. Katsumata, R. L. Burns, M. H. Somervell, R. A. Segalman, C. J. Hawker, and C. M. Bates, "Rapid and Selective Deposition of Patterned Thin Films on Heterogeneous Substrates via Spin Coating," *ACS Appl Mater Interfaces*, vol. 11, no. 23, pp. 21177–21183, Jun. 2019, doi: 10.1021/acsami.9b05190.

[308] A. Szwed-Georgiou, P. Płociński, B. Kupikowska-Stobba, M. M. Urbaniak, P. Rusek-Wala, K. Szustakiewicz, P. Piszko, A. Krupa, M. Biernat, M. Gazińska, M. Kasprzak, K. Nawrotek, N. P. Mira, and K. Rudnicka, "Bioactive Materials for Bone Regeneration: Biomolecules and Delivery Systems," Sep. 11, 2023, *American Chemical Society*. doi: 10.1021/acsbiomaterials.3c00609.

[309] T. J. Keane and S. F. Badylak, "Biomaterials for tissue engineering applications," *Semin Pediatr Surg*, vol. 23, no. 3, pp. 112–118, 2014, doi: 10.1053/j.sempedsurg.2014.06.010.

[310] R. A. Musina, E. S. Bekchanova, A. V Belyavskii, and G. T. Sukhikh, "Differentiation potential of mesenchymal stem cells of different origin," *Bull Exp Biol Med*, vol. 141, no. 1, pp. 147–151, 2006, doi: 10.1007/s10517-006-0115-2.

[311] S. Ding and P. G. Schultz, "A role for chemistry in stem cell biology," Jul. 2004. doi: 10.1038/nbt987.

[312] A. K. Wheaton, M. Velikoff, M. Agarwal, T. T. Loo, J. C. Horowitz, T. H. Sisson, and K. K. Kim, "The vitronectin RGD motif regulates TGF-induced alveolar epithelial cell apoptosis," *Am J Physiol Lung Cell Mol Physiol*, vol. 310, pp. 1206–1217, 2016, doi: 10.1152/ajplung.00424.2015.-Transforming.

[313] K. M. Hennessy, B. E. Pollot, W. C. Clem, M. C. Phipps, A. A. Sawyer, B. K. Culpepper, and S. L. Bellis, "The effect of collagen I mimetic peptides on mesenchymal stem cell adhesion and differentiation, and on bone formation at hydroxyapatite surfaces," *Biomaterials*, vol. 30, no. 10, pp. 1898–1909, Apr. 2009, doi: 10.1016/j.biomaterials.2008.12.053.

[314] J. W. Kim, C. S. Ki, Y. H. Park, H. J. Kim, and I. C. Um, "Effect of RGDS and KRSR peptides immobilized on silk fibroin nanofibrous mats for cell adhesion and proliferation," *Macromol Res*, vol. 18, no. 5, pp. 442–448, May 2010, doi: 10.1007/s13233-010-0514-0.

[315] Z. Y. Guan, C. Y. Wu, J. T. Wu, C. H. Tai, J. Yu, and H. Y. Chen, "Multifunctional and Continuous Gradients of Biointerfaces Based on Dual Reverse Click Reactions," *ACS Appl Mater Interfaces*, vol. 8, no. 22, pp. 13812–13818, Jun. 2016, doi: 10.1021/acsami.6b03908.

[316] I. Brigaud, R. Agniel, J. Leroy-Dudal, S. Kellouche, A. Ponche, T. Bouceba, N. Mihailescu, M. Sopronyi, E. Viguier, C. Ristoscu, F. Sima, I. N. Mihailescu, A. C. O. Carreira, M. C. Sogayar, O. Gallet, and K. Anselme, "Synergistic effects of BMP-2, BMP-6 or BMP-7 with human plasma fibronectin onto hydroxyapatite coatings: A comparative study," *Acta Biomater*, vol. 55, pp. 481–492, Jun. 2017, doi: 10.1016/j.actbio.2017.04.013.

[317] J. Almodóvar, R. Guillot, C. Monge, J. Vollaire, Š. Selimović, J. L. Coll, A. Khademhosseini, and C. Picart, "Spatial patterning of BMP-2 and BMP-7 on biopolymeric films and the guidance of muscle cell fate," *Biomaterials*, vol. 35, no. 13, pp. 3975–3985, Apr. 2014, doi: 10.1016/j.biomaterials.2014.01.012.

[318] J. T. Koepsel, P. T. Brown, S. G. Loveland, ab Wan-Ju Li ab, and W. L. Murphy, "Combinatorial screening of chemically defined human mesenchymal stem cell culture substrates †", doi: 10.1039/c2jm32242k.

[319] C. T. Cheng, P. S. Vyas, E. J. McClain, T.-C. A. Hoelen, J. J. C. Arts, C. McLaughlin, D. T. Altman, A. K. Yu, and B. C. Cheng, "The Osteogenic Peptide P-15 for Bone Regeneration: A Narrative Review of the Evidence for a Mechanism of Action," *Bioengineering*, vol. 11, no. 6, p. 599, Jun. 2024, doi: 10.3390/bioengineering11060599.

[320] R. S. Bhatnagar, J. J. Qian, A. Wedrychowska, M. Sadeghi, Y. M. Wu, and N. Smith, "Design of Biomimetic Habitats for Tissue Engineering with P-15, a Synthetic Peptide Analogue of Collagen," Mary Ann Liebert, Inc, 1999. [Online]. Available: www.liebertpub.com

[321] R. S. Bhatnagar, J. J. Qian, and C. A. Gough, "The role in cell binding of a β1-bend within the triple helical region in collagen αl(i) chain: Structural and biological evidence for conformational tautomerism on fiber surface," *J Biomol Struct Dyn*, vol. 14, no. 5, pp. 547–560, 1997, doi: 10.1080/07391102.1997.10508155.

[322] G. Bullock, J. Atkinson, P. Gentile, P. Hatton, and C. Miller, "Osteogenic peptides and attachment methods determine tissue regeneration in modified bone graft substitutes," Jun. 01, 2021, *MDPI*. doi: 10.3390/jfb12020022.

[323] M.-C. Durrieu and O. Zouani, "Bone substitutes grafted by mimetic peptides of human bmp-2 protein," EP2968660A1, 2019

[324] A. Hachin, T. Buffeteau, J. Hunel, J. P. Salvetat, Y. Roupioz, Se. Bonhommeau, S. E. Mornet, M. Treguer-Delapierre, V. Humblot, and L. Vellutini, "Spin-Coated Amino-Terminated Monolayers to Immobilize Gold Nanorods for Surface-Enhanced Raman Scattering-Active Substrate," *Langmuir*, vol. 41, no. 21, pp. 13430–13442, Jun. 2025, doi: 10.1021/acs.langmuir.5c01196.

[325] R. Kane and P. X. Ma, "Mimicking the nanostructure of bone matrix to regenerate bone," 2013, *Elsevier B.V.* doi: 10.1016/j.mattod.2013.11.001.

[326] K. Klimek and G. Ginalska, "Proteins and peptides as important modifiers of the polymer scaffolds for tissue engineering applications-A review," Apr. 01, 2020, *MDPI AG*. doi: 10.3390/POLYM12040844.

[327] S. Wang, S. Hashemi, S. Stratton, and T. L. Arinzeh, "The Effect of Physical Cues of Biomaterial Scaffolds on Stem Cell Behavior," *Adv Healthc Mater*, vol. 10, no. 3, Feb. 2021, doi: 10.1002/adhm.202001244.

[328] E. H. Schwab, M. Halbig, K. Glenske, A.-S. Wagner, S. Wenisch, E. A. Cavalcanti-Adam, and E. A. Cavalcanti-Adam, "Distinct Effects of RGD-glycoproteins on Integrin-Mediated Adhesion and Osteogenic Differentiation of Human Mesenchymal Stem Cells," *Int. J. Med. Sci*, vol. 10, no. 13, pp. 1846–1859, 2013, doi: 10.7150/ijms.6908.

[329] G. Le Saux, A. Magenau, T. Böcking, K. Gaus, and J. J. Gooding, "The relative importance of topography and RGD ligand density for endothelial cell adhesion," *PLoS One*, vol. 6, no. 7, 2011, doi: 10.1371/journal.pone.0021869.

[330] C. Mangano, A. De Rosa, V. Desiderio, R. d'Aquino, A. Piattelli, F. De Francesco, V. Tirino, F. Mangano, and G. Papaccio, "The osteoblastic differentiation of dental pulp stem cells and bone formation on different titanium surface textures," *Biomaterials*, vol. 31, no. 13, pp. 3543–3551, May 2010, doi: 10.1016/j.biomaterials.2010.01.056.

[331] H. Yang, H. Ding, Y. Tian, C. Wu, Y. Chen, H. Shi, Y. K. Chan, Y. Deng, L. Liao, and S. Lai, "Metal element-fusion peptide heterostructured nanocoatings endow polyetheretherketone implants with robust anti-bacterial activities and in vivo osseointegration," *Nanoscale*, vol. 16, no. 27, pp. 12934–12946, Jun. 2024, doi: 10.1039/d4nr01453g.

[332] M. N. Tamaño-Machiavello, J. C. Marín Payá, S. Flores, L. Cordón, A. Sempere, R. Sabater i Serra, and J. L. Gómez Ribelles, "Maintenance of pluripotency and osteogenic differentiation of human mesenchymal stem cells on acrylate-based substrates exhibiting gelatin or heparin grafting," *Sci Rep*, vol. 15, no. 1, Dec. 2025, doi: 10.1038/s41598-025-05640-7.

[333] G. S. Stein, J. B. Lian, A. J. Van Wijnen, J. L. Stein, M. Montecino, A. Javed, S. K. Zaidi, D. W. Young, J. Y. Choi, and S. M. Pockwinse, "Runx2 control of organization, assembly and activity of the regulatory machinery for skeletal gene expression," May 24, 2004. doi: 10.1038/sj.onc.1207676.

[334] B. Kern, J. Shen, M. Starbuck, and G. Karsenty, "Cbfa1 Contributes to the Osteoblast-specific Expression of type I collagen Genes," *Journal of Biological Chemistry*, vol. 276, no. 10, pp. 7101–7107, Mar. 2001, doi: 10.1074/jbc.M006215200.

[335] P. Ducy and R. Zhang, "Osf2/Cbfa1: A Transcriptional Activator of Osteoblast Differentiation," 1997.

[336] H. Enomoto, T. Furuichi, A. Zanma, K. Yamana, C. Yoshida, S. Sumitani, H. Yamamoto, M. Enomoto-Iwamoto, M. Iwamoto, and T. Komori, "Runx2 deficiency in chondrocytes causes adipogenic changes in vitro," *J Cell Sci*, vol. 117, no. 3, pp. 417–425, Jan. 2004, doi: 10.1242/jcs.00866.

[337] T. Ramesh, "Osteogenic differentiation potential of human bone marrow-derived mesenchymal stem cells enhanced by bacoside-A," *Cell Biochem Funct*, vol. 39, no. 1, pp. 148–158, Jan. 2021, doi: 10.1002/cbf.3596.

[338] D. Zhang and K. A. Kilian, "Peptide microarrays for the discovery of bioactive surfaces that guide cellular processes: a single step azide-alkyne 'click' chemistry approach †," 2014, doi: 10.1039/c4tb00375f.

[339] L. Oliver-Cervelló, H. Martin-Gómez, N. Mandakhbayar, Y. W. Jo, E. A. Cavalcanti-Adam, H. W. Kim, M. P. Ginebra, J. H. Lee, and C. Mas-Moruno, "Mimicking Bone Extracellular Matrix: From BMP-2-Derived Sequences to Osteogenic-Multifunctional Coatings," *Adv Healthc Mater*, vol. 11, no. 20, Oct. 2022, doi: 10.1002/adhm.202201339.

[340] K. M. Hennessy, W. C. Clem, M. C. Phipps, A. A. Sawyer, K. Culpepper, and S. L. Bellis, "The effect of collagen I mimetic peptides on mesenchymal stem cell adhesion and differentiation, and on bone formation at hydroxyapatite surfaces," *Biomaterials*, vol. 30, no. 10, pp. 1898–1909, 2009, doi: 10.1016/j.biomaterials.2008.12.053.

[341] L. Fu, M. Omi, M. Sun, B. Cheng, G. Mao, T. Liu, G. Mendonça, S. E. Averick, Y. Mishina, and K. Matyjaszewski, "Covalent Attachment of P15 Peptide to Ti Alloy Surface Modified with Polymer to Enhance Osseointegration of Implants," *ACS Appl Mater Interfaces*, vol. 11, no. 42, pp. 38531–38536, 2019, doi: 10.1021/acsami.9b14651.

[342] Y. M. Jingying, Z. Eleftherios, T. Xuebin, and B. Yang, "Comparing bone tissue engineering efficacy of HDPSCs, HBMSCs on 3D biomimetic ABM-P-15 scaffolds in vitro and in vivo," *Cytotechnology*, vol. 72, 2020, doi: 10.1007/s10616-020-00414-7.

[343] W. Liu, Q. Wang, H. Liu, S. He, H. Wang, C. Xu, C. Jin, N. Li, and L. Li, "Endowing implants surface with enhanced vascularization and osseointegration via presenting triple-functional peptides," *J Orthop Translat*, vol. 52, pp. 150–166, May 2025, doi: 10.1016/j.jot.2025.03.020.

[344] L. Fan, K. Yang, R. Yu, H. Hui, and W. Wu, "circ-Iqsec1 induces bone marrow-derived mesenchymal stem cell (BMSC) osteogenic differentiation through the miR-187-3p/Satb2 signaling pathway," *Arthritis Res Ther*, vol. 24, no. 1, Dec. 2022, doi: 10.1186/s13075-022-02964-x.

[345] G. Dobreva, M. Chahrour, M. Dautzenberg, L. Chirivella, B. Kanzler, I. Fariñas, G. Karsenty, and R. Grosschedl, "SATB2 Is a Multifunctional Determinant of Craniofacial Patterning and Osteoblast Differentiation," *Cell*, vol. 125, no. 5, pp. 971–986, Jun. 2006, doi: 10.1016/j.cell.2006.05.012.

[346] J. Zhang, Q. Tu, R. Grosschedl, M. S. Kim, T. Griffin, H. Drissi, P. Yang, and J. Chen, "Roles of SATB2 in osteogenic differentiation and bone regeneration," *Tissue Eng Part A*, vol. 17, no. 13–14, pp. 1767–1776, Jul. 2011, doi: 10.1089/ten.tea.2010.0503.

[347] M. Bonilla-Claudio, J. Wang, Y. Bai, E. Klysik, J. Selever, and J. F. Martin, "Bmp signaling regulates a dose-dependent transcriptional program to control facial skeletal development," *Development*, vol. 139, no. 4, pp. 709–719, Feb. 2012, doi: 10.1242/dev.073197.

[348] X. Zhao, Z. Qu, J. Tickner, J. Xu, K. Dai, and X. Zhang, "The role of SATB2 in skeletogenesis and human disease," 2014, *Elsevier Ltd.* doi: 10.1016/j.cytogfr.2013.12.010.

[349] J. Liu, B. Zhao, X. Shen, D. Lu, W. he, X. Zan, L. Li, and Y. Pan, "Enhanced vascularization and osseointegration under osteoporotic conditions through functional peptide coating on implant surfaces," *Mater Today Bio*, vol. 27, Aug. 2024, doi: 10.1016/j.mtbio.2024.101150.

[350] W. K. J. Mosse, M. L. Koppens, T. R. Gengenbach, D. B. Scanlon, S. L. Gras, and W. A. Ducker, "Peptides Grafted from Solids for the Control of Interfacial Properties," *Langmuir*, vol. 25, no. 3, pp. 1488–1494, Feb. 2009, doi: 10.1021/la802864v.

[351] R. Trzcinska, P. Suder, A. Bodzon-Kulakowska, M. Skalska, A. Marcinkowski, J. Kubacki, R. Pedrys, J. Silberring, A. Dworak, and B. Trzebicka, "Synthesis and characterisation of PEG-peptide surfaces for proteolytic enzyme detection," *Anal Bioanal Chem*, vol. 405, no. 28, pp. 9049–9059, Nov. 2013, doi: 10.1007/s00216-013-7082-z.

[352] L. Oliver-Cervelló, H. Martin-Gómez, C. Gonzalez-Garcia, M. Salmeron-Sanchez, M. P. Ginebra, and C. Mas-Moruno, "Protease-degradable hydrogels with multifunctional biomimetic peptides for bone tissue engineering," *Front Bioeng Biotechnol*, vol. 11, 2023, doi: 10.3389/fbioe.2023.1192436.

[353] J. Su, Y. Song, Z. Zhu, X. Huang, J. Fan, J. Qiao, and F. Mao, "Cell–cell communication: new insights and clinical implications," Dec. 01, 2024, *Springer Nature*. doi: 10.1038/s41392-024-01888-z.

[354] Z. Liu, S. Hu, Z. Yun, W. Hu, S. Zhang, and D. Luo, "Using dynamic cell communication improves treatment strategies of breast cancer," Dec. 01, 2021, *BioMed Central Ltd*. doi: 10.1186/s12935-021-01979-9.

[355] K. E. Knewtson, N. R. Ohl, and J. L. Robinson, "Estrogen Signaling Dictates Musculoskeletal Stem Cell Behavior: Sex Differences in Tissue Repair," Aug. 01, 2022, *Mary Ann Liebert Inc.* doi: 10.1089/ten.teb.2021.0094.

[356] J. Waldron, A. McCourty, and L. Lecanu, "Aging differentially affects male and female neural stem cell neurogenic properties," *Stem Cells Cloning*, vol. 3, no. 1, pp. 119–127, 2010, doi: 10.2147/SCCAA.S13035.

[357] J. K. Williams, "Gender, Age and Differences in Stem Cell Expression and Efficacy," *J Stem Cell Res Ther (Edmond)*, vol. 3, no. 2, Sep. 2017, doi: 10.15406/jsrt.2017.03.00097.